University College London (UCL)

Model-based approaches to investigating spread and productivity of Neolithic domesticates

By

Anna Rudzinski

A thesis submitted in fulfilment of the degree of Doctor of Philosophy (PhD)

In the Faculty of Life Sciences

Department of Genetics, Evolution and Environment (GEE)

January 2020

Declaration of Authorship

I, Anna Rudzinski, confirm that the work presented in this thesis is my own. Where information has been derived from other sources, I confirm that this has been indicated in the thesis.

- This work has been done wholly while in candidature for a research degree at the University College London.

- Where I have consulted the published work of others, or myself, this is always clearly acknowledged.

- Where I have quoted from the work of others, the source is always given. With the exception of such quotations, this thesis is my own work.

- I have acknowledged all main sources of help.

Signed:

Date: 03.01.2020

Declaration of Funding

This project was funded by a Marie Curie Initial Training Network, named 'BEAN' – Bridging the European and Anatolian Neolithic, GA no. 289966.

Statement of Originality

Chapter 1:

The archaeological background relevant for Chapters 2 – 6 is discussed in Chapter 1; the introduction of the thesis. The introduction was completely researched and written by me.

Chapter 2:

The idea for the method of inferring locations of origin of domesticated species, was suggested by my primary supervisor, Prof. Mark Thomas (University College London). I wrote the code for the analysis and the plotting in python under Prof. Thomas' supervision.

Chapter 3:

The application of the method was fully performed by myself. I have kindly received data to be analysed from collaborating colleagues, which are:

Dr. Harriett Hunt and Prof. Martin K. Jones (The University of Cambridge), Dr. Yann Dussert (Université Paris-Sud), Dr. Ilaria Grimaldi (University of Oxford), Dr. Laurent A. F. Frantz (Queen Mary University of London) and finally Dr. Ardern Hulme-Beaman (University of Aberdeen).

Chapter 4:

The idea for the method ‘Inferring herd sustainability from age-at-death profiles of domesticated caprines (sheep and goats)’ was initially suggested by my primary supervisor Prof. Mark Thomas in conversations with myself. The design of the method was performed by myself and Prof. Thomas. The application of the method was solely performed by myself. I wrote the code for performing the analysis and plotting of results in ‘R’. The databases on age-at-death profiles were collated by myself (collecting already published age-at-death profiles) and other collaborating colleagues; Dr. Rosalind Gillis (University of Algarve), and Dr. Alfred Galik with Prof. Barbara Horejs (University of Vienna). Dr. Anne Tresset and Dr. Stephanie Brehard (both Muséum national d’Histoire naturelle, Université of Paris) provided insightful expertise concerning the construction of the ethology of Neolithic sheep and goat herds.

Chapter 5:

The conception and design of the method ‘Design and application of Bayesian Markov Chain Monte Carlo method to infer sex-specific mortality profiles and product yields from unsexed Caprini zooarchaeological remains’ was performed by Prof. Thomas, Dr. Diekmann and myself. I contributed by coding a pipeline for the application of the approach as well as the analysis and plotting of results in C++ and in R. I performed all analyses presented in this chapter. I also contributed to the validation process of the method. Furthermore, I collated (a) a database of >200 published and unpublished age-at-death profiles, (b) ethological data on unimproved sheep and goats and (c) archaeological and contemporary sheep and goat herd sex ratios by age. Dr. Rosalind Gillis provided advice and expertise pertaining to the age-at-death databases collation as well as to the archaeological contexts of the analyses.

Dr. Roger Blench provided advice and expertise with respect to the ethological data on unimproved sheep and goats.

Chapter 6:

The application of the method presented in Chapter 5 was applied to three datasets in a meta-analysis (through time, longitude and latitude). The datasets were collated by myself and my colleagues (see Chapter 4). The analyses of more than 200 age-at-death profiles has been entirely performed and coded (in R) by me. Advice and expertise on the archaeological context of milk as a food in the Neolithic, has been kindly provided by Catherine Walker (PhD candidate, UCL).

Chapter 7:

The general discussion was researched and written by me.

Abstract

The domestication of plants and animals during the Neolithic transition marks one of the most important changes in human ecology in the last 300,000 years. Whilst there is a considerable literature on the archaeology of domestic plants and animals, analyses tend to be descriptive and formal model-based inference on the processes of spread and the economic value of those domesticates are less common.

In this research, I developed a model-based approach to inferring the location of origin of a population, based upon the expected monotonic decrease in genetic diversity with distance from origin location, and applied this method to data from broomcorn millet across Eurasia, African pearl millet, taro in Africa, the Pacific rat and three endemic species from the island of Sulawesi. I also developed two approaches to analysing age-at-death data from caprines. The first uses the Dirichlet distribution to infer caprine herd sustainability parameters. The second is a full Bayesian Markov Chain Monte Carlo method for inferring herd sustainability and economic productivity of caprine herds. Under the assumptions of the latter model, I infer a general improvement in the economic productivity of caprine herd slaughter management strategies throughout the Neolithic and into the Middle Ages.

Impact Statement

In this thesis, I address two classes of research question in Neolithic archaeology and develop three model-based approaches to provide some insights into these questions. All approaches contribute to archaeological research on the Neolithic in various parts of the world.

The geographical locations of the origin of expansion of certain plants and animals remain poorly understood for some species. For many years, archaeologists focused their research on identifying the regions of origin of 'founder crops' such as emmer and einkorn wheat, and barley, in the Near East. While this approach resulted in key insights on the crops' location of origin, the origins of spread of crops from different agricultural centres in the world such as crops firstly domesticated in Africa or West Asia, only gained more attention in recent years. I developed and applied a discriminative model-based approach to infer the location of origin of spread of domesticates from georeferenced genetic and morphometric variation data. I applied the method to support archaeological research on the origins of, for example, African pearl millet, Eurasian broomcorn millet and others. Inferring the geographical region of origin of a crop may inform archaeologists about a potential region for archaeological excavations, which have not been considered before, and may in turn lead to other significant archaeological findings.

Furthermore, archaeologists are sometimes interested in understanding the economic targets of past herding strategies for cattle, sheep and goats – the first animal domesticates of the Near East. Age-of-death profiles reflect underlying culling strategies, which may be targeted towards the exploitation of specific animal products such as meat or milk. In a collaborative project, I developed and applied a Bayesian Markov Chain Monte Carlo method to infer sex-specific mortality profiles and animal product yields from a collection of > 200 sheep and goat age-at-death profiles. With this novel approach it is possible to estimate relative herd growth – a proxy for herd

sustainability – product yields, and the economic efficiencies of slaughter strategies from archaeozoological kill-off profiles.

Furthermore, by applying this approach to a dataset spanning different time periods and locations, I investigate one aspect of cultural evolution by studying the change in time and space of herding practises across Europe during the Neolithic. In particular, I consider if the economic efficiency (in terms of calories produced per fodder consumed) of slaughter strategies improves through time. I find evidence that sheep / goat management strategies did improve, with a concomitant shift from meat to milk calories.

This project requires knowledge from Neolithic archaeology, population genetics, computer programming and simulation, and an understanding of statistics, reflecting the cross-disciplinary and collaborative nature of this thesis – perhaps a stimulus for multidisciplinary research in future.

Table of Contents

List of Figures

List of Tables

Acknowledgements

I want to begin to express my infinite gratitude for my supervisor, Prof. Mark Thomas - for all the scientific skills he taught me and made me conquer no matter what, for all the hours in his office to discuss the projects of this thesis, for all his patience throughout the learning of all the skills needed in order to complete this work.

I want to express my deepest thanks to all my colleagues at UCL who helped me to master (or at least understand) the scientific skills to perform the work presented here. I want to thank Dr. Pascale Gerbrault, Dr. Mirna Kovačević and Dr. Adam Powell for their kindness and patience to explain the virtues of modelling and how to translate words into programming code.

Special thanks to Prof. Dallas Swallow, who always cared about me and my work and who provided me with her experienced advice in the field of genetics and, above all, for all her direction in what to focus on during every write-up process of projects, upgrades and this thesis.

Catherine Walker, Dr. Katherine Brown and Dr. Elizabeth Gallagher were my colleagues and friends from the MACE-lab and always there for scientific and life - advice. Special thanks to Catherine, who helped enormously during the write-up process of this work. Her suggestions undoubtfully improved this thesis.

Dr. Yoan Diekmann not only helped in designing the methods described in this thesis but was also the friend who also stayed until night time at the lab. I want to thank him for all the insightful conversations.

I want to thank Adrian Timpson for his unconventionalism in every way, especially regarding science by questioning all those things we take for granted. He, together with Prof. Thomas, always shook up my view of the world and inspired me to stay curious and critical towards the scientific premises and the world we are living in.

I want to thank the entire ‘BEAN’ team with special thanks to Prof. Joachim Burger and Karola, who made all the investigations related to ‘Bridging the European and Anatolian Neolithic’ possible, including an interesting and horizon-widening excursion to West Anatolia. I would also like to express my thanks to Dr. Beatrijs de Groot, who is also part of BEAN and who not only became a close friend but also answered all my questions regarding Neolithic archaeology. I want to thank Prof. Barbara Horejs for taking me on an excavation in Selcuk, during which I learnt plenty about the West Asian Neolithic and Bronze Age. Also, special thanks to Dr. Alfred Galik, who intrigued me with his expertise in zooarchaeology and who, later, was so kind to share some of his data, which I also used in this thesis. I am also grateful to Dr. Roz Gillis and all her advice on animal bones and that she shared her expertise and data on age-at-death profiles.

Last but certainly not least, I want to thank all my friends and family, who always supported me during the process of – hopefully – becoming a doctor.

Publication output

As a result of the work carried during my PhD, I have authored 3 published papers:

Hunt, H. V., **Rudzinski, A**., Jiang, H., Wang, R., Thomas, M. G. & Jones, M. K. (2018). Genetic evidence for a western Chinese origin of broomcorn millet (Panicum miliaceum) **The Holocene,** 0959683618798116.

Frantz, L. a. F., **Rudzinski, A**., Nugraha, A. M. S., Evin, A., Burton, J., Hulme-Beaman, A., Linderholm, A., Barnett, R., Vega, R., Irving-Pease, E. K., Haile, J., Allen, R., Leus, K., Shephard, J., Hillyer, M., Gillemot, S., Van Den Hurk, J., Ogle, S., Atofanei, C., Thomas, M. G., Johansson, F., Mustari, A. H., Williams, J., Mohamad, K., Damayanti, C. S., Wiryadi, I. D., Obbles, D., Mona, S., Day, H., Yasin, M., Meker, S., Mcguire, J. A., Evans, B. J., Von Rintelen, T., Ho, S. Y. W., Searle, J. B., Kitchener, A. C., Macdonald, A. A., Shaw, D. J., Hall, R., Galbusera, P. & Larson, G. (2018). Synchronous diversification of Sulawesi's iconic artiodactyls driven by recent geological events **Proc Biol Sci***,* 285.

Gerbault, P., Allaby, R. G., Boivin, N., **Rudzinski, A**., Grimaldi, I. M., Pires, J. C., Climer Vigueira, C., Dobney, K., Gremillion, K. J., Barton, L., Arroyo-Kalin, M., Purugganan, M. D., Rubio De Casas, R., Bollongino, R., Burger, J., Fuller, D. Q., Bradley, D. G., Balding, D. J., Richerson, P. J., Gilbert, M. T., Larson, G. & Thomas, M. G. (2014). Storytelling and story testing in domestication **Proc Natl Acad Sci U S A***,* 111**,** 6159-64.

I am also an author (stared equal first author) on a paper currently under review in Methods in Ecology and Evolution (note: the contents of this paper are not reported in this thesis):

Hulme-Beaman, A.***, Rudzinski, A.*,** Cooper, J., Lachlan, R., Dobney, K., Thomas, M.G.. GeoOrigins: Trait mapping and geographic provenancing of specimens without categorical constraints**.**

Chapter 1

1 General Introduction

1.1 Context of the work

My PhD work was embedded within a European collaborative programme called BEAN. The BEAN project (Bridging the European and Anatolian Neolithic) is an EU Marie-Curie funded project investigating the Neolithization of Europe by bringing together various disciplines and addressing demographic questions surrounding the spread of technological, cultural and biological components associated with the Neolithic transition across Anatolia into Europe, and involves eight laboratories across Europe. The diverse content of this thesis reflects the broad scope of that project.

1.2 Background to the research

The Neolithic is a prehistoric phase which is characterised by the first developments of farming, the domestication of animals and plants, a sedentary way of life, and polished stone tools. The Neolithic transition took place at different times in different places in the world and is thought to have occurred independently in at least 20 centres (Purugganan and Fuller, 2009). The Neolithic transition first occurred in southwestern Asia, in a region often called the Fertile Crescent, ca. 12,000 years ago.

Various disciplines, such as archaeology, population genetics, statistical modelling, ancient DNA, linguistics and anthropology, have been mobilised to address questions relating to where, when and by what processes the Neolithic transition occurred and spread. The exact timing as well as routes of dispersal of Neolithic lifeways are reasonably well-understood, although the processes by which they spread are not.

1.3 The Origin and Spread of farming

Farming involves the deliberate cultivation and domestication of plants and animals. The onset of farming gave rise to major shifts in human demography. In the past 10,000 years human populations grew rapidly (Bocquet-Appel, 2011), probably due to more food production in less geographical space as compared to a hunting- and gathering-based subsistence.

The development of farming cannot be accredited to a specific population (Broushaki *et al.*, 2016; Lazaridis *et al.*, 2016) , archaeological culture, location in the world or point in time. Archaeological evidence and evidence from other disciplines have shown that plant domestication included a diverse range of taxa and occurred in several independent centres in the world at different times (Richerson, Boyd and Bettinger, 2001; Bellwood, 2005), including western Asia ~13,000 - 9,000 B.P. (Braidwood, 1983), central China ~7,000 – 6,000 B.C (Crawford, 2006), New Guinea ~6,000 B.P (Lebot, 2009), Mesoamerica ~10,000 B.P, the Andes 8,500 – 4,500 B.P, North America 4,500 – 4,000 B.P and possibly India ~5,000 B.P and West Africa ~ 5,000 B.P (Purugganan and Fuller, 2009).

According to Purugganan and Fuller (2009), crop domestication emerged in up to 20 regions independently. In contrast, animal domestication is generally considered to have happened primarily in three centres of domestication: the Andes, China and the Near East. However, it can be challenging to distinguish clearly between the spread of the idea of farming and an independent development.

The earliest evidence for agricultural activities is dated to around 11,500 cal BP in the Near East (Zeder, 2011). Why agriculture might have started at that particular time and location is still debated. However, some scientists claim that a more stabilised climate was the main driving factor leading to the emergence of agriculture (Reed, 1977; Henry, Leroi-Gourhan and Davis, 1981; Richerson, Boyd and Bettinger, 2001). During the Holocene (from 11,700 BCE to present) in the Near East, stable

temperatures and a temperate climate might have facilitated the evolution of methods for intensive exploitation of crops. It has been hypothesised that rapid population growth led to competition among groups for more intensive subsistence strategies (Bronson, 1977; Richerson, Boyd and Bettinger, 2001). Furthermore, wet, warm and stable climates provided a fertile ground for plant domestication. In contrast, during the Pleistocene, which preceded the Holocene, the planet was exposed to extreme temperature fluctuations, hostile and unstable conditions for consistent crop growth (Richerson, Boyd and Bettinger, 2001). Another factor which may have led to the beginnings of agriculture is increased pressures on natural food resources, which may have forced people to find homegrown solutions (Binford, 1968; Flannery, 1969; Bronson, 1977). Others have argued that key social developments were necessary, such as the emergence of property rights (Bowles and Choi, 2013; Gallagher, Shennan and Thomas, 2015) .

Despite the various debates, there are two constants, which hold true for all cases of the emergence of farming: a) the cultivation of wild plants and b) a stable climate. The Holocene alone may not have been sufficient for the origins of farming, since it was developed independently multiple times at different regions of the world well after the beginning of this epoch (Bellwood, 2005), but it provided a condition that permitted the sustained cultivation of plants. Evidence for pre-Holocene 'unsuccessful' experiments for the domestication of rye (*Secale cereale*) in Syria (Hillman *et al.*, 2001), illustrate this point.

1.4 Domestication

Domestication and keeping of sheep, goat, pigs and cattle began around 11,000 to 10,000 years ago in a region between the Levant, the Zagros mountains and Central Anatolia (M. Zeder, 2008). Most of our knowledge on the location and timing of domestication of animals is known from archaeozoological investigations (Zeder,

2006a; Gerbault *et al.*, 2012). However, precise answers for the 'where and the when' still remain elusive (Burger and Thomas, 2011). The domestication of animals is characterised by a reduction in body sizes (Meadow, 1989). However, others have explained reduced animal sizes by culling strategies directed towards younger, female animals (Vigne, Peters and Helmer, 2005).

Some have proposed that the initial plant domestication preceded animal domestication by ~1,000 years in the same geographic regions of the Near East (Bar-Yosef and Meadow, 1995). However, more recent studies indicate that the domestication of both plants and animals occurred simultaneously (Zeder, 2011).

Scientific methodologies other than traditional archaeozoological approaches, such as genetic and stable isotope analyses, in combination with radiocarbon dating, have led to insights into initial livestock and crop domestication and their diffusion (M. A. Zeder, 2008). Modern and ancient DNA, ranging from uniparental systems such as mtDNA, to full genomes, have provided information on the demographic history of humans, as well as domesticated animals and plants; information that would not be available from the study of animal remains alone. This includes estimates of domestication such as effective population size (Bollongino *et al.*, 2012), temporal and geographical range of expansion, single versus multiple dispersal processes, etc. (Scheu *et al.*, 2015). One frequently-asked question is the geographic location of origin of an expansion of a domestic species. In Chapters 2 and 3 I describe the development and some applications of a method for inferring the place of origin of domesticated animals and crops from genetic and morphological data, based on expected patterns of diversity reduction in geographic space (Frantz *et al.*, 2018; Hunt *et al.*, 2018).

1.5 The European and West Asian Neolithic in a context

In the context of the 'BEAN' project, I will refer here to the Neolithic of the Fertile Crescent and Anatolia. The term 'Neolithic Revolution' was coined by Childe (1950) to define a change in subsistence strategies; specifically the beginnings of farming. The more archaeology that has been done on Neolithic sites, the more challenging it has become to distinguish between hunter-gatherers and early farming people, and as such the interest in understanding the origins of agriculture and domestication increased amongst archaeologists in the 1960s (Richerson, Boyd and Bettinger, 2001).

Defining the Neolithic has met with challenges when the aceramic Neolithic or the pre-pottery Neolithic was identified and classified (Colledge and Conolly, 2007; Özdoğan, 2011). The term 'Neolithic package' has been used to refer to material culture, permanent settlements, agriculture and animal farming across Southwest Asia and Southeast Europe (Çilingiroğlu, 2005; Burger and Thomas, 2011). However, there is no clear definition of the actual content of that package. Çilingiroğlu (2005) attempted to define the content of the 'Neolithic package' in Southeast Europe and Southwest Asia as follows:

- The package comprises *material culture* such as red-slipped or/and painted pottery; *stone objects* (e.g. bowls, jewellery), *bone objects, technological or prestigious or symbolic items* (Çilingiroğlu, 2005).
- The *'agricultural package'* consists of the founder crops: emmer, einkorn wheat, wild barley, lentil, chickpea, vetch and flax (Çilingiroğlu, 2005; Colledge and Conolly, 2007).
- *Domesticated animals* include goats, sheep, pigs and cattle.
- The Neolithic is also defined by changing subsistence strategy from hunting and gathering to food production and from a mobile to a sedentary lifestyle (sedentism).
- The development of *architecture and settlements* are also part of the package.

When using the term ‘Neolithic’ in this thesis, I refer to a novel lifestyle centred on crop and animal domestication and the construction of permanent settlements with special-use buildings.

The first evidence of sedentism is observed in the Levant. Sedentary hunter-gathering and fishing communities started to experiment with cereal cultivation during the Pre-Pottery-Neolithic A period (PPNA, ca. 9,500 – 8,700 BCE). By the pre-pottery Neolithic B (PPNB, ca. 8,700 – 7,000 BCE) people had converted to large-scale farming (Düring, 2010). Around 7,000 BCE the ‘Neolithic package’ spread through central Anatolia to southern and western Anatolia and appears simultaneously in the Greek Aegean and the Marmara region by around 6,400 BCE (Burger and Thomas, 2011). However, radiocarbon dates on material from Neolithic excavation sites in western Anatolia indicate an earlier appearance than previously thought and suggest a more complex picture of its spread in the region (Özdoğan, 2011).

For more than 90 years, since the term ‘Neolithic revolution’ was introduced by Childe (1936), considerable uncertainties have remained about the processes of the spread of the Neolithic package from Anatolia into and across Europe (Childe, 1950). Understanding this spread remains one of the most challenging topics in archaeology.

In the 1950’s, archaeological activities, particularly concerning Neolithic tell-sites, were increased in the Balkans (Lichardus and Lichardus-Itten, 1985; Van Andel and Runnels, 1988, 1995; Tringham, 2000; Séfériadès, 2007; Özdoğan, 2011). This revealed rich archaeological records, which indicated the direction of spread of the package into Europe from the Near East via the Balkans (Tringham, 2000). In contrast, Western Anatolia had been largely neglected in terms of Neolithic period excavations. Furthermore, because of discrepancies in dating, uneven distribution of excavation sites and political differences between Turkey and the countries of Southeast Europe, the role of the Neolithic in Anatolia was partly neglected as a potential source location for the Neolithic in the Balkans (Özdoğan, 2011). However,

more recent excavations of Anatolian Neolithic sites suggest that this region might have served as a source for the Balkan Neolithic, giving rise to the concept of the Balkano-Anatolian Neolithic cultural complex (Özdoğan, 2011). Western parts of the Anatolian Peninsula formed the main contact zone during the initial stage of the Neolithic expansion into Europe whereas Southeast Europe was considered to be core area for expansion.

From material culture evidence, two routes have been inferred for the dispersal of Neolithic cultures. On the one hand, the Adriatic Impressa culture and the later Cardial Ware culture spread east via the northern Mediterranean. On the other hand, the Karanovo complex culture and the Starcevo-Körös-Cris complex are associated with a spread via the mainland along the Danube into central Europe. By ~4,100 cal. B.C., the Neolithic package reached the northwestern fringes of the continent (Burger and Thomas, 2011).

1.6 Climate and Geology

Climate stability and the temperate ecologies associated with the Holocene (from 11,700 BCE to present) are thought to have been an important factor shaping the appearance and expansion of farming and sedentism (Richerson, Boyd and Bettinger, 2001; Düring, 2010). Semi-arid zones in close proximity to water sources, and the ability of humans to adapt to new subsistence strategies, are thought to have made permanent settlements possible. The Holocene is an epoch characterised by a warm and stable climate, which led to the growth of dense forest landscapes in Anatolia and the European continent. From 6,000 BCE, farming practices introduce cereals, which changed the landscapes significantly. Between 1,700 BCE – 700 AD, human excessive deforestation started to have a substantial effect on ecology (Düring, 2010).

The changing climate led to rise and fall of sea levels. In the Aegean, which is rich in islands and shallow seas, lowering of sea-levels led to extended coast-lines and may have facilitated human population movement. During the Last Glacial Maximum (LGM), a climatic event characterised by very cold temperatures, which peaked at ~21,500 years ago, sea levels are thought to have been ~100 - 130 meters below those of present day due to the formation of ice covering large regions of the planet (Clark *et al.*, 2009). However, during the onset of the temperate climate, the coastal landscape was restored to its present configuration (Van Andel and Shackleton, 1982). The fluctuation of sea levels had a major impact on the conservation of archaeological sites, and as such, some Neolithic settlements are under water at present times which results in absent or biased evidence for the spread of the Neolithic.

1.7 History of human diet

Studying human diet may give insights into the past, present and future of people (Ungar and Teaford, 2002). Understanding how and what people eat today and ate in the past and how human diet changed through time informs on how and what people will eat in the future and how to react to future dietary changes and necessary quantities to feed future world populations.

Furthermore, understanding past diets can also shed light on other processes such as past animal husbandry, farming, past settlement architecture, culture and religion. For example, eating meat from cattle is very common in Europe while forbidden in parts of India as the animals are respected living beings amongst Hindus. Other examples of how prehistoric farmers handled animals and food is reflected in archaeological remains of Neolithic settlements which show if and where domesticated animals were kept within a village complex. Nowadays, many different disciplines deal with studying human present diets as well as past diets such as

nutritional chemistry, biochemistry, nutrition studies, medicine, evolutionary medicine, anthropology, archaeology, archaeobotany, zooarchaeology and many others. In the following chapters of this thesis, I will perform analyses on domesticated crops and domesticated animals – both from archaeological remains of Neolithic excavations and from modern genetic data.

At the beginnings of the Homo lineages ~2.6 million years ago (mya), diet shifted from a predominantly plant-based diet to an omnivorous diet. Simultaneously, at ~ 2.7 – 2.6 mya, the development of Oldwan stone tools has been proposed to have led to an increase in meat consumption, shifting diets from high volume low-calorie foods to low volume high-calorie and protein-rich foods (Lee-Thorp, Sealy and Van Der Merwe, 1989; Lee-Thorp, van der Merwe and Brain, 1994; Sponheimer and Lee-Thorp, 1999). This dietary shift has been implicated in increasing brain sizes and decreasing length of the gut (Aiello and Wheeler, 1995). A subsequent major change in hominin dietary history is thought to involve the controlled use of fire. Cooking permitted an eased digestion of meats and starch-rich foods (Hardy *et al.*, 2015), as well as reduced pathogen-loads. However, the timing of this transition to controlled fire use and cooking remains contentious – with dates ranging from 1.7 Mya to 120 kya. During the Upper Palaeolithic ~100 – 10 thousand years ago (kya) more advanced stone tools techniques and hunting strategies appear – causing higher human population densities and range expansion. Eventually, with the onset of the agricultural revolution ~10 kya, carbohydrate-rich foods began to dominate the Neolithic diet (Cordain *et al.*, 2005). This is often associated with reduced dietary diversity, increased population sizes and poorer health status. Modern farming, which commenced ~200 years ago, is thought to have resulted in reduced richness of macronutrients, minerals and vitamins and increased protein, carbohydrate and saturated fat intake.

1.7.1 Plant-based diet in the Neolithic across the world

The Near Eastern and European Neolithic diet typically consisted of starch-rich foods such as emmer wheat, einkorn wheat and barley, as well as protein-containing pulses like lentils and chickpeas (Colledge and Conolly, 2007). At the beginnings of farming, crops did not show all the traits associated with domestication (Willcox, 2004). Instead, 'domestication traits' – such as tough rachis and increased seed size – developed over the ensuing millennia.

1.7.2 Plant-based diet during the Neolithic in East-Asia

Outside the Near East a range of different crops were domesticates at other, independent centres of origin (Fig. 1.1 and Fig. 1.2). The oldest records of East Asian agriculture, mainly in present-day China, have been reported at 7,000 – 6,000 B.C (Crawford, 2006). Rice (*Oryza sativa*), foxtail millet (*Setaria italica* subsp. *italica*) and broomcorn millet (*Panicum miliaceum*) were amongst the first cereals cultivated in East Asia (Lee *et al.*, 2007). Later native plant species domesticated in this region include fruit trees like hazelnut, mandarin and peach; legumes like mungbean and soybean; roots and tubers such as yam, ginseng and turnip (Crawford, 2006). While the locations of origins of the Near Eastern 'founder crops' are generally well defined, this is often not the case for grains and root plants from other parts of the world. The location of origin of expansion of domestic broomcorn millet, for example, is explored in this thesis.

In terms of food preparation and common foods eaten in East Asia, archaeologists infer that – with the exception of Japan – agriculture preceded pottery, which was thought to be used for steaming and boiling grains, vegetables and meats, and also for the distillation and boiling of beverages. This stands in contrast to the Near East, where it is argued that agriculture preceded ovens, which were used for baking breads and other foods. These findings may explain differences of cooking

traditions between present-day eastern and western Eurasia (Fuller and Rowlands, 2011; Hodos, 2016).

1.7.3 Plant-based diet in the Pacific Neolithic

Taro, 'probably the oldest crop on earth' (Lebot, 2009), is also one of the domesticated crops considered in this thesis. Tropical tubers such as taro and yams, and fruits like coconut, breadfruit and banana, were originally domesticated in the pacific region, mainly referring to the region ranging from present-day Malaysia to the islands in Melanesia (Crawford, 2006). Via migration routes of Austronesian language-speaking populations from East Asia towards equatorial regions, tubers and tropical fruits started to be cultivated or picked up and planted elsewhere. There is evidence for an independent agricultural origin centre in New Guinea (Fig. 1.1 number '13'), dating back to 7,000 - 10,000 B.P. (Bourke, 2009). Taro in particular is thought to have been grown in tropical Asia for ~10,000 years and was most likely domesticated multiple times in different regions of the Pacific (Lebot, 2009). Despite various efforts, the location of taro domestication in the Pacific remains unknown (Yen and Wheeler, 1968; Lebot and Aradhya, 1991; Matthews, 2002).

1.7.4 Plant-based diet during the Neolithic in the Africa

A range of cultivated crops are thought to have been domesticated in Africa (Purugganan and Fuller, 2009; Harlan, 2011). In the East African uplands, finger millet (*Eleusine coracana) and* teff (*Eragrostis tef*) were domesticated ~4,000 B.P. Yam (*Dioscorea cayenensis)* and the root crop commonly known as Ethiopian banana (*Ensete ventricosum)* were domesticated in the East African lowlands. Although the domestication dates of these crops remain unknown, some claim that the latter was first cultivated some 10,000 years ago (Tsegaye, 2002). Sorghum (*Sorghum bicolor*) is thought to have been domesticated in Sudanic Africa, and fonio

millet (*Digitaria exilis)* and African rice (*Oryza glaberrima)* first cultivated in the West African savanna and woodlands, all around 4,000 BP. In the same region, cowpea (*Vigna unguiculate)* was cultivated a few centuries later ~3,700 BP. And lastly, the West African sub-Sahara served as the agricultural centre for pearl millet (*Pennisetum glaucum*) cultivation ~4,500 BP (Fig. 1.1) (Purugganan and Fuller, 2009; Harlan, 2011). The domestication process of pearl millet did not take the same course as other domesticated crops, of which their changing morphology is usually characterized by increasing seed size and non-shattering. Instead, grain size only changed ~ 2,000 years after domestication, as also observed in pulses from sub-Saharan Africa. Evidence for delayed seed size enlargement may indicate multiple, later attempts at domestication. As such, pearl millet as known today may not descend from the earliest domesticates in Africa (Purugganan and Fuller, 2009).

When it comes to food making, interestingly, manufacturing beers and cooking porridges was common and most probably firstly appeared in Egypt and the Nile valley during the East African Neolithic (Fuller and Rowlands, 2011).

1.7.5 Plant-based diet during the Neolithic in the Americas

Mesoamerica is considered one of the three most important centres for plant domestication in the world; next to those in the Near East and North China (Harlan, 2011). Together with other New World crops (Fig. 1.1 number 1-3), the region provided a range of nuts, tubers, vegetables and fruits which are widely used in modern Western diets. Pumpkin (*Cucurbita pepo*), was domesticated in Mesoamerica, while the lima bean (*Phaseolus lunatus*), giant bean (*Canavalia plagiosperma*) and a type of squash (*Cucurbita ecuadorensis)* were domesticated in Ecuador and Peru ~10,000 BP. Maize was also cultivated in Mesoamerica ca. 1,000 – 3,000 years later. The sweet potato (*Ipomoea batatas*) and the common bean (*Phaseolus vulgaris*) are thought to have been domesticated in a region covered by

present-day Colombia and Venezuela ~9,000 – 8,000 BP. By ~8,000 BP potato (*Solanum tuberosum*) was cultivated in the Andes, and cassava (*Manihot esculenta*) and peanut (*Arachis hypogaea*) were first grown in the Amazon. Following an apparent hiatus for plant domestication in the Americas of 3,000 years, by ~5,000 BP quinoa (*Chenopodium quinoa*) and amaranth (*Amaranthus caudatus)* started to be cultivated in the Andes. Additionally, the sun flower (*Helianthus annuus*) is thought to have been domesticated in northeast America ~4,500 – 4,000 BP. A number of other crops were also domesticated in the Americas – too numerous to list here – some of which are represented in modern Western diets (Harlan, 1971; Purugganan and Fuller, 2009). Domestication of plants was carried out by the native Americans across the whole continent of America, with hotspots in the Andes and the tropics.

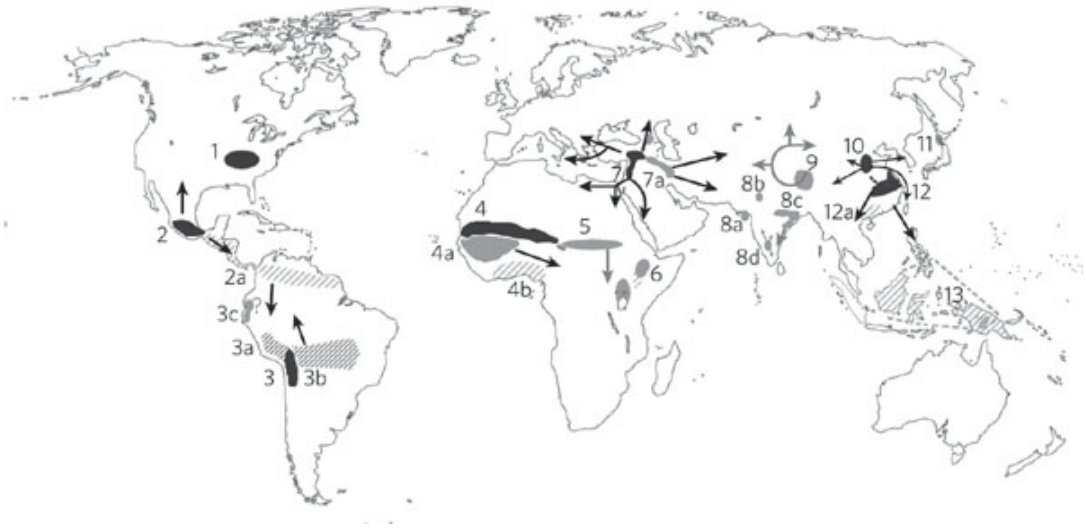

Fig. 1.1 Centres of plant domestication (adapted from Purugganan and Fuller, 2009). Solid-shaded areas and hatched areas indicate regions of important seed-crop domestication and vegecultural crops, respectively. Accepted primary domestication centres are shown in black, and potentially important secondary domestication centres are shown in grey.

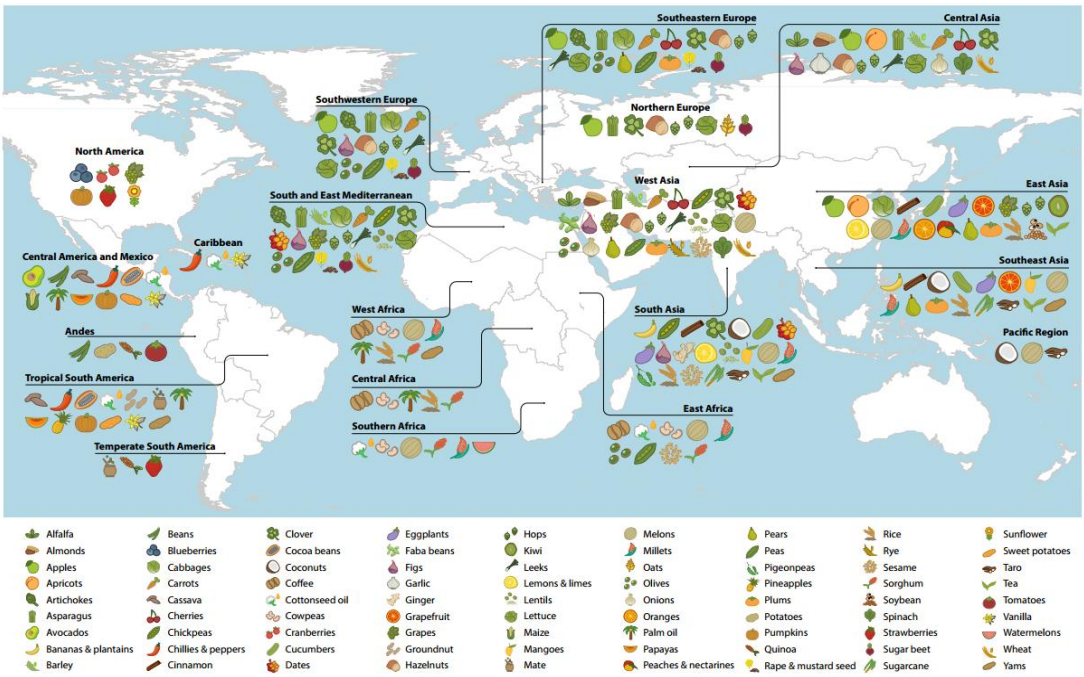

Fig. 1.2 Origins and primary regions of diversity of agricultural crops. Adapted from (Khoury *et al.*, 2016).

1.8 Animals in the Neolithic

The Neolithic Revolution included the domestication of a number of animal species. This process is mostly thought to have occurred after the domestication of plants (Scanes, 2018). In general, the processes of animal domestication were associated with a decrease in body size. Explanations put forward for this phenomenon include: (a) because smaller animals are easier to tame (Clutton-Brock, 1981b), and (b) a preference for smaller newborns from sub-adult breeding, resulting in increasing meat production (Manning *et al.*, 2015). Across Western Europe a continued decrease in size between the Neolithic and Iron Age is seen, particularly for cattle, until the animals started to increase in size again starting from the Roman period onwards (Matolcsi, 1970; Bokonyi, 1974; Méniel, 1984; Audoin-Rouzeau, 1991; Valenzuela-Lamas and Albarella, 2017). However, some archaeozoological evidence for an increase of body sizes starting during Iron Age Italy – earlier than in

the rest of Europe – has also been noted (Trentacoste, Nieto-Espinet and Valenzuela-Lamas, 2018).

Domesticated animals were and continue to be used for several purposes. Sherratt (1981) proposed the 'secondary product revolution', whereby at the beginnings of the Neolithic in the Near East animals were mainly used as meat source and bones were transformed into bone tools, but only later were they exploited for traction, milk, skins, wool and manure (Sherratt, 1981). However, studies have shown that milk exploitation, at least, was a feature of relatively early Neolithic lifeways (Evershed *et al.*, 2008).

While it is commonly accepted that crop domestication generally occurred once for each species, there is archaeological evidence for multiple, independent domestication of the same animals species (Scanes, 2018). Which type of animal was domesticated or appeared at which time across the world varies amongst the centres of origin for agriculture (Fig. 1.1). Cattle, dromedaries, sheep and goats were firstly domesticated in the 'Fertile Crescent' and then introduced to northeastern African regions ~8,000 B.P., followed by migration southwards (Marshall and Hildebrand, 2002). On an East-West axis, domesticates were also introduced into Europe, when the climate started to become drier and the land arid in the Middle East. Cattle are thought to have been domesticated independently in several regions of southern and western Asia. Sheep and goats were thought to have been domesticated twice at different times in the Fertile Crescent, and pigs were independently domesticated in Anatolia, East Asia and possibly western Europe. It has been argued that a major corollary of humans living in close proximity to livestock was the emergence of infectious diseases such as small pox and measles (Furuse, Suzuki and Oshitani, 2010).

1.9 Milk drinking

Evidence for milk drinking dates back to early Neolithic Anatolia ~9,000 – 10,000 years ago, a time when Neolithic adults were as yet unable to digest the milk sugar lactose. To overcome the symptoms associated with the inability to digest lactose, milk was most probably processed into yoghurts, butter fat, cheeses and related dairy products, all of which have lower lactose concentrations (Salque *et al.*, 2012; Warinner *et al.*, 2014). Via strong natural selection, a genetic variant (-13,910*T) causing lactase persistence (Enattah *et al.*, 2002) – the continued expression of lactase into adulthood – increased in frequency in Europe, western and southern Asia. Other genetic variants causing lactase persistence increased dramatically in frequency in other regions of the world where pastoralism and milk consumption were common, such as the Middle East and some regions of Africa. Today, 1/3 of the world population is able to digest lactose from animal milk (Curry, 2013) (Fig.1.3).

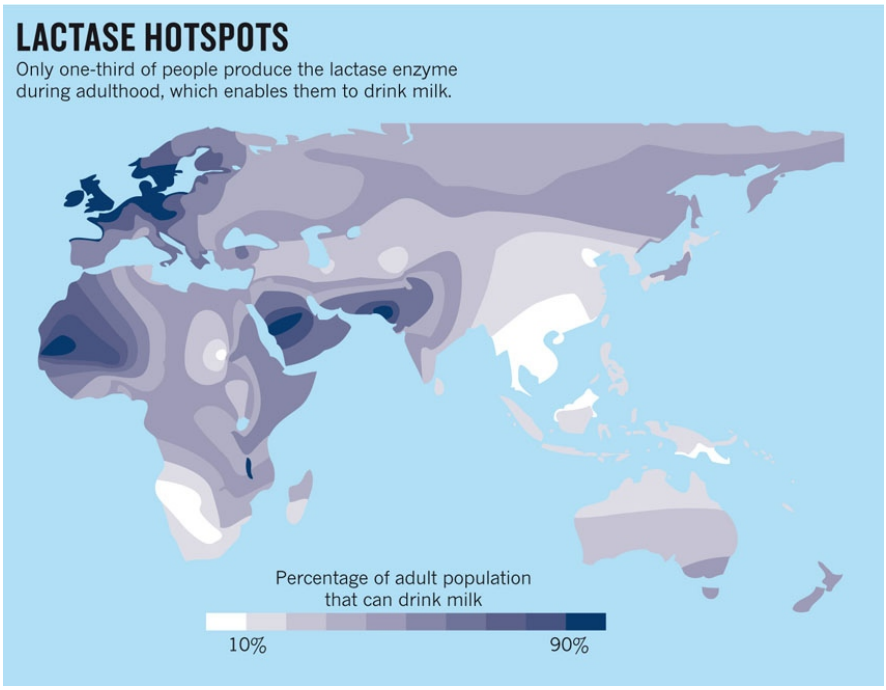

Fig.1.3 Percentage of adult population that can drink milk worldwide today. Adapted from (Curry, 2013).

1.10 Animal exploitation strategies in West Asia and Europe during the Neolithic period

Meat and milk were mainly obtained from cattle, dromedaries, sheep and goats and other wild, hunted animals during the West Asian and European Neolithic period. Cattle, sheep and goats are thought to have been subjected to different slaughtering strategies which were oriented towards the production of milk, meat, fleece, hair or wool (e.g. Helmer and Vigne, 2004). Both sheep and goats were traditionally herded together, although probably for different purposes (Bartosiewicz, 1999). In modern times, sheep and goats are mainly used for milk production in the Mediterranean. However, in northern Europe, sheep are mainly raised for wool production (Boyazoglu and Morand-Fehr, 2001) and cattle (and to a lesser extend goats) are exploited as dairy animals.

Age-at-Death profiles (also called 'Mortality profiles', 'Kill-off profiles', 'age-at-slaughter distribution' or 'culling profiles') are the key source of information used to make inferences about past slaughter practices and animal products produced (Payne, 1973). Target species include cattle, sheep and goats. In Chapters 4, 5 and 6, I will analyse mortality profiles of caprines (sheep and goats) constructed from archaeological remains, which were excavated from European and West Asian archaeological sites.

An age-at-death profile is best characterised by following definition: 'Mortality profiles are histograms of the estimated age frequencies from the archaeozoological remains relative to the width of the age classes used' (Payne, 1973). Most archaeozoologists use the mortality-profile model proposed by Payne (1973), in which the ages are subdivided into 9 classes. This is due to the age estimation system from teeth eruption timings (Ducos, 1968). These mortality profiles from Payne have been modified by Helmer and Vigne (2004) to achieve more detailed information of

mortality profiles, especially when it comes to distinguishing between milk- and meat-oriented slaughtering strategies.

In Chapters 4 and 5, I present the development and application of two methods to infer herd sustainability, product yields and economic efficiencies from caprine age-at-death profiles. Furthermore, I test whether the age-at-death profiles would have reflected sustainable herds over time (Chapter 6).

1.11 Using model-based approaches to study human, animal and crop history

Increasing quantities of genetic and archaeological data have led to numerous studies attempting to explain human and animal past migration trajectories, demography and animal and crop domestication processes (Heun *et al.*, 1997; Edwards *et al.*, 2007). However, the relationship between genetic and archaeological data, and the domestication, demographic or adaptation history that shaped it is noisy, and as a result, it is often challenging to infer histories from data. The reason for this is that (a) in any evolving system that includes stochastic processes, patterns in genetic (or archaeological) data could have been generated under a range of different histories (equifinality); (b) any particular history can potentially give rise to a wide range of different patterns in data [evolutionary variance (Wilson and Balding, 1998)]; and (c) certain demographic or adaptation histories can give rise to counter intuitive patterns in data (emergence) (e.g. Edmonds, Lillie and Cavalli-Sforza, 2004; Allaby, Fuller and Brown, 2008; Excoffier, Foll and Petit, 2009; François *et al.*, 2010).

In recent years, as a result of the issues raised above, there has been increasing interest among archaeologists in explicit, model-based inference approaches. While such approaches are common in population history studies using genetic data, they are by no means universal in this field, and more 'data interpretative' approaches are still common. A model is an explicit and simplified representation of the underlying causative mechanisms in a system and is used to

make predictions about the observed outcomes (data) of that system (Gerbault *et al.*, 2014). In this thesis I consider two classes of models used in historical inference: discriminative models, which fit directly observed data to predicted relationships (e.g., linear regression), and generative models, which are intended to capture the main real-world mechanisms that generate data, and are typically used to produce artificial datasets. Generative models can be used to make inferences from observed data, but in an archaeological context, are more frequently used to reveal some behavioral properties, including counter-intuitive phenomena (Gallagher, Shennan and Thomas, 2019). A particularly popular form of generative modelling for this purpose is agent-based modelling, in which simulated entities called agents are given characteristics that make them capable of autonomous decisions and interaction with each other and their environment. This can be useful for exploring how macro-scale processes can emerge from simpler micro-scale behaviours. However, most model-based approaches for studying the past are concerned with inferring processes from observed data; a model provides a means to exploring how processes relate to data.

For inference, a model should be fitted to observed data, and there are various ways to do this. A challenging aspect of model fitting is how to deal with unknown parameters. In a frequentist framework parameters are treated as fixed, which means that the model specifies imaginary random repetitions of the data generation process (Allaby, Fuller and Brown, 2008; Bramanti *et al.*, 2009; Boyd, Richerson and Henrich, 2011; Kitchen and Allaby, 2012). Using this approach, the researcher might ask 'how frequently does some aspect / descriptive statistic my observed data fall above, or below, or within some range of my simulated data (e.g.: (Rodríguez *et al.*, 2011)?'. While this approach is related to classic frequentist hypothesis testing that is so widely used in science, it has limitations, including not using the full information content of the data and making parameter estimation challenging (but see (Voight *et al.*, 2005; Bollongino *et al.*, 2012).

Given some assumed model of the processes at play, the parameter values that maximize the probability of observing the data (maximum likelihood) provide a useful method to estimate parameters. The main challenge of this approach is the requirement for a likelihood function; a mathematical formula that specifies the probability of the data as a function of parameter values. Unfortunately, and in general, likelihood functions cannot be formulated for anything but the simplest models. However, when they are available, then in theory they can use the full information content of the data in the inference process. Additionally, likelihood values for different models can be compared as a means of model testing.

A full Bayesian approach, like the one described in Chapter 5 of this thesis, also makes use of a likelihood function, but combines it with a prior (prior information about a model's parameters, which helps to focus on plausible regions of parameter space). With the likelihood function and a prior in place, computational techniques such as the Markov Chain Monte Carlo (MCMC) can be used to explore parameter values combinations (parameter space) and produce posterior probabilities of those parameter values. More on Bayesian statistics and MCMC is described in Chapter 5. This Bayesian likelihood-based approach is a powerful inference technique.

The difficulty of computing likelihoods for all but the simplest models has led to the development of a family of techniques known as approximate Bayesian computation (ABC) (Beaumont, Zhang and Balding, 2002; Bertorelle, Benazzo and Mona, 2010). In its simplest form, ABC works by simulating data from a generative model with parameter values chosen at random from their prior distributions. A simulation is accepted if the simulated data resemble the observed data, and rejected otherwise, where the 'resemblance' of datasets is measured using one or more summary statistics. The proposed parameter values that are accepted in this algorithm form a sample from an approximation to the posterior distribution (Gerbault *et al.*, 2014).

1.12 Project Aims and Objectives

The content of this thesis can be subdivided into two broad categories of research question: (a) where was the location of origin of geographic expansion of various animals and crop species (Chapters 2 and 3), and (b) how sustainable and productive was goat/sheep herd management during the Neolithic times (Chapters 4 - 6)? I describe, develop and apply a number of model-based approaches to inferring aspects of animal and crop domestication. I consider genetic data from various crop species, and morphological, genetic and age-at-death data from domestic animals. I use both discriminative and generative modelling approaches. I develop (Chapter 2) a discriminative model-based approach to inferring the location of origin spread of a species or population, and apply it (Chapter 3) to pearl millet (*Pennisetum glaucum)* in Africa, taro (*Colocasia esculenta*) in Africa, broomcorn millet (*Panicum miliaceum*) in China and across Eurasia, the Polynesian rat (*Rattus exulans),* and three endemic mammals from the island of Sulawesi: Anoa (*Bubalus depressicornis*), babirusa (*Babirusa celebensis*), and the Sulawesi warty pig (*Sus celebensis*). I also develop and apply a generative model to predict the sustainability of past caprine herds based on archaeological kill-off profiles (Chapter 4). Finally, I help to develop, parameterize and test and apply (Chapter 5) a full Bayesian method to infer the economic productivity and sustainability of past caprine herds based on archaeological kill-off profiles, and explore how these outputs change through the Neolithic in Europe (Chapter 6). Here, I make use of a generative model-based approach to infer past herd managements from archaeological data (age-at-death profiles). I describe all details of model design and application in the following chapters.

Chapter 2

2 A discriminative model-based approach to inferring the geographic origin of domestic crop and animal species.

2.1 Background

Archaeologists, anthropologists, biologists, and population geneticists are often interested in identifying the location and timing of origins of an expansion of people, other hominin species, wild or domesticated animals, and crops. In this chapter, I describe the development of a discriminative model-based approach to inferring the locations of origins from domesticated crops and animal species.

Searching for the oldest remains of a specific animal or plant species in archaeological excavations, which are usually dated by ^{14}C radiocarbon or material culture context dating, can give insight into the locations of origin of animals or plants e.g. (Huang, 1994; Sweeney and McCouch, 2007). For inferring the location of origin of individuals rather than populations, archaeologists team up with chemists to analyse stable isotopes from skeletal remains in order to trace the origins and migration routes of individuals and animals (Zimmo, Blanco and Nebel, 2012; Bickle and Whittle, 2013).

Various approaches within the field of population genetics have been applied to identify the geographical origins of humans and/or animals and plants. Composite patterns of genetic variation in space have been interpreted as proxies of dispersal routes in humans and other species, for example by performing Principle Components Analysis (PCA) and plotting components explaining large proportions of variation (Cavalli-Sforza, Barrai and Edwards, 1964), or by superimposing phylogenetic trees of modern mitochondrial and Y-chromosome DNA (Jobling, Hurles

and Tyler-Smith, 2013), on maps. Genetic data simulation approaches employing coalescent theory (Nei and Tajima, 1981; Kingman, 1982; Hudson, 1983; Charlesworth and Charlesworth, 2017) in combination with model-fitting approaches such as Approximate Bayesian Computation (ABC) (Beaumont, Zhang and Balding, 2002), have been used to make inferences about more complex scenarios of past human migrations, including inferring the geographic and temporal location of origin of specific variants (Itan *et al.*, 2009), while research on ancient DNA helps to fill in the gaps in genetic history (Slatkin and Racimo, 2016). More recently, computational approaches such as machine learning have been employed to tackle models proposed by population geneticists to explain genetic data structures (Schrider and Kern, 2018).

Other computational approaches, like the method proposed by Silva and colleagues (Silva *et al.*, 2015), calculate the most probable geographical areas for the origins of domesticated rice expansion within the rice-growing domain.

In this chapter I describe the development (in Chapter 3 I describe the applications) of a method for inferring the geographic origin of expansion of a population that is based on the principle that genetic diversity (or morphological diversity) decreases with geographical distance from the location of origin of a population under certain assumptions (Ramachandran *et al.*, 2005; Manica *et al.*, 2007). I add a number of innovations to the approach in order to make it suitable for the analysis of specific plant and animal genetic, and morphometric data, as well as a test for statistical significance for the inference on the geographical origins. I apply this approach to microsatellite and mitochondrial genetic data and morphometric data from various domesticated crop and animal species (Chapter 3).

2.2 Method description

The underlying principle on which the methodologies I describe in this chapter are based on is that of a monotonic decline in population diversity with increasing geographic distance from origin location. When a species spreads from a particular origin location, a negative correlation is expected between the geographic distance from that location and its genetic diversity (Fig. 2.1, 2.2, 2.3). This is because as a population expands in space, genetic variation is sampled (genetic drift) on the wave front of expansion, leading to a loss of diversity (Nei, Maruyama and Chakraborty, 1975; Austerlitz *et al.*, 1997; Klopfstein, Currat and Excoffier, 2005; Ramachandran *et al.*, 2005). While this relationship may not hold under certain conditions (e.g. admixture with in situ populations during the process of spread), it does provide a useful null-model for exploring spatial genetic data. Previous research has examined the spatial distribution of genetic and craniometric data in modern humans in order to identify the origin location where a negative correlation between geographic distance and genetic diversity, or phenotypic variability, is maximized (Manica *et al.*, 2007) (Fig. 2.2 a and b). For this method, it is also assumed that a species has a single as opposed to multiple locations of origins. Some domesticates, such as the domestic pig (*Sus scrofa domesticus* or only *Sus domesticus*) are thought to have undergone multiple events of domestication at different locations (Bosse *et al.*, 2014) and as such this method is not suited for inferring the place of origin of these particular species.

While this broad inference approach has been used before, for example to examine the geographic origin of the expansion of human populations around the world (Ramachandran *et al.*, 2005; Manica *et al.*, 2007), I have developed a number of innovations, allowing application to a selfing species and to where only sparse and geographically unevenly sampled data are available. Selfing species show a high rate of homozygosity and therefore diversity might be challenging to detect from individual samples or those that are in geographic proximity. In addition, I developed an

approach for assessing statistical confidence for inferred regions of origin, via a permutation test.

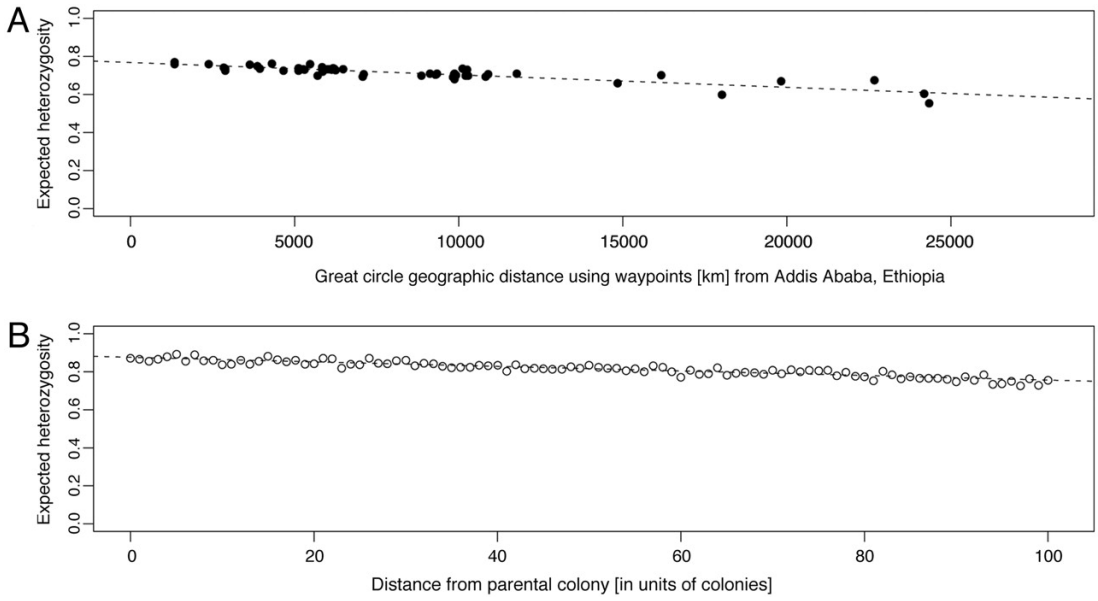

Fig. 2.1 The decay of heterozygosity in human genetic data plotted against geographic distance between populations and a possible origin of expansion in humans. Retrieved from (Ramachandran *et al.*, 2005).

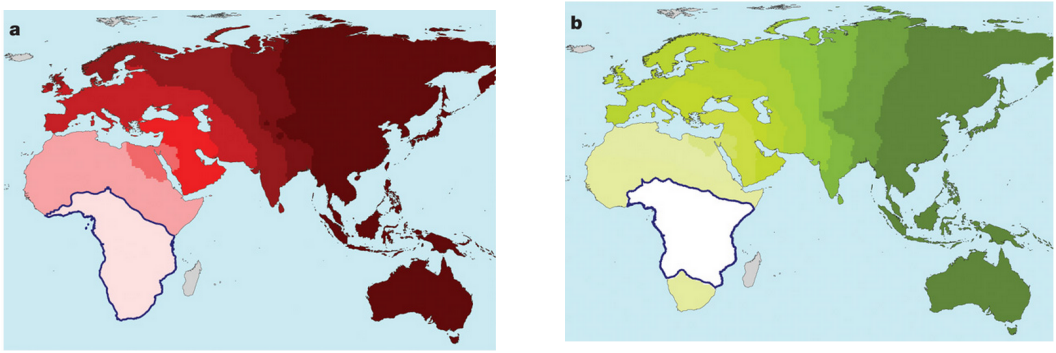

Fig. 2.2 a and b. Maps showing the likely location of a single origin for phenotypic (a) and genetic (b) data. Retrieved from Manica (2007). Lighter colours represent better fits of models of variability as predicted by distance from a location. The area in each panel containing the most likely origin is enclosed by a blue line. Areas of the world not investigated as possible origins (such as Iceland and Madagascar, which would require substantial land bridges to the main continents) are shown in grey.

2.3 Method development

To accommodate the possibility of selfing, which is common in some crops – particularly domestic crops – and the availability of only sparse and unevenly sampled data, I explored a grid of real latitude and longitude values covering the geographic space considered and, using a 500km (or other) radius flat kernel, recorded estimates of the local genetic diversity over regions covered by the kernel that included at least five (or other values) sampled individuals (accepted kernels; Fig. 2.4a). Diversity of genetic data is calculated with various diversity statistics. For microsatellite (also known as short tandem repeat; STR) data I used both Average Square Distance (ASD), which under the STR stepwise mutation model (SSM) is linearly related to divergence time (Goldstein *et al.*, 1995; Slatkin, 1995), and unbiased Heterozygosity (Nei, 1978). For other genetic polymorphism data, I use unbiased Heterozygosity. The size of the kernel radius and the number of samples, which fit into the kernel, are parameterized. I then re-explored the same grid treating each latitude/longitude location as a potential origin location (Fig. 2.4b and c) and calculated the Pearson's correlation coefficient between geographic distance (d) - calculated using the Haversine formula where φ and λ are latitude and longitude values in radians (Robusto, 1957)-

$$a = \sqrt{sin^2\left(\frac{\varphi_2 - \varphi_1}{2}\right) + cos(\varphi_1)\, cos(\varphi_2)\, sin^2\left(\frac{\lambda_2 - \lambda_1}{2}\right)} \quad (1)$$

$$d = 2\, r\, artan\left(\frac{a}{\sqrt{1 - a^2}}\right) \quad (2)$$

to the accepted kernels and local diversity within those kernel locations (Fig. 2.4d). This provided a grid of correlation coefficient values (Fig. 2.4e), which can be interpolated and visualized on a map (Fig. 2.4f). The formula for calculating the Pearson's correlation is:

$$r_{xy} = \frac{\sum_{i=1}^{n}(x_i - \bar{x})(y_i - \bar{y})}{\sqrt{\sum_{i=1}^{n}(x_i - \bar{x})^2 \sum_{i=1}^{n}(y_i - \bar{y})^2}} \quad (3)$$

where x represents values of geographic distance (in km) and y represents the values of genetic diversity.

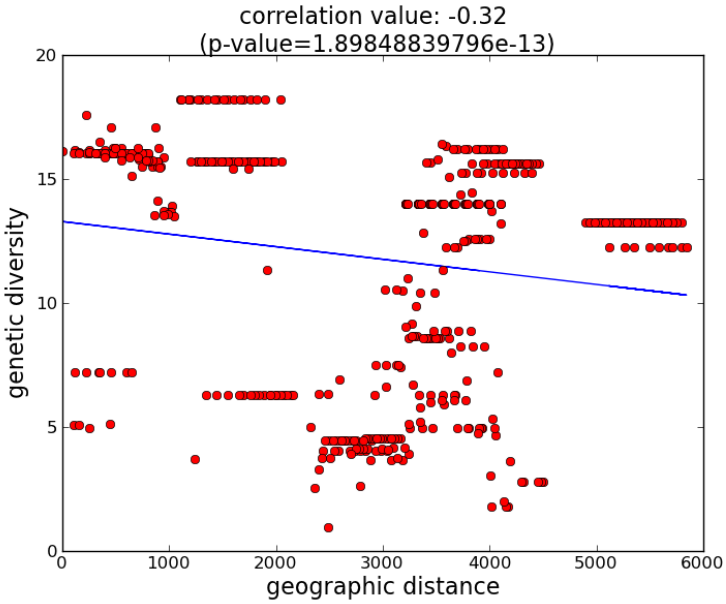

Fig. 2.3 Shows a single example for a correlation value in a grid of correlation values. Genetic diversity from African pearl millet genetic data and geographic distance (in km) are correlated. The blue line represents a polynomial trendline and indicates the correlation gradient.

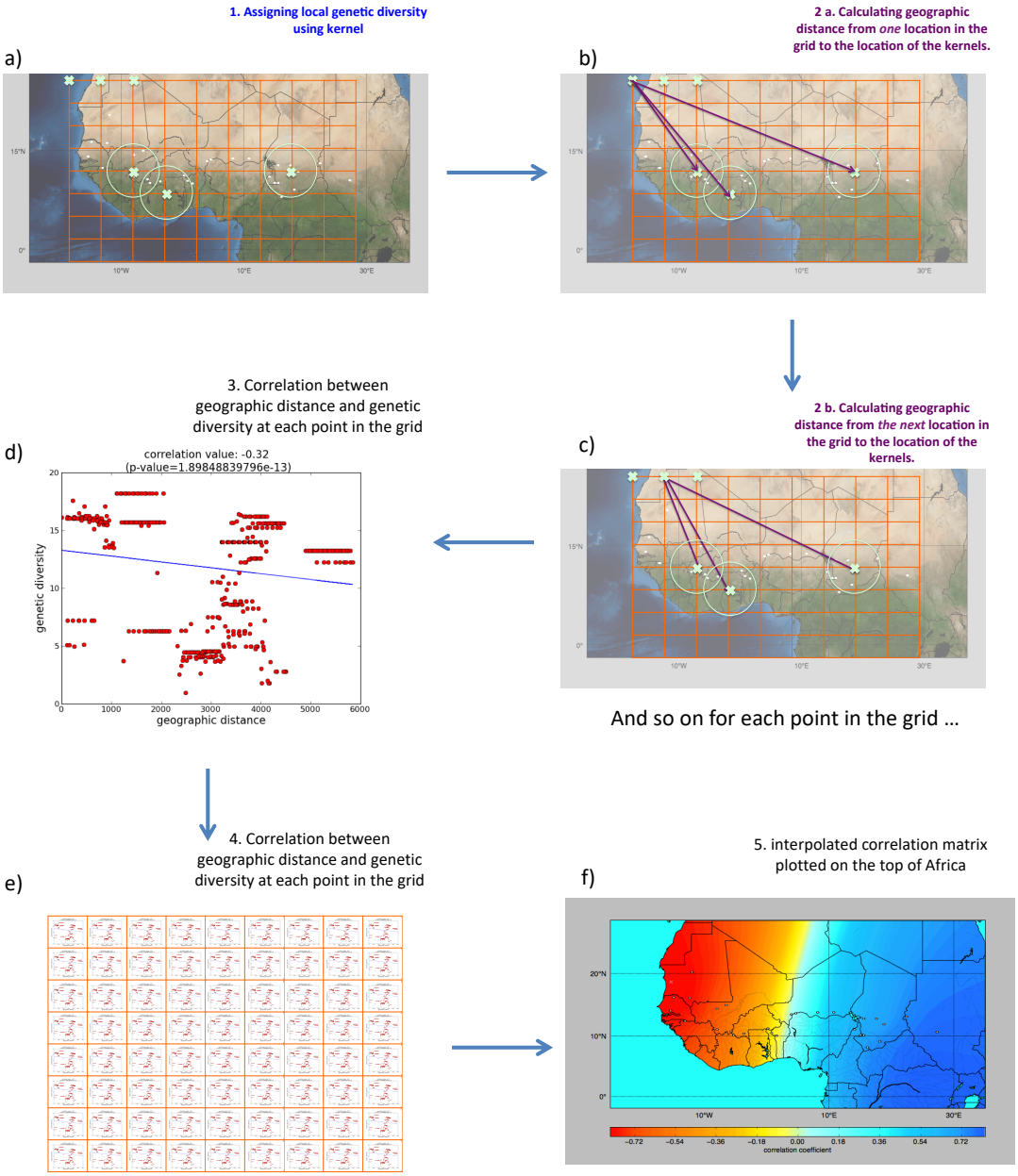

Fig. 2.4 Summary of methodology: a) shows the assessment of local genetic diversity using the kernel (blue circle) and b) and c) show the calculation of geographic distance (purple line) from each point in the grid (orange grid) of real latitude and longitude values to the location of the kernels, using the haversine formula (1) and (2). d) shows the correlation between geographic distances and genetic diversity of samples in the kernels. e) illustrates the idea that a correlation will be generated for each point in the grid. The correlation coefficient matrix is then plotted on a geographic map as an interpolated surface (f).

2.4 Statistical support

To estimate the statistical support for inferred origin locations (i.e. those locations where the negative correlation between geographic distance and genetic diversity is high), I permuted the data among sample sites 1000 times, and for each permuted dataset, I repeat the analysis described above (Fig. 2.4). I then identified grid locations where the negative correlation between geographic distance and genetic diversity was higher than some chosen percentile of those obtained from the permuted data. For each grid location, I also calculate the proportion of permuted correlation values that were more extreme (i.e. more negative) than those obtained from the real data.

2.5 Limitations to the method

There are some limitations to the method described. A decline in genetic diversity in a population sample is not expected to decrease with distance from expansion origin location under a process of admixture with *in-situ* populations, since admixture is expected to increase genetic diversity.

Topographical and other landscape features are not considered in the approach described in this chapter. Instead, geographic distances are calculated using the Haversine formula (formula (1) and (2)), which takes account of the curvature of the earth only. The mode of spread of a species is influenced by such features (deserts, mountains, and bodies of water; the latter can both act as a barrier or facilitate population expansion). In theory it should be possible to take account of topological and other landscape features if their impact on migration were known. For example, such features could be factored into the estimation of geographic distance to produce a composite distance reflecting typical times taken to traverse that region. However, the impact of topological and other landscape features on migration is relatively

unknown, and incorporating such information is beyond the scope of this research (Klopfstein, Currat and Excoffier, 2005).

Analyses presented here were conducted on modern DNA data only; ancient DNA (aDNA) data was not considered. Analysis of aDNA may provide important information on past movements and spreads using different modelling approaches for example, see (Loog *et al.*, 2017).

Multiple centres of domestication have been hypothesized for some domesticated crops, such a pearl millet in Africa (Dussert *et al.*, 2013; Manning and Fuller, 2013), or broomcorn millet in China or eastern Europe (Hunt *et al.*, 2008). The approach presented in this chapter and Chapter 3 is designed for situations where there was a single area of origin of expansion, and it is not clear how the inference methodology would behave if there were multiple domestication or dispersal events. However, for cases where two different locations of origins of dispersal of a population are hypothesised, an additional permutation test can be applied – as performed for the Chinese broomcorn millet study (see Chapter 3) – to assess which of those locations is best supported by the data under the model of a monotonic decline in population diversity with increasing geographic distance from origin location. The principles and application of this additional permutation test are described in Chapter 3.

Chapter 3

3 Application of model-based approach to inferring geographic origins on various genetic and morphometric animal and crop data.

In this chapter I apply the model-based approach to inferring the geographic origin of spread of a population, as described in Chapter 2, to a range of domesticated crop and animal species. These species including pearl millet (*Pennisetum glaucum)* (Fig. 3.1) in Africa, a taro (*Colocasia esculenta*) (Fig. 3.6) in Africa, and broomcorn millet (*Panicum miliaceum*) (Fig. 3.11) in China and across Eurasia, all using genetic data. They also include the Polynesian rat (*Rattus exulans),* using morphometric data (Fig. 3.16), and three endemic mammals from the island of Sulawesi: Anoa (*Bubalus depressicornis*), babirusa (*Babirusa celebensis*), and the Sulawesi warty pig (*Sus celebensis*) (all shown in Fig. 3.22), all using genetic data.

I will first give a more general background on the origins and spread of African, East Asian and Southeast Asian agriculture as the domesticates analysed in this chapter either came or spread from those regions.

3.1 Origins and spread of agriculture in Africa

The Sahel zone and the Sahara have been suggested to be the main region for a beginning of agriculture in Africa (Harlan, 1971; Gautier, 1987; Hanotte *et al.*, 2002; Marshall and Hildebrand, 2002; Prendergast *et al.*, 2019). A second centre is suggested to have been located in present-day Ethiopia and Sudan, where different crops such as Guinea yam (*Dioscorea rotundata*) and finger millet (*Eleusine coracana)* have been cultivated (Vavilov, 1951). Egypt has also been considered to be a centre for African agriculture origins because the region was influenced by

agricultural practises from the Fertile Crescent (Hassan, 1988; Wenke, 1989). For some time, it was even considered that the region surrounding the Nile river in present-day Egypt was the location of origin for Southwest Asian agriculture (Hassan, 1986).

The beginnings and mode of agricultural and herding lifeways in Sub-Saharan Africa, which possibly started during the Late Holocene, more specifically between the third and fourth millennium B.C. (Harlan, 1971; Manning and Fuller, 2013; Ozainne *et al.*, 2014), are substantially different to those inferred for Europe or the Near East. The herding of cattle, for example, preceded the introduction of domesticated crops (Marshall and Hildebrand, 2002; Manning and Fuller, 2013). Cattle were present in North Africa during the end of the Pleistocene and possibly started to become already domesticated by mobile groups; perhaps even independently from the Southwest Asian locus of domestication. The first appearances of goats and sheep in North Africa at around 6,000-5,000 cal BCE, are suggested to be due to their introduction from Southwest Asia (MacDonald, 2000).

Because of ecological and climate changes (e.g. increased aridity), it has been hypothesized that a secondary livelihood was required to augment mobile herding lifeways (Ozainne *et al.*, 2014). The details of the location and mode of the appearance of agriculture in the form of domesticated crops within a well-established food production system consisting of cattle and fishing, remains uncertain. The selection of which type of crop to domesticate differed from the choices made in the Near East and Europe. Before 3,000 cal BCE, parts of what is now the Sahara were wetland (Manning and Fuller, 2013) and the selection of domesticated crops was linked to climate conditions such as summer rain-fall. Cereals, particularly pearl millet, African rice (*Oryza glaberrima*) and sorghum (*Sorghum bicolor*) are known to have been grown in this period. In addition, taro (*Colocasia esculenta;* see below) and yams (*Oxalis tuberosa*) were introduced into Africa, probably from Indonesia. However, the routes and exact timings of their introduction are not very well resolved.

African agriculture spread slowly southwards (Bellwood, 2005); diseases infesting cattle such as the trypanosomiasis, caused by the tsetse fly, or the rinderpest amongst others, being hypothesised to be the main reason for the slow pace of spread. As a result, agriculture – mainly in form of cattle herding – arrived in central Africa only around 1,500 BCE, although hunter-gatherer communities continued to be the main human occupants of the terrain. Following this, an impactful agricultural spread reaching from the rain forest in Cameroon to the southeastern side of sub-Saharan Africa followed the expansion of Bantu language-speaking peoples. This population expansion was relatively rapid, taking less than one thousand years. In parallel, another migratory wave with agricultural components appears to have reached Africa. Indonesian populations have been suggested to have contributed crops such as yams, bananas and taro, via Madagascar, to east Africa around 1,500 years ago (Bellwood, 2005). Evidence of banana phytoliths, at around 500 BCE, suggests much earlier trading routes and cultural influences between Indonesia and Africa. However, the introduction of taro, which is one of the crops analysed in this chapter, might have had other routes of entry in to Africa.

3.2 Origins and spread of agriculture in East Asia

The earliest evidence for agriculture in East Asia is found in present-day China, specifically the region around the Yangzi and Yellow Rivers (Fig. 3.12). The fertile region between the rivers is and was rich in rainfalls and reliable monsoons, and has been proposed to be the location of early rice (*Oryza sativa*) agriculture. On the other hand, the Yellow river region was dryer and better-suited for the development of crops such as broomcorn millet (Zhao, 2011).

Although the location of taro domestication is hypothesised to lie somewhere in the Pacific region, South China, particularly along the Zhujiang River (see Fig. 3.12), shows substantial evidence for tuber cultivation and root plants such as taro, too. The

possibility of the cultivation of tubers in South China forms a potential third subcentre of agriculture in China (Fig. 3.12).

3.3 Spread of human populations into Southeast Asia

I this chapter I infer the location of origin of the spread of the Pacific rat (hypothesised migration routes visualised in Fig. 3.17); a possible marker of human migrations in the region (White, Clark and Bedford, 2000). In the following, I will give a brief overview on the movements of human populations into Melanesia and Polynesia. Furthermore, I focus on the spread of certain endemic species on one island in Melanesia; the island of Sulawesi, as I analyse the population dispersal of three domesticates within the island.

The dispersal of agricultural Austronesian-speaking people probably commenced in southern China and Taiwan, spreading through Southeast Asia and into the Pacific, to as far as Easter Island, in various stages between 5,000 to 1,000 years ago. On route, the Austronesian-speaking people came into contact with, and to a greater or lesser extent mixed with, mostly hunter-gatherer populations who colonised Southeast Asia ca. 35,000 years ago (Bellwood, 2004; Lipson *et al.*, 2014, 2018; Skoglund *et al.*, 2016). Inferring the location of origin of spread of the Pacific rat, which probably occurred in parallel to the migration of Austronesian-speaking populations - or other, earlier or later movements - may give additional insight into the complex human migration history of Southeast Asia.

Crop agriculture and animal husbandry were vital for the people who inhabited many Pacific islands due to limited wild resources available. Among the cultivated crops were typical tropical crops such as rice, yams coconuts and taro, which probably has its origins somewhere in the Pacific (see section on taro 3.5 p.68). As far as for animals, the Austronesian-speaking people took along domestic pigs and dogs (Bellwood, 2004). However, the three endemic animals, the Sulawesi warty pig

and the babirusa belonging to the swine family and the dwarf buffalo, were probably brought to the island of Sulawesi as a result of human-mediated dispersal during the Middle/Late Pleistocene by a migration wave prior to the hunter-gatherer expansion 35,000 years ago. These animals were domesticated much later – probably by agricultural populations (Groves, 1984; Rozzi, 2017). In this chapter, I analyse the location of origin of the population expansion of these three Sulawesian animals, of which the results are combined with geological research to identify associations between geological activities in the region and the peculiar biodiversity of Sulawesi (Frantz *et al.*, 2018).

3.4 Inferring the location of origin of pearl millet (*Pennisetum glaucum*) in the Sahel (North/Central Africa).

Fig. 3.1 Pearl millet grown at present times. Adapted from USDA-ARS, 2005.

3.4.1 Background

Pearl millet probably first appeared in the Sahel and Savannah zone of Africa (Fig. 3.2) around the second half of the 3rd millennium cal BCE. Empirical evidence for domesticated pearl millet cultivation is found between 2,000 – 1,500 cal BCE in Mauritania and Ghana (Bellwood, 2005). Archaeobotanical remains of pearl millet provide some of the earliest evidence for domestication in Africa. Some scholars

hypothesize that pearl millet, amongst other crops, was challenging to cultivate, due to constant cross-pollination with wild species (Zohary, Hopf and Weiss, 2012), which means that earlier cultivation attempts may have remained undetected. A late entry of crop cultivation into sub-Saharan Africa may also be due to a lack of transmission of ideas and skills required for farming due to insufficient human population densities (Powell, Shennan and Thomas, 2009). Others have argued that there may have been a lack of push or pull factors, such as those which led to farming in other regions; low local carrying capacities and population growth – so called 'push factors' – as well as the lack of positive attractions such as uninhabited and arable land – also termed 'pull factors' - may have reduced migrations in to the region and delayed the onset of agriculture (Svizzero, 2015).

Pearl millet may have undergone multiple domestication events, which complicate any inferences for detecting the location of its origin performed with the approach presented here (see paragraph 'Limitations to the method' in Chapter 2). Whether its domestication occurred in a single west Sahelian centre followed by a second expansion in the eastern Sahel (Tostain, 1992) continues to be debated (Dussert *et al.*, 2013). Fuller (2003) and Oumar (2008) have suggested the centre of pearl millet domestication to be in south-eastern Mauritania and/or north-eastern Mali (Fig. 3.2). Other researchers suggest a monophyletic domestication event of pearl millet between the Inner Niger Delta and the Air Mountains (Ozainne *et al.*, 2014) (region 2 in Fig. 3.2). A recent study conducted by Burgarella and colleagues (2018), who used whole-genome sequencing and considered gene flow between wild and domestic species, suggest the Toaudeni Basin as the location for pearl millet domestication – a region close to but somewhat removed from the locations proposed by Fuller (2003) and Oumar (2008). Contrary to the Fuller (2003) and Oumar (2008) hypothesis of a western origin, a single event of domestication in central / east Africa, between Niger and Sudan, was inferred using Approximate Bayesian Computation

(ABC) based on microsatellite and nucleotide sequence data (Dussert *et al.*, 2013; Dussert, Snirc and Robert, 2015); much further east than previously proposed.

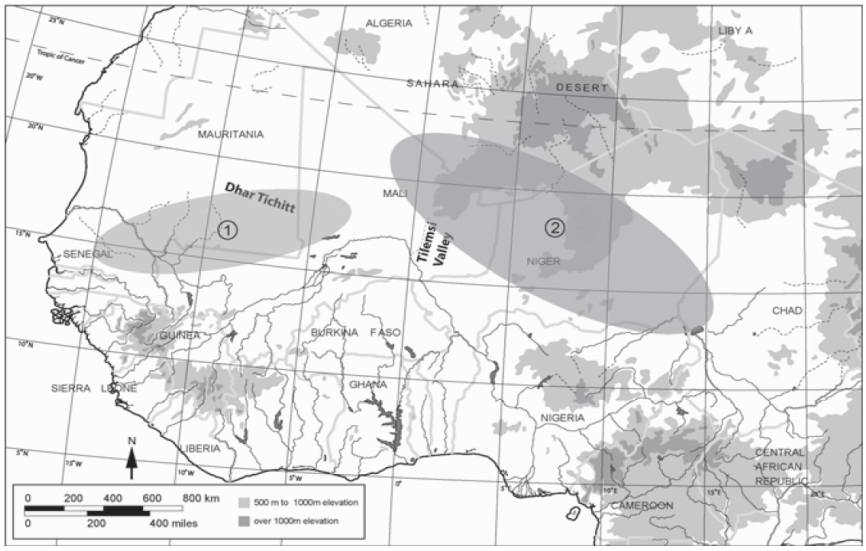

Fig. 3.2 Proposed centres for pearl millet domestication in Africa. Adapted from Manning and Fuller (2013).

The goal of the analysis performed here is to infer the location of origin of spread of domesticated pearl millet in the African Sahel-belt using the approach to inferring the geographic origin of spread of a population described in Chapter 2. However, it should be noted that it is generally believed that the crop underwent a slow domestication process (Fuller, 2003; Manning and Fuller, 2013). Thus the location where the crop was domesticated in Africa for the first time may not be the same as the location of origin of spread, and it is only the latter that the approach described in Chapter 2 is designed to address.

3.4.2 Data and analysis

The dataset comprises repeat counts for 11 short tandem repeats (STRs; also known as microsatellites) from 848 samples of domesticated pearl millet, spread mainly over the African Sahel-belt. Given the number of samples and STRs, it is the richest dataset analysed with the method described in Chapter 2. Since the method I

developed is spatially-explicit, it performs best with a heterogeneous distribution of sample locations and a large sample number. Our collaborator kindly converted microsatellite fragment lengths into repeat numbers, as required for the calculation of the Average Square Distance (ASD) (Goldstein *et al.*, 1995; Slatkin, 1995); the diversity statistic chosen for the pearl millet study.

A spatial grid of latitude and longitude ranges, covering the geographic area of the Sahara and the Sahel zone (from 2° 0' 0" S to 38° 0' 0" N and from 25° 0' 0" W to 37° 0' 0" E), was searched at a resolution of 0.1 degrees by 0.1 degrees. At each point in these searches where five or more genetic samples were present within a radius of 100 km, the mean (across loci) genetic diversity was calculated. The grids were then re-explored with each latitude/longitude location treated as a potential origin location of pearl millet expansion. At each location, I recorded the Pearson's correlation coefficient between geographic distance to the accepted kernels and local diversity at those kernels (Fig. 3.3). I also performed the permutation test (Fig. 3.4 and 3.5).

3.4.3 Results

Fig. 3.3 shows an interpolated surface of a grid of correlation coefficients of pearl millet genetic diversity from microsatellites and the geographic distance for the grid of different hypothesised origin locations. This result indicates a West African site for origin of expansion of domesticated pearl millet.

By applying a cut-off of 0.05 of the observed correlation coefficients obtained from permuted (among sites) data, I inferred the location of origin of expansion of domesticated pearl millet, to range between eastern Mauritania and north-western Mali (Fig.3.4). This result is consistent with the hypothesis and results of Fuller (2003), Oumar (2008) and Burgarella (2018), who proposed a south-eastern Mauritanian and/or north-eastern Malian origin for domesticated pearl millet. With a cut-off of

observed negative correlation values lower than 0.001 of those obtained from permuted (among sites) data, the inferred location of origin for pearl millet narrows to mostly central Mauritania (Fig. 3.5).

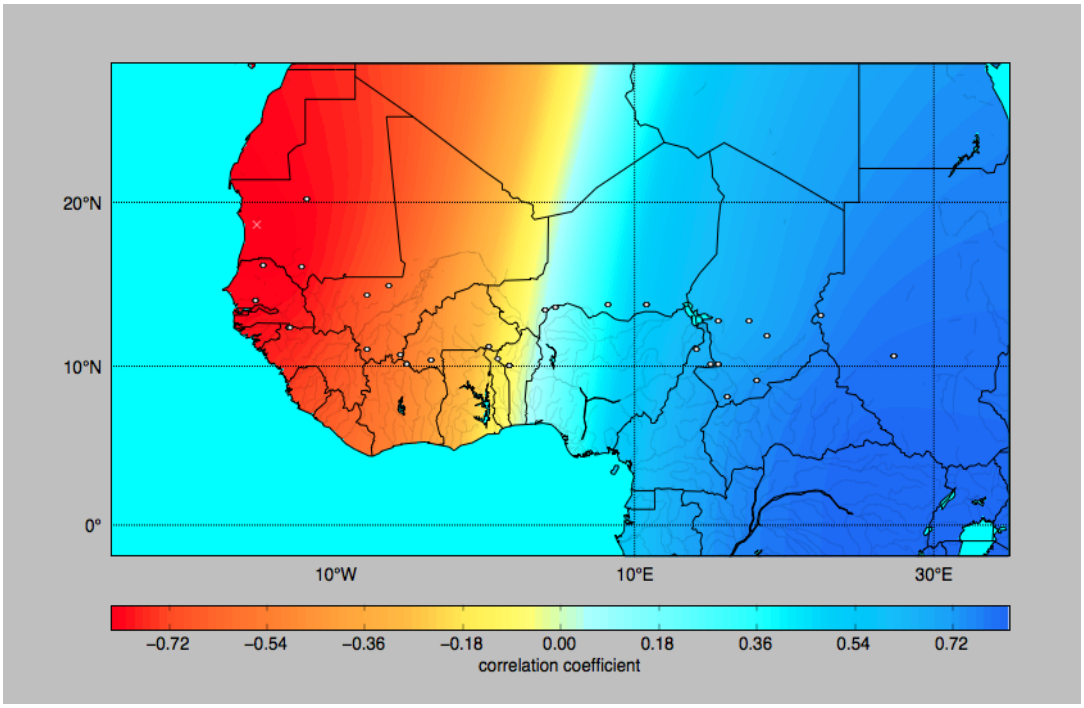

Fig. 3.3 Interpolated surface of a grid of correlation coefficients of genetic diversity of pearl millet microsatellites versus geographic distance. Negative correlation values are coloured in red, gradually turning blue the more positive they become. White dots represent sample location of domesticated pearl millet.

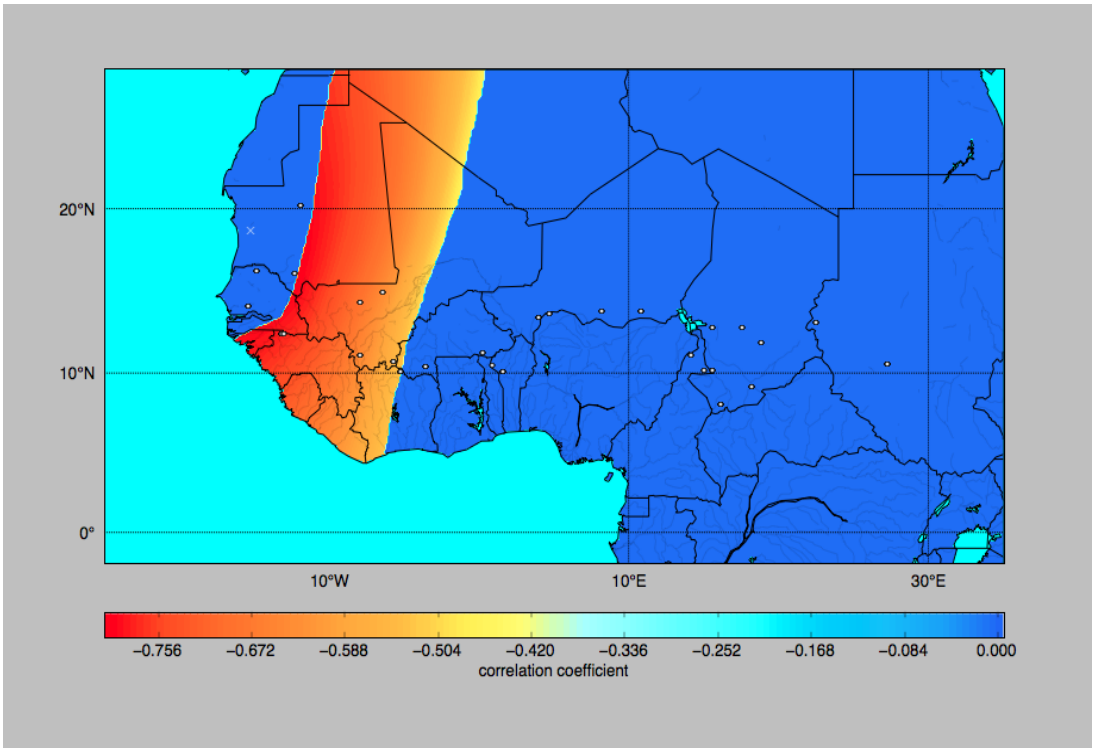

Fig. 3.4 Cut-off of observed correlation values (correlation between genetic diversity of pearl millet microsatellites versus geographic distance) at 0.05 of those obtained from permuted data.

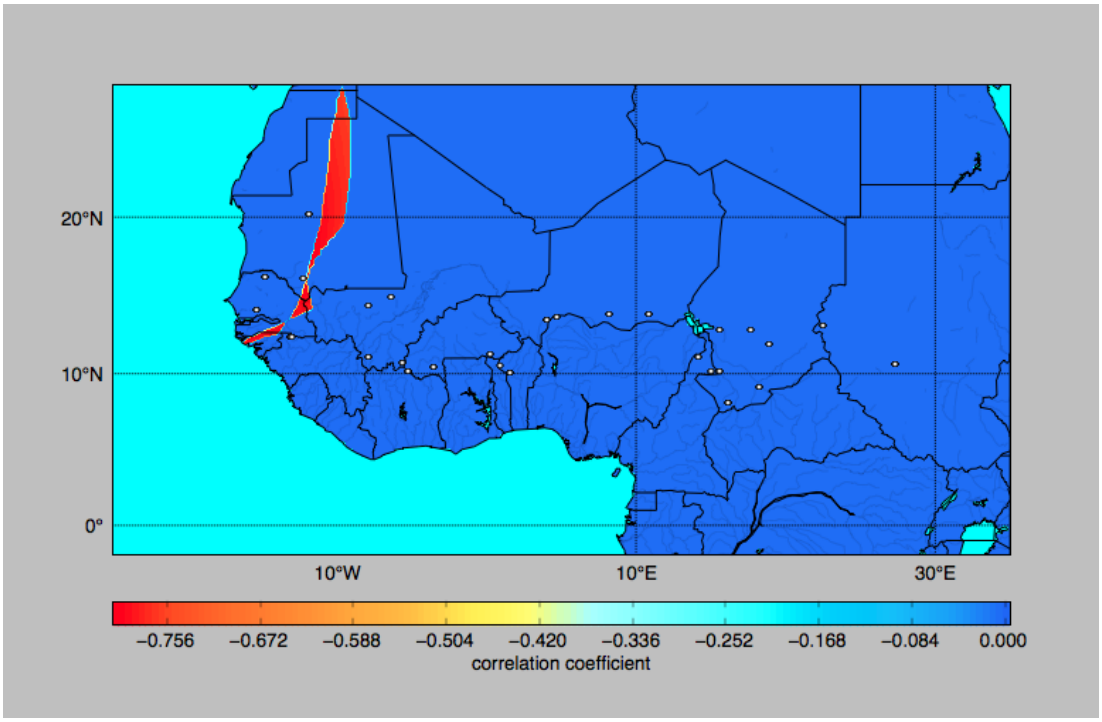

Fig. 3.5 Cut-off of observed correlation values (correlation between genetic diversity of pearl millet microsatellites versus geographic distance) at 0.001 of those obtained from permuted data.

3.4.4 Discussion

A strong signal for a West-African origin of expansion of domesticated pearl millet is presented in Fig. 3.3, 3.4 and 3.5. The pearl millet dataset is large and the sampling is throughout the Sahel region, and this is reflected in the precision of the inferences presented in Fig. 3.4 and Fig. 3.5. In particular, with a very stringent cut-off of correlation coefficients – those more negative than 0.001 of those obtained by data permutation among sites – a region is still returned (Fig. 3.5).

Comparing hypotheses of different regions of origin of expansion would be desirable but at present not possible with the method presented here, since this method allows to differentiate between two hypothesized locations of origins (see section on broomcorn millet), while the number of locations hypothesised for pearl millet exceeds two (see above background on pearl millet).

A scenario of multiple domestication events has been suggested, as reflected in the different flowering patterns of the crop (personal communication with Dr. Yann Dussert). Further work on pearl millet should be aimed at identifying differences between late and early flowering types of pearl millet, and infer their locations of origin or expansion separately.

3.4.5 Collaborators

3.5 Inferring the location of origin of spread of taro (*Colocasia esculenta*) in Africa.

Fig. 3.6 Taro root.

3.5.1 Background

Taro is a tropical root plant rich in starch, native to Asia (De Candolle, 1883; Vavilov, 1951; Burkill, 1966) but now also cultivated widely in Africa as a food crop. It might have already been used as a food crop as early as the late Pleistocene in the Pacific region. There is evidence for taro grain remains from the Salomon Islands (Loy, Spriggs and Wickler, 1992), Papua New Guinea (Denham, Haberle and Lentfer, 2004) and Borneo (Barton *et al.*, 2009). The location and timing of its spread within Africa remains debated (Blench, 2009). However, historically, three main hypotheses about the route by which taro was introduced into Africa exist (Fig. 3.7): taro might have entered a) via the Nile valley, b) via southeast Asia into east Africa/Madagascar (De Candolle, 1883; Murdock, 1959; Beaujard, 2011), as mentioned above, and c) via west Africa (Jones, 1971). The third hypothesis is the most controversial and has been highly criticised by other scholars (Blench, 1996). In the following, I infer the location of entry of domesticated taro into Africa using the approach to inferring the geographic origin of spread of a population described in Chapter 2.

Fig. 3.7 Hypothesised entries of taro into Africa.

3.5.2 Data and analysis

The dataset comprises 570 samples of taro, spread mainly over central Africa with fewer samples in North Africa and Europe. Two microsatellites, Xutem84 and Xutem88, are used for the inference. According to our collaborator the microsatellites do not lie within (or around) regulatory regions, which qualifies them as neutral marker for calculating genetic diversity. Originally, only microsatellite PCR fragment lengths were provided by our collaborators. Knowing the repeat unit of the two microsatellites, it was possible to determine the repeat number via binning the raw microsatellite PCR fragment size distributions and then converting these fragment sizes into repeat numbers.

A spatial grid of latitude and longitude ranges, covering the geographic area of the African and parts of the European continent (from 51° 0' 0" S to 68° 0' 0" N and from 22° 0' 0" W to 85° 0' 0" E), was searched at a resolution of 1 degree by 1 degree. At each point in these searches where five or more genetic samples were present within a radius of 500 km, the mean (across loci) genetic diversity was calculated.

The grids were then re-explored with each latitude/longitude location treated as a potential origin location of taro expansion. At each location, I recorded the Pearson's correlation coefficient between geographic distance to the accepted kernels and local diversity at those kernels. The grid of correlation values was then interpolated and visualized on a map (Fig. 3.8). I also performed the permutation test (Fig. 3.9 and 3.10).

3.5.3 Results

A. The results indicate an origin of African taro expansion in west Africa, since the most negative correlation coefficients are in the central west (red colour in Fig. 3.8).

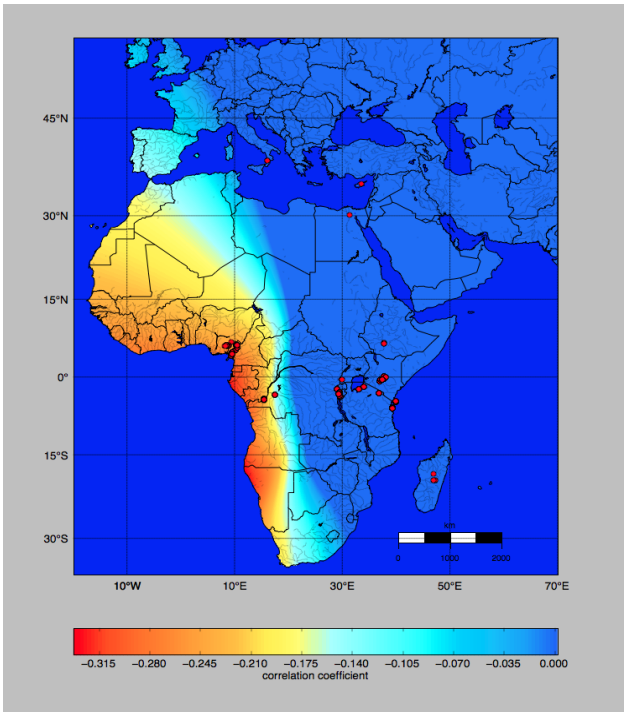

Fig. 3.8 Correlation coefficients of genetic diversity of taro versus geographic distance. Most negative correlation values are coloured in red gradually turning blue when becoming more positive. Red dots represent sample locations.

B. A matrix of empirical p-values, generated from the proportion of permuted correlation values that are more extreme (i.e. more negative) than those obtained

from the real data, for each hypothesised origin location on the grid, was plotted on a geographic map of Africa (Fig. 3.9). It should be noted that even though negative correlations are highest, and empirical p-values are lowest, in the south west, in no location was the negative correlation obtained from the real data more negative than 95% of those obtained from the permuted data. As such, this analysis can only be interpreted as weakly indicative of origin of the spread of taro in west Africa. The lowest p-value recorded was 0.28 (Figure not shown). Fig. 3.10 shows correlation coefficient values, where the negative correlation between geographic distance and genetic diversity is more extreme (i.e. more negative) than 65% of those obtained from the permuted data.

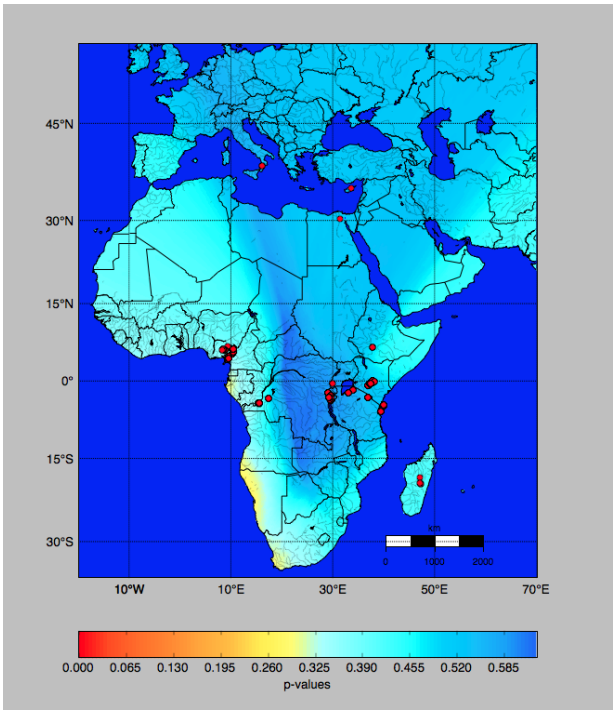

Fig. 3.9 P-values of generated, permuted correlation values (correlation values between genetic diversity of taro versus geographic distance). More significant values are coloured in warmer colours whereas non-significant p-values are coloured in a colder colour. Red dots represent sample sites.

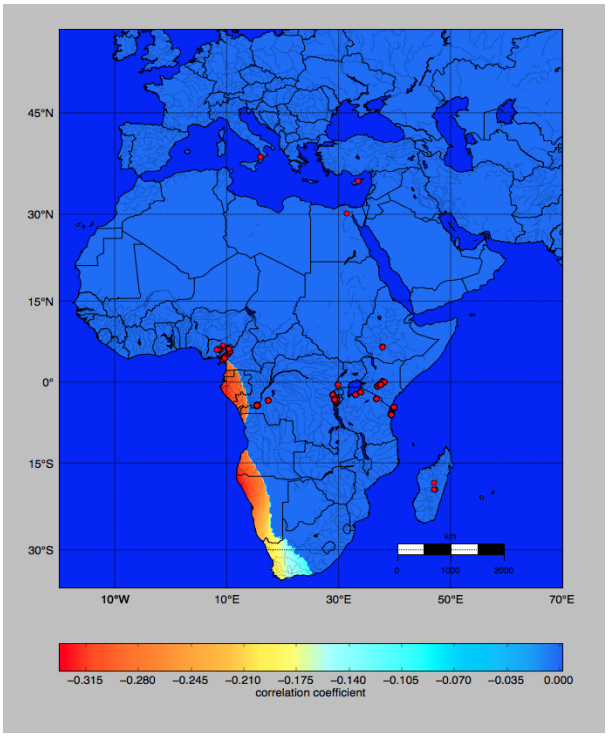

Fig. 3.10 Cut-off of observed correlation values at a p-value of 0.35 from those obtained by permuted correlation coefficients.

3.5.4 Conclusion

In conclusion, the results from the analysis performed are most consistent with hypothesis c); the route of entry via south west Africa. However, in contrast to the results shown for pearl millet, there is insufficient signal in the data to reject other origin locations. This may result from a low number of microsatellites used per sample (two), with a rather heterogenous sampling region over a large area encompassing the entire African continent, or possibly too low geographic structuring of genetic variation for those microsatellites.

3.5.5 Collaborators

[redacted]

[redacted]

[redacted]

[redacted]

[redacted]

[redacted]

[redacted]

[redacted]

[redacted]

[redacted]

[redacted]

[redacted]

3.6 Inferring the location of origin of broomcorn millet (*Panicum miliaceum*) in China.

Fig. 3.11 Present-day broomcorn millet growing. Photo by Santosh Rajput

3.6.1 Background

Panicum milicaeum was among the world's earliest domesticated cereals, of comparable antiquity to wheat and rice (Lu *et al.*, 2009), and one of the first crops

domesticated in north China. At the beginnings of Chinese agriculture, foxtail millet (*Setaria iatlica*), broomcorn millet (*Panicum miliaceum),* rice *(Oryza sativa),* which are native, and common wheat (*Triticum aestivum*), which was introduced, were the dominating crops (Zhimin, 1988; Zhao, 2011).

Broomcorn millet, also referred to as common millet or proso millet, is nowadays grown around the world, mainly in under-developed countries, as a cereal crop. Millet is grown by farmers living in arid areas as it grows at high temperatures and in dry climates, and also has a short growth period. The crop is known to have been grown 8,000 to 10,000 BP (Lu *et al.*, 2009) somewhere along the Yellow River. Due to short life cycles and high water use efficiencies, early Chinese farmers discovered the crop's favourable cultivation conditions (Baltensperger, 2002). Therefore, broomcorn millet could be integrated into mobile agro-pastoral communities, which used wide ranges of ecological zones for its cultivation (Spengler *et al.*, 2014).

The earliest empirical evidence for broomcorn millet archaeological remains, alongside reliable radiocarbon dates, are found in the Cishan archaeological site, which is located in the centre of the Yellow River region, and date to 7,600-8,100 cal BP (Zhao, 2011). Research on millet phytoliths and biomolecular components extend the earliest domestication of broomcorn millet to as far back as 10,300 cal yr BP, followed by foxtail millet after 8,700 cal yr BP (Lu *et al.*, 2009). However, exact timings and location(s) of the beginnings of agriculture of rice and millet in China still remain a matter of debate. Furthermore, studying the archaeology of broomcorn millet, and as such understanding the geographical location of origin for its domestication, may give answers for a wider range of archaeological questions such as the nature, timings and transition of agriculture in China, as well as the contact of early farmers and domestication processes between Eastern and Western Eurasia (Jones *et al.*, 2011).

The archaeobotanical evidence for an almost simultaneous appearance of broomcorn millet at ca. 7,000 cal BP in Eastern Europe and China, has sparked a debate amongst archaeologists. Both a single versus multiple domestication events of broomcorn millet, and a rapid migration and agricultural adaptation processes by Neolithic people of both zones, have been proposed (Jones, 2004; Hunt *et al.*, 2008, 2011; Motuzaite-Matuzeviciute *et al.*, 2013).

By applying the model-based approach presented in Chapter 2 to broomcorn millet, I aim to examine both whether the crop's expansion commenced in East or West Eurasia, and if in East Eurasia, which of the two main hypothesised geographical origin locations within China (Fig. 3.12) best explain patterns of modern genetic diversity.

Fig. 3.12 Three possible centres of agriculture in China.Yellow River (blue), Yangtze River (red) and Zhujiang River (yellow).

3.6.2 Data and analysis

The collated datasets comprise a) 188 genetic data samples spread over China (green dots Fig. 3.13) and b) 333 samples from pan-Eurasia (including the Chinese samples) (green dots Fig. 3.14). Both datasets are available in the Supplementary Information within the publication of Hunt and colleagues (Hunt *et al.*, 2018) as the results of this work have already been published. Both datasets comprise data for 16

microsatellite loci. Analysis was performed on the two datasets using unbiased heterozygosity as the summary statistic representing genetic diversity (Nei, 1978).

A spatial grid of latitude and longitude ranges covering the geographic space between Europe and Japan (7°W to 153°E, 9°N to 67°N) for the pan-Eurasian microsatellite dataset, and ranges covering China (95°E to 135°E, 30°N to 50°N) for the Chinese dataset, were searched at resolutions of 0.1 by 0.1 and 0.01 by 0.01 degrees, respectively. At each point in these searches where five or more genetic samples were present within a radius of 500 km (accepted kernels), the mean (across loci) genetic diversity was calculated. The reason this approach was taken, as discussed in chapter 2, is that broomcorn millet is a largely selfing species. Selfing leads to high levels of observed homozygosity, and so the extent of selfing would skew estimates of diversity if based on individual plants. However, by estimating expected heterozygosity across multiple plants, the effects of selfing should be ameliorated. The grids were then re-explored with each latitude/longitude location treated as a potential origin location of broomcorn millet expansion. At each location, I recorded the Pearson's correlation coefficient between geographic distance to the accepted kernels and local diversity at those kernels. The grid of correlation values was then interpolated and visualized on a map (Fig. 3.13 and Fig. 3.14). Since genetic diversity is expected to decrease with geographic distance from the origin of an expansion, regions yielding more negative correlation values represent more plausible locations for the source of spread of broomcorn millet.

3.6.2.1 Testing two hypothesised locations for the origin of broomcorn millet domestication

For each of the two datasets (pan-Eurasian and China-specific), I compared two hypothesised locations of origin, each based on archaeobotanical evidence for early broomcorn millet. For the pan-Eurasian dataset, I compared a Ukrainian site

(Sokol'tsy) against Xinglonggou in China, and for the Chinese dataset, I tested Dadiwan in the Gansu province against Xinglonggou (white stars in Fig. 3.13 and Fig. 3.14). To quantify support for one location to be the origin of population expansion over the other, I first calculated the difference in correlation values for the two hypothesised origin sites considered. To test if these differences were greater than expected by chance, I permuted (randomly distributed) the site data among sample sites 1000 times, and for each of these 1000 permuted datasets, I repeated the above analysis and recorded the difference in correlation values for the two hypothesised origin locations. This gives an expected distribution of difference in correlation values between each pair of sites under the null hypothesis of no geographic structure in the genetic data. Finally, I compared the differences in correlation values for the observed data with those generated from permuted data to calculate two-tailed p-values (Fig. 3.15a and Fig. 3.15b).

3.6.3 Results

The multidisciplinary study has already been published (Hunt *et al.*, 2018) and the analyses and results described in the following contributed to that publication. Using the spatially explicit discriminative modelling approach, the most negative correlation values between distance from hypothesised location of origin and genetic diversity for the China-only dataset are in north-western China, approximately in the south-eastern part of Gansu province; negative correlation coefficients are shown in red and positive coefficients in blue (Fig. 3.13). The sites of Dadiwan and Xinglonggou – two hypothesised source locations for the expansion of broomcorn millet within China based on archaeobotanical evidence – are marked '1' and '2', respectively, on Fig. 3.13; correlations are more negative for Dadiwan. To test if the difference in correlation values between Dadiwan and Xinglonggou is more extreme than that expected under the null hypothesis of no geographic structure in the genetic data, I performed the permutation procedure described above. This returned a two-tailed p-

value of 0.192 (see Fig. 3.15b) suggesting that the data are insufficient to discriminate between these hypothesised source locations using this approach.

For the pan-Eurasian dataset, the most negative correlation values between distance from hypothesised origin location and genetic diversity were for northeast Eurasia, and the most positive were for western Eurasia (see Fig. 3.14). Thus, under the model of a monotonic decline in genetic diversity with distance from origin location, my analyses do not support a western Eurasian origin for the expansion of broomcorn millet, but do permit the possibility of an eastern Eurasian origin. Two hypothesised source locations for the domestication of broomcorn millet in Eurasia– the sites of Sokol'tsy and Xinglonggou – are indicated with marked '1' and '2', respectively. Again, I tested if the difference in correlations between these two sites is more extreme than that expected under the null hypothesis of no geographic structure in the genetic data (Fig. 3.15a). I obtained a two-tailed p-value of 0.047, indicating the data favour an eastern Eurasian origin for the expansion of broomcorn millet under the assumption of a monotonic decline in genetic diversity with distance from origin location and that the difference in these values for these two sites is significant.

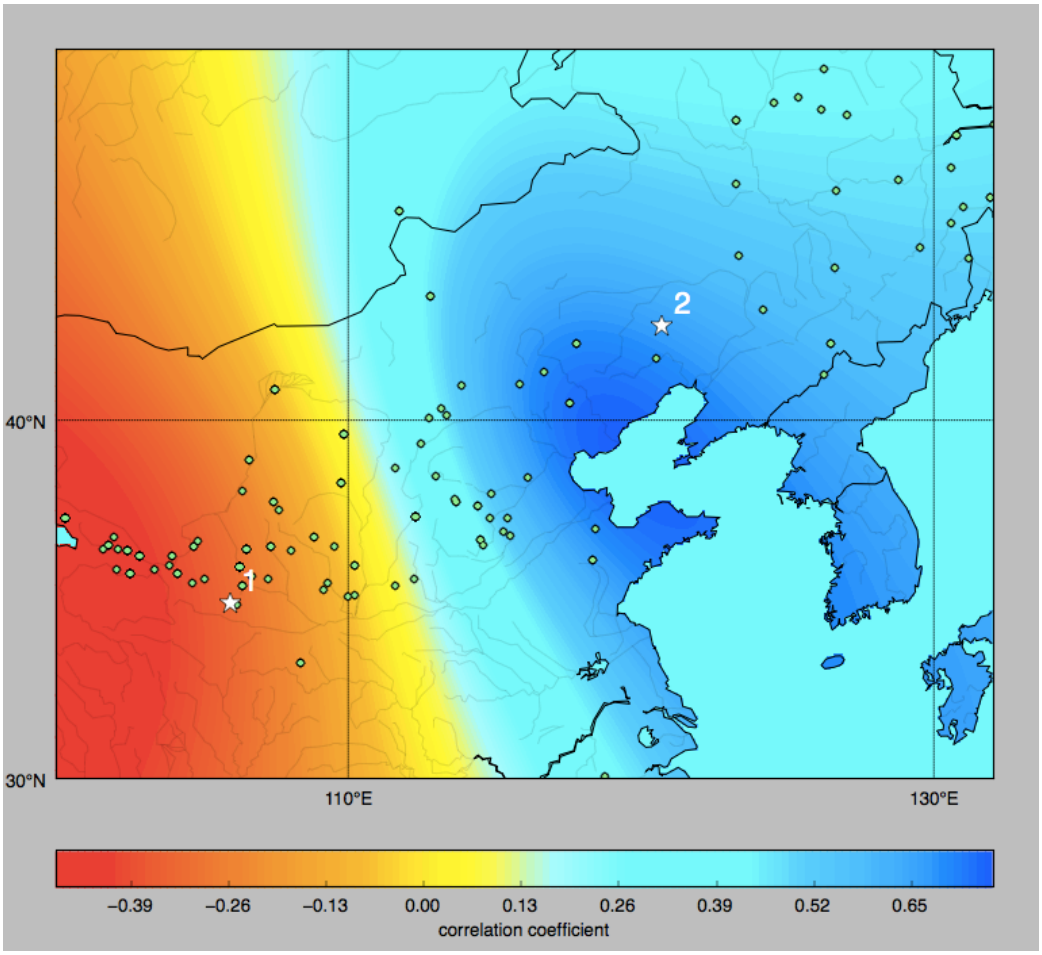

Fig. 3.13 Interpolated surface of correlation coefficient values between genetic diversity (unbiased heterozygosity of Chinese broomcorn millet microsatellite data recorded in kernels) and geographic distance. Red colour shows negative correlation values, gradually turning blue the more positive the correlation values become. Since genetic diversity is expected to decrease with geographic distance from the origin of an expansion, regions yielding more negative correlation values represent more plausible locations for the source of spread of broomcorn millet. Green dots show the sample locations. White stars indicate the locations of Dadiwan (1) and Xinglonggou (2).

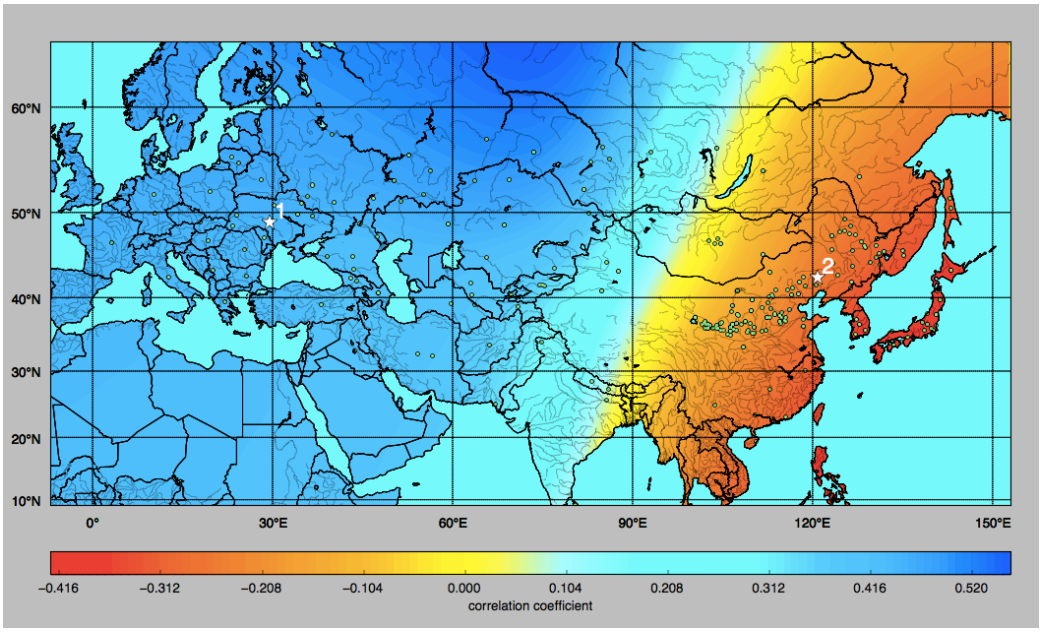

Fig. 3.14 Interpolated surface of correlation coefficient values between genetic diversity (unbiased heterozygosity of panEurasian broomcorn millet microsatellite data recorded in kernels) and geographic distance. Red colour shows negative correlation values, gradually turning blue the more positive the correlation values become. Since genetic diversity is expected to decrease with geographic distance from the origin of an expansion, regions yielding more negative correlation values represent more plausible locations for the source of spread of broomcorn millet. Green dots show the sample locations. White stars indicate the locations of Sokol'tsy (1) and Xinglonggou (2).

3.6.4 Results from permutation test

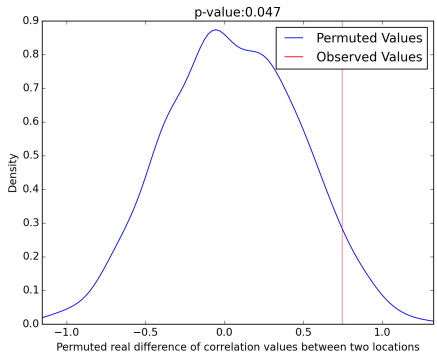

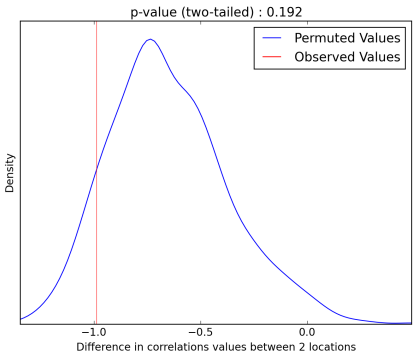

3.15a Fig. 3.15b

Fig. 3.15a Comparison of the observed difference in Pearson's correlation coefficients (red line) between Sokol'tsy ('1' in Fig. 3.14) and Xinglonggou ('2' in Fig. 3.14) generated with the panEurasian dataset, to the distribution of those generated by permuting (randomly distributing) the site data among sample sites 1000 times (blue line). The p-values represent the probability of obtaining the observed difference in correlation values under the null hypothesis of no geographic structure in the genetic data. This can be interpreted as a measure of how well the data favour one site over the other as a location for the source of spread of broomcorn millet, given the assumption that genetic diversity decreases with geographic distance from the origin of expansion. Fig. 3.15b Comparison of the observed difference in Pearson's correlation coefficients (red line) between Dadiwan ('1' in Fig. 3.13) and Xinglonggou ('2' in Fig. 3.13) generated with Chinese dataset, to the distribution of those generated by permuting (randomly distributing) the site data among sample sites 1000 times (blue line). The *p*-values represent the probability of obtaining the observed difference in correlation values under the null hypothesis of no geographic structure in the genetic data. This can be interpreted as a measure of how well the data favour one site over the other as a location for the source of spread of broomcorn millet, given the assumption that genetic diversity decreases with geographic distance from the origin of expansion.

3.6.5 Discussion

This work is embedded in an already published study presenting an archaeological and genetic research on the origins of domestication and expansion of broomcorn millet in China and Pan Eurasia (Hunt *et al.*, 2018).

The question of whether cultivated broomcorn millet populations originated in China and/or central-eastern Europe (Jones, 2004), has stimulated much novel work in archaeobotany, genetics and stable isotope analysis across Eurasia. In a previous

survey of microsatellite diversity in Eurasian *P. miliaceum* (Hunt *et al.*, 2011), it was suggested that the observed pattern of variation is somewhat more consistent with a Chinese origin and centre of dispersal. Speculation about European, Caucasus or Central Asian origins of broomcorn millet arose from multiple sites in central and eastern Europe, and the Caucasus, dating to 5,000 BC and older – a similar time period to those archaeological sites located in China (Hunt *et al.*, 2008). In contrast, direct dating of macrofossils from central and eastern Europe showed that their previous early Neolithic assignments were incorrect, and they were dated much later – to around 1,500 BC (Motuzaite-Matuzeviciute *et al.*, 2013). In the Caucasus, excavations and re-evaluation of earlier reports have resulted in a similarly revised chronology for broomcorn millet, with the earliest evidence of the crop at 1,200-1,000 BC (Trifonov *et al.*, 2017). Archaeobotanical analysis in Central Asia has recovered *P. miliaceum* from sites dating from ~2,200 BC (Spengler *et al.*, 2014). In consistence with archaeobotanical evidence, studies on human and animal prehistoric diets (Lightfoot, Liu and Jones, 2013), indicate that broomcorn millet was used as a food between the 2nd and 1st millenium BC in Europe, and as such, provides additional evidence for a later entry of broomcorn millet into Europe, when compared with the timing at which broomcorn millet first appeared in China. All those studies indicate a later appearance of broomcorn millet in central and west Asia than in east Asia.

With the model-based approach described in Chapter 2, it was possible to formally test previous assumptions of a Chinese versus west Asian/eastern European location of origin for broomcorn millet expansion. The results presented here indicate an east Asian origin of expansion of broomcorn millet when analysing the pan Eurasian dataset (Fig. 3.14), and a central west Chinese expansion of the crop when analysing the China-only dataset (Fig. 3.13). Results on the pan Eurasian dataset resonate with other proxies, which have also shifted the focus of early *P. miliaceum* exploitation to the East, through both positive evidence at early dates in China (Ren *et al.*, 2016) and comparative negative evidence further west (Lightfoot, Liu and

Jones, 2013; Motuzaite-Matuzeviciute *et al.*, 2013). Furthermore, the results are supported by more studies (Hunt *et al.*, 2011), which indicate a Chinese/East Asian origin for the dispersal of broomcorn millet and not a European centre of origin of the crop's dispersal, as also hypothesised by the collaborators in this study (Jones, 2004; Hunt *et al.*, 2008).

Although the results on testing two hypothetical locations of origin for broomcorn millet expansion within China (Ren *et al.*, 2016) are not statistically significant (Fig. 3.15b), they are nonetheless indicative, and consistent with research from Madsen and Elston (2007), who suggested early cultivation of wild millet in the region of the Loess Plateau (surrounding the region of the site Dadiwan, '1' Fig. 3.13). They assumed that the distribution of wild millet was centred in the Yellow river valley - a hypothesis which resonates with the Yellow river narrative for the origins of millet agriculture by Liu (2009) and Zhao (2011) (Fig. 3.12).

3.6.6 Collaborators

[redacted]

[redacted]

3.7 Inferring the location of origin of spread of the Polynesian rat (*Rattus exulans*) in the Pacific.

Fig. 3.16 *Rattus exulans.*

3.7.1 Background

The Pacific rat (*Rattus exulans*) most likely dispersed as a human commensal, in parallel to human movements, and as such constitutes a useful model organism to track human migrations. The location of origin of dispersal of the Pacific rat remains unknown (Roberts, 1991; Thomson *et al.*, 2014). Unlike other species that have been analysed in this chapter, *R. exulans* is not a domesticated species. Speciation was suggested to have taken place in the Philippine-Borneo-Java region followed by an eastwards expansion into the Pacific (Roberts, 1991). Recent studies have investigated the location of origin by conducting analysis on the diversity of the animal's mitochondrial DNA (mtDNA) and allozyme electrophoresis data (Thomson *et al.*, 2014). The island of Flores showed the highest diversity for these data, and as such was inferred to be the homeland of *R. exulans* (Thomson *et al.*, 2014). Here, I compare inferences on the centre of expansion from previous research with results from the model-based approach described in Chapter 2, as applied to morphometric data.

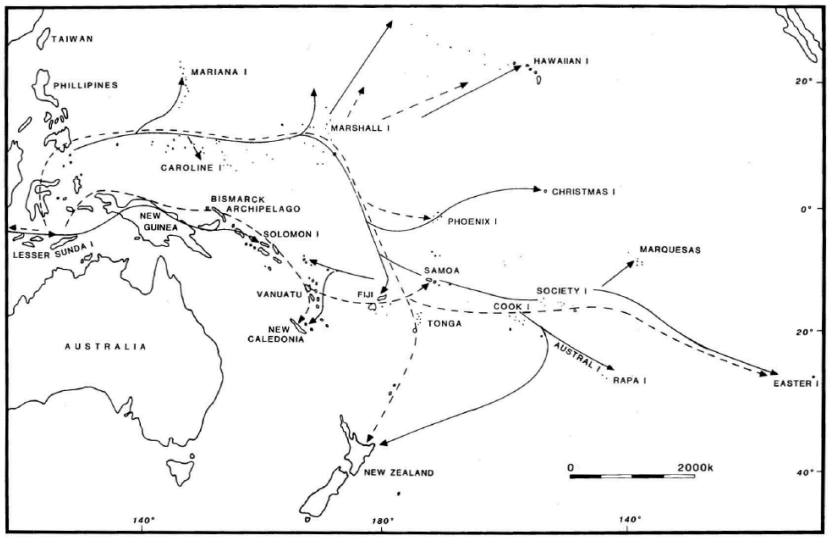

Fig. 3.17 Hypothesized insular Pacific dispersal routes (Roberts, 1991) of *Rattus exulans*.

3.7.2 Data and analysis

Analyses were performed using morphometric data, as opposed to the genetic data used in other analyses presented in this chapter. The diversity statistic used with this morphometric data is the 'mean of Procrustes distance', which was provided by Dr. Ardern Hulme-Beaman. Procrustes distances (PA) are a measure of shape difference. They are used to quantify the similarity or dissimilarity of 2- or 3-dimensional shapes (Al-Aifari, Daubechies and Lipman, 2013), which are usually presented as landmark coordinates. They are calculated strictly pairwise because removing non-shape variation (Procrustes superimposition) is performed on the landmarks of the paired shapes of the objects or individuals. The pairwise transformation means that these distances are invariant of the specimens in the total dataset — these distances are solely based on the minimum rotation between two sets of landmarks. The mean of pairwise comparisons among individuals provides a useful metric of diversity within population samples. In this study, Procrustes distances were calculated from geometric morphometric coordinates of dental morphology of *R. exulans* specimen.

A spatial grid of latitude and longitude ranges, covering the geographic area of Southeast Asia (from 22° 0' 0" S to 23° 0' 0" N and from 95° 0' 0" E to 177° 0' 0" E), was searched at a resolution of 0.1 degrees by 0.1 degrees. The grids were then re-explored with each latitude/longitude location treated as a potential origin location of *R. exulans* expansion. At each location, I recorded the Pearson's correlation coefficient between geographic and mean of Procrustes distances. The grid of correlation values was then interpolated and visualized on a map (Fig. 3.18). I also performed the permutation tests, as described in Chapter 2 (Fig. 3.19, 3.20 and 3.21).

3.7.3 Results

The region inferred as the location of origin of dispersal for the Polynesian rat ranges between the islands and Sumatra and Java, as seen in Fig. 3.18, where negative correlation values are coloured in red. After the permutation test, the inferred region of expansion origin includes the countries of Thailand, Vietnam, Cambodia, Laos to the island of Borneo. Fig. 3.19 shows a cut-off of observed correlation values more negative than 95% of those obtained by permutation among sites. With that cut-off value placed at 0.99 of those obtained by permutation of the data among sites, the inferred location of origin for *R. exulans* covers a region including the countries of Thailand, Cambodia, Laos, west Borneo and east Java (Fig. 3.20). With a cut-off of observed correlation values placed at 0.999 of those obtained by permutation of the data among sites, the inferred location of origin for *R. exulans* covers a region of the western tip of Borneo and eastern tip of Java (Fig. 3.21).

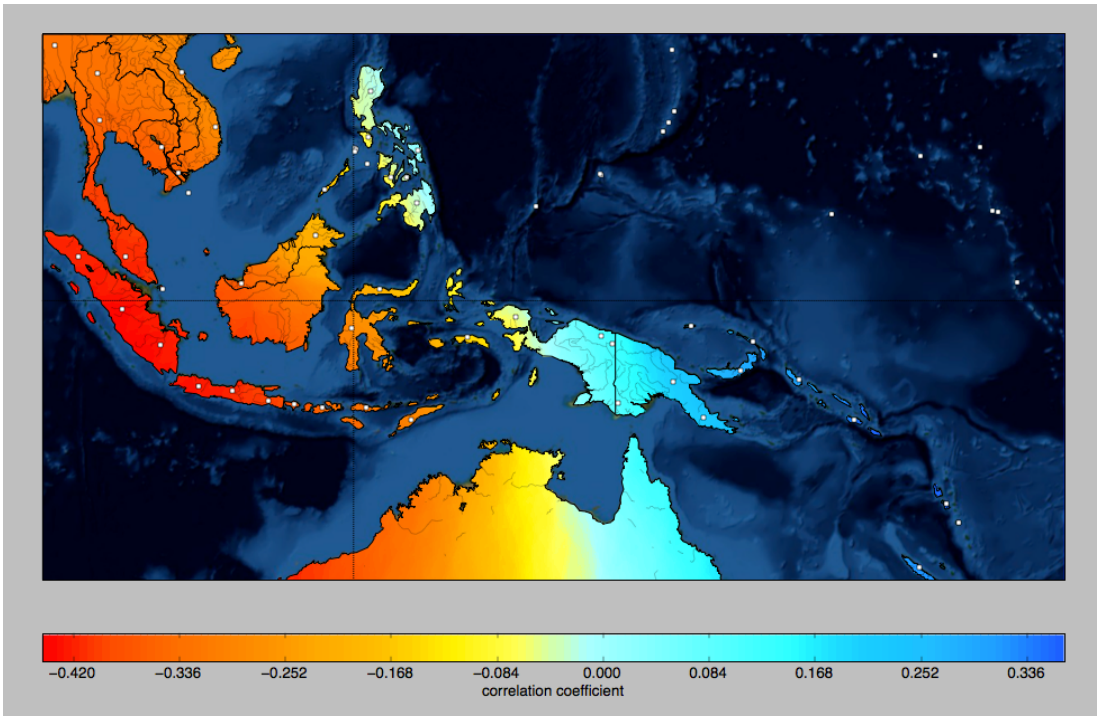

Fig. 3.18 Correlation coefficient of morphometric diversity of the Polynesian rat versus geographic distance. Most negative correlation values are coloured in red. White dots show population locations.

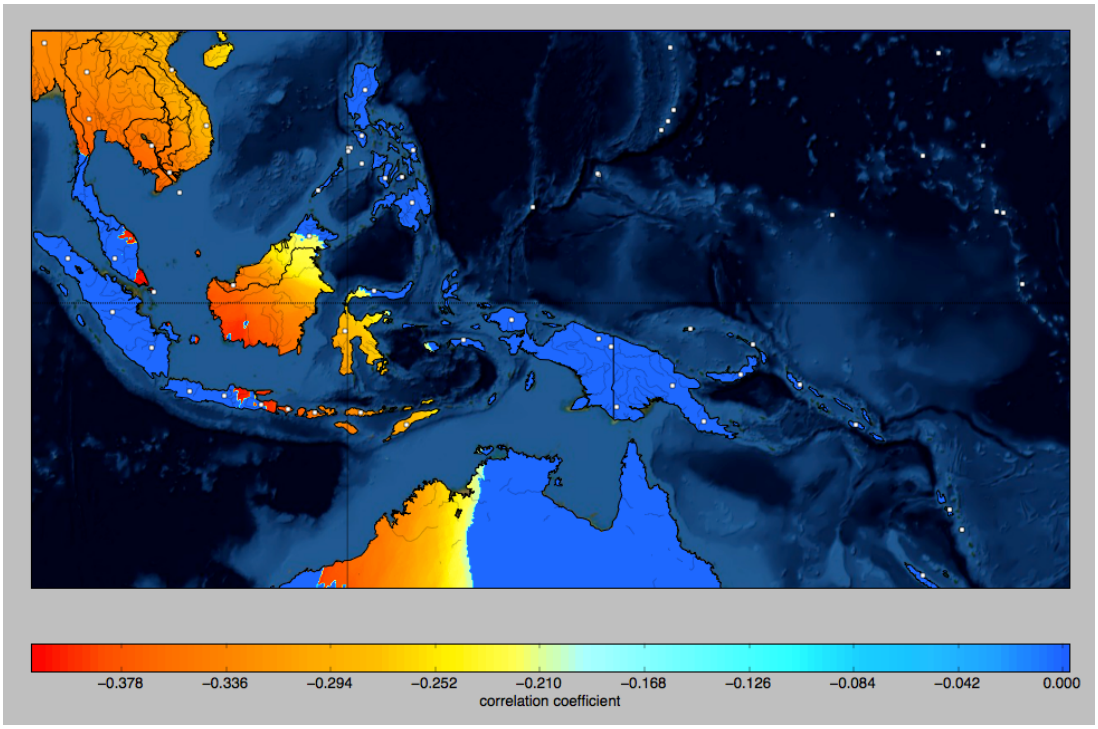

Fig. 3.19 Cut-off of observed correlation values at a p-value of 0.05 from those obtained by permuted correlation coefficients.

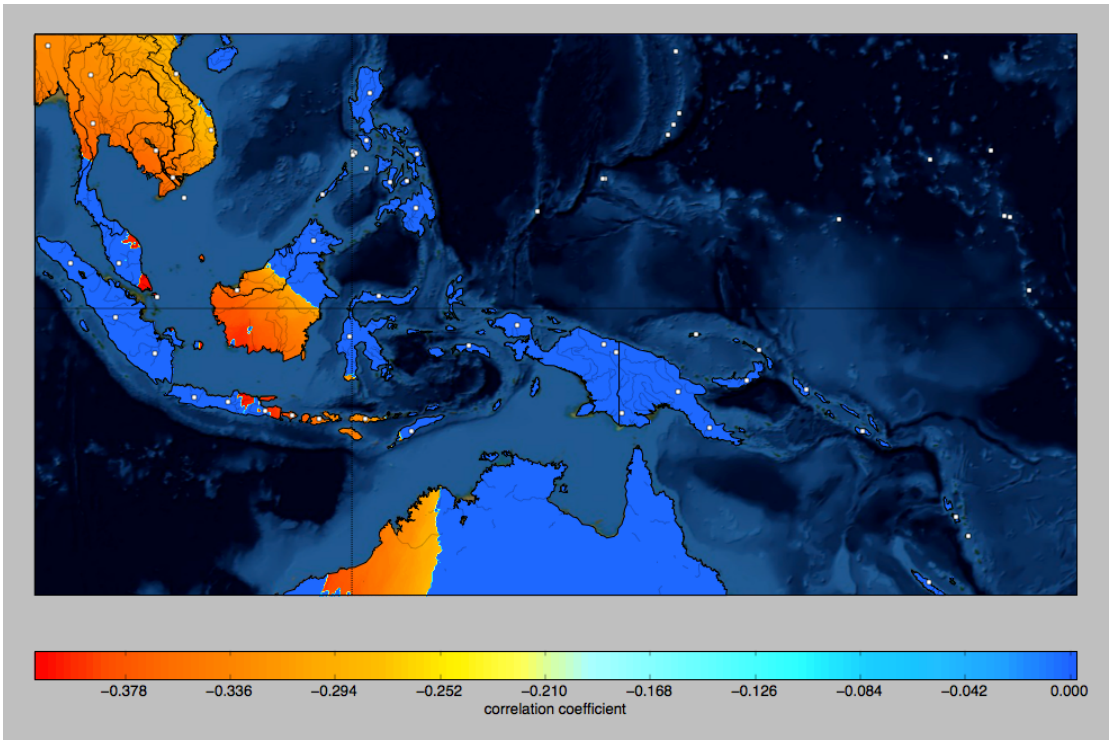

Fig. 3.20 Cut-off of observed correlation values at a p-value of 0.01 from those obtained by permuted correlation coefficients.

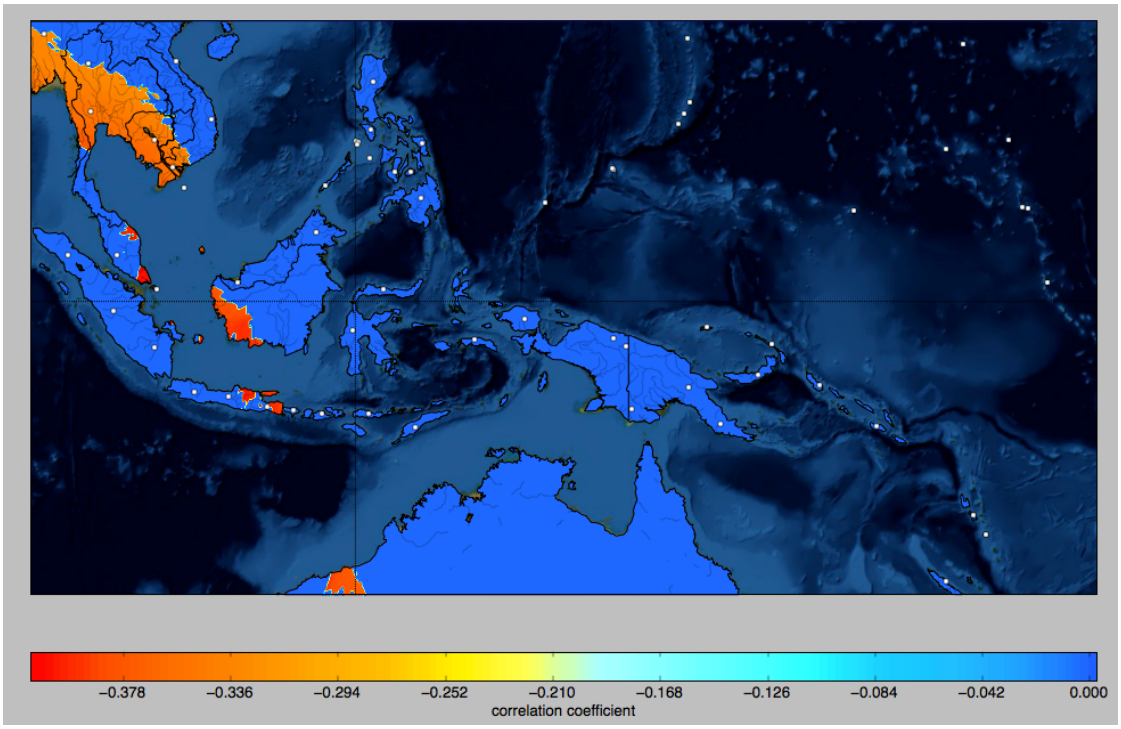

Fig. 3.21 Cut-off of observed correlation values at a p-value of 0.001 from those obtained by permuted correlation coefficients.

3.7.4 Conclusion

Previous analyses were only able to narrow down the inferred location of origin of expansion of the Polynesian rat to a relatively wide region, covering the Philippines, Borneo and the Java (Roberts, 1991). The most recent analyses, based on genetic data, inferred the location of origin of *R. exulans* to lie on the island of Flores (Thomson *et al.*, 2014). My results (shown in Fig. 3.19 and 3.20) are broadly consistent with these results, although favouring an origin somewhat to the west of Flores. It is interesting to note that regions were found where correlation values were more negative than 0.999 of those obtained by permutation of the data among sites, indicating very strong spatial structuring of morphological diversity in the data.

3.7.5 Collaborators

[redacted]

3.8 Inferring the location of origin of dispersal of three endemic species from the island of Sulawesi.

Fig. 3.22 Anoa - also called dwarf buffalo (left), babirusa (middle) and the Sulawesi warty pig (right)

3.8.1 Background

The island of Sulawesi is thought to have been primarily formed by an uplift process around 15 million years ago and in combination with subsequent uplifts and sea level changes the island gained its structure today (Fig. 3.23). The hypothesis of a recent increase in land area (Van den Bergh, de Vos and Sondaar, 2001) can be tested by comparing the population histories of multiple species on the island. Analyses of genetic and morphometric variability can be used to infer the timing and trajectories of dispersal, and the geographical and temporal origins of expansion. For example, if land area had increased, from a single smaller island, extant species now living on Sulawesi would all have expanded from the same area. In addition, under this assumption, within the same geographical region their respective diversifications would be expected to have been roughly simultaneous.

The work described in this section formed part of a multidisciplinary collaborative study which has already been published (Frantz *et al.*, 2018) and the analyses and results described in the following contributed to the research. By inferring the geographical origins of the population expansions of three endemic mammal species and considering these inferred origin locations with inferences on colonisation timings derived from genetic and morphometric data, and with information on recent geological uplifts (Fig. 3.23), the study identified associations between the geology and biodiversity on the island. Here, I contribute to the study by inferring the locations of origin of expansion within the island of Sulawesi. The three species analysed are Anoa (*Bubalus depressicornis*) – commonly referred as the miniature buffalo, babirusa (*Babyrousa* spp.) also named deer-pig, and the Sulawesi warty pig (*Sus celebensis*); all show in Fig. 3.13., which are characterised by their unique anatomic features found nowhere else in the world. As the common name already implies, Anoa can only grow up to ca. 1 m tall, usually inhabits rainforests and is related to indigenous bovids from East Asia. The babirusa belongs to the Suidae family and its most prominent characteristic features are the extraordinary curved upper canine

tusks in males (Ito *et al.*, 2017). The Sulawesi warty pig also belongs to the Suidae family but is more closely related to the common European wild pigs, and is characterised by facial warts of the males. Sulawesi warty pigs usually inhabit rainforests and swamps throughout the southeast Asian islands. The populations of all three species have diminished in recent years, probably due to anthropogenic processes such as overhunting and habitat reduction from agricultural use, and are marked as 'threatened' on the IUCN Red list.

3.8.2 Data and analysis

For the multidisciplinary investigation of the three animals, genetic and morphometric data were gathered from wild populations, museums and zoos, of which only the genetic data were used for the analysis presented here. The datasets consist of 13 microsatellite loci from 163 Anoa, 14 microsatellite loci from 238 Sulawesi warty pigs and 13 microsatellite loci from 182 babirusa. No conversion of microsatellite fragment lengths into repeat numbers was required as this step has already been performed by my colleagues, who provided the data. In order to obtain as much information from the genetic data as possible, ASD was used as the measure for genetic diversity.

A spatial grid of latitude and longitude ranges, covering the geographic area of the island of Sulawesi (from 6° 0' 0" S to 1° 0' 0" N and from 118° 0' 0" E to 124° 0' 0"), was searched at a resolution of 0.05 degrees by 0.05 degrees. At each point in these searches where five or more genetic samples were present within a radius of 500 km for Sulawesi warty pigs and Babirusa, and 350 km for Anoa (i.e. accepted kernels), the mean (across loci) genetic diversity was calculated using ASD and recorded for that grid location. The grids were then re-explored with each latitude/longitude location treated as a potential origin location of the population expansion of each species. At each location, Pearson's correlation coefficient between geographic distance to the accepted kernels and local diversity at those

kernels was recorded. This provided a grid of correlation values, which was then interpolated and visualised on a map. Regions with the highest negative correlations were considered the best hypothesized origin locations. To quantify statistical support for inferred origin of expansion locations, the data were permuted among sample sites 1000 times, and for each permuted data set the above analysis was repeated. Following this, I plotted only the grid locations where the negative correlation between geographic distance and genetic diversity was more extreme than 0.99 (0.98 for Anoa) of those obtained from the permuted data (Fig. 3.23 b, c, d).

3.8.3 Results

To assess whether these Plio-Pleistocene uplifts were a possible explanation for a synchronous expansion, the geographical origin of expansion was inferred using microsatellite data under a model of reduction in genetic diversity with distance from expansion origin. These estimates were obtained independently of, and uninformed by, either the geological reconstructions or modern phylogeographical boundaries inferred from other species. I inferred that the location of origin of expansion for both Sulawesi warty pig and babirusa was in the east central region of Sulawesi (Fig. 3.23 c, d), and the location of origin expansion of Anoa was in the west central region (Fig. 3.23 b). The origins of the population expansions of both Sulawesi warty pig and babirusa occurred in an area of Sulawesi that only emerged during the Late Pliocene to Early Pleistocene (Fig. 3.23 a). On the other hand, Anoa's most likely origin of diversification lies in a region that was submerged until the Pleistocene, consistent with palaeontological evidence (Rozzi, 2017) and with the more recent TMRCA (The Most Recent Common Ancestor) inferred for this species (Frantz *et al.*, 2018).

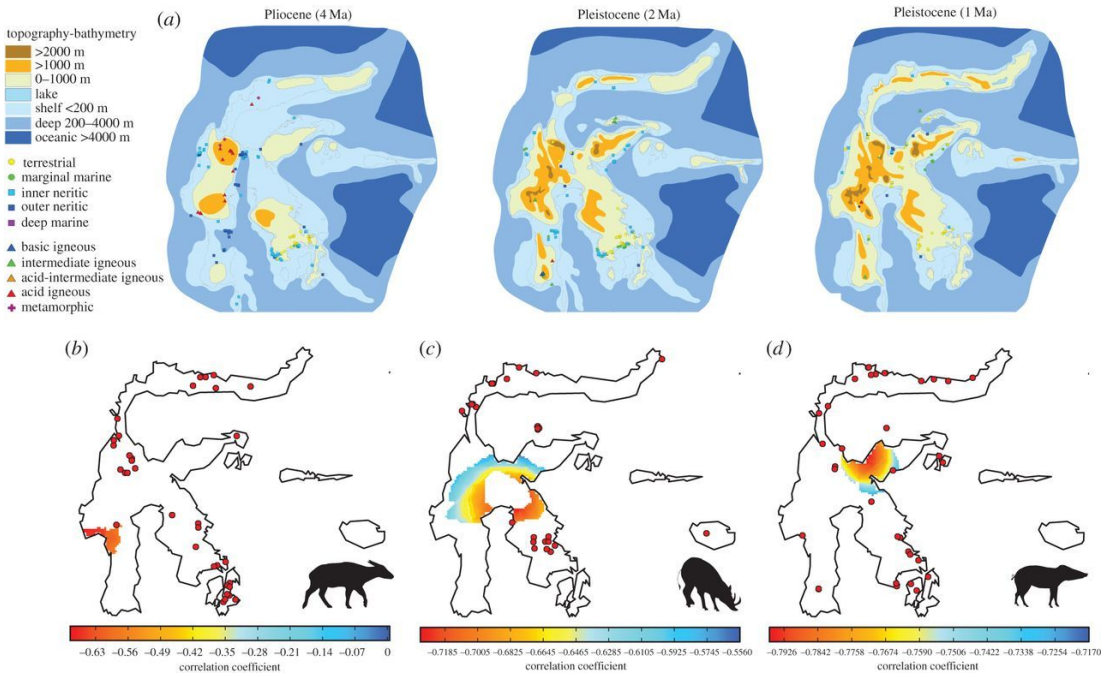

Fig. 3.23 Adapted from Frantz et al., 2018 and Nugraha and Hall (2018). Geological maps of Sulawesi and the geographical origin of expansion. (a) Reconstruction of Sulawesi over the last 5 Myr (adapted from Nugraha and Hall (2018) and origin of expansion of (b) Anoa, (c) babirusa and (d) Sulawesi warty pig. Red dots represent the location of the samples used for this analysis. Low correlation values in red (between distance and genetic diversity) represent most likely origin of expansion.

3.8.4 Discussion

Results from the geological analysis on the formation of the island of Sulawesi indicate that, while the different geological components of Sulawesi were assembled at about 23 Myr ago, the island only acquired its distinctive modern form in the last few million years. By 3 Myr ago there was a large single island at its modern centre, but the complete connection between the arms was established more recently (Fig. 3.23a). The increasing land area associated with Plio-Pleistocene tectonic activity is likely to have provided the opportunity for the expansion of the animals of Sulawesi.

While the origin of population expansion of babirusa and the Sulawesi warty pig was inferred to be in central Sulawesi, the origin of population expansion of Anoa was inferred to lie in the west of the island. In combination with the geological reconstructions of Sulawesi and the results on the TMRCA inferred from the genetic

data of Anoa (1.06 million years ago), babirusa (2.49 million years ago) and SWP (2.19 million years ago), it is suggested that the increased land area gave opportunity for a synchronous expansion of the three endemic mammals from the centre of the island - see Frantz and colleagues (2018). Nevertheless, the conclusion of an association between the expansion of the animal populations and geological activities of the island of Sulawesi at around ca. 1 - 2.5 million years ago, requires further testing. Even then, it is important to keep in mind that correlation does not mean causation and that the modes of expansion of Anoa, babirusa and the Sulawesi warty pig may have been shaped by different processes.

Inferring population expansions in combination with results from other scientific disciplines exceeds the original motivation of developing this approach to inferring the locations of origins of domesticated animal and crop species and may be also applied beyond research concerned with the domestication of animals. It can also contribute to explain the dispersal of endemic species on an island (Frantz *et al.*, 2018).

3.8.5 Collaborators

[redacted]

Chapter 4

4 Inferring herd sustainability from age-at-death profiles of domesticated caprines (sheep and goats).

4.1 Background

The Neolithic transition in the Near East witnessed major changes in subsistence that altered the course of human prehistory. A transition from a mobile hunting-gathering to a sedentary, food producing lifestyle, with the associated domestication of animals and plants, are considered to be the most important changes (Hesse, 1982; Stein, 1986; Zeder, 2001; Çilingiroğlu, 2005; Atici, 2007; Balaresque *et al.*, 2010; Haak *et al.*, 2010). Domesticates include the founder animal species: cattle, goats, sheep and pigs, and founder crops, including emmer and einkorn wheat, and barley (Çilingiroğlu, 2005; Manning and Shennan, 2013; Peters *et al.*, 2013). Animal husbandry and plant cultivation is thought to have resulted in a reduction in dietary breadth (Peters *et al.*, 2013). Animal domestication is typically characterized by size reduction, increased docility and various morphological changes. In addition, changes in culling patterns (the ages at which animals are killed) have been observed relative to hunted wild animals (Hesse, 1982; Stein, 1986; Zeder, 2001).

The study of animal bones from archaeological assemblages is relevant for archaeologists as it informs on the fauna of the environment, the diet of the people in the past, the symbolic roles of animals, and potentially the management strategies employed. Scholars have therefore been interested in identifying the species, age and sex of animal remains. Age at death estimations of archaeozoological remains can be made based on changing size, shape, structure, wear patterns and composition of teeth and bones. Teeth structure and eruption are most suitable for age estimation because teeth suffer the least from taphonomic modification processes. An additional advantage of tooth analysis is that teeth become

progressively more worn with age, which is reflected in distinctive wear patterns. Tooth wear can also provide insights into the diets and habitats of the animals.

The most widely-used method used to estimate the age of sheep and goat remains is from tooth wear, and was developed by Sebastian Payne in the 1970s and 1980s (Payne, 1988). Other methods have also been developed, based on measuring crown height and annual growth rings (cementum increments) and tooth crown and root development (Fairnell, 2014). Cementum increment analysis permits very accurate age estimation. However, it is a destructive and time-consuming method. Tooth crown and root development can also be analysed by X-radiography or by breaking down the mandibles directly e.g. (Klein *et al.*, 1981; Carter, 1997), although this alternative is also destructive and costly.

As with tooth wear, bone fusion is also progressive with age, allowing for age at death estimation from material other than teeth. Age estimation from fusing bones is powerful for assigning age of younger animals, but bones are usually all fused by early adulthood (Fairnell, 2014).

A demographic profile (mortality profile) can be constructed after identifying the species and estimating the ages at death in an archaeological assemblage. From those mortality profiles it is possible to make inferences on animal herding and slaughter management strategies. For decades zooarchaeologists have studied herding strategies in Europe and the Near East during the Epipaleolithic and Neolithic periods (Zeder, 2001; Helmer and Vigne, 2004; Atici, 2007; Helmer, Gourichon and Vila, 2007; Gillis, Chaix and Vigne, 2011). Animal bone remains from archaeological sites can give insight into a herd's age structure, into the choice of domesticates, the culling profiles, the ratio of hunted, wild versus captive animals, and early domestication strategies (Stein, 1986; Zeder, 2001; Helmer and Vigne, 2004; Helmer, Gourichon and Vila, 2007; Gillis, 2012).

Today, animal herding and slaughter strategies are optimized for high product yields, such as meat, milk and other dairy products, and hides, from cattle, pigs, sheep and goat. However, during the beginnings of agriculture, animal management was likely to have been experimental and targeted towards multiple products (Stiner *et al.*, 2014). Asıklı Höyük, an archaeological site in central Anatolia, is a potential example of these first attempts at animal management (Stiner *et al.*, 2014). It has been shown that in Asıklı Höyük, over only a few centuries, from the Pre-Pottery Neolithic (PPN) (9,000 cal BC.) to the later Neolithic (8,200 cal BC.), subsistence strategies changed from wild ungulate animals to caprines (Stiner *et al.*, 2014). It is unknown to what extent herding was practiced in other sites in Anatolia and Europe during the beginnings of agriculture and whether it was optimized towards particular products (Hesse, 1982; Zeder, 2001). The first attempts may have not necessarily yielded any surplus of product or may have even resulted in non-sustainable herds.

Age-at-death profiles (also called 'mortality profiles', 'kill-off profiles', 'age-at-slaughter distribution', 'harvest profiles' or 'culling profiles') are constructed from age at death estimations made from measurements of archaeological bone and tooth specimens taken from animals interpreted as having been domesticated (Zeder, 2001; Helmer and Vigne, 2004; Helmer, Gourichon and Vila, 2007; Manning and Shennan, 2013; Peters *et al.*, 2013). Constructing such culling profiles requires a sound understanding of population demography, age and sex composition. Acquiring this information from archaeological remains is challenging and current techniques for the determination of sex and age of skeletal components are limited (Zeder, 2001). Another problem is that of distinguishing species of similar morphology such as sheep and goat, which is why both species are usually combined into one age-at-death profile. However, each species might have undergone different kill-off patterns, because sheep and goats are usually herded for different exploitation goals. One approach to tackling this problem is thorough metric analysis of modern goat/sheep herds in order to understand detailed morphological information, which is then applied

to archaeological remains (Zeder, 2001). Also, by analysing long bone epiphyseal fusion, systematic differences between sheep and goat can be detected (Zeder, 2001). However, for the method presented here, I combine both sheep and goat to generate a single kill-off profile.

Age-at-death (AaD) profiles are usually represented as histograms with the widths of the columns being proportional to the duration of the discernible age (Fig. 4.1). Because teeth of younger animals undergo many changes, the resolution for distinguishing between ages is higher for younger animals (Fig. 4.1). This explains the differences in the widths of the vertical bars in the histogram. To give an example, Age class A shows animals of 0-2 months in age whereas Class D shows animals of 1-2 years (Fig. 4.1). Consequently, the area - and not the height - of the column represents the frequency of elements.

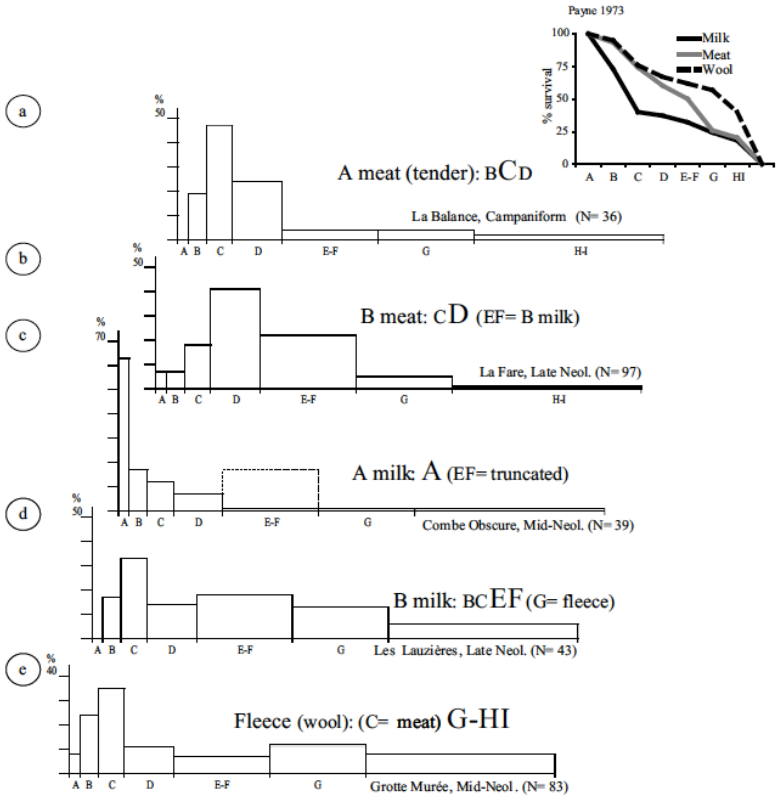

Fig. 4.1 Archaeological representation of idealised mortality profile models of caprines (Payne, 1973; Vigne and Helmer, 2007). Image retrieved from Fig. 5 in Vigne and Helmer, 2007.

The division of animal bones into particular age classes is not standardised and therefore depends on the researcher and also on the level of preservation at an archaeological site. For example, in the case of sheep/goat culling-off profiles, Zeder (2001) uses nine age class categories (A,B,C,D,E,F,G,H,I) (Payne, 1973), whereas other researchers usually use seven age class categories (A,B,C,DE,F,G,HI) (Helmer and Vigne, 2004; Gillis, 2012). For the approach presented in this chapter, I will look into age-at-death profiles of caprines, which were constructed according to Helmer and Vigne's age class system (Fig. 4.2) (Helmer, Gourichon and Vila, 2007).

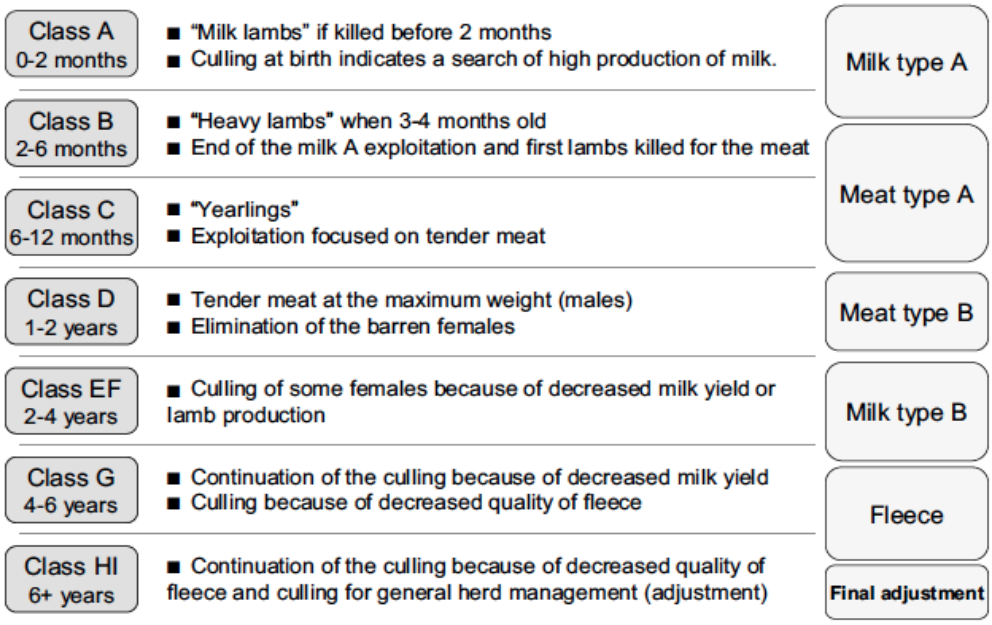

Fig. 4.2 Caprine management within the present-day herding systems in the southeast of France (Helmer and Vigne, 2004; Blaise, 2006); the age classes are associated with the products sought. Taken from (Vigne and Helmer, 2007).

Archaeological age-at-death profiles have been compared by simple visualization to reference age-at-death profiles, which are idealised for particular product proposed by Payne (1973), Redding (1981) and Helmer and Vigne (2004; 2007). This permits some inference of the targets of slaughtering strategies from archaeological material. However, it is unlikely that ancient herds were ever managed in such a way as to optimise the production of a single product.

Caprines, comprising both sheep and goats, were traditionally herded together (Bartosiewicz, 1999). In the Mediterranean sheep and goats are mainly used for milk production in modern times. However, in northern Europe sheep are mainly raised for wool production (Boyazoglu and Morand-Fehr, 2001) and cattle (and to a lesser extent goats) are used as meat source and dairy animals. Herds of wild sheep and goats consist mostly of adult animals. Evidence of a natural mortality rate is reflected in a small percentage of young dead lambs/kids, as those individuals are more likely to die during epidemics or through other environmental causes (Stein, 1986). On the other hand, age profiles of ancient domesticated herds show a high number of young deaths. Herders would selectively cull young males for a) meat and b) to prevent excessive exploitation of resources required for the milk-producing goats. In milk producing herds, it has been inferred that infant caprines were slaughtered at around 1-2 months, whereas when there was more balanced milk and meat production, slaughter occurred later in life. Females were probably kept in the herds as long as possible, which means up to an age of 6 years (i.e. while they had good health, high fertility and high milk yield, even though domesticated goats can live up to 20 years) (Malher, Seegers and Beaudeau, 2001).

The killing of young male goats can be interpreted as a dairying strategy. Thus, female goats remain and increase milk productivity as they get older. Unlike a dairying strategy, a strategy for meat exploitation might be characterised by slaughtering young males between the ages 2 and 4 years, when they reach full body size and when good-quality meat exploitation can be optimized. When herders target wool exploitation, most adult animals would be expected to survive until (and beyond) the age of 6 years. The diagram in Fig. 4.2 lists some proposed subsistence strategies inferred from preferred slaughter at age classes (Helmer, Gourichon and Vila, 2007).

4.1.1 Age-at-death idealised models

A number of different idealised mortality-profile models have been proposed. Probably the most used is the model proposed by Payne (1973) (Fig. 4.3). Mortality profiles from Payne have been modified by Helmer and Vigne (2004) in an effort to achieve a more realistic and detailed picture (see Fig. 4.1), especially when it comes to distinguishing milk and meat and combined milk/meat production strategies. Payne's idealised mortality-profiles consist of three predictive models (meat, fibre, milk) whereas Helmer and Vigne added two additional models, which represent a combined herd management strategy (milk and meat) (Peters *et al.*, 2013).

Age class	Eruption/wear stage	Estimated age*
A	D4 still unworn	0-2 months
B	D4 in wear, M1 is unworn	2-6 months
C	M1 in wear, M2 unworn	6-12 months
D	M2 in wear M3 unworn	1-2 years
E	M3 in wear, posterior cusp unworn	2-3 years
F	Posterior cusp of M3 in wear, M3 pre	3-4 years
G	M3 M2	4-6 years
H	M3	6-8 years
I	M3 post	8-10 years

Fig. 4.3 Payne age classes from studying 20 Turkish sheep mandibles. Adapted from Payne, 1973 (Payne, 1973a).

Helmer and Vigne's (2004; 2007) 'Milk type A', 'Meat type A' and 'Fleece' idealised slaughter profiles are derived from Payne's (1973) milk, meat and fleece idealised models, whereas Helmer and Vigne's (Helmer, Gourichon and Vila, 2007) two mixed-economy profiles 'Meat type B' and 'Milk type B and Meat type A' (or in some publications just termed 'Milk Type B' (Helmer and Vigne, 2004; Vigne and Helmer, 2007)) models (see Fig. 4.1) were novel. In Meat type A most slaughtering occurs in age class C, and in Meat type B, slaughtering is more balanced between age classes C-F, having a peak at age class D. Milk type A is characterised by a slaughter peak at age class A, indicating a high rate of infant slaughter (Fig. 4.2). The

modified model also proposes to combine two slaughter strategies targeting both milk and meat production, where killing happens in a more balanced manner spread throughout the age classes, having a peak at age classes A and B for young animals, representing a milk production management, and killing off females for meat at classes EF due to decreasing milk productivity (see Fig. 4.1).

Given a kill-off pattern, survivorship curves represent the inferred percentage of the herd surviving at a particular age (Hesse, 1982; Stein, 1986; Zeder, 2001). As a result, different slaughter practises will result in distinctive survivorship curves, or demographic profiles. Given that animals only begin to reproduce after around 15 months (although this number may vary), a survivorship curve will influence the average number of offspring an individual will have throughout its life, and so the sustainability of the overall herd. Since different targeted products (e.g. meat, milk or wool production) will favour different slaughter practises and thus different survivorship curves, the probability of the herd being sustainable will depend to an extent on what the herd is being kept primarily for (Fig. 4.4, example of survivorship curve from Stein, 1986).

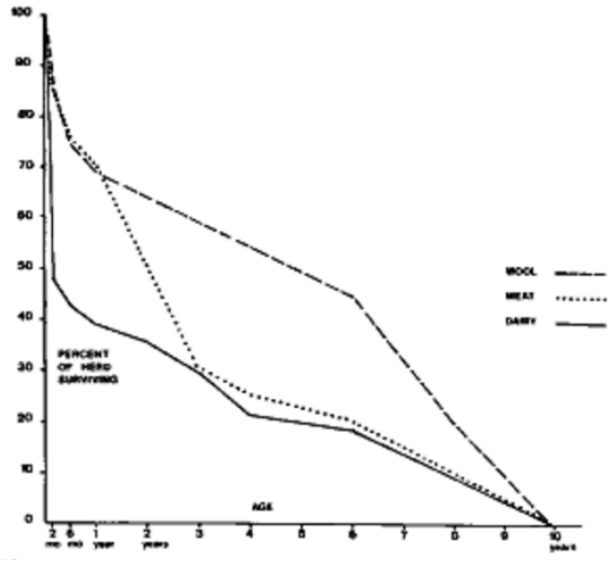

Fig. 4.4 Example for survivorship curves for three different herding strategies: wool, meat and dairy (adapted from Stein, 1986). Original caption: Survivorship curves for sheep and goats under different herding strategies. The vertical axis shows the percentage of the herd

surviving; the horizontal axis shows the age of the animal. At birth (age 0 months on the left), 100 percent of the herd is alive. As the animals grow older, they are culled from the herd so that virtually none survive beyond the age of ten years (reflected by a survivorship of 0 percent at the bottom right side of the graph). The ages at which the animals are culled will depend on what products the herders are emphasizing. As a result, meat, dairy and wool (or fibre) production each yield distinctive survivorship curves. (After Payne 1973).

An issue with using archaeological data to infer kill-off profiles, and thus survivorship curves and the targets of herd management, is the relatively small samples sizes associated with archaeological assemblages. Small sample sizes generate sampling uncertainty, whereby the proportions observed in each age class in the sample poorly reflect the proportions in each age class in the actual population. This is a universal problem with small samples, but one that has received only limited attention in studies of archaeozoological kill-off profiles (but see (Gerbault *et al.*, 2016; Gillis *et al.*, 2017; Timpson *et al.*, 2018).

4.2 Aim of the project

In this chapter, I present the development of an approach to evaluate sustainability/viability of domesticated caprines herd from archaeozoological kill-off profiles that accommodates sampling uncertainty. I use information on expected ages at reproduction. Because we do not know underlying birth rates in Neolithic herds, I treat this as a free parameter. This enables me to identify the birth rates that would be required to make a herd sustainable given the inferred kill-off profile from a finite sample. I present results of the application of this method to a range of datasets covering the Epipaleolithic, Neolithic and Bronze Age.

4.3 Data

I collected more than 200 age-at-death profiles from the literature (Gejvall *et al.*, 1969; Payne, 1973; Wolff, 1975; Chaix, 1976; Halstead and Jones, 1980; Redding, 1981; Meniel, 1987; Barker *et al.*, 1990; Wilkens, 1996; Halstead, 1998; Munson, 2000; Braguier, 2000; Greenfield and Fowler, 2005; Atici, 2007; Bartosiewicz and Gál, 2007; Vigne and Helmer, 2007; Orton, 2008; El Susi, 2008; Blaise, 2009; Stiner and Munro, 2011; Salque *et al.*, 2012; Gillis, 2012; Stiner *et al.*, 2014; Horejs *et al.*, 2015; Molloy, 2016) and from collaborators who shared their data with me (Dr. Rosalind Gillis from the University of Algarve and Dr. Alfred Galik from the University of Vienna).

Age-at-death profile data are provided in either number of elements (e.g. teeth) or in Minimum Number of Individuals (MNI), which is a transformation from element counts (White, 1953).

For the approach described below, the following three datasets will be used:

- Dataset-A; skeletal element counts
- Dataset-B; minimum number of individuals (MNI)
- Dataset-C; idealized models formulated by other researchers (Payne, 1973; Redding, 1981; Vigne and Helmer, 2007)

The locations of the archaeological sites, from which the archaeozoological remains were collected, comprise Europe and West Asia, and range chronologically from the Epipalaeolithic to modern times (see Figs. 4.5 to 4.10). Most age-at-death profiles are from Neolithic sites. Some of the locations and the ages of the archaeological sites are approximate. Those age-at-death profiles have not been provided with the exact chronology (i.e. radiocarbon dates of archaeological sites) nor the exact latitude and longitude values. The chronology is of variable quality.

4.3.1 More detailed information and general statistics on datasets

4.3.1.1 Dataset-A

Dataset-A contains >200 age-at-death profiles (Table A.1 in Appendix). The number of skeletal elements are recorded in seven age classes (see Table 4.1 below) as proposed by Vigne and Helmer (Helmer and Vigne, 2004). The map in Fig. 4.5 shows the locations and ages (in BP) of archaeological sites, from which the age-at-death profiles were harvested. Locations are spread over Europe and West Asia and sampling clusters can be seen around the northern Mediterranean, the Balkans and West Asia. Few data are available from north Europe and none from Scandinavia. Fig. 4.6 visualizes the density of sampling and shows that one location in West Anatolia (archaeological site Cukurici Hüyök) occurs multiple times with different site phases in the given dataset. Here, many Neolithic site phases are processed for one archaeological site. Age class EF (24 – 48 months of age) is most frequently represented in the profiles of dataset-A (Fig. 4.7a). Age class B (2 – 6 months of age) is least frequently represented in this dataset. Fig. 4.7b shows that most profiles are from the years 5,000 – 7000 BCE (~ca. 7,000 – 9,000 BP respectively). This time period is a good representation of the European Neolithic.

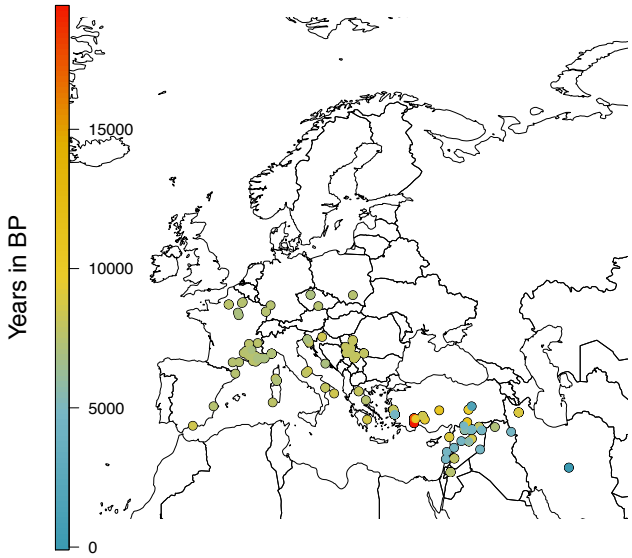

Fig. 4.5 Locations of archaeological sites from which >200 age-at-death profiles (dataset-A)) were collected. The colours are representative of the age (years in BP) of the sites; red dots representing sites from the Epipalaeolithic and gradually turning blue when approaching the modern times.

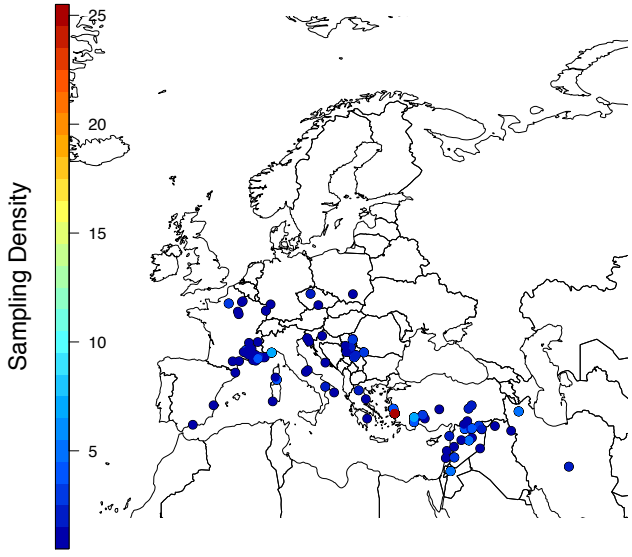

Fig. 4.6 Locations of archaeological sites from which >200 age-at-death profiles were collected. The colours are representative of sampling density; red dots represent sites, from which there are a high number of age-at-death profiles spread over many site phases and gradually turning blue when there is only one age-at-death profile per aracheological site.

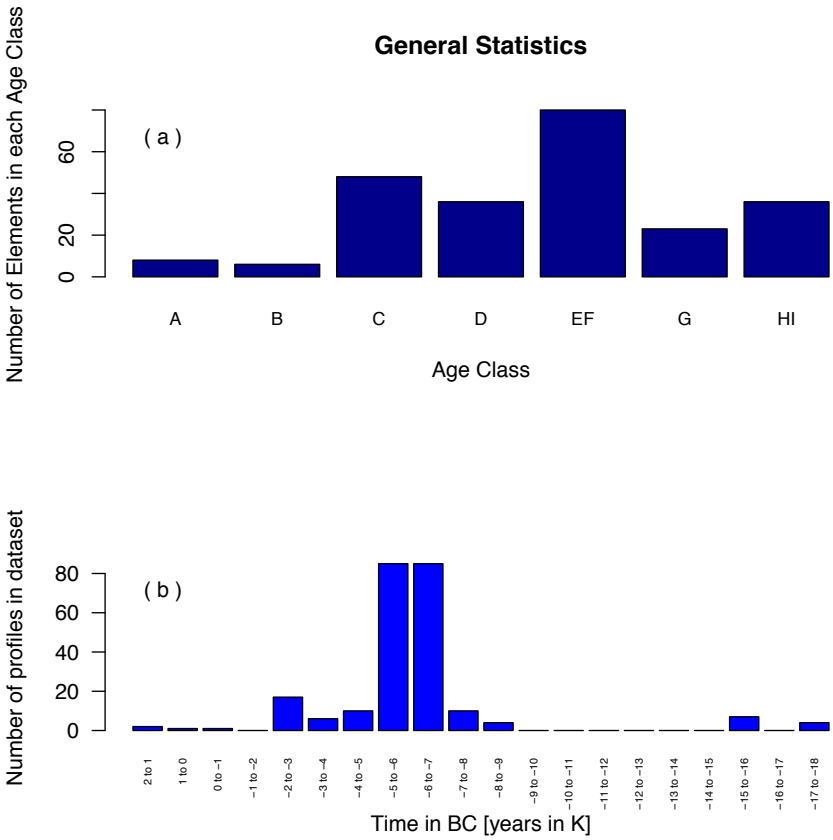

Fig. 4.7 Frequency of skeletal elements in each age classes (a) and number of age-at-death profiles in particular time period (b) from dataset-A.

4.3.1.2 Dataset-B

The MNI dataset was collated by my colleague Dr. Rosalind Gillis (Table A.2 in Appendix). It contains 76 age-at-death profiles, which differ from dataset-A in that the MNI dataset is a translation of the number of skeletal elements into the number of individuals. As such, most profiles in the MNI dataset stem from the same archaeological locations and publications as dataset-A. The profiles are also mostly from the Neolithic era and the archaeological sites are concentrated within Europe (Fig. 4.8). The age of the sites is based on relative chronologies. The reason for having two datasets is that the MNI dataset provides information on the number of individuals rather than skeletal elements and is as such a more accurate proxy for simulating population frequencies of different age classes.

The map in Fig. 4.8 shows the locations and ages (in BCE) of archaeological sites from which the age-at-death profiles were harvested. Dataset-B has been provided in times in BCE and the original format of time has been kept (time format in dataset-A was mainly provided in BP and has been converted to BP, when originally provided otherwise). The locations of archaeological sites are mainly placed in central Europe. Clusters are found in the Balkan and Franco-Iberian regions. Few data are available from north Europe and none from Scandinavia. Fig. 4.9 visualizes the density of sampling. It shows that the maximum number of profiles from one site is in the Southern Adriatic region with five age-at-death profiles per site. As well as in dataset-A, age class EF (24 – 48 months of age) is most frequently represented in dataset-B (Fig. 4.10a). Age classes A, B and HI are least frequently represented in dataset-B. Fig. 4.10b shows that most profiles are from the years 7,000 – 5,000 BCE (ca. 9,000 – 7,000 BP respectively).

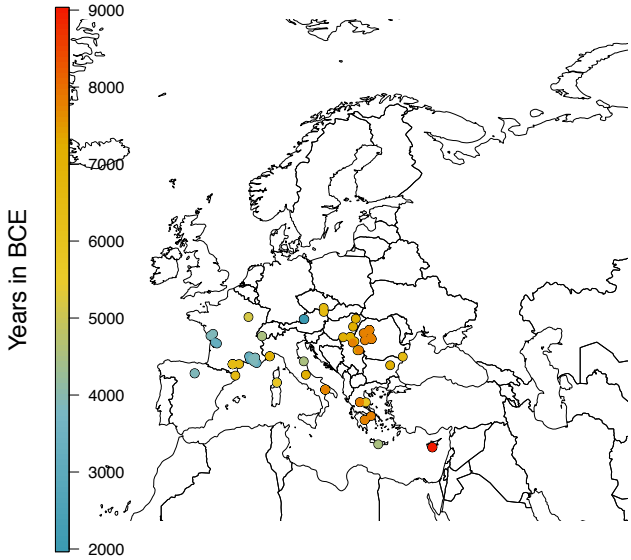

Fig. 4.8 Locations of Neolithic archaeological sites from which 76 age-at-death profiles were collected. For this dataset, the sites were dated relatively (relative chronology). The colours are representative of the age (years in BCE) of the sites; red dots represent sites ranging from ~ 9,000 BCE to 2,000 BCE.

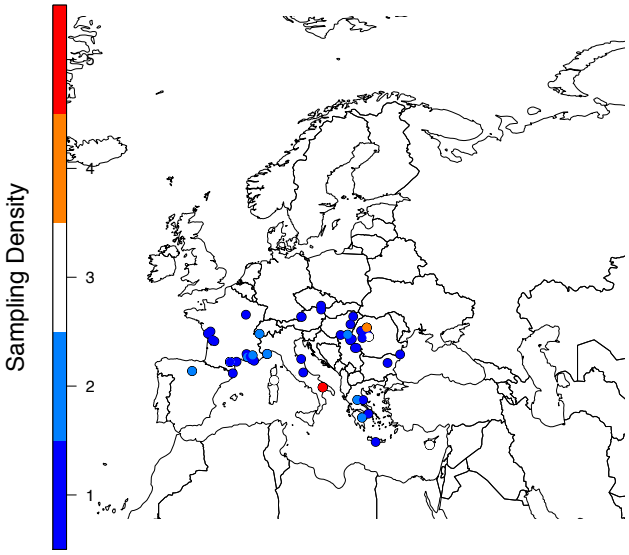

Fig. 4.9 Locations of archaeological sites from which 76 age-at-death profiles were collected. The colours are representative of sampling density; red dots represent sites, from which there are a high number of age-at-death profiles spread over many site phases and gradually turning blue when there is only one age-at-death profile per aracheological site.

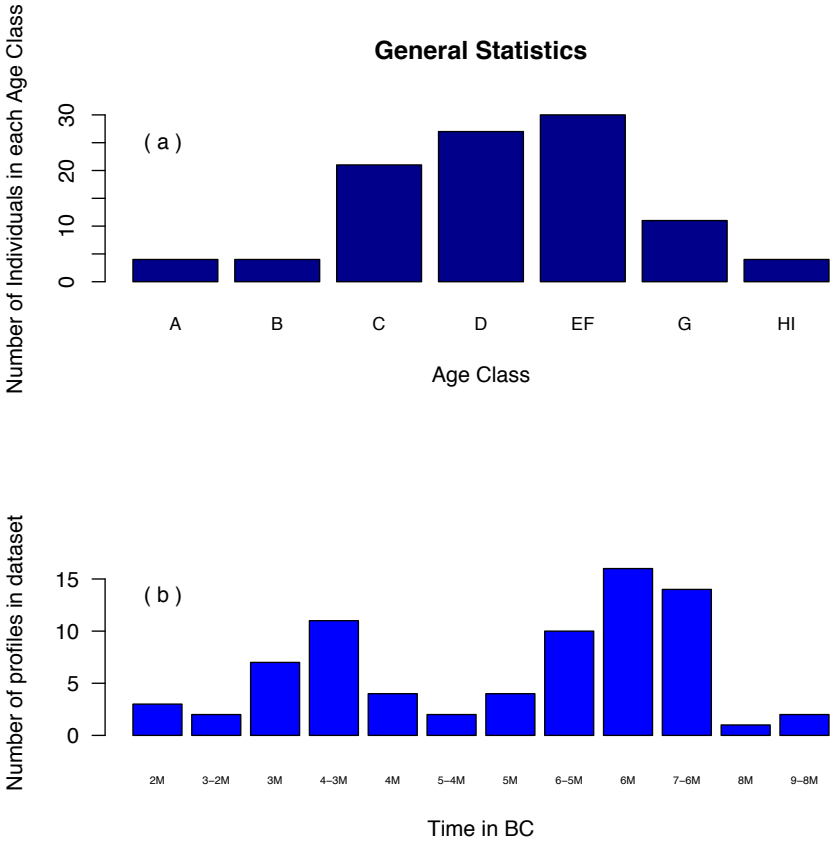

Fig. 4.10 Frequency of individuals in each age classes (a) and number of age-at-death profiles in particular time period (b) from dataset-B.

4.3.1.3 Dataset-C

I collected a total of ten idealized age-at-death profiles (tables A.3-6 in Appendix). Payne (1973) proposed three Caprini model kill-off profiles, each based on nine age classes (table 4.1). Redding (1981) proposed two Caprini model kill off profiles, each based on 10 age classes (table 4.1); one proposed to optimised energy yield and one proposed to maximise herd security (i.e. herd growth rate). Vigne and Helmer (2007) identified five archaeological Caprini mortality profiles, each based on seven age classes (table 4.1), which they interpreted as different combinations of five distinct slaughter strategies practiced in modern stock in southeastern France: Milk type A, Meat type A, Meat type B, Milk type B and Meat type A, and Fleece. These five distinct slaughter strategies were themselves based on observed preferential culling ages, whereas Payne's and Redding's models were constructed based on proportions of each age class.

Table 4.1 . Breakdown of age classes into months by Payne, Redding as well as Vigne and Helmer.

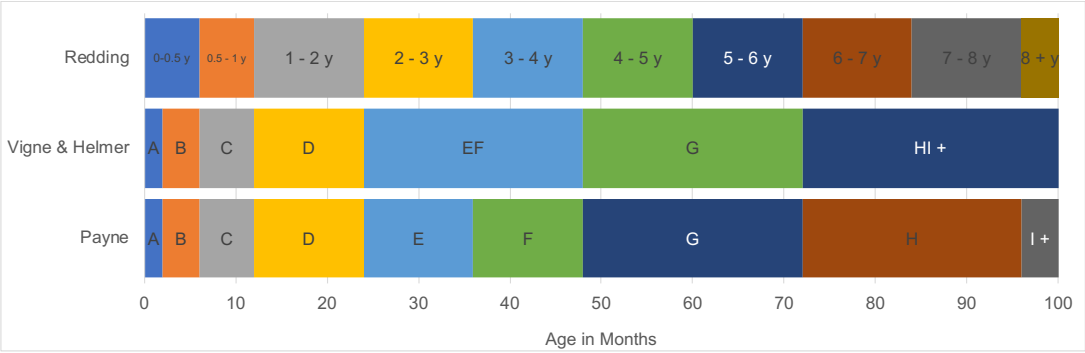

As dataset-C comprises model age-at-death profiles for particular target products, or combinations thereof, it is not associated with a particular time period or location. For this reason, no summary statistics were generated.

4.4 An approach to infer herd growth rates

4.4.1 Overview of the approach

Age class frequencies can be combined with an assumed birth rate and an age of reproduction to calculate the average number of animals produced per animal born (Fig. 4.11). This requires certain assumptions, such as those concerning sex-ratios in different age classes.

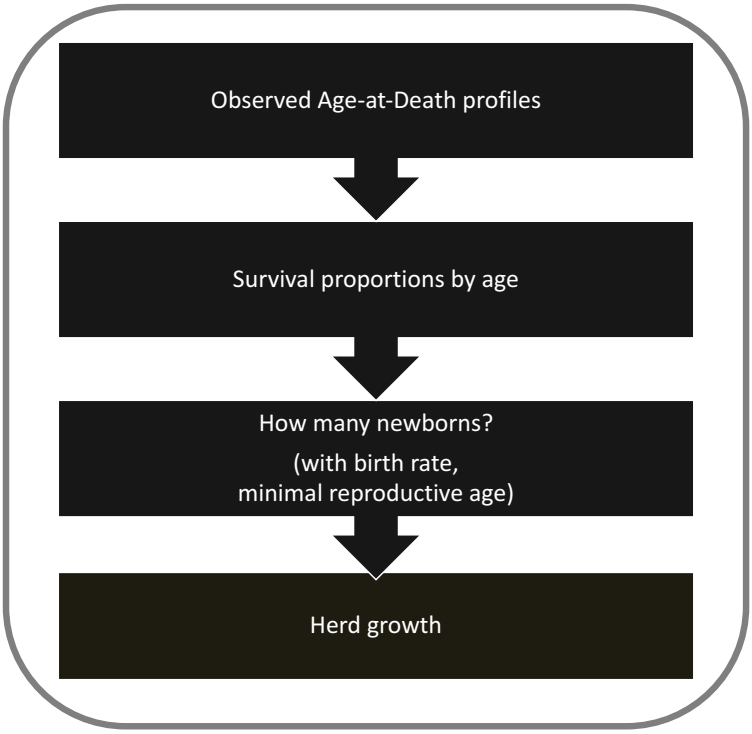

Fig. 4.11 Overview of approach

4.5 Detailed description of the approach

Age class categories were transformed to ages in months. Then, the proportions of killed animals were distributed across the months in each age class equally. Next, survivorship curves were generated, which show the percentage of surviving animals at a particular age in months (Fig. 4.12 middle right). From the survivorship curves, an assumed birth rate (e.g. 1 kid/lamb per year per female), and a minimum reproductive age (from 15 months onwards was used here), the numbers of newborns

per surviving animal for each month of age can be calculated (Fig. 4.12 middle left). Note that in this analysis I assume an equal sex ratio throughout the age range of the herd. The sum of all newborns then represents the average number of animals produced per animal born over its lifespan (ΔN_{ls}). From this we can calculate the intrinsic per mean lifespan growth rate as $\Delta N_{ls} - 1$. Because we do not know the actual birth rates, we explored a range of possible values ranging from 0.2 – 2 per female per year, which translates to approximately 0.00833 to 0.0833 newborns per animal per month (Fig. 4.12 bottom middle).

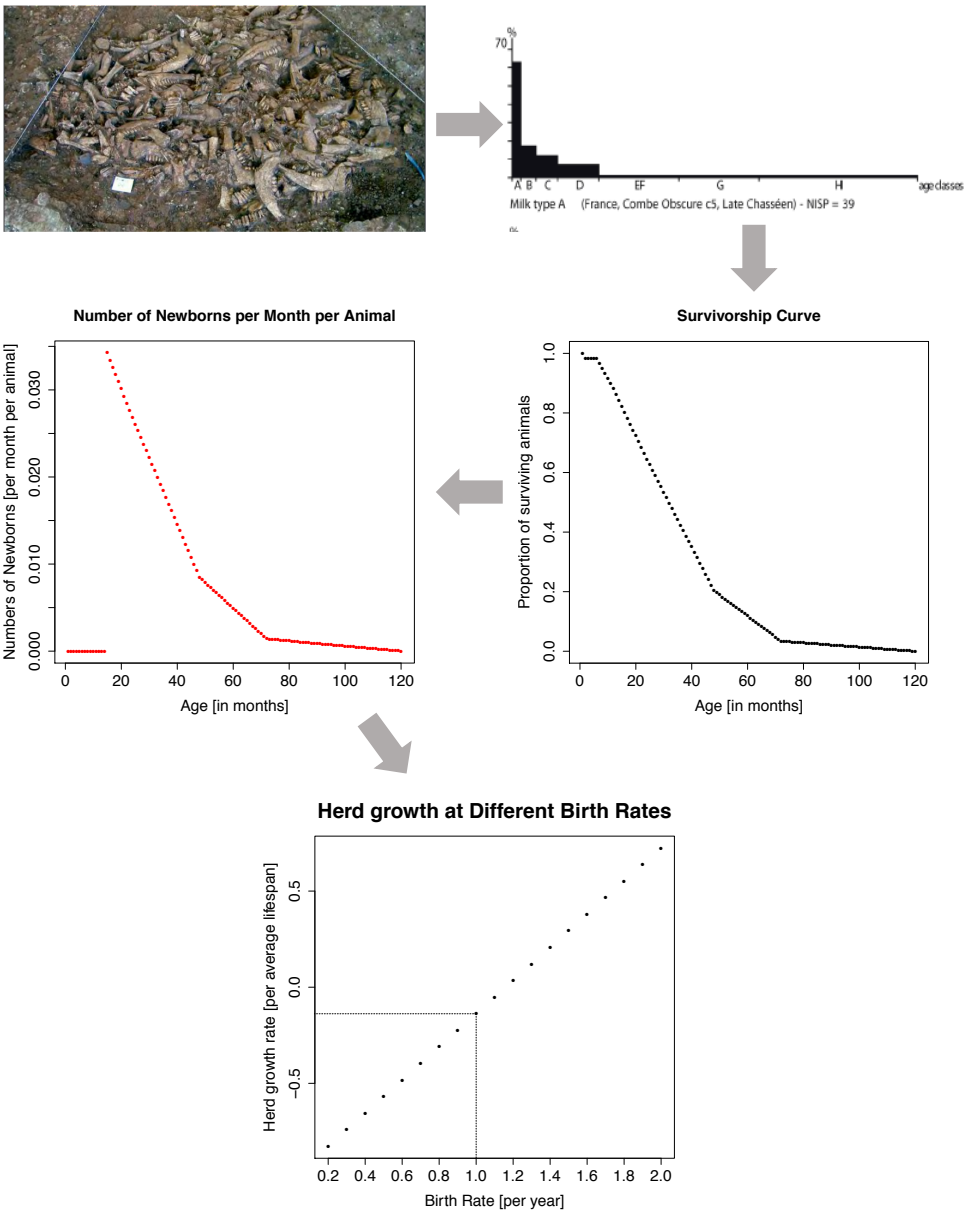

Fig. 4.12. Detailed description of the approach. Top left: Example of archaeozoological remains. Top right: example of an age-at-death profile typical for a milk yielding strategy, which is constructed from archaeozoological remains. Middle right: Survivorship curve constructed from profile. Middle left: From the survivorship curve, the number of newborns per female per year was worked out. Bottom middle: Herd growth at different birth rates (x-axis).

4.6 Sampling uncertainty

Age-at-death profiles are usually constructed from a small number of bone or teeth remains, and as such the small size of the data results in sampling uncertainty. In order to overcome sampling uncertainty, random deviates of population age class

frequencies for a particular age-at-death profile (the observed data), were generated 1000 times using the Dirichlet distribution. The Dirichlet distribution is a multivariante probability distribution and is the conjugate prior of the multinomial distribution. As such, it provides a Bayesian method for estimating the probability distributions of population frequencies of three or more types, given the sample counts of those types, and a prior. We use a uniform prior, which in the Dirichlet function means adding 0.5 to each of the counts. The previously described procedure (see Fig. 4.13 top) is then repeated with the random Dirichlet simulated age class population frequencies, resulting in a distribution of number of animals produced per animal born in its lifetime, reflecting sampling uncertainty (Fig. 4.13 middle). As described previously, growth rates are then explored for different assumed birth rates ranging from 0.2 – 2 (Fig. 4.13 bottom) kids/lambs per female per year.

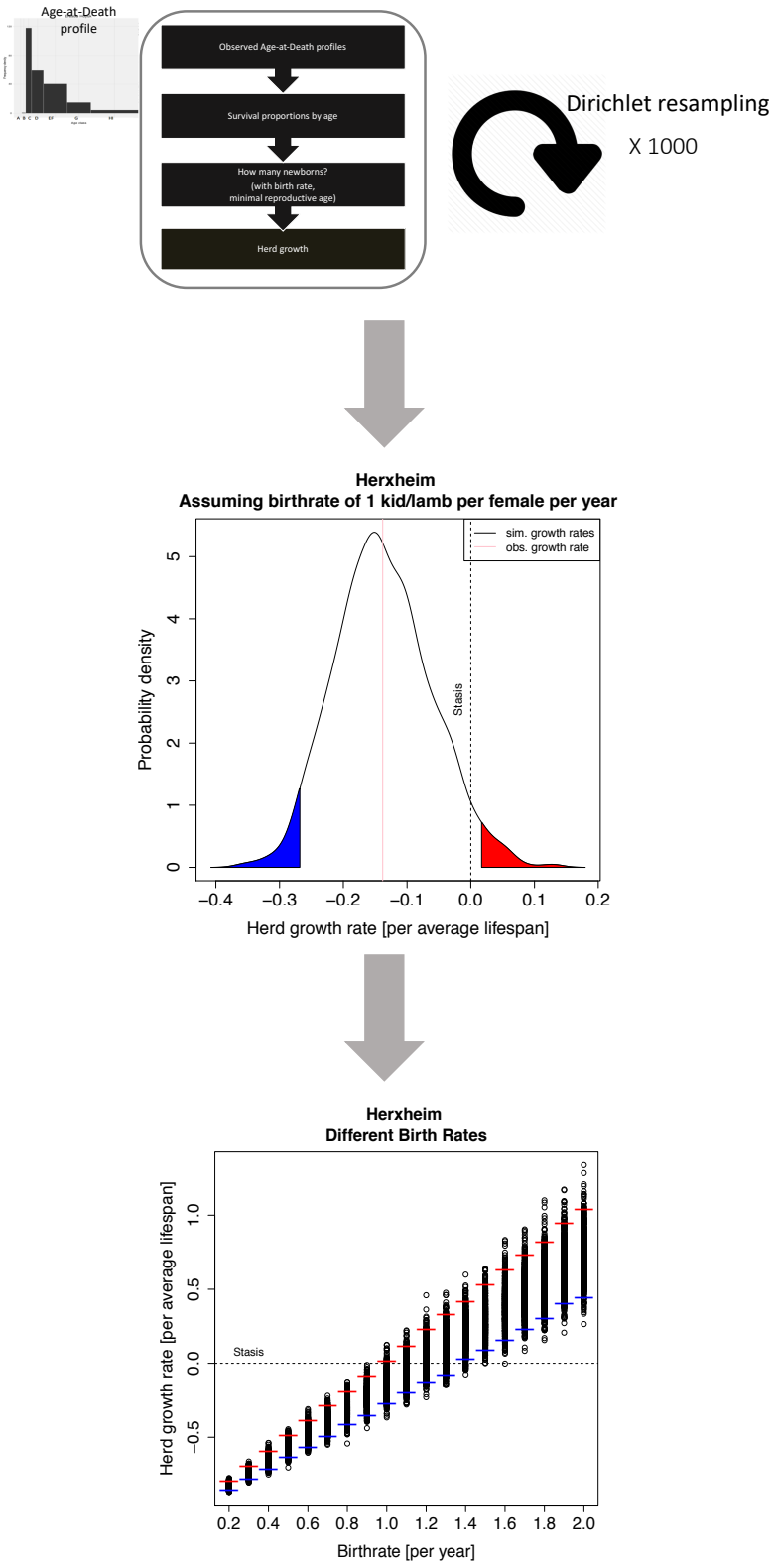

Fig. 4.13 Top: Procedure repeated 1000 times with simulated age class population frequencies. Middle: Distribution of herd growth rates. Bottom: Distributions of herd growth rates at birth rates ranging from 0.2 – 2.0. Blue and red shaded areas of the probability density show equal-tailed 95% credible intervals.

4.7 Interpreting the results

The reasoning behind defining herd sustainability is that the results of the method generate negative or positive herd growth rates. Growth rates greater than zero indicate a growing herd, and hence a sustainable slaughter management strategy, given equal sex ratios and the assumed birth rate. Growth rates smaller than zero indicate a declining herd, and hence an unsustainable slaughter management strategy. A herd with herd growth of zero is in stasis, which means no growth but also no decline.

4.8 Limitations to the method

There are some limitations to the method. The sex of animals can be determined by analysing the morphology of the bones of the animals. Due to the difficulty of assessing the sex from remains such as teeth, from which age-at-death profiles are usually constructed, the ratios between females and males in profiles are only rarely provided. Since offspring and milk are only produced by females, it would be necessary to know about the ratio of females within a herd. To overcome the absence of information of the sex of the animals, another method has been developed, which incorporates the sex ratios (Chapter 5). For the method described in this chapter, a sex ratio of 50:50 is assumed in all age classes.

4.9 Results

I applied the approach presented here to the three age-at-death profile datasets (see above), which consist of (A) >200 age-at-death profiles, (B) 76 profiles, (C) 10 idealised profiles by Payne, Redding as well as Vigne & Helmer. Profiles are of different sample size, location and time period (if the information is provided).

4.9.1 Results for Dataset-A

4.9.1.1 Herd Growth

Example Herxheim:

Fig. 4.14 Age-at-death profile from archaeological site Herxheim (left) and distribution of herd growth rate per lifetime distribution assuming 1 kid/lamb per female per year (right).

Results are illustrated here using the archaeological site Herxheim, an open Neolithic site in North-west Europe (Nowadays southwest Germany) with a profile containing 165.95 skeletal elements in total. Fig. 4.14 shows the age-at-death profile from this archaeological site. The most intense period of slaughter is in age class B (2-6 months of age) although the greatest number of deaths occurs in age class EF. By applying the previously described approach with 1000 random Dirichlet simulations, the probability density (black line Fig.4.14) of the herd growth rates per animal lifetime, assuming a birth rate of 1kid/lamb per female per year and a sex ratio of 50:50, is generated. The vertical red line shows the growth rate estimated from the observed age-at-death profile. The vertical dashed line is placed at a growth rate of 0, indicating ‘stasis’, which means the herd is neither growing nor declining. Blue and red shaded areas of the probability density are the equal-tailed 95% credible intervals. Credible intervals are applied in Bayesian statistics and show the interval which

unobserved parameter values (here growth rates) fall within a particular probability. For Herxheim, higher probability densities for negative growth rates are inferred, and as such, it is unlikely that the Herxheim herd was sustainable, given the assumptions of the model used here, and a birthrate of 1kid/lamb per female per year (Fig. 4.14).

4.9.1.2 Exploring the birth rates

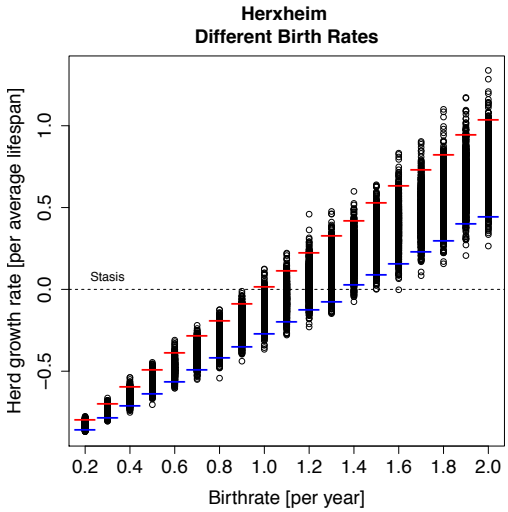

Fig. 4.15 Distribution of herd growth rates at increasing birth rates (from 0.2 – 2.0) for age-at-death profile from Herxheim.

Although I infer that a birth rate of 1 kid or lamb per female would not be sufficient to sustain the Herxheim herd, I can also use the model to identify what birth rates would make this herd sustainable. In the analysis illustrated in Fig. 4.15 I found that a minimum birth rate of ca. 1.2 is required in order to permit the possibility of a sustainable herd.

In order to summarise the results on all profiles from dataset-A, I record the birth rates necessary to ensure that more than 50% of the inferred growth rate distributions are above zero, indicating likely sustainable herds. Fig. 4.16 shows the distribution of birth rates needed for likely sustainable herds, across all profiles in dataset-A.

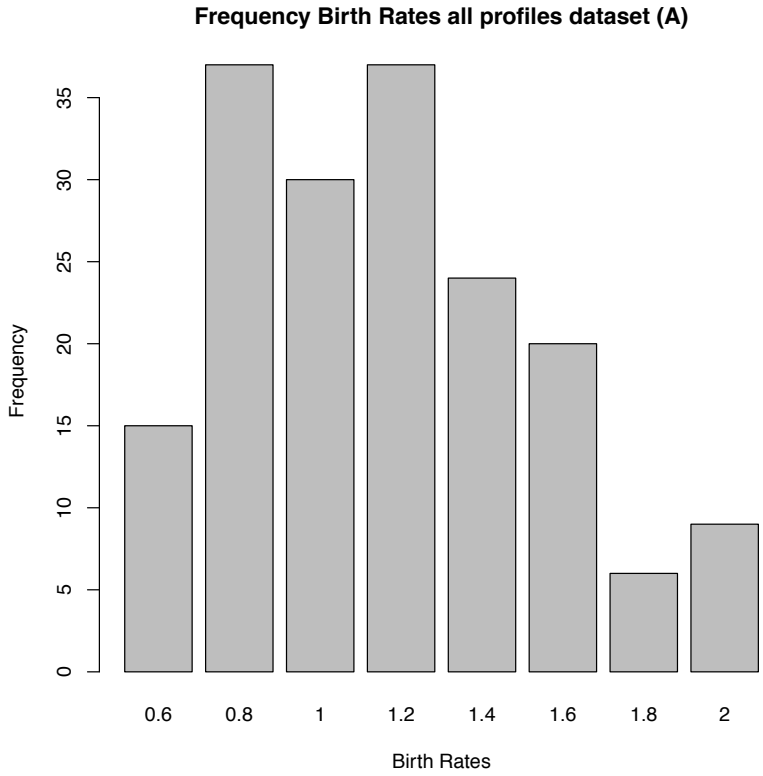

Fig. 4.16 Frequency of birth rates required for stable/growing herds from dataset-A.

4.9.2 Results for Dataset-B

The results for all profiles from dataset-B were recorded. Fig. 4.17 summarises the distribution of birth rates needed for likely sustainable herds across all profiles in dataset-B.

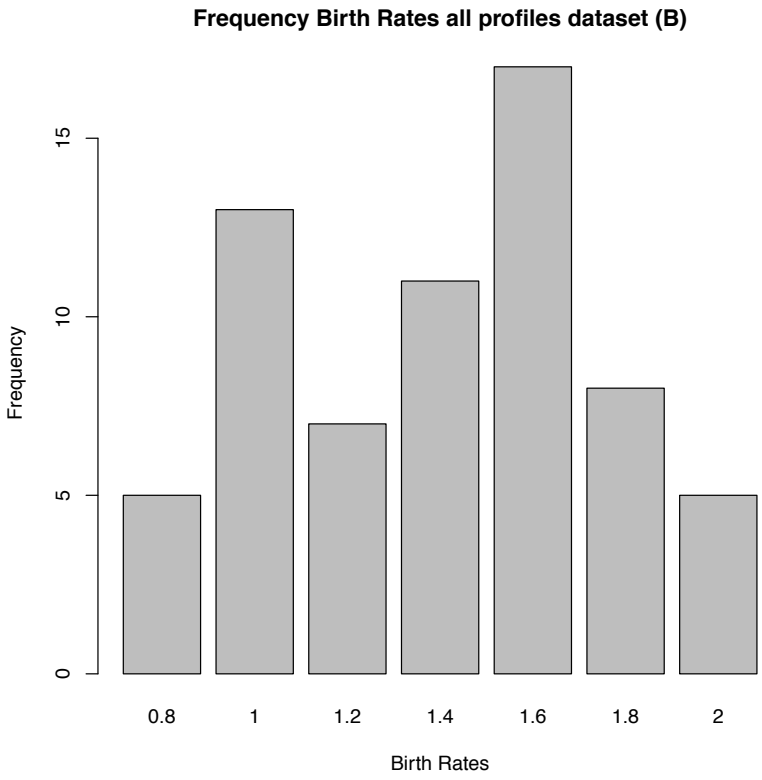

Fig. 4.17. Frequency of profiles from dataset-B with birth rates at which a herd is sustained.

4.9.3 Results for Dataset-C

4.9.3.1 Vigne and Helmer models

The models proposed by Vigne and Helmer (2007) differ from age-at-death profile models by Payne (1973) and Redding (1981) in that Vigne and Helmer use observed data to construct examples of culling profiles, to represent profiles idealised for the production of meat, milk and fleece/wool. Five profiles are proposed: 'Meat Type A', 'Meat Type B', 'Milk Type A', 'Milk Type B' and 'Fleece' (Fig. 5 in Vigne and Helmer, 2007). Below, I reconstructed the profiles given the data from Helmer and colleagues (Helmer, Gourichon and Vila, 2007) (Fig. 4.18). The description of Fig. 5 in Vigne and Helmer (2007) provides information on the archaeological site from which each profile was derived. From this, I inferred which dataset in the Appendix of

Helmer et al., 2007 was used for a reconstruction. This was necessary to check whether the raw data provided in the publication by Helmer and colleagues (2007) was that used for the age-at-death pattern seen in Fig. 5 of Vigne and Helmer (2007) (please note that I am describing two different publications from the same year with Helmer being an author on both papers).

The ‘Meat type A’ profile shows an elevated number of killings in age class C, animals of 6 - 12 months of age. At this age animals show a good tenderness of meat. ‘Meat Type B’ shows many killings in age class D, animals of 12 – 24 months of age, which is when the animals reached their maximum height and weight.

Model ‘Milk Type A’ shows a high number of killings in age class A (0 - 2 months of age). Very young animals are culled so that the milk of the does or ewes can be used for human consumption. ‘Milk type B’ model shows a combination of both, a herding strategy to aim for the production of meat and milk. Many killings are shown in age classes C and EF. And lastly, model ‘Fleece’ shows a moderate number of killings in all age classes (except age class A) to guarantee many animals of all ages producing wool and fleece. Furthermore model ‘Fleece’ shows elevated killings in classes C and G, when animals reach an idealised weight for meat and wool production or reach an old age.

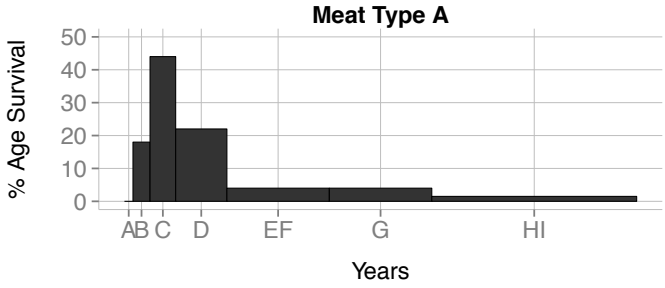

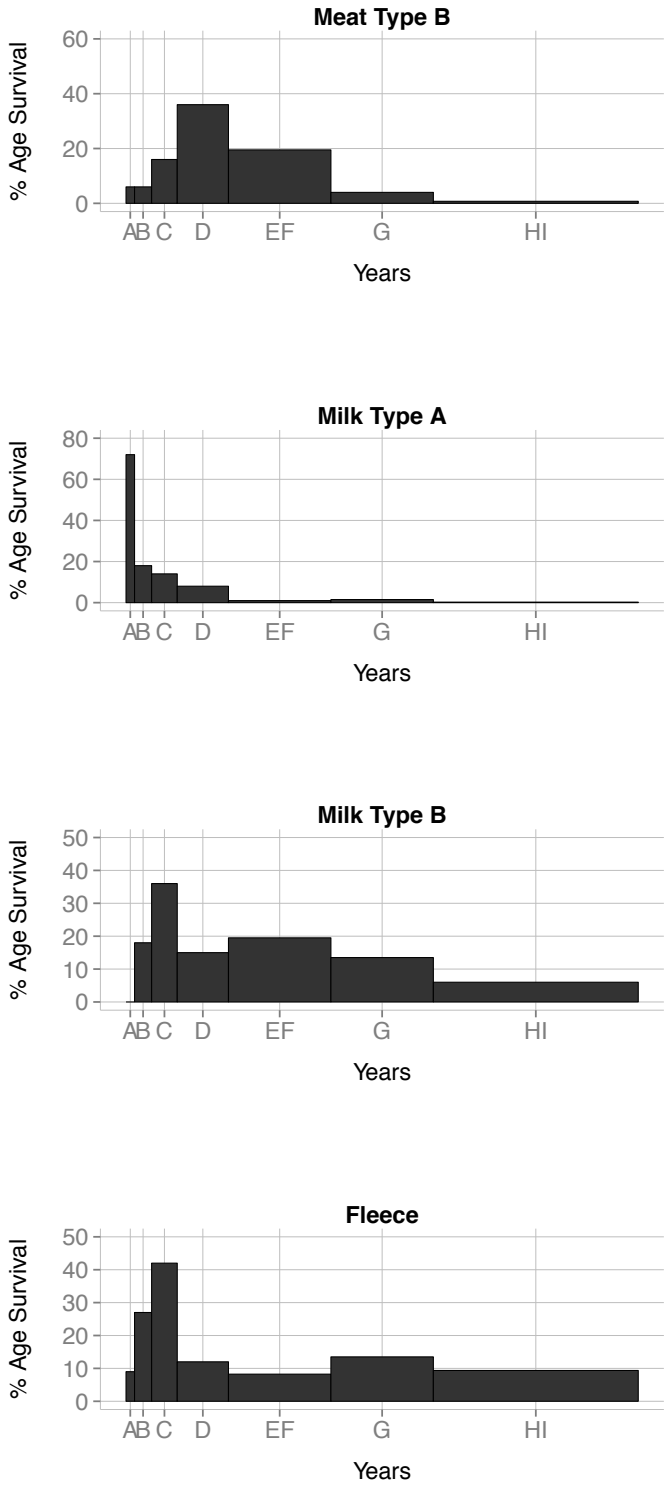

Fig. 4.18 a - e. Reconstruction of Vigne and Helmer's models from Fig. 5 in Vigne and Helmer, 2007 given data from Helmer et al., 2007: 'Meat Type A' (a),' Meat Type B' (b), 'Milk Type A' (c), 'Milk Type B' (d) and 'Fleece' (e).

The method presented in this chapter is not designed to infer optimal herding strategies for a particular product, but to make inferences about the sustainability of the herd. An approach for inferring product yields is presented in Chapter 5. By applying the analyses described above (Fig. 4.19), a profile interpreted as being idealised for meat production, shows mainly negative growth rates at a birth rate of 1 kid/lamb per female per year. The same is inferred for the second profile, also idealised for meat production (Fig. 4.19). Most negative growth rates, indicating a declining herd, are seen for the 'Milk Type A' profile (Fig. 4.19), in which the youngest animals are culled in high numbers. A profile with mixed strategies for milk and meat yields ('Milk Type B', Fig. 4.19), shows mostly positive growth rates but the distribution of growth rates does not exclude negative values. Unlike the other four profiles, a herding strategy oriented towards harvesting fleece results in a sustainable herd (Fig. 4.19) assuming a birth rate of 1 kid/lamb per female per year.

The 'Meat Type A' profile requires a birth rate of around 1.3 to generate a likely sustainable herd (Fig. 4.20), whereas the 'Meat Type B' profile requires a birth rate of ~1.4 (Fig. 4.20). Birth rates of 1.8 and greater are required to make the 'Milk Type A' profile likely sustainable (Fig. 4.20), and rates of 0.8 and greater are required for the mixed 'Milk Type B' profile (Fig. 4.20). Unsurprisingly, a lower birth rate of 0.6 is required for the 'Fleece' profile to be likely sustainable (Fig. 4.20).

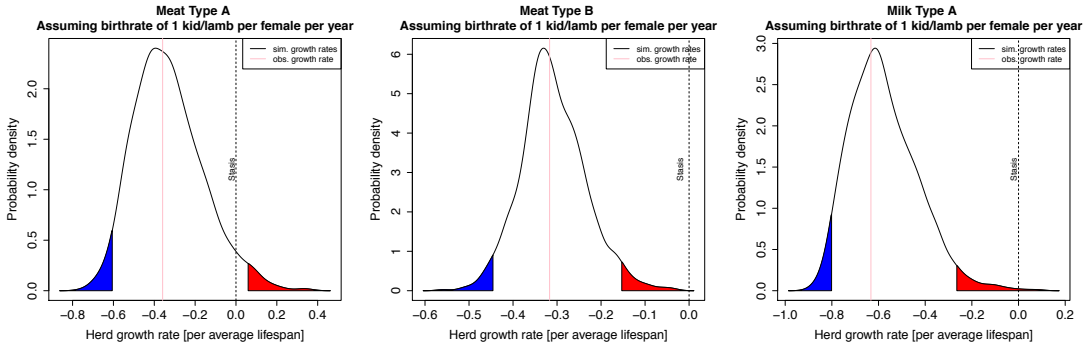

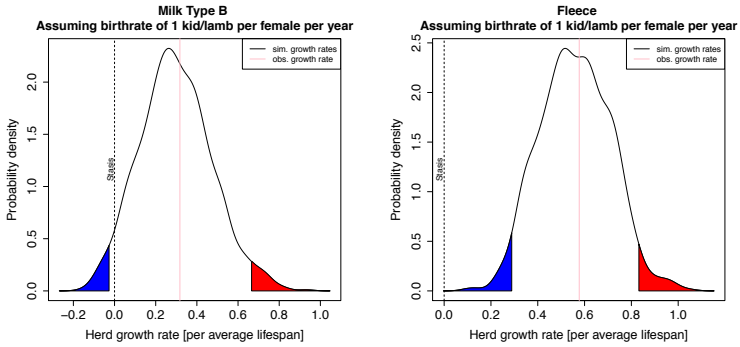

Fig. 4.19 Distribution of herd growth rates per lifetime distribution assuming 1 kid/lamb per female per year for Helmer models 'Meat Type A' (upper left),' Meat Type B' (upper middle), 'Milk Type A' (upper right), 'Milk Type B' (lower left) and 'Fleece' (lower right).

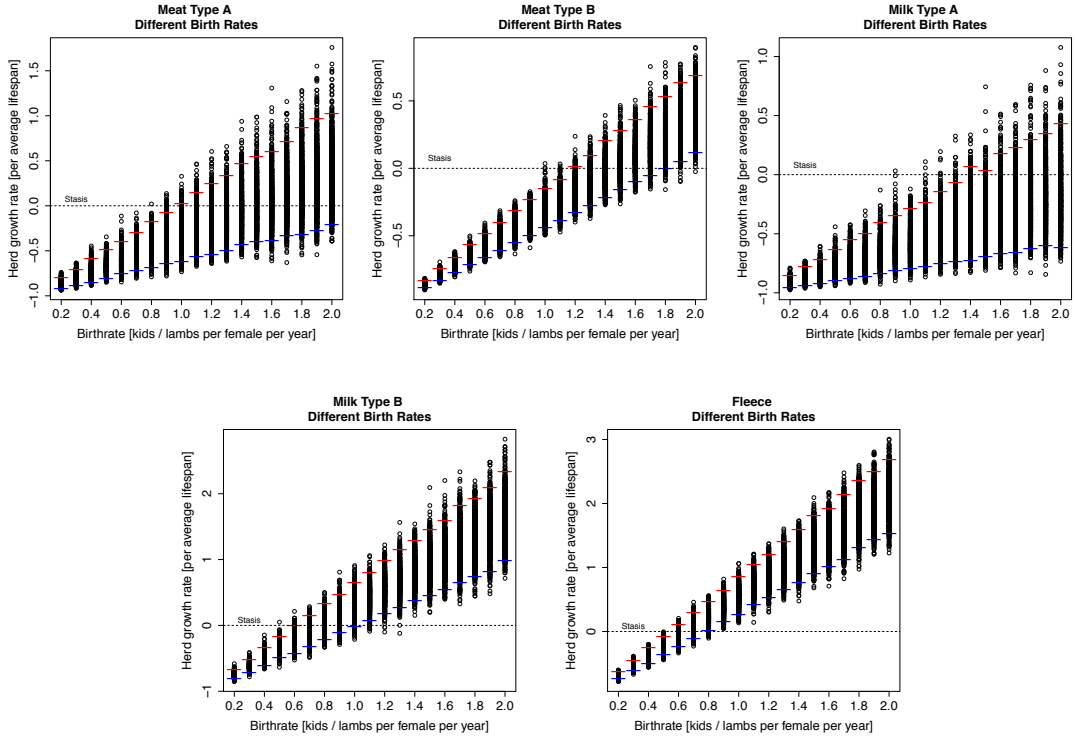

Fig. 4.20 Distribution of herd growth rates at increasing birth rates (from 0.2 – 2.0) for Helmer models 'Meat Type A' (upper left),' Meat Type B' (upper middle), 'Milk Type A' (upper right), 'Milk Type B' (lower left) and 'Fleece' (lower right).

4.9.3.2 Payne models

Payne has proposed idealised goat and sheep age-at-death profile models for maximizing milk, meat and fleece yields (Fig. 4.21). The figures below were reconstructed from the Payne publication (Payne, 1973). In these idealised profiles,

Payne (1973) was not constrained to archaeologically determinable age classes, and so recorded killings for 10 age classes, each representing one year of age of an animal. The 'milk' profile shows a high number of killings in the first year of an animal's age (corresponding to Payne's archaeological age classes A, B and C) as compared to all older animals (age classes D – I). Payne's 'meat' profile shows a high number of killings in the first three years of life and some killings in older animals. According to Payne, the model to obtain a high yield of fleece shows a high level of killing during the first year of life, a small number of killings in years 1-6 and a relatively high number of killing in later ages (6 – 10 years). When comparing all three of Payne's models, the 'milk' profile shows the highest number of killings (60 %) in the first year of age and also the lowest number of killings for ages 4-6 with 2%.

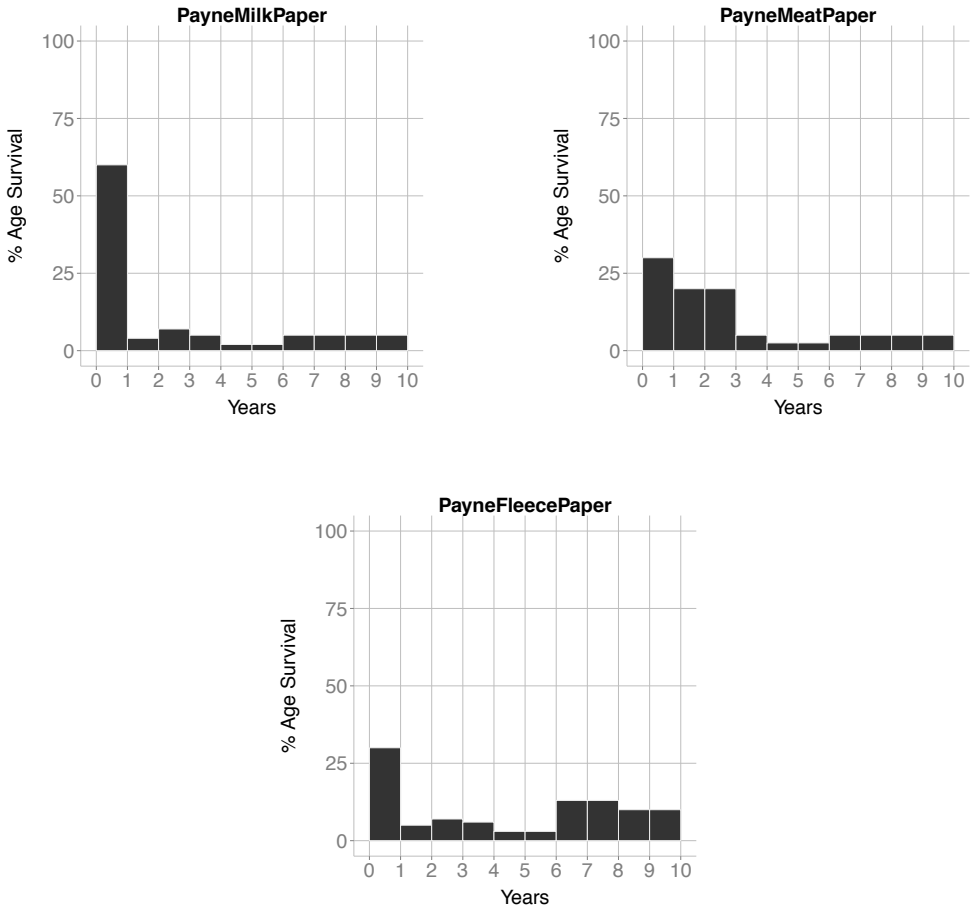

Fig. 4.21. Payne models (Payne, 1973) milk (upper left), meat (upper right) and fleece (lower middle).

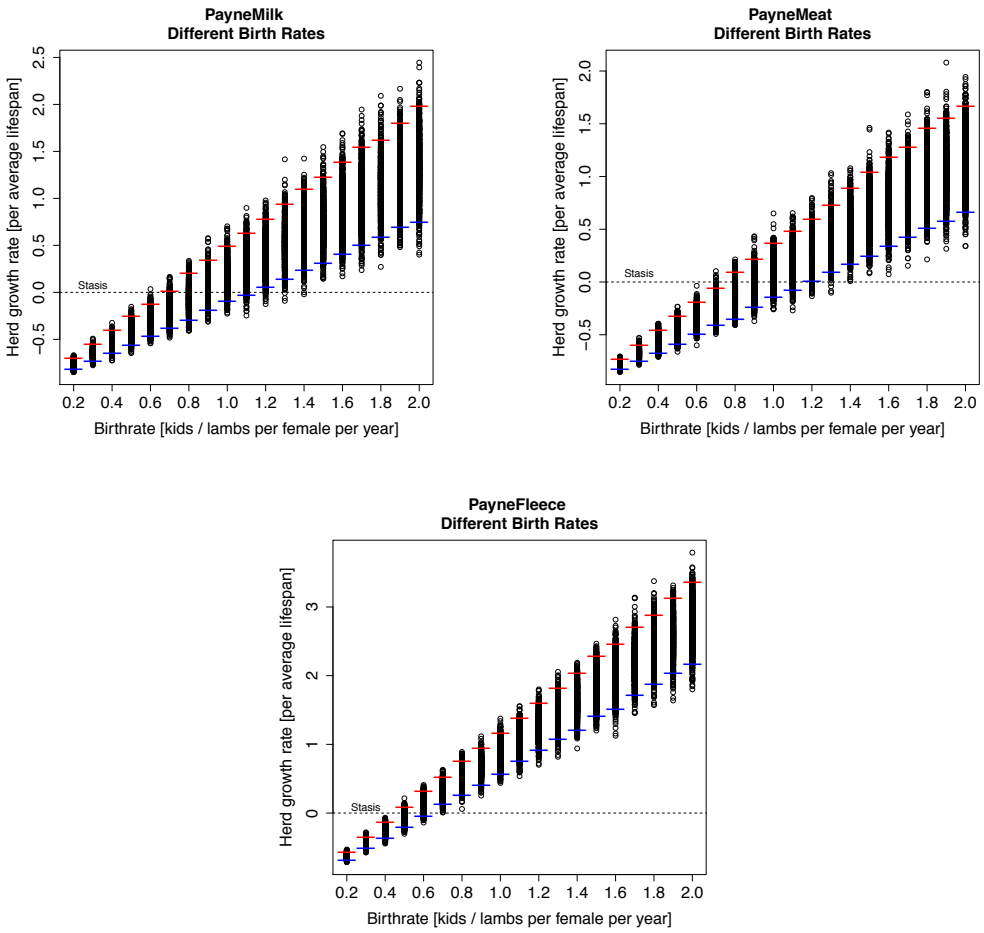

Fig. 4.22. Distribution of herd growth rates at increasing birth rates (from 0.2 – 2.0) for Payne's age-at-death models: 'milk' (upper left (a)) and 'meat' (upper right (b)) and 'wool/fleece' (lower middle (c)). Note: Pseudo-samples were generated by multiplying the proportions in each age class by 1000. The credible intervals presented have no meaning for idealised profiles as those profiles are models, not samples, and are not affected by sampling uncertainty. However, I retain the presentation of credible intervals based on pseudo-samples for comparison with those plots obtained from empirical data.

Payne's 'wool/fleece' model results in likely positive simulated growth rates under birth rate values greater than 0.5 (Fig. 4.22a). Payne's 'milk' and 'meat' profile growth rates are positive under a birth rate of ~ 0.8 and 1 (Fig. 4.22 a and b). Interestingly, higher growth rates are shown with a strategy oriented towards milk production rather than meat production.

4.9.3.3 Redding models

Redding proposed two idealised age-at-death profile models maximizing herd security and energy offtake (Fig. 4.23). The ‘security’ profile shows a high number of killings in the second age class and a small number of killings in the later age classes. The ‘energy’ profile shows a high number of killings during the first three years of life of an animal and a small number of killings during older age classes.

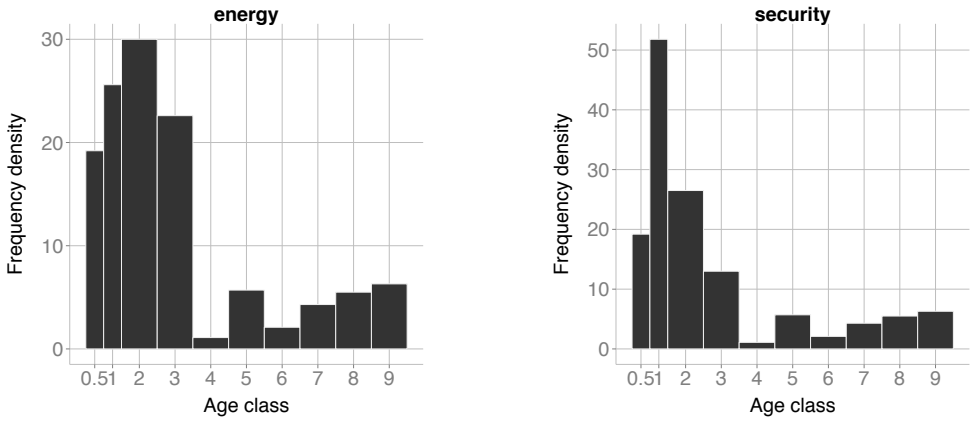

Fig. 4.23. Redding models (“energy” and “security”) (Redding, 1981).

Since Redding proposes a model for herd security, I expect the results to show positive growth rates at comparatively small birth rates. For the profile ‘energy’, I expect results with high numbers in meat/milk yield estimates (discussed in Chapter 5).

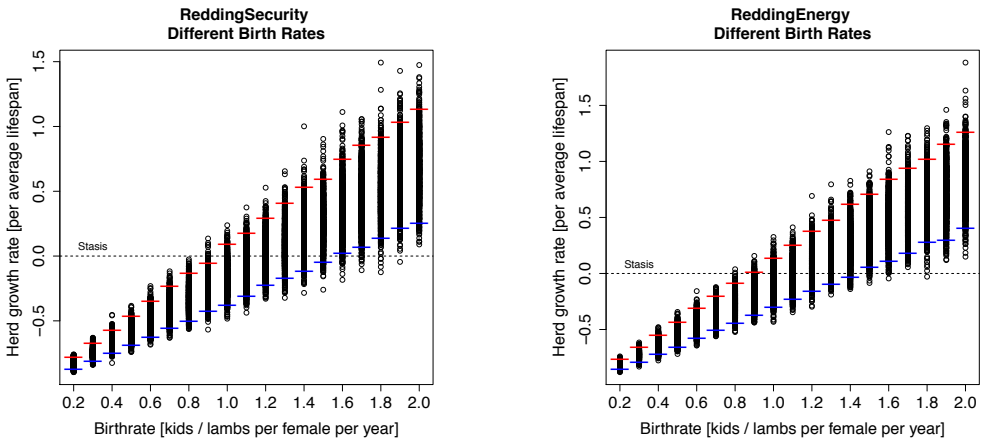

Fig. 4.24. Distribution of herd growth rates at increasing birth rates (from 0.2 – 2.0) for age-at-death profile models 'security'(left) and 'energy' (right). Note: Pseudo-samples were generated by multiplying the proportions in each age class by 1000. The credible intervals presented have no meaning for idealised profiles as those profiles are models, not samples, and are not affected by sampling uncertainty. However, I retain the presentation of credible intervals based on pseudo-samples for comparison with those plots obtained from empirical data.

Redding's 'security' model results in likely positive simulated growth rates under birth rate values greater than >~1.2 (Fig. 4.24 left), while the 'energy' model results in likely positive growth rates under birth rate values greater than ~1.1.

4.10 Discussion

The shape of an age-at-death profile may have been altered by past events such as taphonomic disruptions, epidemics and predation, affecting the animal population at the time of site occupation, or the extent to which the archaeologically-derived kill-off profile represents the true management strategy. Furthermore, various techniques for age determination of the animal bones exist and the method of choice for age determination can differ amongst archaeologists (personal communication with Dr. Katie Manning). Another issue is that changes in size of individuals can be the result of difference in sex, domestication, poor diet or early farmers simply preferred small

animals. All those factors might have had an effect on the shape of the mortality profile and thus its interpretation regarding animal exploitation strategies.

Additional limitations of the method described in this chapter include the assumption of an equal sex ratio in all age classes, and assumptions about the starting age of reproduction of the does/ewes. Since sex-asymmetric culling usually involves killing more males in early life, it is likely that the assumption of equal sex rations in all age classes will result in underestimation of the sustainability of herds. However, such assumptions, and other parameters, should affect analyses of different sites in a similar way. As such, the results presented for different sites should be considered in relative terms.

The approach presented here is novel in that it systematically attempts to estimate and compare herd sustainability based on both archaeological data and idealised kill-off profiles, and in that it attempts to accommodate sampling variation. Although related methods have been proposed to accommodate sampling variation when dealing with zooarchaeological data (Millard, 2006; Gerbault *et al.*, 2016; Price, Wolfhagen and Otarola-Castillo, 2016; Timpson *et al.*, 2018), none attempt to infer sustainability from age-at-death profiles.

Consideration of the herd sustainability inferences for individual site profiles is beyond the scope of this chapter. However, some general patterns can be discerned. Firstly, among the idealised model kill-off profiles, those directed towards fleece production generated the most easily sustained herds, followed by those directed towards meat, and then milk. This is unsurprising since more animals are expected to live until late into the reproductively active stage of their life when being raised for fleece.

When considering the inferences from archaeological data, it is interesting to note that for the majority of sites in dataset-A a birth rate between 0.8 – 1.2, and for datasets-B a birth rate of ~1.6 kid / lamb per female per year is required to make the

herds likely sustainable. Given the assumptions of the model employed, this raises the question: Were these herds truly unsustainable or were birth rates higher than 1 kid / lamb per female per year commonplace?

A detailed survey on the herding of unimproved sheep and goat herds – used here as a proxy for Neolithic caprine herds – states that both sheep and goats usually have birth rates > 1 kid or lamb per year (Dahl and Hjort, 1976). There are differences between the two species when it comes to lambing/kidding. In general, goats give birth more often than sheep, and additionally, twins and even triplets occur more often in goats. In addition, sheep tend to be more sensitive towards their environment, with the probability of twinning being higher in Welsh mountain sheep than in Sub-Saharan sheep, which are often exposed to droughts. Despite their differences, both species show birth rates > 1 kid/lamp per year. This resonates with the results from the analyses performed here, which also show that across all age-at-death profiles from the Neolithic period, birth rates > 1 would be required to make the herds likely sustainable (Fig. 4.16 and 4.17).

Redding's 'security' model shows a distribution of mainly negative growth rates and suggest that Redding's model would result in a declining, unsustainable herd rather than fulfilling its suggested purpose to secure animal numbers, unless underlying birth rates were high.

The model-based inference methodology presented here could be improved by including the possibility of inferring female:male sex-ratios, from which sex-specific product outcomes could be generated such as herd growth rates and milk yield estimates, which are only produced by females. This can be performed by including a sex ratio parameter as described in Chapter 5.

4.11 Conclusion

The method described in this chapter has given insight into whether an age-at-death profile from different time periods and archaeological contexts (datasets-A and B) or a profile representing a particular herding strategy (dataset-C) would have resulted in positive or negative herd growth rates. It also provides a means of estimating the underlying birth rates necessary to make herds sustainable given a particular culling strategy. This approach served as a stepping stone for a more powerful method described in the following chapter, which allows to incorporation of more information (e.g. information on the sex ratio in age-at-death profiles) needed to infer various product yields and economic efficiencies.

4.12 Collaborators

The work in this chapter is in direct collaboration with Dr. Rosalind Gillis, Dr. Anne Tresset, Stephanie Brehard, Prof. Barbara Horjes and Dr. Katie Manning. My role in the collaborations was to develop and apply the method described above to age-at-death profiles that were provided by these collaborators. Furthermore, I was provided with information on the ethology of sheep and goats, which was required for the approach described in this chapter and Chapter 5 by Dr Roger Blench, Dr. Anne Tresset and Stephanie Brehard.

[redacted]

Dr. Anne Trevet

Muséum national d'Histoire naturelle

UMR 7205 du CNRS

Archéozoologie, archéobotanique

55 rue Buffon - CP 56

75005 Paris (France)

Prof. Vigne Jean Denis

Muséum national d'Histoire naturelle

UMR 7205 du CNRS

Archéozoologie, archéobotanique

55 rue Buffon - CP 56

75005 Paris (France)

Stephanie Bedard

Muséum national d'Histoire naturelle

UMR 7205 du CNRS

Archéozoologie, archéobotanique

55 rue Buffon - CP 56

75005 Paris (France)

Prof. Barbara Helga

Institut für Orientalische und Europäische Archäologie

Österreichische Akademie der Wissenschaften

Fleischmarkt 22-02

A-1010 Wien

Dr. Nelia Hanning

UCL Institute of Archaeology,

31-34 Gordon Square,

London WC1H 0PY UK

Dr Roger Mason

McDonald Institute for Archaeological Research, University of Cambridge

8, Grant Road

Cambridge, CB1 2HL

United Kingdom

Chapter 5

5 Design and application of Bayesian Markov Chain Monte Carlo method to infer sex-specific mortality profiles and product yields from unsexed Caprini zooarchaeological remains

5.1 Background

The analysis of age-at-death profiles permits a view into the past by inferring prehistoric hunting strategies and decision-making related to herd practices. (Higham, 1968; Payne, 1973; Redding, 1981; Vigne, 1988; Helmer, 1992; Halstead, 1998; Helmer *et al.*, 2005; Vigne and Helmer, 2007; Price, Wolfhagen and Otarola-Castillo, 2016). Mortality curves (also called survivorship curves) are inferred from age-at-death profiles and can provide insights into the economic relationships of prehistoric farmers and their domesticates. In principle, when additional information on the ethology of an animal is provided, together with the mortality profile, it is possible to extract further information on herd sustainability and product yields. The previous chapter described a method for caprine herd sustainability inference that incorporates the sampling uncertainty associated with small sample sizes typically gathered from archaeological sites. In this chapter, I describe a full Bayesian Markov Chain Monte Carlo method to infer various productivity parameters, including herd growth rates, milk and meat yields, macronutrient and calorie yields, and herd economic efficiency, from archaeological age-at-death profiles from the Neolithic period and the Middle Ages in Europe. The method is designed, coded, tested and applied in collaboration with colleagues Dr. Yoan Diekmann (UCL), Dr. Rosalind Gillis (University of Algarve) and Prof. Mark Thomas (UCL).

Not only is it possible to infer herd growth rates with the method presented here, but also estimate meat and milk yields, which are derived from inferred sex-specific survival curves. This is informative to archaeologists, who have proposed to characterise and date but also to estimate the secondary product revolution, which involved an increasing exploitation of domesticates for their renewable products, such as milk and fleece/wool and the use of traction, during the fourth-third millennia BC within Europe and West Asia (Payne, 1973; Sherratt, 1981; Halstead, 1998; Vigne and Helmer, 2007). This method also permits to identify the relative quantity of those products produced per animal and per forage / fodder consumed.

5.2 Sex ratios

Estimating the age from dental eruption, replacement and wear pattern or epiphyseal fusion data of animal remains, has proven challenging but several techniques exist for age estimation (Payne, 1973; Zeder, 2006b). However, determining the sex of sheep or goat archaeological remains is even more challenging and, as such, kill-off profiles are only rarely provided with information on the sex of the animals. The method presented here permits the inference of sex-specific survival curves from unsexed age-at-death profiles, thus enabling estimation of food product yields and herd growth rates. This is because – of course – only females are able to produce offspring and milk and therefore are almost solely responsible for herd growth rates and milk production outcomes (only a very small number of males are required for reproduction). Meat yields, on the other hand, are generated from female and male animals. In addition to meat and milk estimates, economic efficiency rates of various slaughter practices are estimated by incorporating information on forage and fodder consumed, which serves as a proxy for the economic costs of animal keeping.

5.3 Overview of the method

It is well-known that modern herd management strategies usually involve differential slaughter of males and females at different ages (Meniel, 1987; RIM., 1992; Zeder, 2001; Zeder *et al.*, 2006; M. A. Zeder, 2008; ETHIOPIA and AGENCY, 2011). The reasons for this are various but include: (a) females can produce young and milk throughout their adult life whereas the returns on the only food product of males – meat – is maximised as they approach full adult size; (b) culling young animals increases milk availability from their mothers. As such, it is likely that sex-asymmetric slaughter was also a feature of past herd management. Thus, we expect sex ratios to change throughout the age range of managed animals according to some pattern. A simple model of sex-ratio change by age is a sigmoidal decay in sex ratios, starting at 1 (i.e. an equal number of males and females are born) and declining at a rate determined by a single parameter sigma (σSR). Other models include linear decay and exponential decay in the sex ratio, again starting at 1. A convenient feature of these and other models is that they each have only one parameter. This means that if one of these models of sex-ratio change by age can be shown to operate in modern unimproved and sexed archaeological herds, then its parameter value can be estimated from unsexed age-at-death profile, since the value for that parameter constrains the kill-off profile.

Below I give a step-by-step, simplified overview of a full Bayesian Markov Chain Monte Carlo method to infer sex-specific mortality profiles and product yields from unsexed Caprini zooarchaeological remains, integrating a model (and its associated parameter value) of herd sex-ratio change by age. A more detailed explanation can be found in the method section of this chapter.

An unsexed kill-off profile is constructed from skeletal remains from an archaeological site. The probability of an observed kill-off profile can then be calculated given the proportion of animals killed in each age class, and a value of

sex-ratio change by age parameter (Fig. 5.1a). The formulation of this calculation is known as a likelihood-function. The parameter space of the proportion of animals killed in each age class, and a value sex-ratio change by age parameter is then explored using the Metropolis Hastings (Hastings, 1970) Markov-Chain-Monte-Carlo (MCMC) algorithm. This is a Bayesian inference approach that correctly samples the joint posterior distribution of the parameters of interest, given the kill-off profile data and model. Each sample from the MCMC chain represents a possible set of values of the proportion of animals killed in each age class, and a value sex-ratio change by age parameter (Fig. 5.1b). From this – using estimates of milk, meat and offspring yields, and milk and fodder consumed, per animal for each age value – an estimate of overall productivity per animal lifetime, and per unit of fodder consumed, can be calculated (Fig. 5.1c). Since each sampled step in the Markov-Chain represents a random sample from the joint posterior distribution of the parameters of interest, each set of estimates of overall per productivity animal per lifetime, and per unit of fodder consumed, represents a random sample from the joint posterior distribution of those outcomes, given the kill-off profile data and model (Fig. 5.1d). In practice, I usually ran the Monte-Carlo Markov-Chain for around 20 million steps, to ensure good sampling of parameter space.

(a)

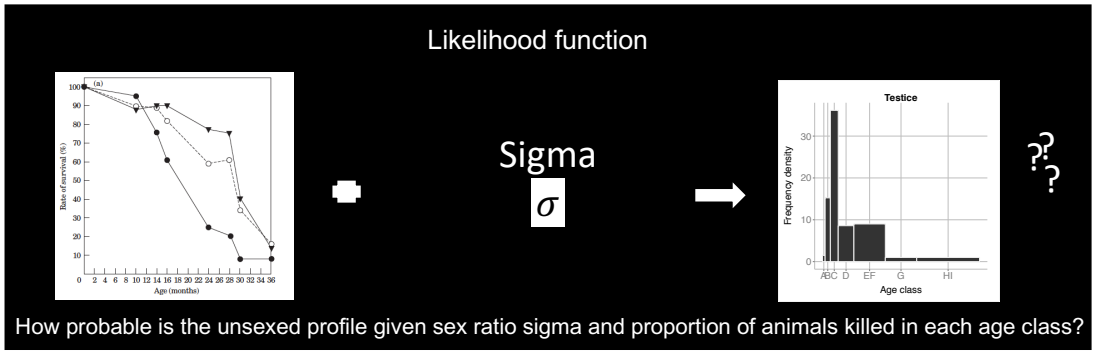

Estimation of parameters (e.g. female and male proportions) using MCMC employing Metropolis Hasting algorithm

(b)

Joint posterior distributions for sex ratio parameter, females (red), males (blue), total (black) for each age class.

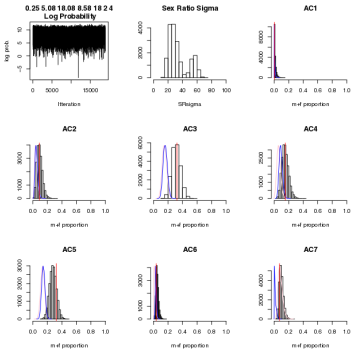

x million simulations

(c)

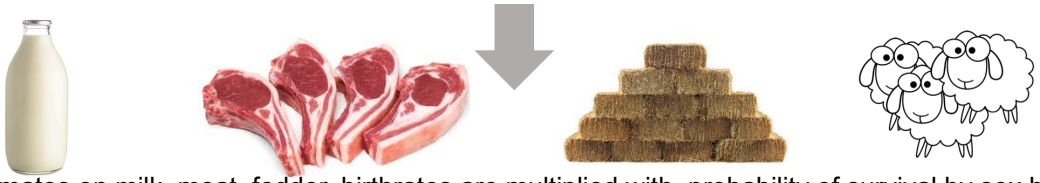

Estimates on milk, meat, fodder, birthrates are multiplied with probability of survival by sex by age for each month

(d)

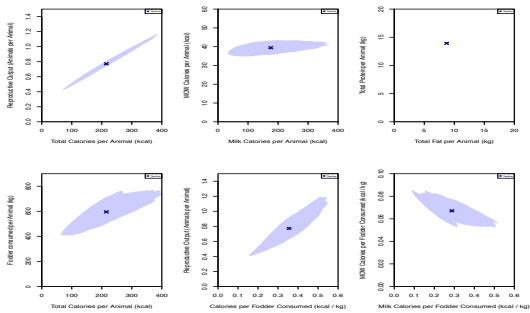

Joint posterior distributions of various productivity outcomes

Fig. 5.1 Overview of method

5.4 Input parameters

Information on estimates for product yields generated per animal per age, ethological information such as birth rates in does/ewes, information on fat or protein in meat and milk and quantities of fodder consumption of the animals, was gathered from literature (Dahl and Hjort, 1976; Mourad, 1992; Tresset, 1996; Food and Organization, 2003; Todaro *et al.*, 2015) and public databases (the U.S. Department of Agriculture National Nutrient Database for Standard Reference). For each MCMC sample, probabilities of survival by sex per month and the ethological information result in estimates of overall productivity per animal lifetime, and per unit of fodder consumed. More specifically, by summing across all months of life and then multiplying by the probabilities of female animals being alive and expected yields at different ages (for overall milk and offspring yields), of young animals that are dependent on their mother's milk, and expected milk consumed at different ages (for overall milk consumed) and of dead animals of both sexes and expected meat yields at different ages (for overall meat yields), product yields per animal per lifetime are obtained. The ethological data are provided in a separate table (Table B.1 in Appendix) The data table shows information on meat, macronutrient yields and milk consumed by kids/lambs for ovicaprines aged 1 to 96 months.

Mean milk yield estimations (kg per female per month) were retrieved from a publication on modern Egyptian goats (Mourad, 1992). This work, which is based on an unimproved herd, is the closest information available to approximate caprine stock yields from the Neolithic. It is assumed that, on average, milk production begins at 15 months of age, allowing 12 months for the females to become fertile and 3 months of pregnancy (Dahl and Hjort, 1976). Furthermore, one lactation per year per doe/ewe is assumed (Todaro *et al.*, 2015). After 78 months of age, milk yields successively reduce (Dahl and Hjort, 1976; Todaro *et al.*, 2015). Milk consumed by kids/lambs in kg per month (Food and Organization, 2003) is then subtracted from the overall milk yields in order to obtain an estimation for milk yields remaining for human

consumption. For the milk parameters, the milk yield is multiplied with the estimated proportions of surviving females and then the milk consumed by the kids/lambs is subtracted from the overall milk yield.

Meat and offal weight (MOW) in kg per animal at each month of age was considered for human consumption (Tresset, 1996). The MOW parameter has been calculated by incorporating information on growth rates of the ovicaprines and live weight in kg per animal per month (Vigne, 1991; Tresset, 1996). This calculation was performed according to the 'meat and offal method' in Vigne (1991), which was then optimized by Tresset (1996). If multiple datasets were gathered giving information on one estimation, for example meat yields (See tables B.4 – B.21 in Appendix), the mean for MOW in kg of all meat datasets was calculated. For MOW, the inferred proportions of female plus male dead animals are multiplied by the MOW at different ages.

Information on the fodder consumption per animal (Food and Organization, 2003), which is supplementary hay provided in addition to grazing, serves as a general proxy for the economic costs of animal keeping, but is not an absolute measure of quantity of food consumed. I estimate the overall economic efficiency of different slaughter strategies by dividing the estimates described above by consumed fodder.

Information on macronutrients (here fat and proteins of milk and meat) and energy content (calories in kcal) of the animal products, is incorporated into the method. Meat and milk have a protein content of ~0.21 kg protein in MOW per kg/month (Redding, 1981; U.S. Department of Agriculture, 2015) and ~0.05 kg protein in milk kg/month from females (Redding, 1981; U.S. Department of Agriculture, 2015) and a fat content of ~0.02 kg fat in MOW kg/month (U.S. Department of Agriculture, 2015) and ~0.04 kg fat in milk kg/month from females (U.S. Department of Agriculture, 2015). If more than one reference for meat or milk macronutrients is available (tables

B.4 – B.21 in Appendix) the mean from all references is calculated. The values for protein and fat (kg) in MOW are then multiplied by the inferred proportions for males plus females while the values for protein and fat (kg) in milk are multiplied by the proportions for females only.

Estimates for calorie content are ~1887 kcal per kilo of MOW (U.S. Department of Agriculture, 2015) and ~874 kcal per kilo of milk (Redding, 1981; U.S. Department of Agriculture, 2015).

A conservative estimate for birth rates of one kid/lamb per female per year were taken from Dahl (1976), who observed many different caprine herds and their birth rates throughout a long time-span.

5.5 Overview on the output estimates

With the method presented here, I infer estimates of milk, MOW, macronutrient and energy yields, and of the economic efficiency of keeping goat/sheep herds from kill-off profiles. The distributions of these estimates are plotted in various combinations (Fig. 5.1d). It should be noted that the estimate distributions reflect sampling uncertainty in the kill-off profiles, but do not reflect uncertainty in the estimates of product yields based on modern unimproved herds.

The underlying parameters estimated are: (1) sex ratio change parameter, (2) probability of survival for females for each age class (ranging between 7 – 10 age classes), (3) probability of survival for males for each age class (ranging between 7 – 10 age classes) (Fig. 5.1 c). From these parameter estimates, the following derivative yield estimates are generated by performing calculations on the underlying parameter estimates using ethological data: (1) Reproductive output (animals per animal), (2) Milk yields per animal (kg), (3) Milk consumption by lambs/kids (kg), (4) Milk available for human consumption (kg), (5) Milk protein per animal (kg), (6) Milk fat per animal (kg), (7) Milk calories per animal (kcal), (8) MOW yields per animal (kg), (9) MOW

protein per animal (kg), (10) MOW fat per animal (kg), (11) MOW calories per animal (kcal), (12) Fodder (hay) consumed per animal (kg), (13) Total protein per animal (kcal / kg), (14) Total fat per animal (kcal / kg), (15) Total calories per animal (kcal), (16) Proportions of total calories from milk, (17) Milk yields (kg) per animal per fodder consumed, (18) MOW yields (kg) per animal per fodder consumed, (19) Milk calories per fodder consumed (kcal / kg), (20) MOW calories per fodder consumed (kcal / kg), and (21) total calories per fodder consumed (kcal / kg).

5.6 Interpreting the results

Estimates of total calories per fodder consumed is used as a proxy for the underlying economic efficiency of a kill-off strategy. In order to show predictions for economic efficiency, I plot parameter 'Fodder (hay) consumed per animal (kg)' versus 'total calories per animal (kcal)' as shown in an example in Fig. 5.2, which is one of the six plots in Fig. 5.1d. An example for macronutrient outputs would be plotting parameters 'Total protein per animal' against 'Total fat per animal' (Fig. 5.1d). Here I infer protein versus fat yields, which a herd would have produced given a particular profile (in Fig. 5.2 inferred from the archaeological site Testice; a Neolithic site located in the North-West of Europe). This is one example of how results obtained from the method described in this chapter can be visualised.

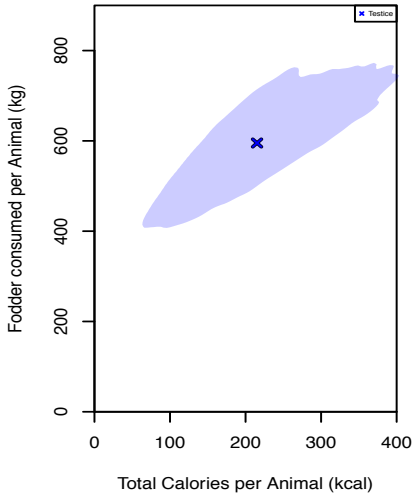

Fig. 5.2. Example for inferring economic efficiency from age-at-death profile from Testice archaeological site.

5.7 Key components of the method: A short introduction to Bayesian statistics, Markov Chain Monte Carlo (MCMC) and the Metropolis-Hastings algorithm.

Bayesian Statistics are a form of conditional probability that employ prior knowledge about parameters of a model, and are often seen as an alternative to the more commonly used frequentist approach to statistical inference. The latter treats probabilities as the result of some number of trials such as throwing a coin, which will eventually result in some proportion of landing head or tail (Bayes, Price and Canton, 1763).

Bayesian Statistics are underwritten by Bayes Theorem, which is expressed in the following equation:

$$P(A|B) = \frac{P(B|A)P(A)}{P(B)} \qquad (1)$$

This equation formulates how we can calculate the probability (P) of a model (A) given (or conditional on, denoted by '|') some data (B) (i.e. P(A|B), otherwise known as the posterior) in terms of the probability of the data given the model (i.e. P(B|A),

otherwise known as the likelihood), the prior probability of the model (i.e. P(A), also known as the prior) and the probability of the data (i.e. P(B), otherwise known as the marginal). The formula is actually true more generally in the realm of conditional probability (i.e. A and B could be any events that have dependency), but in most modern applications of Bayesian inference, A refers to some model / hypothesis / parameter value, and B refers to some data.

The main challenges of implementing Bayesian inference with anything but the simplest models are (1) formulating P(B|A), the likelihood function, and (2) finding a method to search the often very large set of possible parameter value combinations (i.e. the parameter space) in a computationally efficient manner. The first of these challenges is often unsurmountable (although fortunately not here), even for apparently simple models. For the second challenge there are, fortunately, a number of computational solutions, of which the Metropolis Hastings (Hastings, 1970) Markov-Chain-Monte-Carlo (MCMC) algorithm is the oldest, and a widely used example.

In the context of this chapter the above formulation means that, given the archaeological data, the inference method estimates posterior probabilities on sex ratio change by age and the male and female survival proportions per age class.

Metropolis-Hastings (Hastings, 1970) MCMC algorithm is computational method for randomly sampling from the joint posterior distribution of a set of parameters. This means that it produces a large set of values of parameters, which can then be plotted using a density function (for example, kernel density) to generate a posterior distribution. The Monte Carlo part of the MCMC process refers to an inherent randomness in how the algorithm searches parameter space. The Markov chain part of the MCMC process refers to a sequence of parameter values in which each value is dependent on the previous value in the sequence only. By applying a set of rules for deciding how to move in this parameter space, the Metropolis-Hastings algorithm

achieves its aim of sampling from the joint posterior distribution. These rules involve deciding which proposed parameter values to accept or reject, based on their prior values and the likelihood.

5.8 A model for sex asymmetry by age

For the above approach to be applied to unsexed kill-off data, we require a simple model of sex ratio change by age. We tested six one-parameter models (negative exponential, uniform, linear, power function, rational function and sigmoidal) by examining which of a range of archaeological and modern observed sex ratio datasets is best explained (see Appendix, Table B.3) by each model. This model-fitting is performed by minimizing the sum of squared differences between modelled and observed sex ratios (the model fitting was performed by my colleague Dr. Yoan Diekmann). The results of this testing are presented below, but because the final choice of model of sex ratio change by age is relevant for the following sections, I note here that the best fitting model was a sigmoidal decay model.

5.9 Model for sexed age-at-death profiles

The following description and formulation of the likelihood function was provided by Dr. Yoan Diekmann: We consider n age classes with upper limits $\boldsymbol{u} = u_1, \dots, u_n$. For convenience, we set $u_0 = 0$. The input data consists of counts $\boldsymbol{c} = c_1, \dots, c_n$ quantifying the number of individuals (of unknown sex) per age class for which skeletal remains were found. We treat the age class inferred for a given individual as a "hard" classification, *i.e.* we do not consider the uncertainty associated to assigning skeletal remains to age classes as for example in Caussinus and Courgeau (2010).

The model is based on a series of assumptions: (1) the male to female sex ratio is modelled by a sigmoidal decay function $r_\sigma(x) = e^{-\frac{x^2}{2\sigma^2}}, \sigma > 0$, over continuous time

x, implying that the sex ratio at birth ($x = 0$) is one (*i.e.* males and females are born in equal proportions, and that males outnumber females at no time). (2) we do not allow for the possibility that animals join the herd at a later age class (*i.e.* the number of births equals the number of deaths). As such the model does not permit the possibility of animals having been brought into the herd from the outside. Note that the last two assumptions imply that sex ratio change is driven solely by excess killing of males. (3) beyond the killing of males required to match a given sex ratio, males and females are killed in equal proportions. (4) no individual survives beyond the last age class (*i.e.* at time point u_n all individuals are dead and as such this model does not permit for the possibility of animals to be taken away from the herd). Examples for such a scenario would be selling stock, predation, and death due to diseases, which cause an animal to die outside of the archaeological site, and may result in an unbalanced number of animal input-output.

In order to formalise the above assumptions, we introduce the following parameters besides the sigmoidal decay parameter σ. Let $\boldsymbol{f} = f_1, \dots, f_n$, $\boldsymbol{m} = m_1, \dots, m_n$, $\boldsymbol{a} = a_1, \dots, a_{n-1}$, and $\boldsymbol{b} = b_1, \dots, b_{n-1}$ be the proportion of females surviving per age class, the proportion of surviving males, the proportion of males killed due to sex ratio, and the remaining proportion of animals killed per sex, respectively. Note that proportion of animals killed per sex b_i is the same, single value for males and females, due to the third assumption. By definition we have the relations $f_{i-1} - b_i = f_i$ and $m_{i-1} - (a_i + b_i) = m_i$, $1 \leq i \leq n-1$, with $f_0 = m_0 = \frac{1}{2}$ and $f_n = m_n = 0$ following from the first and last assumption respectively. Furthermore, the second assumption constrains a_i and b_i to be positive, *i.e.* $a_i \geq 0$ and $b_i \geq 0$. Lastly, the first assumption requires that males and females survive in proportions dictated by the sigmoidal decay function. We discretise $r_\sigma(x)$ using the definition of the mean of a function, *i.e.*

$$\bar{r}_\sigma(i) := \frac{1}{u_i - l_i} \int_{l_i}^{u_i} r_\sigma(x)\, dx = \frac{m_i}{f_i} \text{ for } 0 \leq i \leq n-1.$$

To infer probable parameter values for $\boldsymbol{\theta} = \{\boldsymbol{f}, \boldsymbol{m}, \boldsymbol{a}, \boldsymbol{b}\}$ and σ from observed counts $\boldsymbol{c}$, we derive an expression for the joint probability of the model parameters given the input data, $P(\boldsymbol{\theta}, \sigma | \boldsymbol{c})$. We begin by transforming the probability term (applying the definition of conditional probability and Bayes' rule in line 1 and 3 and the definition of independence in line 2)

$$\begin{aligned} P(\boldsymbol{\theta}, \sigma \mid \boldsymbol{c}) &= P(\sigma|\boldsymbol{\theta}, \boldsymbol{c})\, P(\boldsymbol{\theta}|\boldsymbol{c}) \\ &= P(\sigma|\boldsymbol{\theta})\, P(\boldsymbol{\theta}|\boldsymbol{c}) \\ &= \frac{P(\boldsymbol{\theta}|\sigma)\, P(\sigma)\, P(\boldsymbol{\theta}|\boldsymbol{c})}{P(\boldsymbol{\theta})}. \end{aligned}$$

If we define the three factors in the numerator and discard the denominator, which is independent of the data, we obtain an expression that is proportional to the true joint probability. That is enough for parameter inference, for example with MCMC. First, counts $\boldsymbol{c}$ are linked to proportions of surviving and killed animals $\boldsymbol{\theta}$ using the Dirichlet distribution, here with uniform prior

$$P(\boldsymbol{f}, \boldsymbol{m}, \boldsymbol{a}, \boldsymbol{b} \mid \boldsymbol{c}) = \mathrm{Dir}(a_1 + 2b_1, \ldots, a_{n-1} + 2b_{n-1}, f_{n-1} + m_{n-1};\ \alpha_i = 1 + c_i).$$

Note that $(a_1 + 2b_1, \ldots, a_{n-1} + 2b_{n-1}, f_{n-1} + m_{n-1})$ is the inferred age-at-death profile, with $f_{n-1} + m_{n-1}$ for the last age class following from the fourth assumption above. Second, relating σ and the inferred age-at-death profile works by ensuring that both are compatible. For example, whenever the sex ratio does not change over time, there cannot be any inferred additional male killings, *i.e.* $\sigma \gg 0 \Rightarrow a_i \approx 0$. As at most one σ can satisfy the constraints $\frac{m_i}{f_i} = \bar{r}_\sigma(i)$, $0 \le i \le n-1$, for given proportions $\boldsymbol{f}$ and $\boldsymbol{m}$, compatibility can be modelled by the likelihood function

$$P(\boldsymbol{f}, \boldsymbol{m}, \boldsymbol{a}, \boldsymbol{b} \mid \sigma) = \begin{cases} 1 \text{ if } \dfrac{m_i}{f_i} = \bar{r}_\sigma(i) \text{ holds for all } i \in \{0, \ldots, n-1\} \\ 0 \text{ else} \end{cases}$$

and an arbitrary prior distribution $P(\sigma)$ on σ, informed, for example, by data from modern unimproved herds. As already discussed above, the normalising factor $P(\boldsymbol{\theta})$ is not required in the context of MCMC.

5.10 Model parameter inference

The parameter inference starts by setting the initial MCMC parameter values. The initial value for sigma is sampled uniformly within the domain of 0 and 100. The initial age-at-death profile is computed by randomly sampling the vector for the proportion of males killed due to the initial sex ratio. From that vector the other parameters can be inferred. The very next new AaD death profile is sampled from the Dirichlet distribution. This procedure will be performed x number of times, eventually resulting in distributions with the inferred male, female and combined posteriors for each age class. There is a burn-in stage, which means discarding the initial parameter values inferred until the MCMC chain has stabilised, and a thinning, which defines the interval by which the parameter will be recorded (to avoid autocorrelation in parameter samples).

Number of simulations, the thinning, burn-in and the proposal function parameter space are meta-parameters and their setting depends on the results of the posterior distributions and (MCMC)-chain mixing. One may increase the number of simulations, for example, in order to increase confidence in the inference. To check sufficient thinning, the level of autocorrelation between successive values in the chain needs to be analysed. A small autocorrelation indicates sufficient thinning. The Gelman and Rubin shrink factor (Gelman and Rubin, 1992) indicates whether the numbers for the burn-in and simulations are sufficient. This part of the method has been developed by Prof. Thomas and Dr. Diekmann.

5.11 Methodology validation

In order to validate the method, its behaviour needs to be tested by simulating data under the model conditions and known parameter values and compare those to the values obtained from the MCMC. The parameters to be simulated under the model are the vector (size of vector depending on the number of age classes) for the proportions of males killed, from which the rest of the to be inferred parameters can be calculated to obtain the proportions for an AaD profile. The sampling of the proportions of males killed, is performed uniformly. As mentioned above, the model inference underlies a number of assumptions, one being that the males never outnumber the females. The sampling is therefore limited (sampling in between upper bound (blue) and lower bound (red) in Fig. 5.3). In order to obtain counts for an AaD profile, the full proportions of animals per age class, resembling the proportions of a full AaD profile, are sampled from a multinomial distribution. Parameter sigma is sampled from the prior distribution, which is a distribution of sigmas generated with a kernel density smoothing method of sigma values obtained by the least square optimisation from 23 observed archaeological and modern sex ratios datasets (Table B.3. in Appendix) (Meniel, 1987; RIM., 1992; Zeder, 2001; Zeder *et al.*, 2006; M. A. Zeder, 2008; ETHIOPIA and AGENCY, 2011). To assess the accuracy of the method, the validation is performed for different total number of counts (n= 10, 20, 50, 75, 100, 150, 200) and for 50 different sigma values.

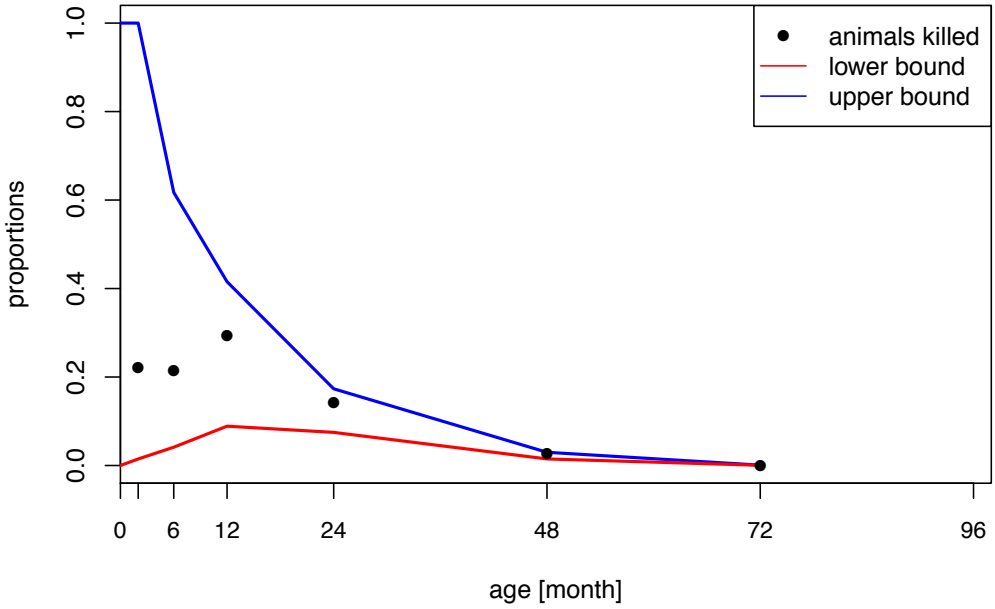

Fig. 5.3. The bounds on the female and male proportions, forming the age-at-death profile, for the simulation scheme detailed in this chapter. The underlying value for σ is 17. Graph was provided by Dr. Diekmann.

5.12 Data used and estimation of derived quantities

All age-at-death profile datasets have been thoroughly described in Chapter 4. The method described here is applied on a subset of the MNI dataset (see Appendix) i.e. dataset-B, which contains the Minimum Number of Individuals per age class. The values for the MNI datasets usually derive from an age estimation performed on whole jaws, while the values for the datasets given in 'Number of Elements' derive from tooth wear stages. Currently, the statistics between the two are poorly understood, which is why we have chosen the MNI datasets here. However, the Meta-Analysis, which is described in Chapter 6, will also involve the datasets containing the data provided in number of elements for each age class i.e. dataset-A. From 76 profiles, I have elected to examine the ten AaD profiles with the smallest total number of samples and ten profiles with the ten largest total number of samples (Table. B.2 in

Appendix). With differing total samples sizes, we can illustrate the credible intervals generated with small samples versus large samples, showing that sampling uncertainty within the small sample sizes leads to wider credible intervals (Fig. 5.5). The archaeozoological data come from 18 Neolithic sites (20 phases), that span from the early Neolithic period (Silourokambos, Cyprus: 9th to 8th millennia BC) to the late Neolithic (Mondsee, Switzerland, 2nd millennium BC; Phaistos, Greece, 4th millennium BC; Champ Durand and La Fare, France, 4th-3rd millennia BC). The majority are early Neolithic sites of the Balkans (Miercurea Sibiului, Pojejena Nucet and Ecsegfalva), the Mediterranean (Prodromos, Greece; and Arma dello Stefanin Colle Santo Stefano and La Draga, Italy) dating from the 7th-6th millennia BC. The remaining sites are representative of the Middle Neolithic: Trasano (Italy, 5th millennium BC), La Barmez sur Collembey (Switzerland, 4thmillennium BC), Lerna and Dimini (Greece, 6th-5th millennia BC).

In addition, I analysed ten published 'idealised profiles' (i.e. dataset-C from Chapter 4). I aim to show how the idealized profiles perform under the Bayesian inference method. I expect that the results inferred from the idealized profiles on animal productivity are reflected in elevated quantities for the milk or meat yields for Vigne's and Helmer's models and high growth rate values inferred from Redding's 'herd security' model.

To examine if inferred productivity and reproductive output rates increased after the end of the Neolithic, I also analysed 12 published age-at-death profiles from various archaeological sites ranging from the Bronze Age to modern times (Payne, 1973; Albarella and Davis, 1996; Albarella, 1999; Albarella *et al.*, 2009). As opposed to the archaeological profiles mentioned above, these profiles are based on number of elements within each age class and not MNI. Out of these 12 archaeological sites, the earliest (second half of 2nd millennium BC) is La Stanza in south Italy (Albarella, 1999). Caprine mandibles have been arranged into nine age classes following tooth eruption stages as suggested by Payne (1973). The archaeological site, Asvan Kale,

in Eastern Anatolia, provides three kill-off profiles from the Roman and Medieval times (provided in number of elements into nine age classes) and one profile from modern times with estimates on kill-off numbers (ten age classes in proportions) from Iranian herders (Payne, 1973). Archaeologists unearthed caprine bones at Norwich Castle in East England, of which five kill-off profiles were constructed spanning the time during the early Saxon era to post-medieval times (Albarella *et al.*, 2009). Data are given in counts of number of elements of tooth eruption stages, which are arranged into 9 age classes. The same age class system is used for the three age-at-death profiles from Launcenston Castle in Cornwall, West England (Albarella and Davis, 1996). The accuracy of the data of the profiles varies in quality, as some of the profiles are inferred from published graphs.

5.13 Sex ratio datasets

Twenty-six sex-ratio by age datasets (Table B.3. in Appendix) on archaeological and modern, unimproved sheep and goat herds, were gathered (Meniel, 1987; RIM., 1992; Zeder, 2001; Zeder *et al.*, 2006; M. A. Zeder, 2008; ETHIOPIA and AGENCY, 2011). Of these, 16 datasets were from modern unimproved sheep and goat herds from Ethiopia and Nigeria. One dataset comprises mixed, wild and domesticated animals, whilst the other five are from strictly unimproved herds. While some data stem from pastoralists and comprise only one herd, other data stem from a survey comprising all available animals in the country. As such the total number of individuals varies between 28 (RIM., 1992) and 22786947 (ETHIOPIA and AGENCY, 2011). Categorising goat/sheep into ‘unimproved’, ’wild’ or ‘domesticated’ categories proved challenging, as sufficient information was not always available. In some cases, these are estimated based on details found in the literature. For example, the Nigerian modern caprini were put into the category ‘unimproved’, because those herds are

mainly used by local farmers and have not been bred as extensively as goats/sheep in developed countries.

Similarly, the sheep/goats sex-ratio datasets from Ethiopia were retrieved from a livestock survey conducted in 2010/2011 (ETHIOPIA and AGENCY, 2011). It was not specifically stated that the herds were unimproved. However, the animals were from private peasant holdings in rural sedentary areas of the country, and the animals were not likely to have been under extensive and/or strategically selective breeding.

Most of the ten archaeological datasets are recorded as so called 'Long Bone fusion scores', a formula designed by Zeder and colleagues (2008), which is based on the computation of the number of fused or unfused bone elements, instead of animal counts as presented in the sex-ratio datasets of modern, unimproved herds. The archaeological datasets mostly comprise domesticated animals (eight datasets). However, one dataset is a mixed herd (wild and domesticated animals) and another dataset comprises wild gazelles. It is expected that the wild gazelles do not show any asymmetry of sex ratios, as opposed to the managed caprini herds.

5.14 Results

5.14.1 Testing models of sex ratio change by age

Six proposed single parameter models of sex ratio change by age were tested for fit to observed sex ratio values gathered from modern and archaeological datasets. The sigmoidal model provided the best fit in most cases, as can be seen in the figure below (Fig. 5.4).

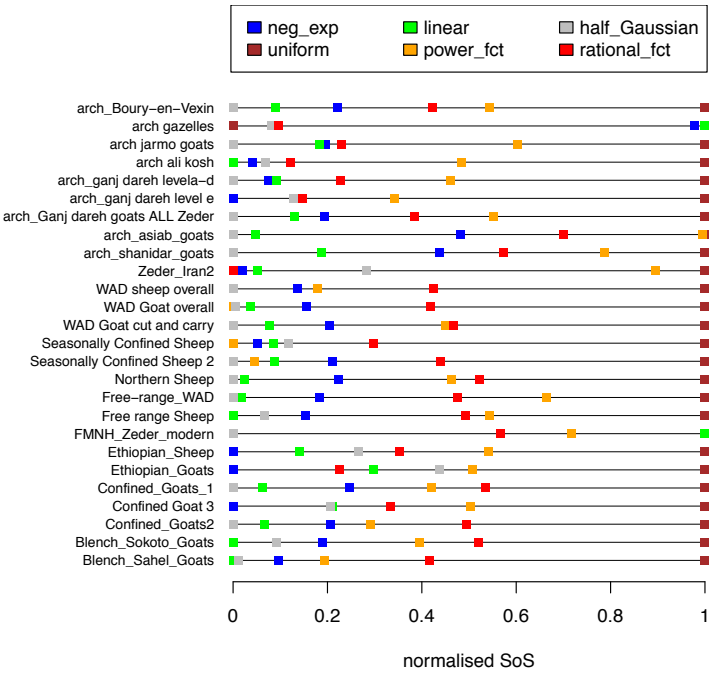

Fig. 5.4. Six single-parameter models (negative exponential function, blue box; linear function, green box; half Gaussian (with parameter sigma) function, grey box; uniform function, brown box; power function, orange box and rational function, red box) are tested (Sums of Squares - Sos) for their best fit on 26 modern and archaeological sex ratio datasets. Plot generated by Diekmann.

In general, the modern sex ratio datasets fitted better to this model than the archaeological profiles. Three datasets show sum of squares values greater than 100, indicating poor fits. As the three outliers were data gathered from wild herds (one of them gazelles), a poor fit is expected, and serves as a sanity check. Details on the results can be seen in the table below (Table 5.1).

Table 5.1 For each of 26 datasets I list the total number of individuals when available, the best fitting parameter of a sigmoidal model (LSQ: least sum squares), its observed deviation, the statistically supported 'deviation', and a classification as domesticated, unimproved or wild. Note that deviations and the corresponding p-value cannot be computed in cases where data sets lack the information on absolute number of individuals.

data set	nb. of individuals	LSQ sigma	obs. deviation	stat. deviation	stat. deviation emp. p-value.	wild / unimproved herd
Blench_Sahel_Goats	189	16.8	0.00858471660360152	0.0033	0.0545	unimproved
Blench_Sokoto_Goats	647	12.6	0.000409552801744769	0.00012	0.0845	unimproved
Confiend_Goats2	28	9.8	0.00077264978800544	0.00044	0.0879	unimproved
Confined Goat 3	83	4.8	0.00223781588851267	0.007	0.0508	unimproved
Confined_Goats_1	106	8.8	0.000329400458730411	3,00E-04	1	unimproved
Ethiopian_Goats	22786947	28.6	0.00645142939313702	0.0016	0.0565	unimproved
Ethiopian_Sheep	25509004	24	0.00433314487805901	7,00E-04	0.0671	unimproved
FMNH_Zeder_modern	244	102.6	0.00238940771441024	0.0026	0.063	mix wild/domesticated, mainly wild
Free range Sheep	134	9	0.000410988446588545	3,00E-04	1	unimproved
Free-range_WAD	157	3.6	0.00177552508366134	0.003	0.0509	unimproved
Northern Sheep	1010	16	0.00461613430848309	0.0011	0.0776	unimproved
Seasonally Confined Sheep 2	58	11.6	0.0136314593185168	0.0055	0.0969	unimproved
Seasonally Confined Sheep	45	10.2	0.01508640030645	0.039	0.0523	unimproved
WAD Goat cut and carry	212	10.8	0.00480390788530438	0.0222	0.0508	unimproved
WAD Goat overall	673	9.2	0.000819195170502115	0.0204	0.0513	unimproved
WAD sheep overall	363	11	0.000543971148382741	0.0084	0.0555	unimproved
Zeder_Iran	100	201	0.171978218260708	0.038	0.0529	mix wild/domesticated, mainly wild
arch_shanidar_goats	*NA*	26.4	*NA*	*NA*	*NA*	domesticated
arch_asiab_goats	*NA*	21.8	*NA*	*NA*	*NA*	domesticated
arch_Ganj dareh goats ALL Zeder		17.4	*NA*	*NA*	*NA*	domesticated
arch_ganj dareh level e	*NA*	19.4	*NA*	*NA*	*NA*	domesticated
arch_ganj dareh levela-d	*NA*	19.8	*NA*	*NA*	*NA*	domesticated
arch ali kosh	*NA*	33.2	*NA*	*NA*	*NA*	domesticated
arch jarmo goats	*NA*	55.6	*NA*	*NA*	*NA*	domesticated
arch gazelles	*NA*	500	*NA*	*NA*	*NA*	wild
arch_Boury-en-Vexin	99	17.8	0.00819908930058486	0.0055	0.0568	domesticated

As discussed in the methods section, the sex ratio dataset sample size variation was considered by applying an approach akin to 'effect size' in statistics. The statistical deviation was represented by an empirical p-value. For all modern sex ratio datasets and one archaeological dataset (total of 19 datasets), the modelled sex ratios fitted the data within 4% deviation, and in all but four cases below 1%. Out of 26 sex ratio datasets, 19 datasets contain real counts on female and male animals. The 'effect size' approach was applied to the 19 datasets, as this approach requires real counts of individuals. The other, mostly archaeological sex ratio datasets were

provided in Zeder ‘scores’ and as such are unsuitable for the ‘effect size’ approach. Deviation is supported by an empirical p-value, which is = or < 0.05 in 11 out of 19 cases.

5.14.2 Results on Bayesian method validation

The performance of the Bayesian inference method presented here can be tested by comparing simulated kill-off profiles generated under known model parameters with the results of the inference. We calculate the quantity (in percentages) of the true value falling into the posterior distribution (95% Highest Posterior Density, HPD). Fig. 5.5 shows (a) that it performs generally well with all age classes but shows worst performance for the last two age classes (above 80 % of true value falling into 95% HPD of posterior distribution for age classes 1 – 4 and above 60 % for age classes 5 and 6), and (b) that the method performs well with small as well as large sample numbers (ranging from an N = 10 - 200).

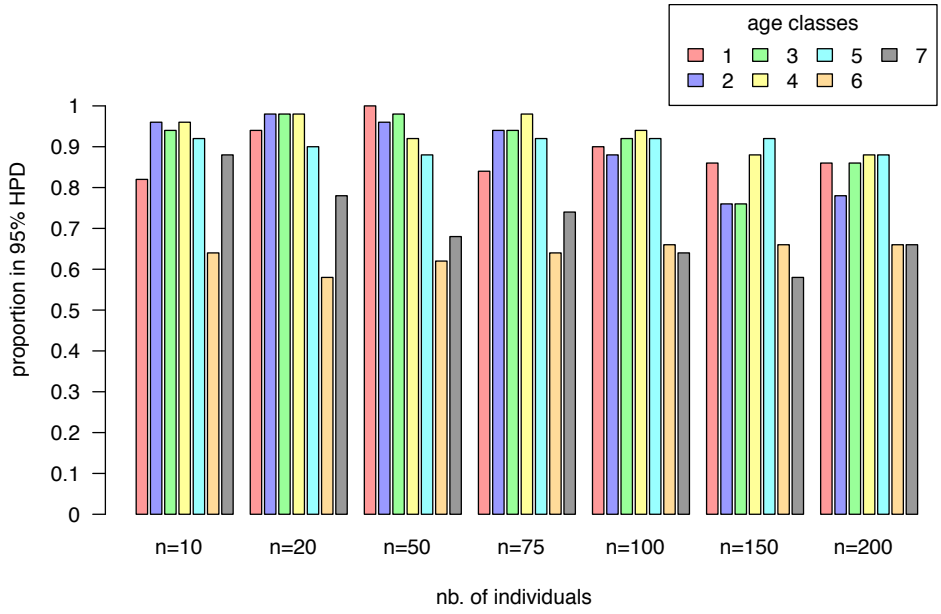

Fig. 5.5. Model performance measured by quantity of true value falling into the 95% HPD (in percentages). Plot provided by Dr. Diekmann.

5.14.3 Results on archaeological age-at-death profiles and idealized models

As discussed in the methods section, there are meta-parameters which need to be set individually. For the results generated here, the number of simulations is set to 20 million with a burn-in of 1 million and a thinning rate that results in MCMC samples being recorded every 1000th iteration. Posterior distributions for male (blue line), female (pink line), male plus female (black histogram) for each age class (AC1 – AC7 for profiles following the Helmer and Vigne age class system), sex ratio sigma and the log probability per recorded iteration on the 20 Neolithic age-at-death profiles are shown in Fig. 5.6 A - T. It should be noted that the number of age classes differs for each of the three idealised models (see Chapter 4), and with it the number of inferred female and male proportions. One of the major advantages to the Bayesian inference method presented here is that inferences from datasets with different numbers of age classes can be fairly compared. Red vertical lines represent the observed age-at-death profile from which the posteriors were inferred. Note that sampling uncertainty caused by small sample sizes is reflected in the 95% credible intervals, which are wider for profiles with smaller samples sizes than those with larger sample sizes.

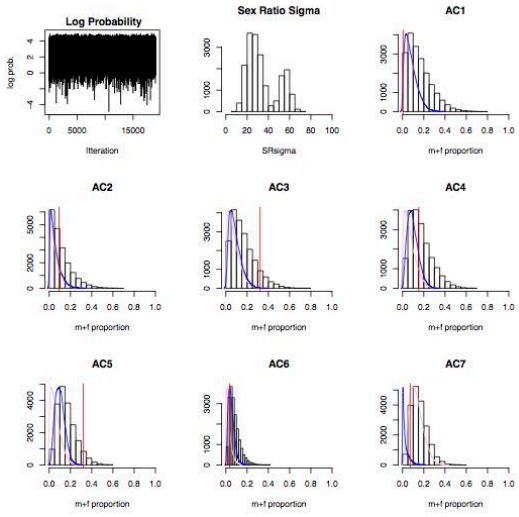

Fig. 5.6A Total (black), female (magenta), male (blue), sigma posterior distribution and log probability inferred from age-at-death profile from Araguina-Sennola III.

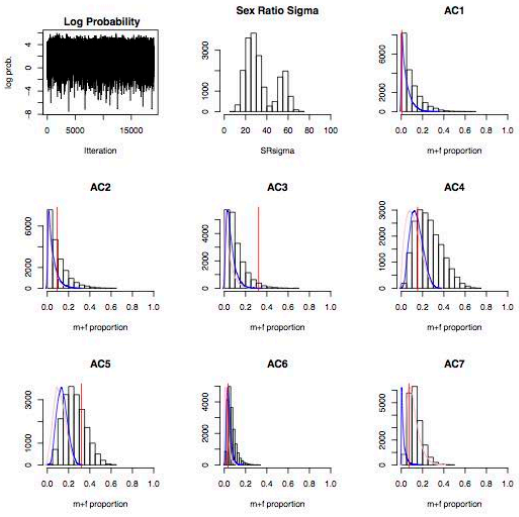

Fig. 5.6B Total (black), female (magenta), male (blue), sigma posterior distribution and log probability inferred from age-at-death profile from Arma dello Stefanin.

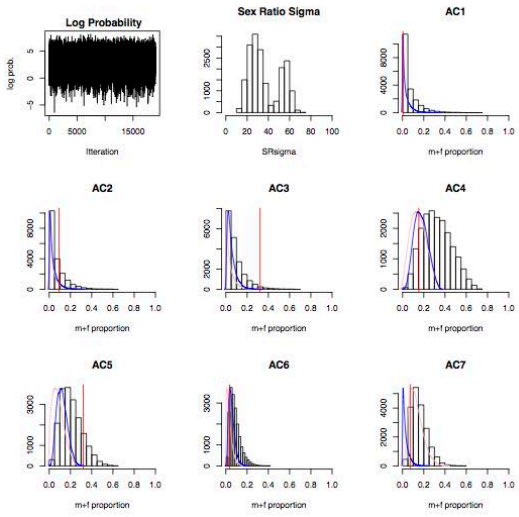

Fig. 5.6C Total (black), female (magenta), male (blue), sigma posterior distribution and log probability inferred from age-at-death profile from Silourokambos1.

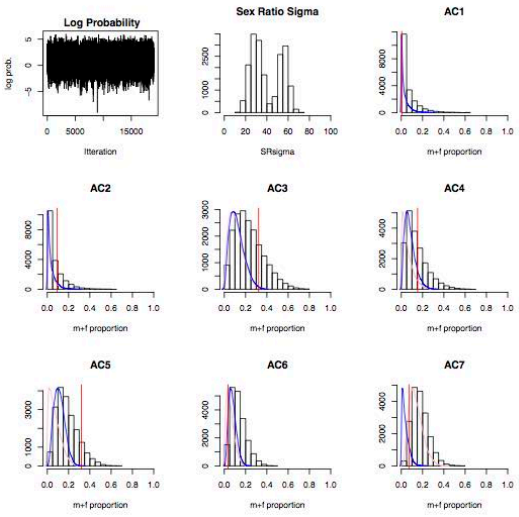

Fig. 5.6D Total (black), female (magenta), male (blue), sigma posterior distribution and log probability inferred from age-at-death profile from Silourokambos2.

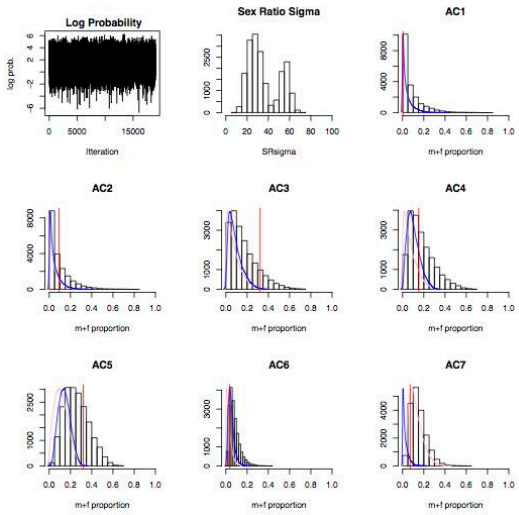

Fig. 5.6E Total (black), female (magenta), male (blue), sigma posterior distribution and log probability inferred from age-at-death profile from Silourokambos3.

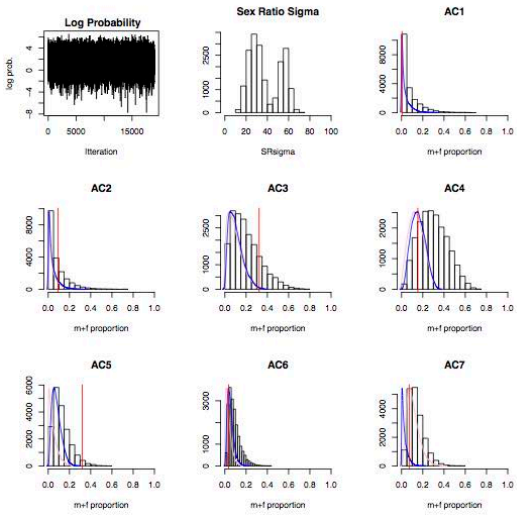

Fig. 5.6F Total (black), female (magenta), male (blue), sigma posterior distribution and log probability inferred from age-at-death profile from Pojejena Nucet IIA-IB.

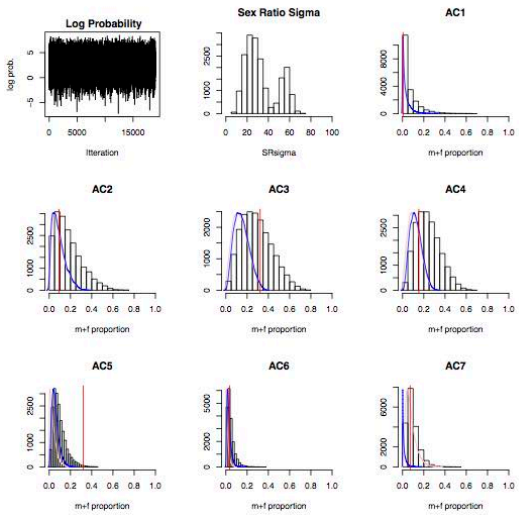

Fig. 5.6G Total (black), female (magenta), male (blue), sigma posterior distribution and log probability inferred from age-at-death profile from Phaistos.

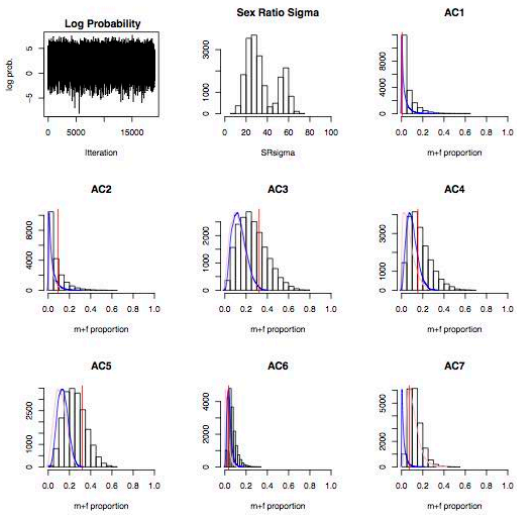

Fig. 5.6H Total (black), female (magenta), male (blue), sigma posterior distribution and log probability inferred from age-at-death profile from Gornea-L I-IIB.

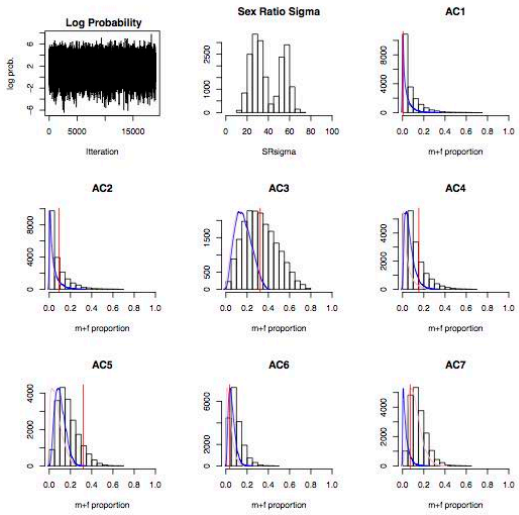

Fig. 5.6I Total (black), female (magenta), male (blue), sigma posterior distribution and log probability inferred from age-at-death profile from Le Barmaz sur Collombey1.

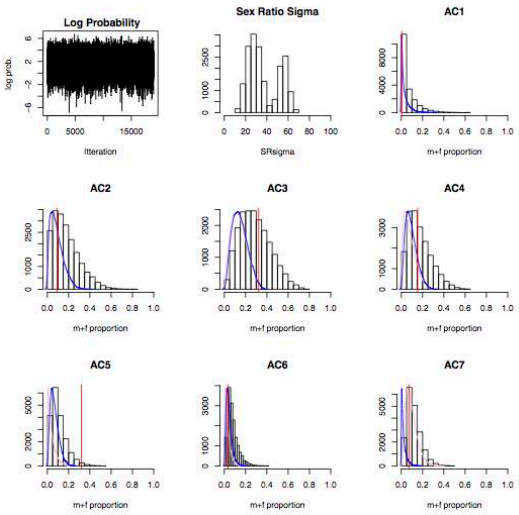

Fig. 5.6J Total (black), female (magenta), male (blue), sigma posterior distribution and log probability inferred from age-at-death profile from Miercurea Sibiului IIB-IIA.

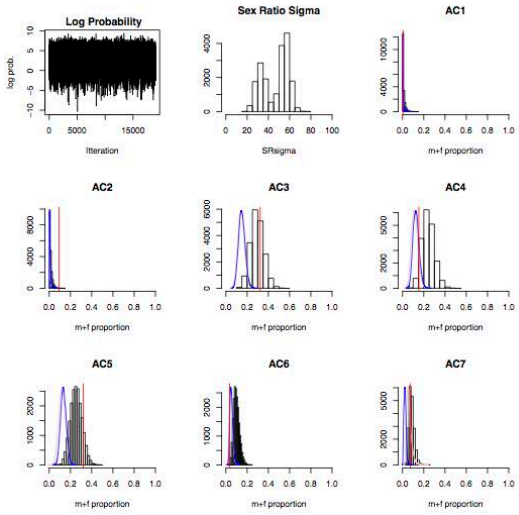

Fig. 5.6K Total (black), female (magenta), male (blue), sigma posterior distribution and log probability inferred from age-at-death profile from Prodromos II.

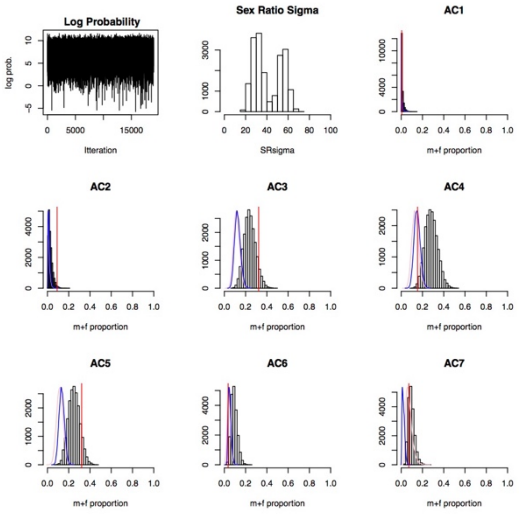

Fig. 5.6L Total (black), female (magenta), male (blue), sigma posterior distribution and log probability inferred from age-at-death profile from Trasano IV.

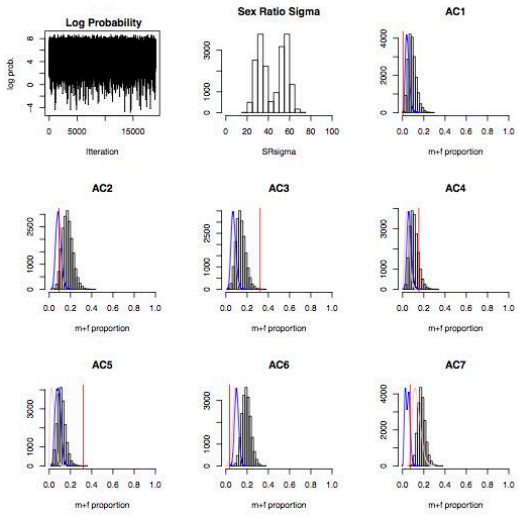

Fig. 5.6M Total (black), female (magenta), male (blue), sigma posterior distribution and log probability inferred from age-at-death profile from Champ-Durand.

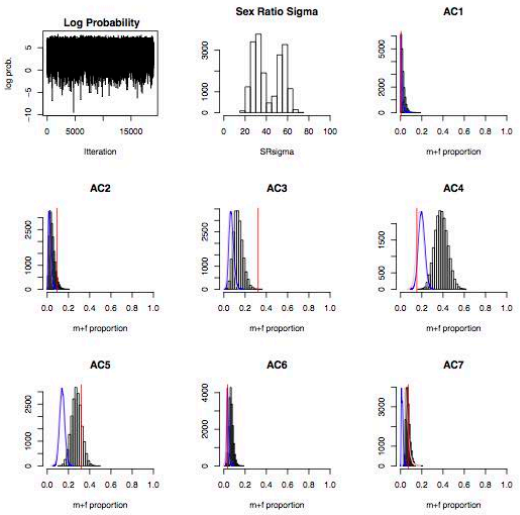

Fig. 5.6N Total (black), female (magenta), male (blue), sigma posterior distribution and log probability inferred from age-at-death profile from La Draga.

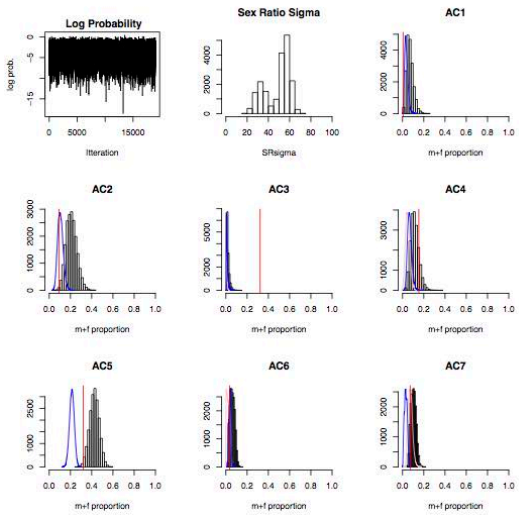

Fig. 5.6O Total (black), female (magenta), male (blue), sigma posterior distribution and log probability inferred from age-at-death profile from Lerna2.

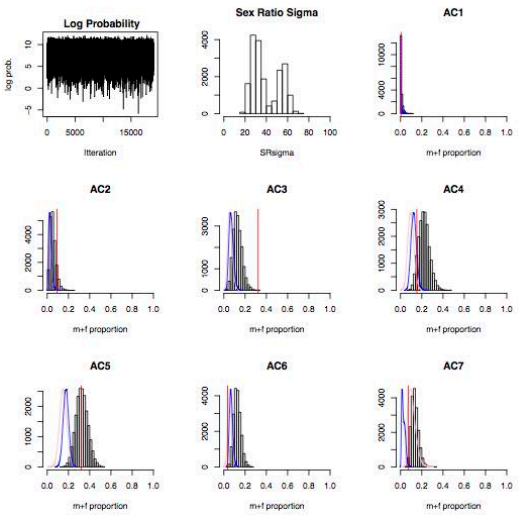

Fig. 5.6P Total (black), female (magenta), male (blue), sigma posterior distribution and log probability inferred from age-at-death profile from Fare1.

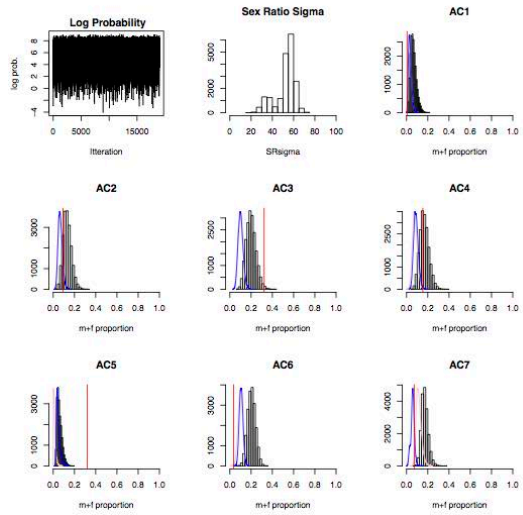

Fig. 5.6Q Total (black), female (magenta), male (blue), sigma posterior distribution and log probability inferred from age-at-death profile from Mondees.

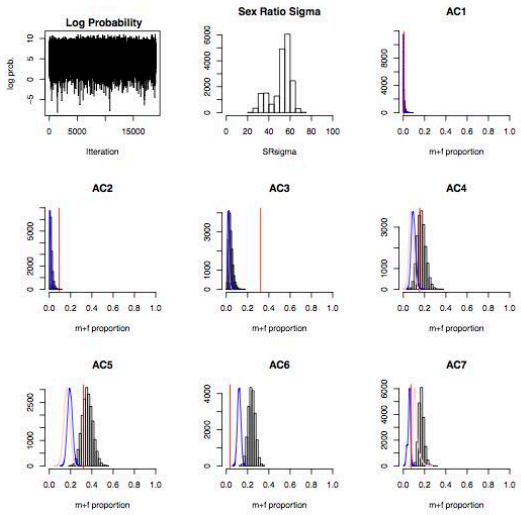

Fig. 5.6R Total (black), female (magenta), male (blue), sigma posterior distribution and log probability inferred from age-at-death profile from Colle Santo Stefano.

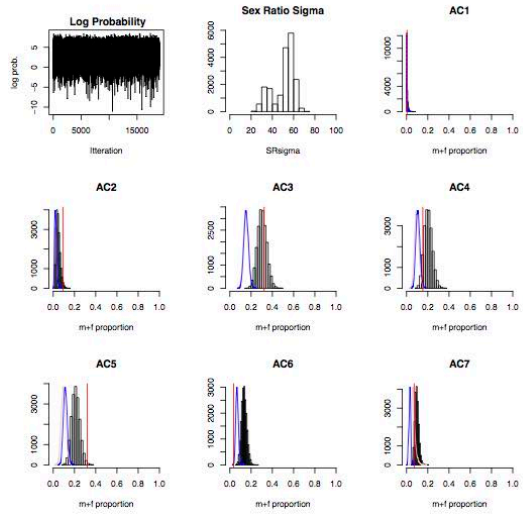

Fig. 5.6S Total (black), female (magenta), male (blue), sigma posterior distribution and log probability inferred from age-at-death profile from Dimini.

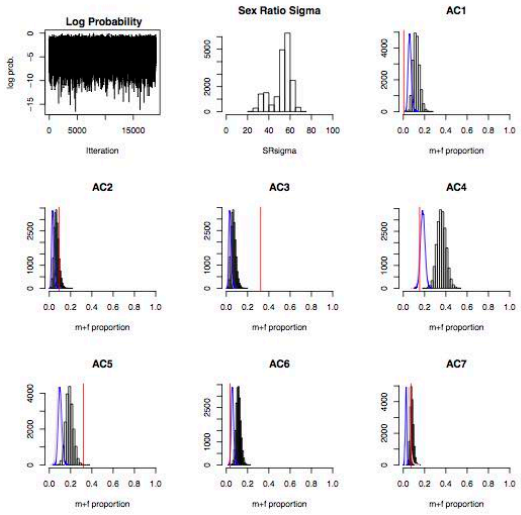

Fig. 5.6T Total (black), female (magenta), male (blue), sigma posterior distribution and log probability inferred from age-at-death profile from Ecsegfalva 23.

The 10 idealised profiles consist of different numbers of age classes. This parameter is adjusted within the analysis code for each profile individually. Furthermore, since the idealised models are presented as proportions, they have to be multiplied by an arbitrary high number (here by 1000) in order to simulate large

datasets. The reason for that strategy is to mimic real data based on a model, which itself does not have an actual sample size.

Calculations are performed on the inferred male and female proportions using nutrient input parameters to obtain information on macronutrient outputs and animal product yields. In the next step, those variables are plotted against each other in order to get some insight on, for example, milk and MOW yields or economic efficiency of keeping a herd, given a particular kill-off profile. Furthermore, I gain some insight on herd sustainability with estimates of reproductive output. Perhaps the most informative plots are those plotting reproductive output against calories per fodder consumed, since these outcomes – representing sustainability and the economic efficiency of nutritional energy production, respectively – are, and likely were the most important targets of any herd management strategy. Fig. 5.7 and 5.8 are plots of the abovementioned combinations of estimates for profiles with the 10 smallest and 10 largest sample sizes, and the 'idealized' profiles. As already seen in the results showing the posterior distributions of male and female proportions per age class Fig. 5.6 A – T, the results in Fig. 5.7 and 5.8 also reflect difference in sample sizes in the 95% credible intervals; profiles with smaller sample sizes show wide credible intervals whereas credible intervals are narrow with the larger sample sizes.

5.14.3.1 On archaeological age-at-death profiles

Focusing on the 10 sites with the largest sample sizes, across sites I infer a broad positive correlation between inferred total calories (milk and MOW) produced per fodder consumed and reproductive output rates (Fig. 5.8d). From an economic point of view these are likely the two most valuable targets in any slaughter strategy; the former to maximise nutritional return and the latter to maximise herd resilience. The means of the estimates for these target outcomes (see Appendix Table B.22) range

approximately 1.7 and 2-fold across sites, respectively, suggesting a lack of optimization for these targets at most sites.

Unsurprisingly, there is a positive correlation between inferred total calories (milk and MOW) produced per animal and fodder consumed (Fig. 5.8a), as well as between the former and reproductive output rates (Fig. 5.7a). Interestingly, we see a broad negative correlation between inferred total milk calories produced per fodder consumed and inferred total MOW calories produced per fodder consumed. This implies that – to an extent – these two target outputs are traded off against one another economically. However, it should be noted that at the 10 sites with the largest sample sizes, milk is predicted to provide between 2.9 and 10.5 times more calories than MOW (per fodder consumed), depending on slaughter strategy. Previous authors have highlighted the efficiency of milk production over meat production, and its importance in supporting larger populations (Ingold, 1980; A. Legge, 1981). This model also predicts a very strong correlation between total protein per animal and total fat per animal, reflecting the similar ratios of these macronutrients in meat and offal on the one hand, and milk on the other.

5.14.3.2 On idealised profiles

Of Payne's (1973) three idealised profiles, the 'meat' profile generates the most MOW calories per fodder consumed but not the most MOW calories per animal, whereas Payne's 'milk' profile generates neither the most milk calories per animal nor the most milk calories per fodder consumed (Fig. 5.7f and 5.8i). However, it should be noted that Payne also proposed sex-specific kill-off profiles, which may not conform to the sigmoidal decrease in sex ratios through time assumed in the model presented here. Of Redding's (1981) two idealised profiles, it is noteworthy that his optimised herd security profile generates the lowest reproductive output rates under

our model, although the mean estimate is only marginally smaller than his maximum energy yield profile (Fig. 5.7c).

Under the assumed model of a sigmoidal decrease in sex ratios, I found that the Vigne and Helmer's 'Fleece' profile generates the highest milk calorie, MOW calorie, total calorie, total fat and total protein yields per animal, as well as the highest reproductive outputs; presumably because it involves culling animals mostly later in life (Fig. 5.7c and 5.7f). However, while their 'Fleece' profile also generates the highest milk calories per fodder consumed, it generates the lowest predicted MOW calorie yields per fodder consumed; 'Milk type A' generates the highest MOW calorie yields per fodder consumed (Fig. 5.8i).

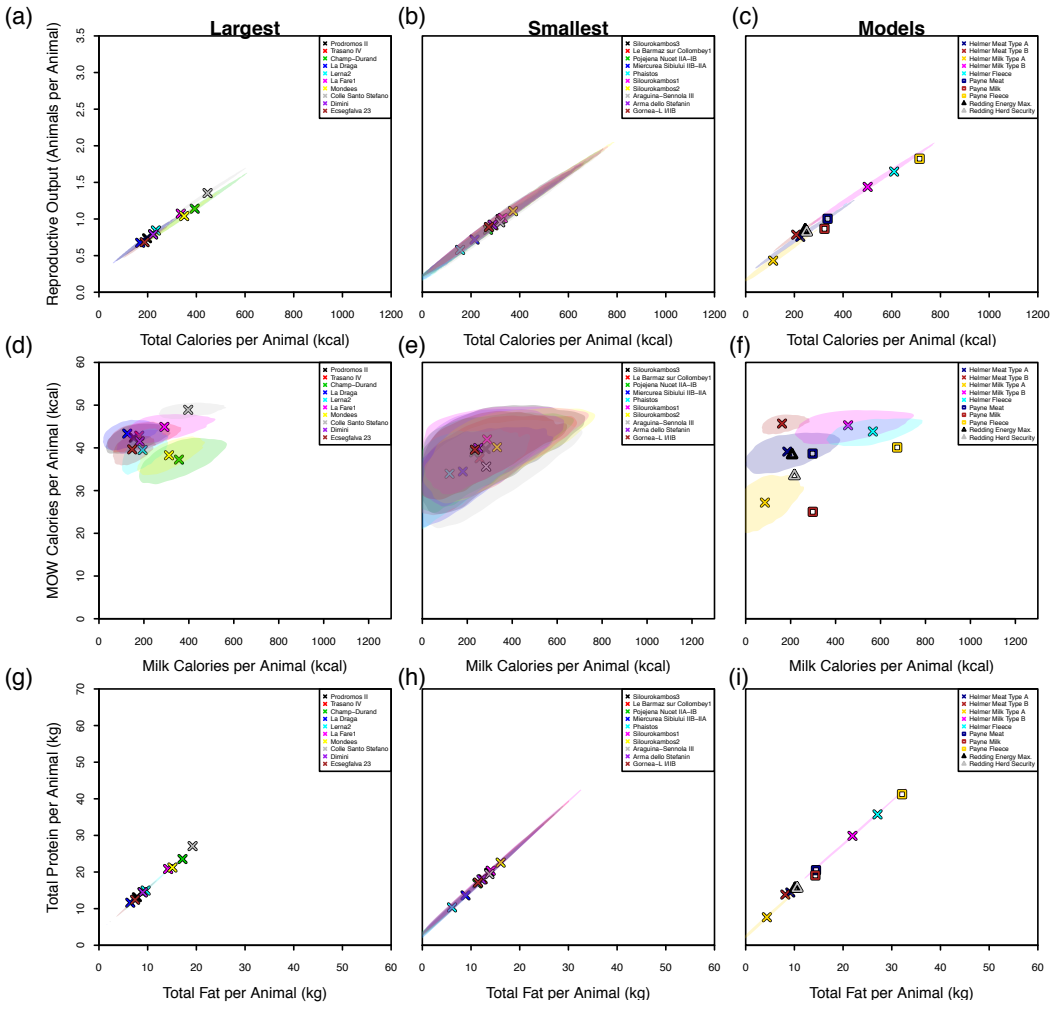

Fig. 5.7. Animal Product yields, macronutrient and reproductive output rates of 20 Neolithic sites with the 10 largest sample sizes, the 10 smallest sample sizes and 10 idealised models.

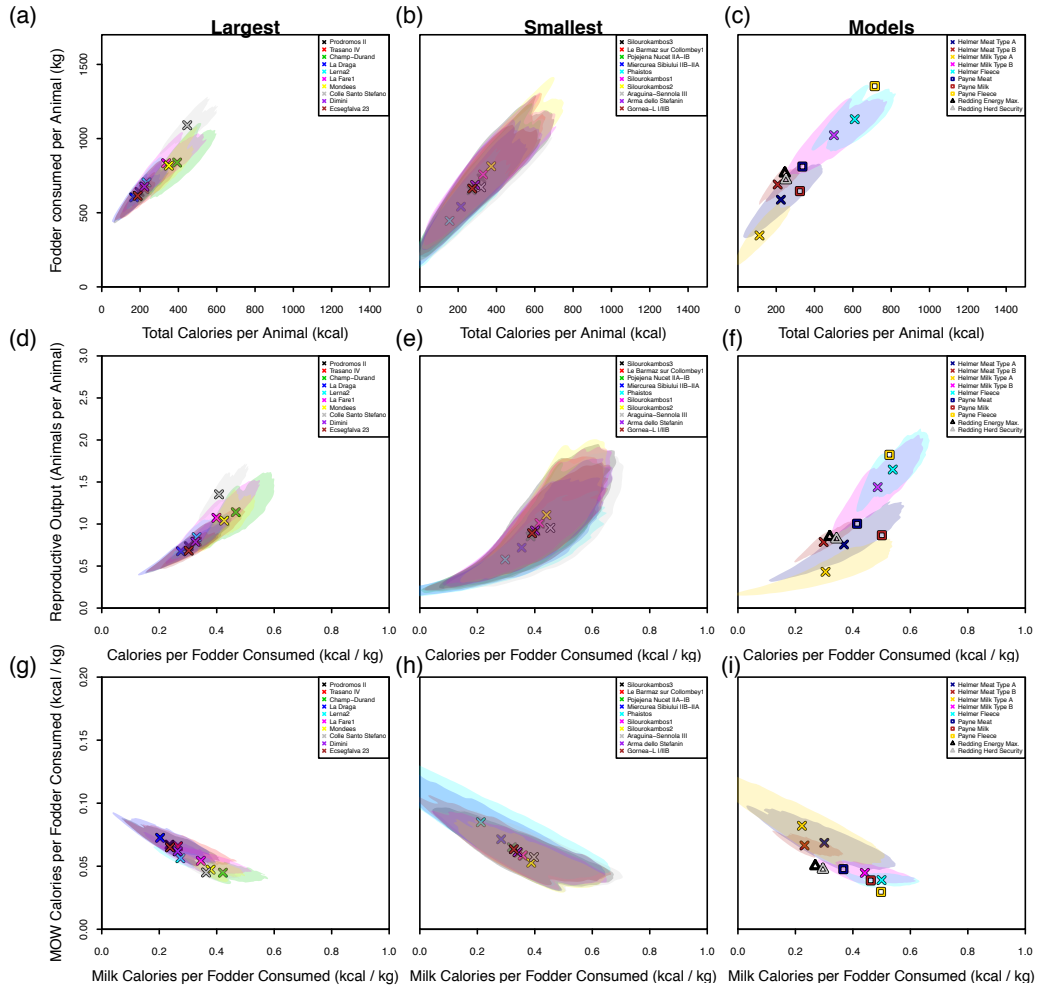

Fig. 5.8. Macronutrient and reproductive output rates as well as economic efficiency of 20 Neolithic sites with the 10 largest sample sizes, the 10 smallest sample sizes and 10 idealised models.

5.14.4 Exploration of parameter space to optimise calorie and reproductive output

The model presented here can be used not only to estimate various yields for different slaughter strategies, but also to identify slaughter strategies that maximise various yields. We performed a slaughter parameter space search to identify age-at-death profiles that would maximise two target outcomes: economic efficiency of calorie production and reproductive output rate, given the per individual per age consumption and yield parameters for unimproved stock used above. This parameter space search was performed by Dr. Diekmann. We performed 2 searches, one

constrained to the sigmoidal decay process assumed in all inferential analyses presented in this study, and one unconstrained (i.e. one where males and females can be killed at any rate in each age class independently). Both interestingly and encouragingly, the former of these 2 searches identified kill-off strategies with both the highest economic efficiencies of calorie production and the highest reproductive output rates (Fig. 5.9; table B.22 in Appendix). Furthermore, the maximum of these target outcomes was around two-fold greater that the modal estimates for the various archaeological sites analysed. This result indicates that Neolithic slaughter strategies were far from optimal. It also indicates that a sigmoidal-like approach to additional male killing would have aided experimentation to find better kill-off strategies.

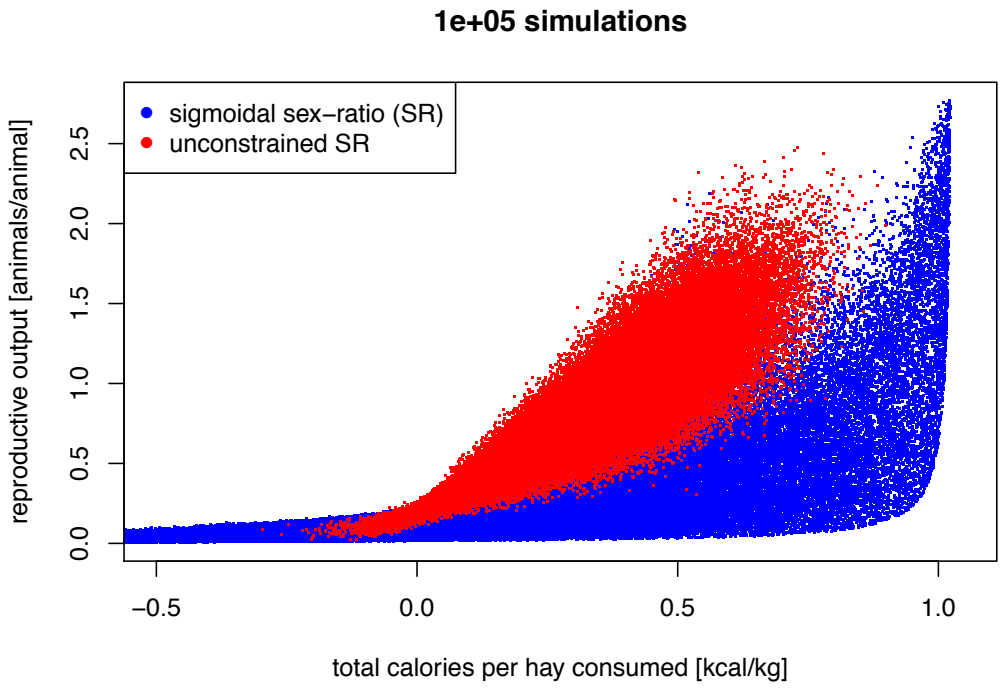

Fig. 5.9 Predicted economic efficiencies of calorie production and reproductive output rates generated in a search of kill-off parameter space (1) constrained to the sigmoidal decay process assumed in all inferential analyses presented in this study (blue), and (2) unconstrained (i.e. one where males and females can be killed at any rate in each age class independently; red). Plot provided by Diekmann.

5.14.5 Results on post-Neolithic age-at-death profiles

I analysed changes in economic efficiency between Neolithic and more recent archaeological sites. Additional post-Neolithic age-of-death profiles ranging from the Bronze Age to modern times are considered for analysis as seen in Fig. 5.10. I added 12 age-at-death profiles to the 10 sites with the largest sample sizes from Dataset-B (Chapter 4) as shown in Fig. 5.8d. Here, I examine if post-Neolithic slaughter strategies would generate higher economic efficiencies of calorie production and reproductive output rates, compared to the Neolithic sites. As can be seen from Fig. 5.10, while there is overlap, there is a general trend of increased economic efficiencies of calorie production and higher reproductive output rates at the later, post-Neolithic sites.

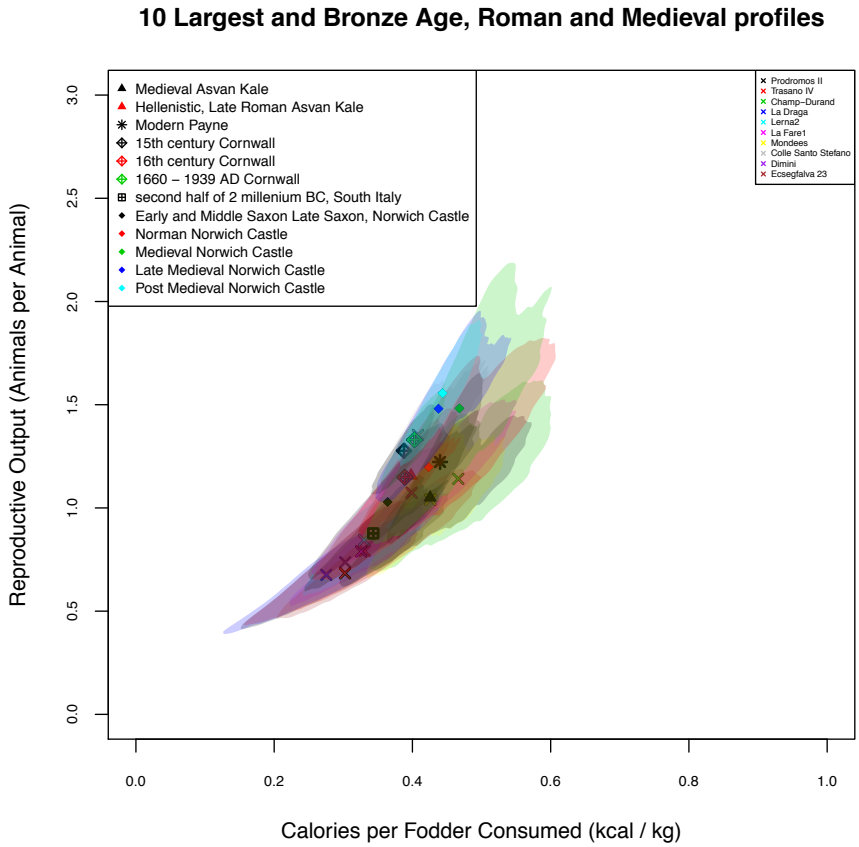

Fig. 5.10 Calorie production and reproductive output as proxy for economic efficiency of 12 age-at-death profiles from the Bronze Age to modern times and 10 Neolithic sites with the 10 largest sample sizes.

5.14.6 Summary of results

As seen in Fig. 5.9, for Neolithic sites there is room for improvement when it comes to the economic efficiency of their slaughter strategies, but the results show a general trend of improvement over time (Fig. 5.10). However, under the assumptions made here, even the idealised models are not 'ideal', and as such should be reconsidered as optimised age-at-death profiles for milk/meat/fleece (or combined) production, or herd resilience.

Among the sites with the 10 largest sample sizes from dataset-B, the profile from Calle Santo Stefano shows the highest rates in almost all estimated yield combinations. La Draga's profile shows the lowest rates for almost all estimated yield combinations presented here. For the profiles with the 10 smallest sample sizes, Phaistos and Silourokambos 2 show the two extremes of lowest and highest outputs. For the idealised models, Payne's and Helmer's fleece models show highest values for most estimated yield combinations, while Helmer´s Milk Type A showed the lowest values (Fig. 5.7 and Fig. 5.8). Furthermore, milk calories per fodder consumed and meat calories per fodder consumed show a negative correlation across the 20 archaeological sites and the 10 idealised models, implying a trade-off between the two animal products.

5.15 Discussion

I present a full Bayesian Markov Chain Monte Carlo method for inferring sex-specific survival curves from Caprini archaeological age-at-death profiles that generates posterior estimates of herd growth rate, milk and MOW yields, macronutrient and calorie yields, and fodder consumed per animal. This approach makes one key assumption – that changes in herd male to female sex ratios through time follow a sigmoidal "half Gaussian" decay pattern. This assumption is supported by data on managed unimproved modern, and archaeological herds, and

encouragingly, is not supported by data from wild herds. Nonetheless, it is necessarily a simple (one parameter) model of sex ratio change through time, and as such, it will not represent the full complexity of sex-specific slaughter strategies. As with all models, this assumption is wrong (Box, 1976), but I contend that it is right enough to be very useful. Interestingly, I also find that making such an assumption aids in finding kill-off strategies with both the highest economic efficiencies of calorie production and the highest reproductive output rates.

By combining primary and secondary product (Sherratt, 1981) yield estimates with estimates of fodder consumed at different ages in unimproved herds (e.g. Food and Agriculture Organization, 2003), I was able to estimate key components of the economic efficiency of various slaughter strategies in terms of milk, meat and offal, total calorie, and total macronutrient production. It is important to note that the estimates I used for fodder consumed (Food and Agriculture Organization, 2003) do not represent the total food consumed by each animal. Rather, I use them as a general proxy of the economic costs of keeping animals at different ages. For this reason, the units of our estimates of product yield per fodder consumed should only be considered in relative terms, rather than as an absolute measure of product yields per food consumed. Likewise, the estimates of reproductive output, milk yields and MOW yields per animal (and their derivatives such as protein, fat and calorie yields) are based on estimates of mean milk produced (Dahl and Hjort, 1976; Mourad, 1992; Todaro *et al.*, 2015) milk consumed by kids / lambs (Food and Agriculture Organization, 2003), meat and offal weight (MOW) produced (Tresset, 1996) and probability of giving birth (Dahl and Hjort, 1976) for each month of life in unimproved herds. I recognise that prehistoric values for such parameters may have been different; in most cases, likely lower. However, the methodology my colleagues and I have developed is not tied to the particular values of these parameters used here, and other values – if better informed – could be used. Nonetheless, predicted yields per animal from this model scale linearly with these parameter values, so while our

absolute yield estimates may be misleading, their relative values in cross site and site/model comparisons should be reasonably secure.

Analyses of the 10 sites with the smallest number of samples (ranging from three to six individuals) generated primary and secondary product (Sherratt, 1981) yield estimates that were substantially overlapping, rendering site to site comparison largely uninformative. However, while 95% credible intervals for some product yield estimates were overlapping for the 10 sites with the largest number of samples (ranging from 52 to 123 individuals), some were not, and some broad correlations could be discerned. Notably, reproductive output and total calories produced per fodder consumed are positively correlated across sites (Fig. 5.8d). Given the importance of these target outcomes, it therefore seems likely that there was considerable scope for improvement and optimization of Neolithic slaughter strategies through cultural evolutionary processes. In support of this view, I identified theoretical kill-off profiles which were still constrained to the sigmoidal sex-ratio decay pattern used in this study, but that predicted approximately 2-fold improvements in the economic efficiency of calorie production and reproductive outputs over the modes of those inferred for Neolithic sites. We also inferred broadly increased economic efficiencies of calorie production and higher reproductive output rates for a set of later, post-Neolithic sites dating from the Bronze Age to modern times. However, it should be noted that many animal deaths at Neolithic sites may have been premature and not under the control of the stock keepers (e.g. due to predation, disease or other natural causes), and that post-Neolithic predation risk was reduced.

Given the sufficient number of sites with informative age-at-death data, as those collected in datasets-A and B, I apply the methodology described here in a meta-analysis to test if there was any significant improvement through the Neolithic in herd sustainability or the economic efficiency of primary and secondary production, and overall caprine calorie yields during the Neolithic. The meta-analysis is described in the next chapter (Chapter 6).

Chapter 6

6 Meta-analysis of archaeological caprine age-at-death profiles to infer herd growths and animal product yield change throughout the European Neolithic.

6.1 Abstract

A Bayesian method for inferring sex-specific survival curves from caprine archaeological age-at-death (AaD) profiles that generates estimates of herd growth rate, milk and meat yields, macronutrient and calorie yields, and fodder consumed per animal, has been described in Chapter 5. These yield and fodder consumption estimates permit estimation of the economic efficiency of calorie and other nutrient production from different archaeological sites. In the following Chapter, I perform a meta-analysis of European and southwest Asian archaeological sites spanning the Neolithic period using this Bayesian method. The main broad questions I aim to address in this meta-analysis are:

(1) Do herd slaughter strategies change so as to improve the sustainability and economic efficiency of animal product production throughout the Neolithic?

(2) Are there systematic geographic differences in the sustainability and economic efficiency of animal product production during the Neolithic?

The first of these questions can be related more broadly to the field of cultural evolution (Boyd, Richerson and Henrich, 2011). Just as genetic variants undergo selection to improve the fitness of individuals, culturally transmitted practices and skills – including herd management / slaughter strategies – can undergo selection to improve the resilience of human populations. Whilst it is beyond the remit of this chapter to explore the cultural evolution literature in detail, any indication of

improvements in culturally transmitted practices and skills would be relevant to that field.

6.2 Background

Archaeological age-at-death profiles reflect aspects of herd management strategies of past peoples. In previous chapters of this thesis, I described the development and application of two methods to infer herd growth rates (methods described in Chapter 4 and Chapter 5) and goat/sheep product yields (milk and meat), macronutrient outputs and economic efficiency rates (method described in Chapter 5) from archaeological caprine age-at-death profiles and age-at-death profile models. In Chapter 5, the application of a Bayesian method was mainly performed on a set of age-at-death profiles from the Neolithic and more recent periods (i.e. Bronze Age and Middle Ages) from various archaeological sites spread throughout Europe and the Near East. The focus of Chapter 5, on applying the method was, firstly, to test its performance, and secondly to shed some light on particular goat/sheep herding strategies during the European Neolithic. Dataset-B contains age-at-death profiles from the Neolithic period, whereas Dataset-A contains age-at-death profile data dating from the Epipaleolithic to modern times. The two datasets differ in their presentation of counts per age class. Dataset-B is presented as number of individuals whereas dataset-A is presented in number of hard tissue elements, mostly teeth, per age class. In this Chapter, I perform meta-analyses of both datasets, but focusing only on Neolithic sites, and also perform a meta-analysis on a single site (Çukuriçi Höyük) which has 9 site-phases – permitting a through-time analysis.

Cultural evolution is the process by which behaviours and skills that are transmitted by learning changes through time. Darwin coined the term of ‘sociocultural evolution’ for the first time (Darwin, 1859). Nowadays, the concept of cultural evolution is used in various disciplines such as linguistics, biology, genetics,

history and anthropology (Maschner, 2003). Cultural changes through time may show correlations to human biology. Perhaps the best known example of this is the correlation of lactase persistence (LP) with the practice of pastoralism milk production (Simoons, 1979; Holden and Mace, 2009). Other scholars employ a Darwinian perspective of cultural change to understand human psychology and human prehistory (Mithen, 1996; Maschner, 2003; Shennan, 2009). Shennan (2009) explores the idea of an evolving culture by analysing population growth, male to female roles, material culture, warfare and subsistence.

As shown in Chapter 5, Fig. 5.10, a positive trend of increased economic efficiency of calorie production from caprine herds through time is indicated from an analysis of 10 Neolithic age-at-death profiles and 12 profiles dating from the Bronze Age to modern times. I aim to broaden this analysis to the whole Neolithic period using datasets-A and B.

6.3 Case study Çukuriçi Höyük

The archaeological site of Çukuriçi Höyük presents one of the oldest or even the oldest human settlement (together with the site Ulucak VI, located on the coast north of Çukuriçi Höyük) in Western Anatolia, beginning at ca. 9,000 years BP (radiocarbon dated). Western Anatolia, and as such the site Çukuriçi Höyük, is often referred to as the ‘gateway’ of the spread of Neolithic lifeways from West Asia into Europe. It is located south of the city of Izmir in present-day Turkey, ca. 1 km south of the Roman archaeological site of Ephesos, near the town Selcuk (Fig. 6.1).

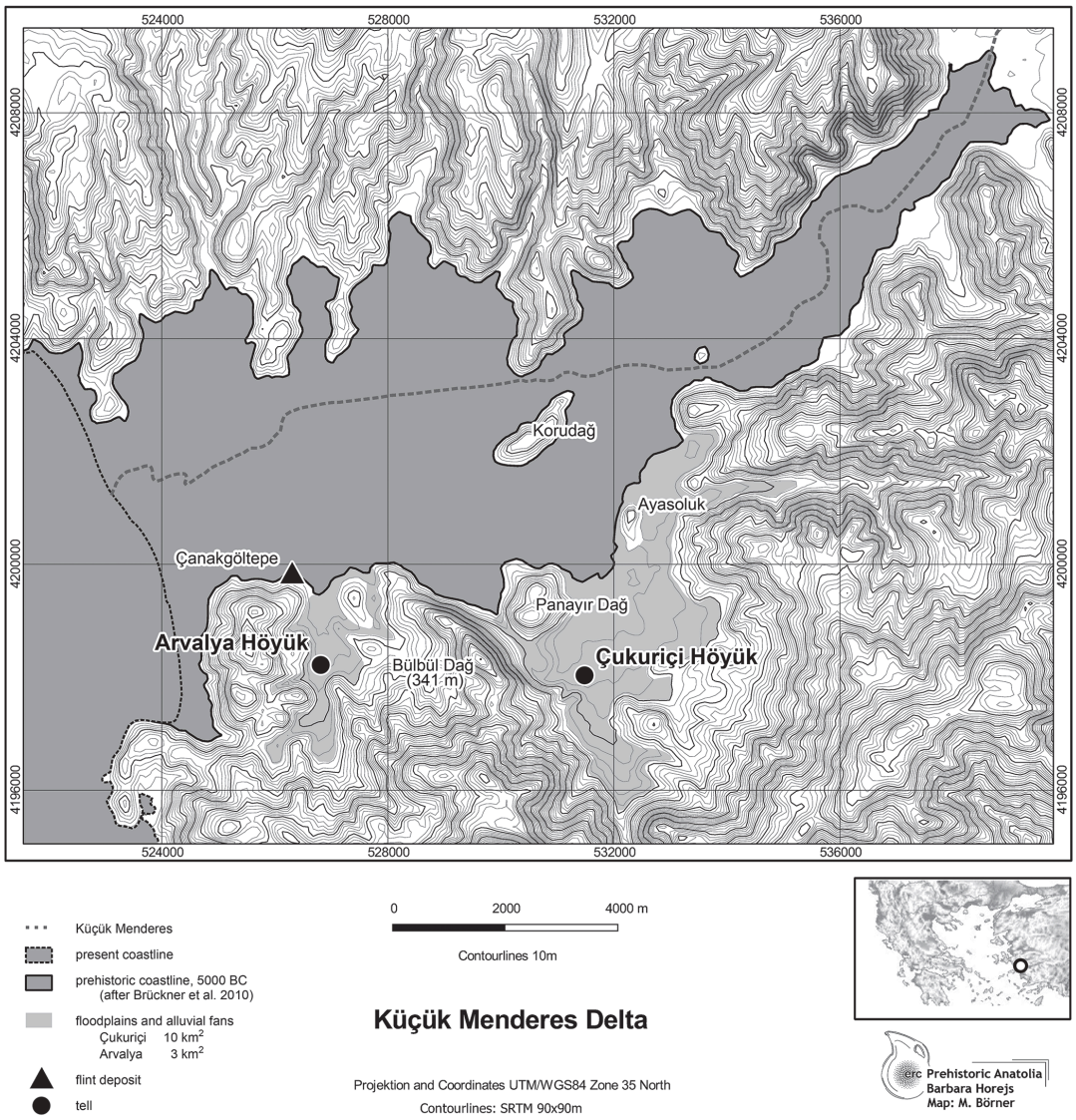

Fig. 6.1 Reconstructed prehistoric environment around Çukuriçi Höyük (map by M. Börner/ ERC Prehistoric Anatolia after Brückner 1997; Stock (2013)). From Horejs (2016).

Çukuriçi Höyük used to be an Aegean coast settlement, which was occupied during the Early Neolithic (7th millennium BC), then abandoned for ca. 2,600 years for reasons yet to be determined. It was reoccupied during the 2nd half of the 4th millennium BC. Nowadays, the archaeological site is located a few km away from the coast (Fig. 6.1). As a result of its direct connection to the sea, the subsistence of early Çukuriçi Höyük farmers mainly consisted of marine animals and domesticated

caprines, pigs and cattle, supplemented with wild animals. Stock farming, rather than hunting, dominated the mammalian assemblages of the site (Horejs *et al.*, 2011; Çakırlar, 2012; Horejs, 2016). The highest numbers of archaeozoological domesticate remains are from goats and sheep, as opposed to cattle and pigs, as reported in the NISP statistics (Fig. 6.2a and 6.2b).

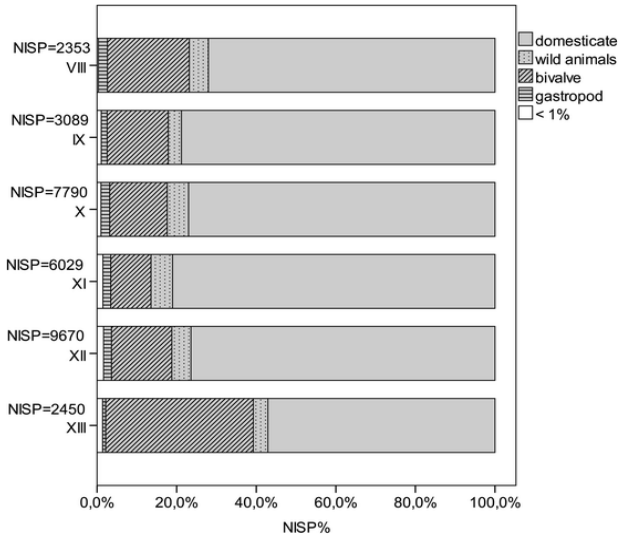

Fig. 6.2 a Quantification of **animal remains** from different site phases of Neolithic Çukuriçi Höyük (A. Galik). Adapted from Horejs (2015).

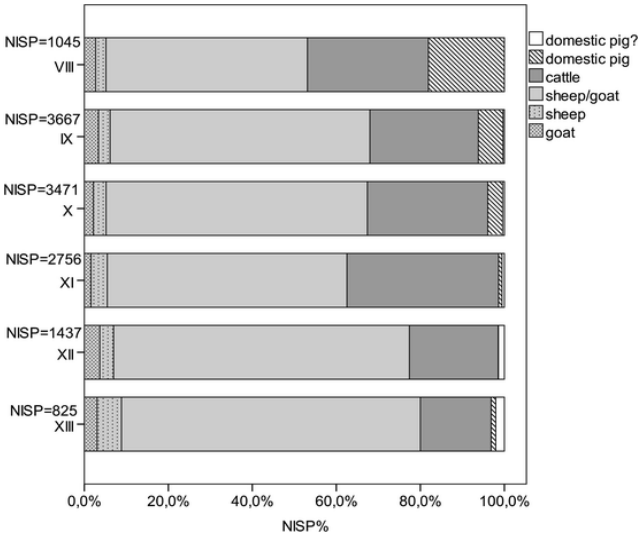

Fig. 6.2 b Quantification of **domesticates** from different site phases of Neolithic Çukuriçi Höyük (A. Galik). Adapted from Horejs (2015).

Çukuriçi Höyük shows similarities in livestock numbers to other coastal and mainland Neolithic sites from mainland Greece and the Greek islands, and represents

a typical Aegean coast settlement (Horejs, 2016). Typical of a Neolithic diet, the Çukuriçi Höyük settler's subsistence also consisted of fruits such as grapes, cereals like wheats and barley, and pulses. However, plant remains are rare archaeobotanical findings. Additionally, there is evidence of extensive exploitation of marine animals, such as tuna, dolphins, various types of mussels, shells, oysters, as well as many species of littoral and pelagic fish, and even whale (Horejs *et al.*, 2015). The pattern of subsistence remained similar throughout all Neolithic site phases (Fig. 6.2a and 6.2b).

Trade, farming and deep-sea fishing were all most probably performed by the first Çukuriçi Höyük settlers. The coastal location also allowed for vigorous trade of goods produced or mined in the Aegean such as obsidian from the island of Melos, ca. 300 km away by sea route. The first settlers are assumed to have come over the sea rather than from inland migrations (Horejs *et al.*, 2015). Stone tool and pottery technology was well established and influenced by Mesopotamian, Eastern Anatolian and Aegean technologies (Bergner, Horejs and Pernicka, 2009).

Following the abandonment of Çukuriçi Höyük, it was re-occupied during the Chalcolithic by a technologically more advanced culture bringing stone housing, textile production, metallurgy and extensive agriculture (Britsch and Horejs, 2014). From ca. 3,000 BC, during the early Bronze Age, a different, more dense architecture with ovens and stoves, a central place and multiple rooms used for living, as well as workshops (e.g. for copper object production) dominated the site. During this period, and in contrast to the Neolithic phases, the focus of lifestyles was in craft industries rather than farming, which was probably performed elsewhere (Horejs *et al.*, 2011). The differences in farming of the Bronze Age and Neolithic occupations may be reflected in changes in herd management strategies. However, subsistence during the Bronze Age is similar to that in the Neolithic. Usually, sheep and goat bones are challenging to distinguish; however, the archaeozoological remains found in the

Bronze Age trenches, were preserved well enough to distinguish between the two animals, showing more goat than sheep bone remains (Fig. 6.3).

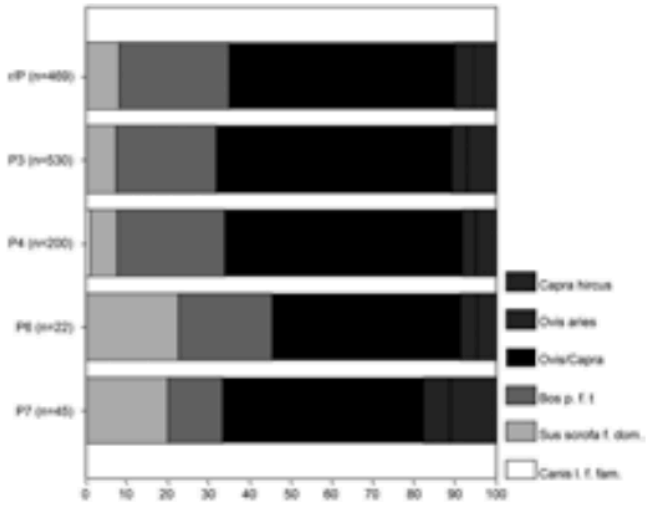

Fig. 6.3 Quantification (number of bones, NISP) of **domesticates** from different site phases of the Chalcolithic and Bronze Age Çukuriçi Höyük. Adapted from (Horejs *et al.*, 2011). Labelling on the right from top to bottom repeated due to illegibility: Capra hircus, Ovis aries, Ovis/Capra, Bos p.f.t, Sus scrofa f. dom., Canis f. fam.

Cattle herding seemed to dominate the early Bronze Age (Horejs and colleagues (2011), Fig. 16, not shown), but then retreated again, with more caprine herding becoming apparent. In general, more cattle bone remains are observed during the Chalcolithic and Bronze Age compared to the Neolithic periods. However, sheep and goats were still dominating the numbers of domesticates during both the Neolithic as well as the Chalcolithic/Bronze Age periods. Dietary diversity seems to have increased during the Chalcolithic/Bronze Age periods, by a few additional animals and plants species (e.g. snails, various types of nuts and fruits such as figs as well as lentils, olives, among others). There is also a change in diet with respect to cereals, with an increased focus on wheats in the Chalcolithic and Bronze Age, while barley was predominant during the Neolithic (Horejs *et al.*, 2011). However, this apparent increased food diversity may be the result of reduced taphonomic loss on Chalcolithic

and Bronze Age remains, compared to older Neolithic remains. Interestingly, domestic dog (*Canis familiaris*) remains first appear during the early Bronze Age; even if only in small numbers.

Age-at-death profile data were gathered from ovicaprines from 9 site phases in Çukuriçi Höyük spanning the Neolithic, Chalcolithic and Bronze Age, with a hiatus of occupation of 2,600 years between the Neolithic and Chalcolithic (table 6.1, hiatus coloured in yellow). The data were kindly provided by my colleague Dr. Galik from Vienna University. In order to have one value for the chronologies instead of age ranges, I have chosen the middle value of the radiocarbon dates (Horejs, 2014, 2016; Horejs and Schwall, 2015; Horejs *et al.*, 2015; Horejs and Weninger, 2016) to allow for a meta-analysis of the various phase sites from Çukuriçi Höyük. For consistency with results presented in Chapters 4 and 5, dates have been converted from BC to BP. Note: the age-at-death profiles from table 6.1 are reported in an age class system with 9 age classes with varying durations, rather than the durations proposed by Payne or Helmer and Vigne, and were constructed from postcranial bone remains of varying number, of total sample sizes n = 1 - 277. In this chapter, I have analysed the age-a-death profiles presented in table 6.1.

Çukuriçi Höyük is an important site to study in order to understand the spread of the Neolithic from West Asia to East Europe, the connections of people and trade in the Aegean and the timings of the transition Neolithic period to the Bronze Age in Western Anatolia.

6.4 Data

Three datasets are considered for the meta-analyses: datasets-A and B from Chapter 4, and age-at-death profiles from Çukuriçi Höyük. Some edits were performed to dataset-A from Chapter 4 and age-at-death profiles from Çukuriçi Höyük:

- I restricted the data used in the meta-analysis of dataset-A to the Neolithic period.
- The original dataset for the site Çukuriçi Höyük (table 6.1) contained 25 age-at-death profiles with profiles for sheep, goats and mixed animals. For consistency with profiles from datasets-A and B and because more data were available for the Ovis/Capra profiles from Çukuriçi Höyük, I have analysed the Ovis/Capra profiles only. This dataset presents a good-quality dataset which contains age-at-death profiles constructed from post-cranial bones with appreciable total number of elements with an individual age class system. The time range spans 6,684 – 2,740 BC.

Table 6.1. Goat/Sheep age-at-death profile data (postcranial) from archaeological site Çukuriçi Höyük, West Anatolia, with site phases of different time periods.

Phase	0-2m	2-4m	4-6m	6-12m	<18m	<24m	<30m	<36m	<48m	total	Cal. BC	Relative Chronology
I	0	3	0	1	1	1	1	1	2	10	2.74	Early Bronze Age
III	6	9	11	44	10	30	18	4	98	230	2.82	Early Bronze Age
VII+VI	0	3	3	3	0	0	3	3	12	27	3.2	Chalcolithic
VIII	9	9	9	14	2	3	10	2	19	77	6.2	Late Neolithic
IX	32	22	14	42	15	20	29	13	60	247	6.2	Late Neolithic
X	51	21	13	52	21	14	43	9	53	277	6.2	Late Neolithic
XI	41	16	12	18	3	7	42	2	40	181	6.592	Early Neolithic
XII	20	5	18	25	7	6	24	3	34	142	6.592	Early Neolithic
XIII	3	1	2	9	2	0	14	1	13	45	6.684	Early Neolithic

6.5 Methods

Datasets-A and B, and the Çukuriçi Höyük age-at-death profiles (table 6.1) were each analysed independently. Below, results on product yields and herd sustainability are plotted versus time, and versus space (latitude and longitude) are shown. Whilst dataset-B (based on minimum number of individuals) was from Neolithic sites only, dataset-A and the Çukuriçi Höyük dataset included sites dating to the Epipalaeolithic, Neolithic, Chalcolithic, Bronze Age, Iron Age and modern Times. In the following

analyses, only Neolithic sites were considered for dataset-A, and only Neolithic, and Chalcolithic sites were considered for the Çukuriçi Höyük dataset. After restricting dataset-A to Neolithic sites only, the time period covered ranges from ~11,000 BP – ~7,000 BP. Of the 21 productivity outcomes inferred, I consider the 10 most relevant to herd managers to be:

1. Reproductive Output (animals per animal)
2. Total Protein per Animal (kg)
3. Total Fat per Animal (kg)
4. Fodder consumed per Animal (kg)
5. Milk Calories per Fodder consumed (kcal/kg)
6. MOW Calories per Fodder consumed (kcal/kg)
7. Total Calories per Fodder consumed (kcal/kg)
8. Total Calories per Animal (kcal)
9. MOW Calories per Animal (kcal)
10. Milk Calories per Animal (kcal).

In order to show results plotted against location, the dataset has been sorted (a) from West to East Europe and (b) from South to North Europe with ascending longitude (West to East) and ascending latitude (South to North) values. Note that latitude/longitude information was missing for archaeological site 'Fontbelle', so this site was excluded from the geographic analyses.

As discussed in the methods section of Chapter 5, there are meta-parameters to this (and all other Bayesian MCMC) method, which were set individually. For the results generated in this chapter, the same meta-parameter preferences were set, as for the results generated in Chapter 5: 20 million simulations, with a burn-in of 1 million and a thinning, which is set to record the outcomes of every 1000^{th} iteration.

To assess the significance of any relationship between date, latitude or longitude and estimates of sustainability and production parameters, I employed two approaches:

1. The means of the productivity outcome estimates (i.e. the means of the thinned MCMC samples; n=19,000) were correlated against the date, latitude or longitude of sites using the 'lm' and 'summary' functions in R, and the regression coefficient and p-value recorded.
2. One of the 19,000 thinned MCMC samples for each productivity outcome for each site was taken and correlated with date, latitude or longitude of sites, and the regression coefficient calculated as above, and recorded. This is repeated for all 19,000 thinned MCMC samples to give a distribution of regression coefficients. The proportion of these regression coefficients that are greater than zero is then calculated.

Of these two approaches to assessing the significance of any relationship between date, latitude or longitude, and estimates of sustainability and production parameters, the first is simpler and perhaps easier to understand, but the second is, in my view, a more natural way to treat Bayesian posterior estimates of output parameters, and is more informative. With respect to the second approach, I consider 1% or less, or 99% or more, of the regression coefficients of MCMC samples against time, latitude or longitude being greater than zero, as being 'persuasive evidence' of a relationship between date, latitude or longitude and estimates of sustainability and production parameters.

6.6 Results

6.6.1 Results for dataset-A (minimum number of elements)

6.6.1.1 Product output estimate trends against time

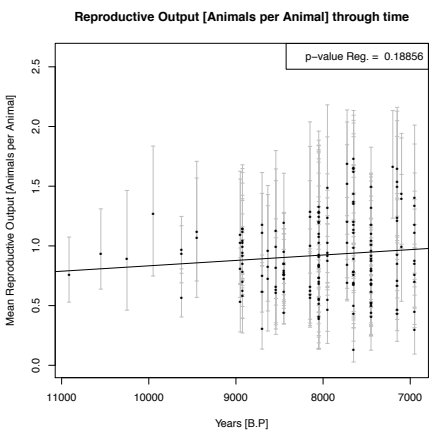

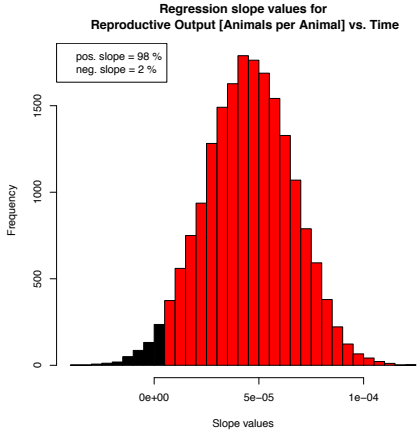

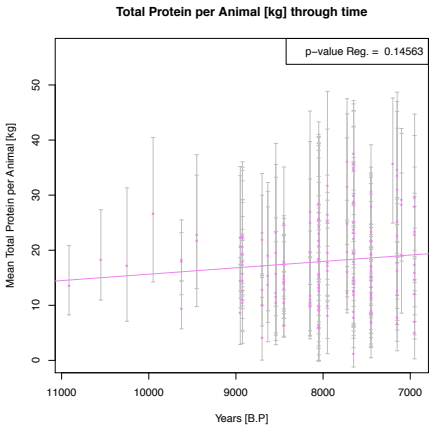

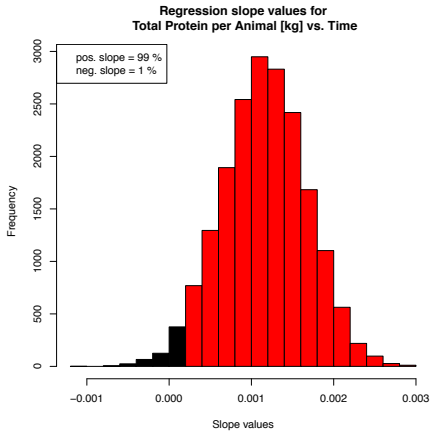

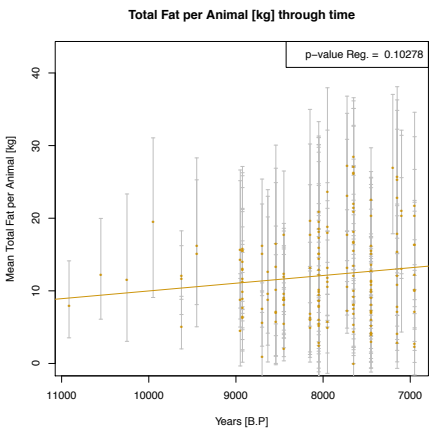

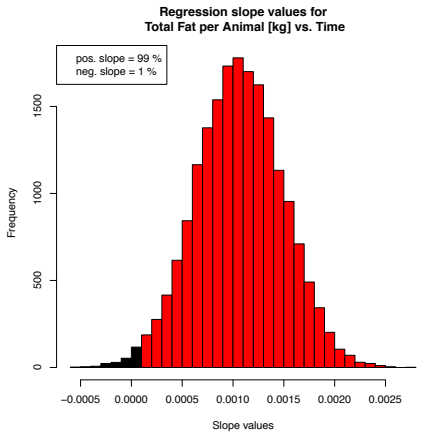

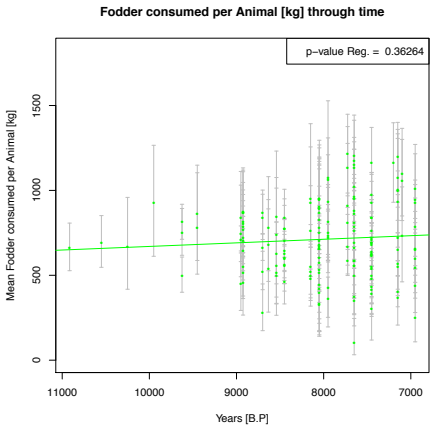
Fodder consumed per Animal [kg] through time
p−value Reg. = 0.36264
Mean Fodder consumed per Animal [kg]
0
500
1000
1500
11000
10000
9000
8000
7000
Years [B.P]

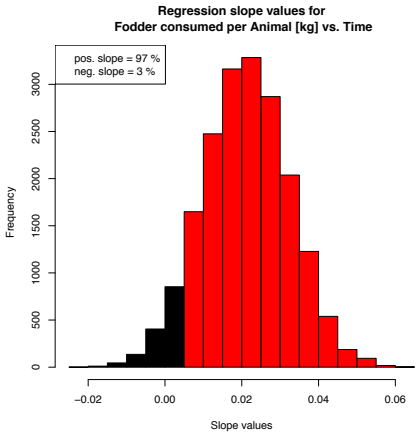
Regression slope values for
Fodder consumed per Animal [kg] vs. Time
pos. slope = 97 %
neg. slope = 3 %
Frequency
0
500
1000
1500
2000
2500
3000
−0.02
0.00
0.02
0.04
0.06
Slope values

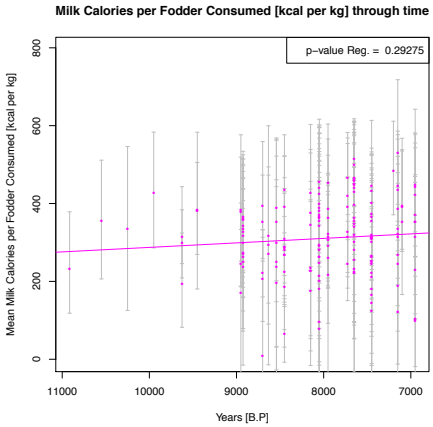
Milk Calories per Fodder Consumed [kcal per kg] through time
p−value Reg. = 0.29275
Mean Milk Calories per Fodder Consumed [kcal per kg]
0
200
400
600
800
11000
10000
9000
8000
7000
Years [B.P]

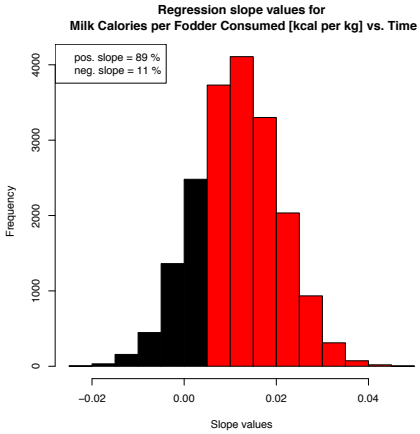
Regression slope values for
Milk Calories per Fodder Consumed [kcal per kg] vs. Time
pos. slope = 89 %
neg. slope = 11 %
Frequency
0
1000
2000
3000
4000
−0.02
0.00
0.02
0.04
Slope values

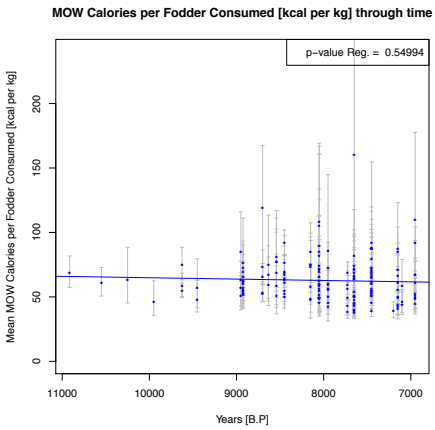
MOW Calories per Fodder Consumed [kcal per kg] through time
p−value Reg. = 0.54994
Mean MOW Calories per Fodder Consumed [kcal per kg]
0
50
100
150
200
11000
10000
9000
8000
7000
Years [B.P]

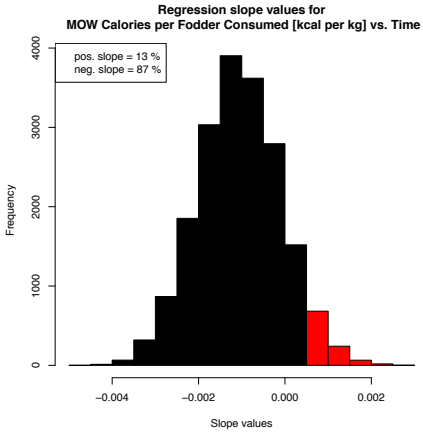
Regression slope values for
MOW Calories per Fodder Consumed [kcal per kg] vs. Time
pos. slope = 13 %
neg. slope = 87 %
Frequency
0
1000
2000
3000
4000
−0.004
−0.002
0.000
0.002
Slope values

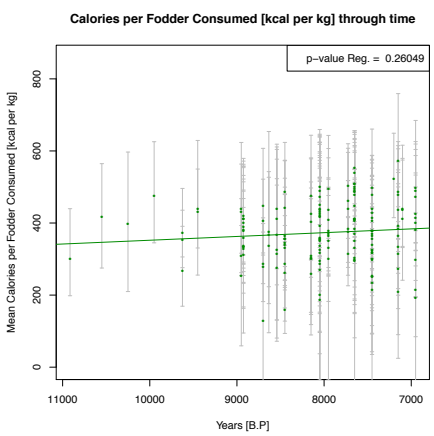
Calories per Fodder Consumed [kcal per kg] through time
p−value Reg. = 0.26049
Mean Calories per Fodder Consumed [kcal per kg]
0
200
400
600
800
11000
10000
9000
8000
7000
Years [B.P]

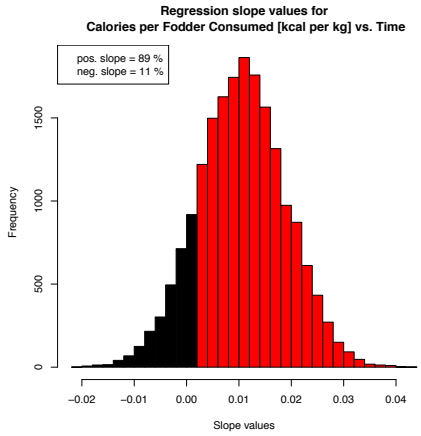
Regression slope values for
Calories per Fodder Consumed [kcal per kg] vs. Time
pos. slope = 89 %
neg. slope = 11 %
Frequency
0
500
1000
1500
−0.02
−0.01
0.00
0.01
0.02
0.03
0.04
Slope values

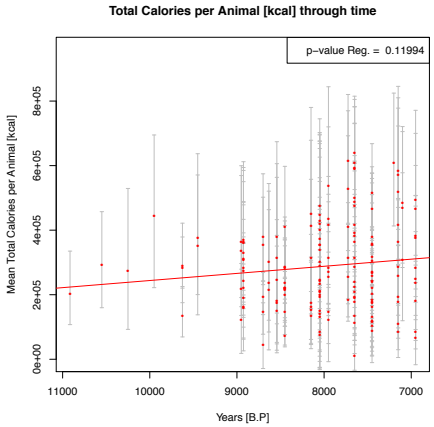
Total Calories per Animal [kcal] through time
p−value Reg. = 0.11994
Mean Total Calories per Animal [kcal]
0e+00
2e+05
4e+05
6e+05
8e+05
11000
10000
9000
8000
7000
Years [B.P]

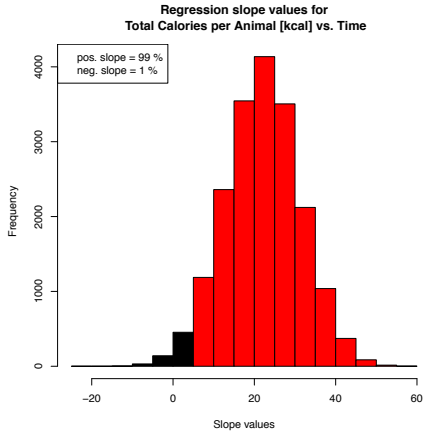
Regression slope values for
Total Calories per Animal [kcal] vs. Time
pos. slope = 99 %
neg. slope = 1 %
Frequency
0
1000
2000
3000
4000
−20
0
20
40
60
Slope values

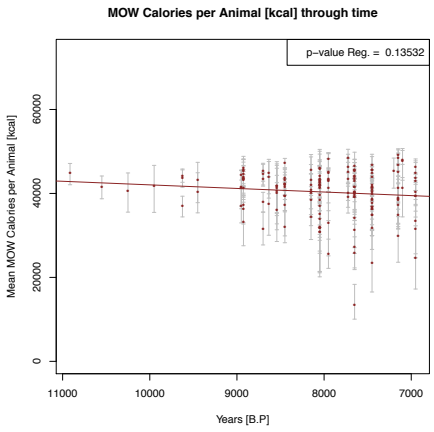
MOW Calories per Animal [kcal] through time
p−value Reg. = 0.13532
Mean MOW Calories per Animal [kcal]
0
20000
40000
60000
11000
10000
9000
8000
7000
Years [B.P]

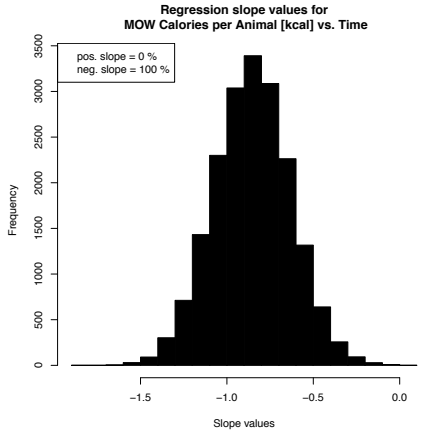
Regression slope values for
MOW Calories per Animal [kcal] vs. Time
pos. slope = 0 %
neg. slope = 100 %
Frequency
0
500
1000
1500
2000
2500
3000
3500
−1.5
−1.0
−0.5
0.0
Slope values

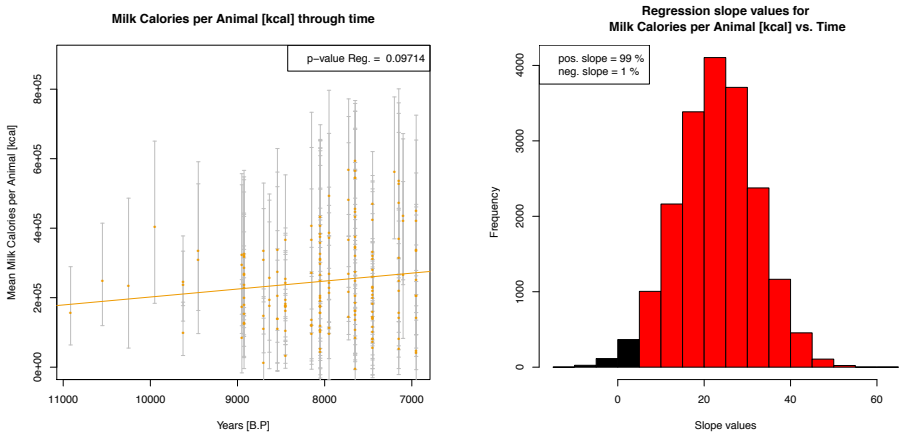

Fig. 6.4. Reproductive Output, animal product yields and macronutrient outputs inferred from 166 age-at-death profiles plotted versus time (~11,000 BP – 7,000 BP). Left hand plots show the means and standard deviations of the ten production estimates, plotted against time, together with the correlation coefficients and p-value. Right hand plots show the distribution of regression coefficients of MCMC samples against time; red = positive slopes, black = negative slopes.

All but two estimates show a positive trend through time, although none of the mean regressions has a p-value <0.05. However, by considering the more informative distribution of regression coefficients of MCMC samples against time, I obtain persuasive evidence of an increase in protein, fat and total calories produced per animal, and milk calories per animal, and persuasive evidence of a decrease on MOW calories per animal, throughout the Neolithic.

6.6.1.2 Product output estimate trends against longitude

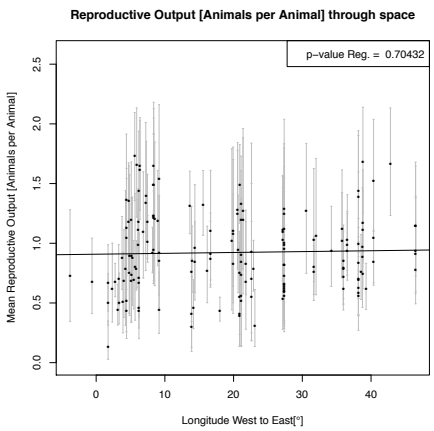

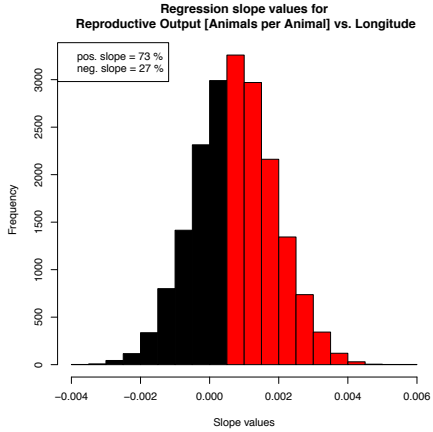

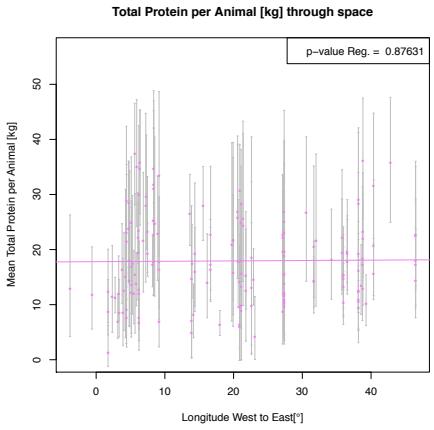

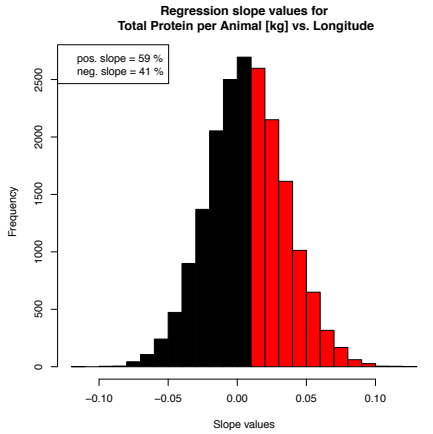

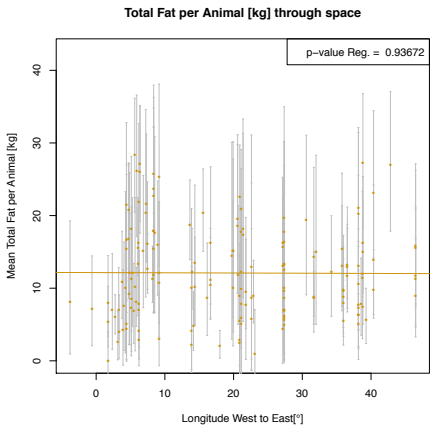

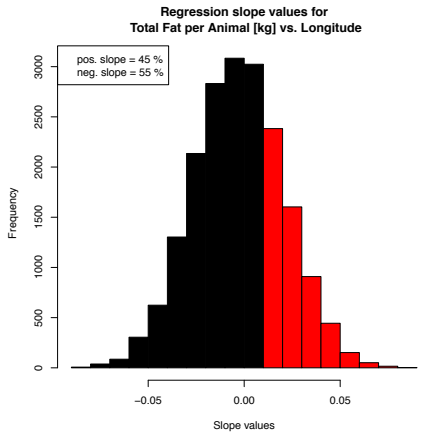

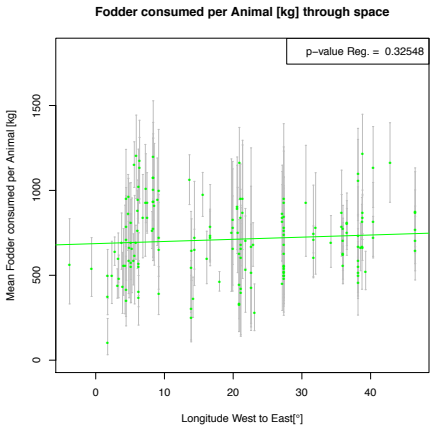
Fodder consumed per Animal [kg] through space
p−value Reg. = 0.32548
Mean Fodder consumed per Animal [kg]
Longitude West to East[°]

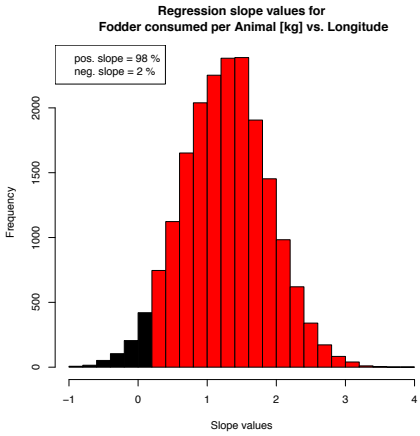
Regression slope values for
Fodder consumed per Animal [kg] vs. Longitude
pos. slope = 98 %
neg. slope = 2 %
Frequency
Slope values

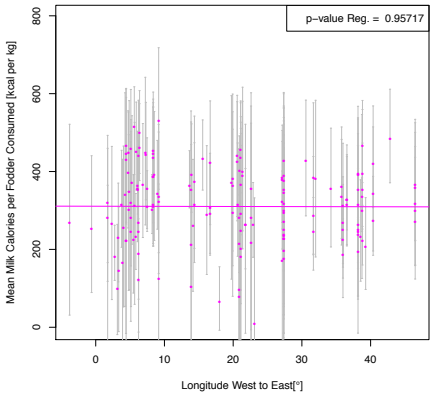
Milk Calories per Fodder Consumed [kcal per kg] through space
p−value Reg. = 0.95717
Mean Milk Calories per Fodder Consumed [kcal per kg]
Longitude West to East[°]

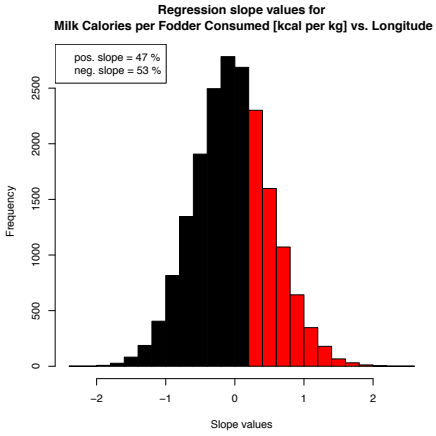
Regression slope values for
Milk Calories per Fodder Consumed [kcal per kg] vs. Longitude
pos. slope = 47 %
neg. slope = 53 %
Frequency
Slope values

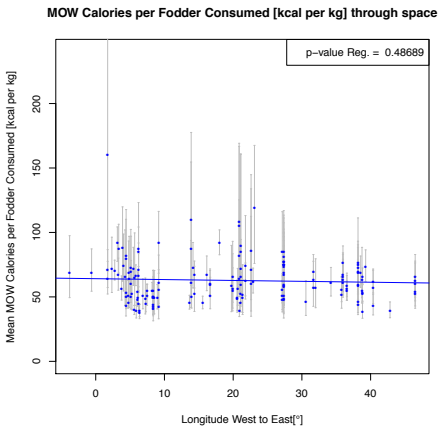
MOW Calories per Fodder Consumed [kcal per kg] through space
p−value Reg. = 0.48689
Mean MOW Calories per Fodder Consumed [kcal per kg]
Longitude West to East[°]

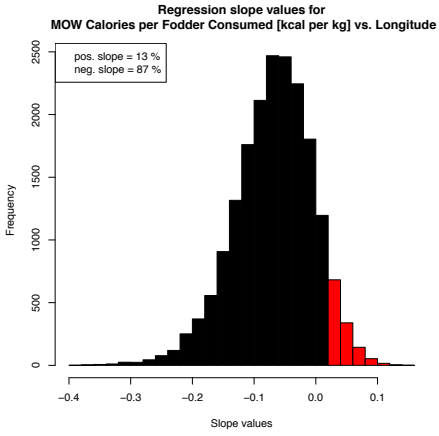
Regression slope values for
MOW Calories per Fodder Consumed [kcal per kg] vs. Longitude
pos. slope = 13 %
neg. slope = 87 %
Frequency
Slope values

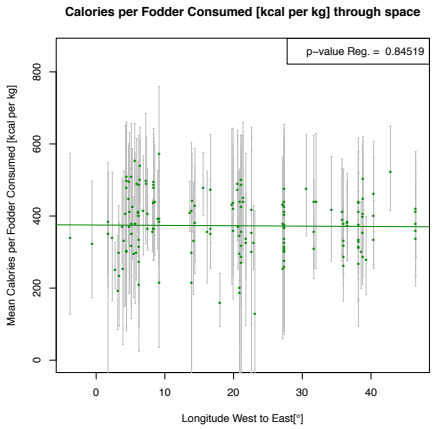
Calories per Fodder Consumed [kcal per kg] through space
p−value Reg. = 0.84519
Mean Calories per Fodder Consumed [kcal per kg]
0
200
400
600
800
0
10
20
30
40
Longitude West to East[°]

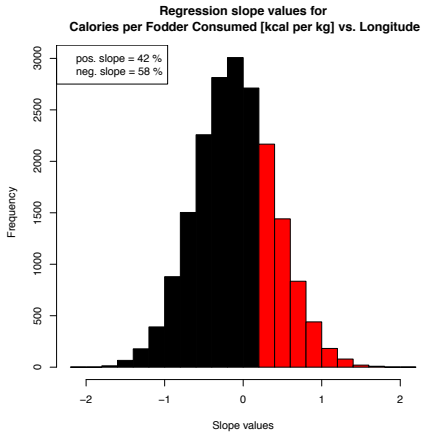
Regression slope values for
Calories per Fodder Consumed [kcal per kg] vs. Longitude
pos. slope = 42 %
neg. slope = 58 %
Frequency
0
500
1000
1500
2000
2500
3000
−2
−1
0
1
2
Slope values

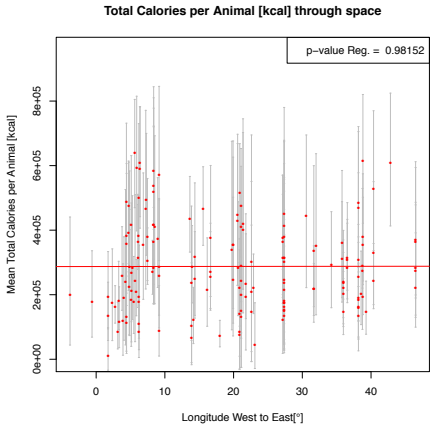
Total Calories per Animal [kcal] through space
p−value Reg. = 0.98152
Mean Total Calories per Animal [kcal]
0e+00
2e+05
4e+05
6e+05
8e+05
0
10
20
30
40
Longitude West to East[°]

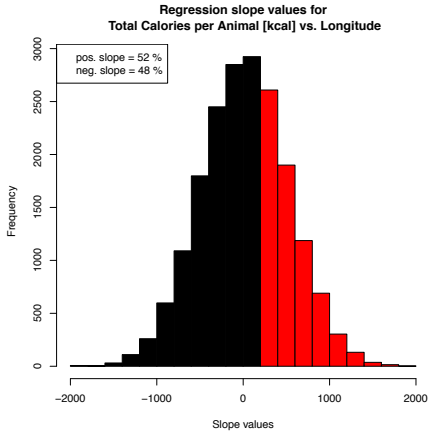
Regression slope values for
Total Calories per Animal [kcal] vs. Longitude
pos. slope = 52 %
neg. slope = 48 %
Frequency
0
500
1000
1500
2000
2500
3000
−2000
−1000
0
1000
2000
Slope values

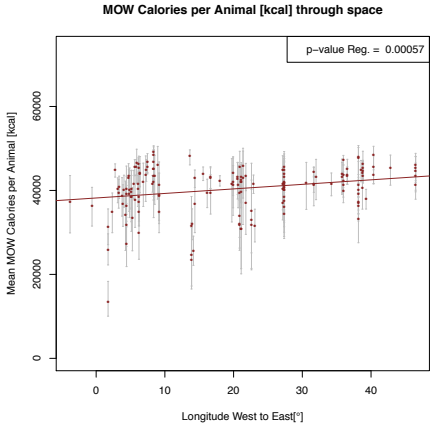
MOW Calories per Animal [kcal] through space
p−value Reg. = 0.00057
Mean MOW Calories per Animal [kcal]
0
20000
40000
60000
0
10
20
30
40
Longitude West to East[°]

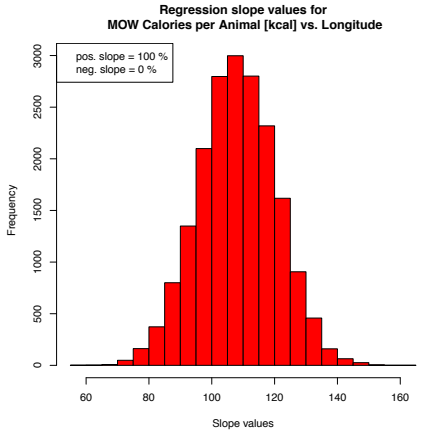
Regression slope values for
MOW Calories per Animal [kcal] vs. Longitude
pos. slope = 100 %
neg. slope = 0 %
Frequency
0
500
1000
1500
2000
2500
3000
60
80
100
120
140
160
Slope values

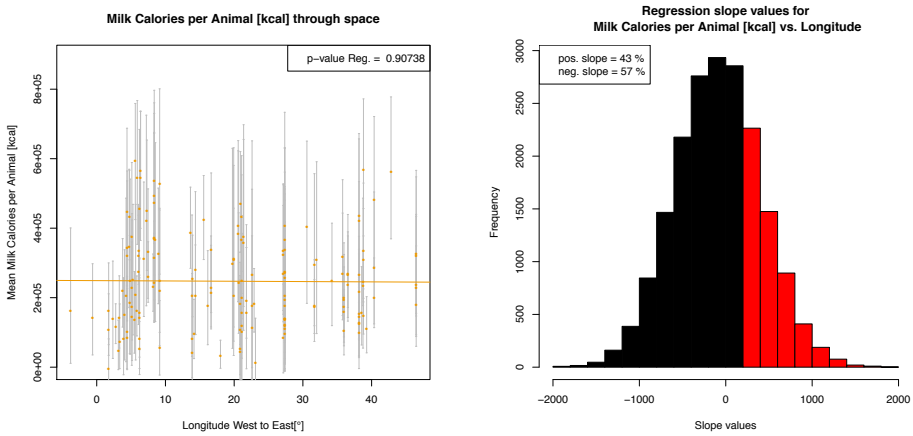

Fig. 6.5. Reproductive Output, animal product yields and macronutrient outputs inferred from 166 age-at-death profiles plotted versus longitude. Left hand plots show the means and standard deviations of the ten production estimates, plotted against longitude, together with the correlation coefficients and p-value. The range of analysed longitudes spans from -3.52 (3° 31' 12" W) to 46.48 (46° 28' 48" E) degrees. Right hand plots show the distribution of regression coefficients of MCMC samples against longitude; red = positive slopes, black = negative slopes.

Out of ten estimates, five show a positive trend with increasing longitude, although all but one of the mean regressions have a p-value >0.05. This one estimate is MOW calories per animal. By considering the more informative distribution regression coefficients of MCMC samples against time, I also obtain persuasive evidence only of an increase of MOW calories per animal with increasing longitude.

6.6.1.3 Product output estimate trends against latitude

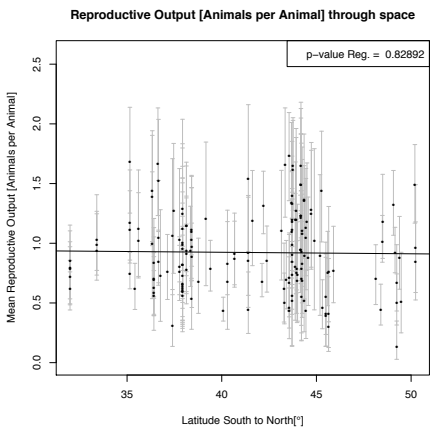

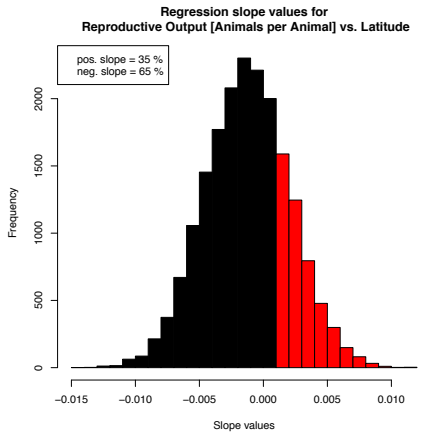

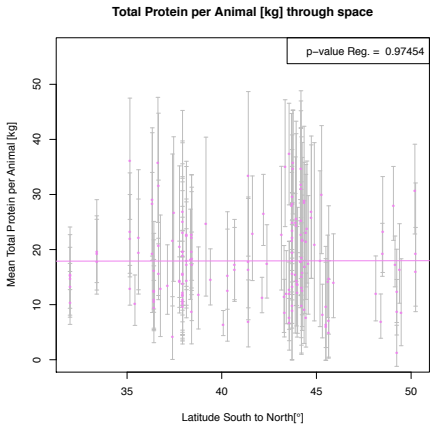

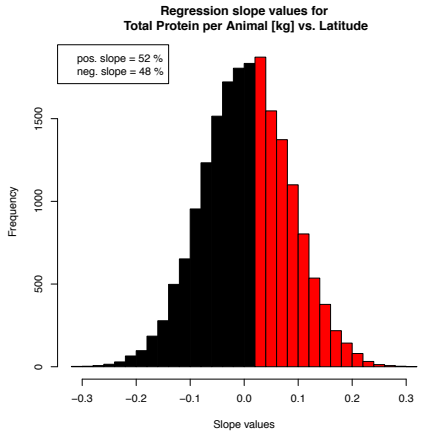

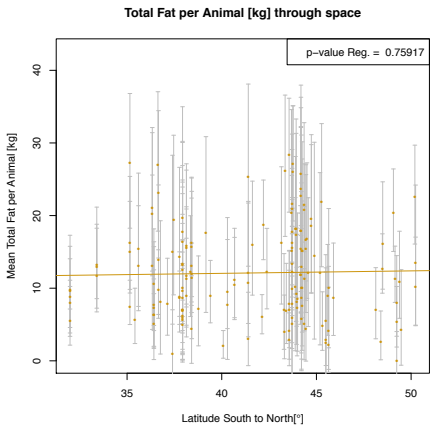

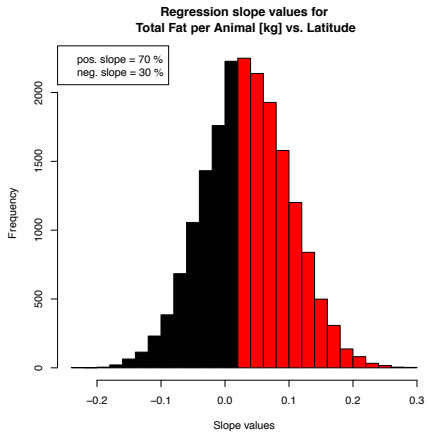

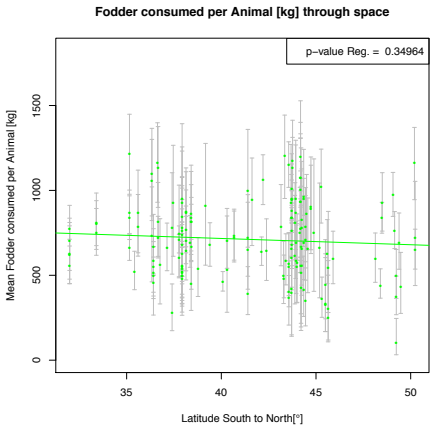
Fodder consumed per Animal [kg] through space
p−value Reg. = 0.34964
Mean Fodder consumed per Animal [kg]
0
500
1000
1500
35
40
45
50
Latitude South to North[°]

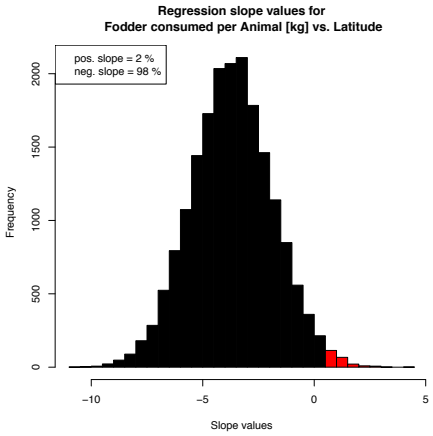
Regression slope values for
Fodder consumed per Animal [kg] vs. Latitude
pos. slope = 2 %
neg. slope = 98 %
Frequency
0
500
1000
1500
2000
−10
−5
0
5
Slope values

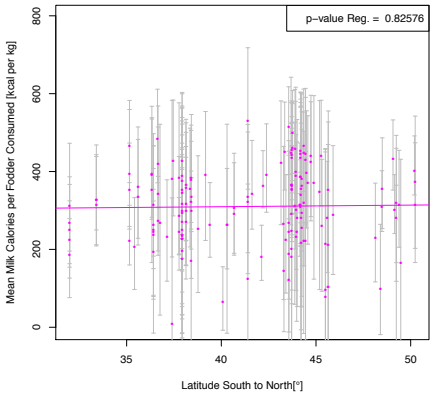
Milk Calories per Fodder Consumed [kcal per kg] through space
p−value Reg. = 0.82576
Mean Milk Calories per Fodder Consumed [kcal per kg]
0
200
400
600
800
35
40
45
50
Latitude South to North[°]

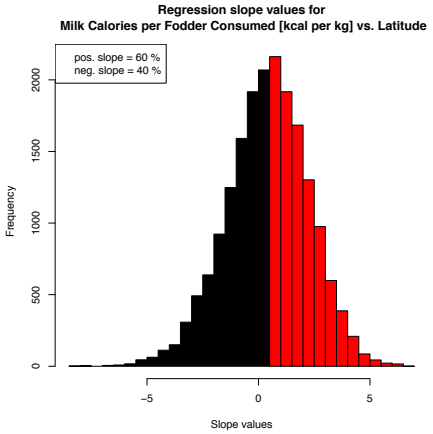
Regression slope values for
Milk Calories per Fodder Consumed [kcal per kg] vs. Latitude
pos. slope = 60 %
neg. slope = 40 %
Frequency
0
500
1000
1500
2000
−5
0
5
Slope values

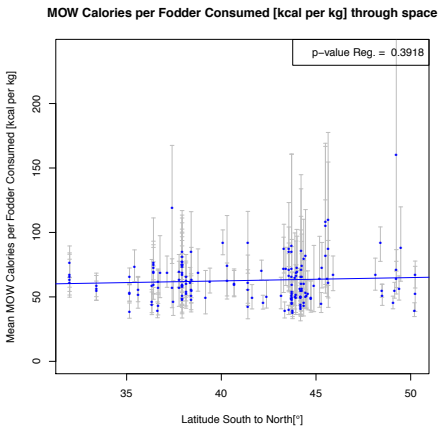
MOW Calories per Fodder Consumed [kcal per kg] through space
p−value Reg. = 0.3918
Mean MOW Calories per Fodder Consumed [kcal per kg]
0
50
100
150
200
35
40
45
50
Latitude South to North[°]

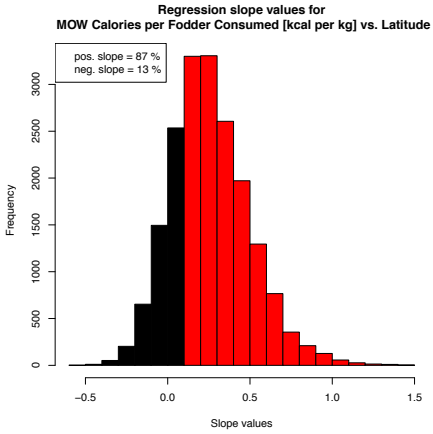
Regression slope values for
MOW Calories per Fodder Consumed [kcal per kg] vs. Latitude
pos. slope = 87 %
neg. slope = 13 %
Frequency
0
500
1000
1500
2000
2500
3000
−0.5
0.0
0.5
1.0
1.5
Slope values

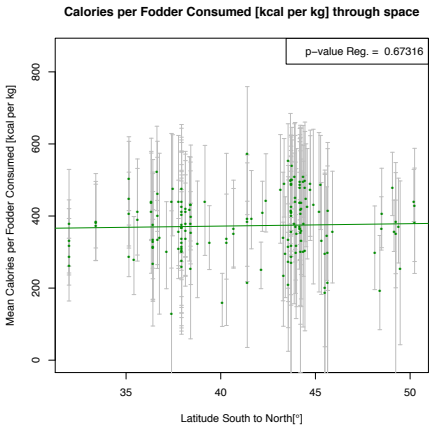
Calories per Fodder Consumed [kcal per kg] through space
p−value Reg. = 0.67316
Mean Calories per Fodder Consumed [kcal per kg]
0
200
400
600
800
35
40
45
50
Latitude South to North[°]

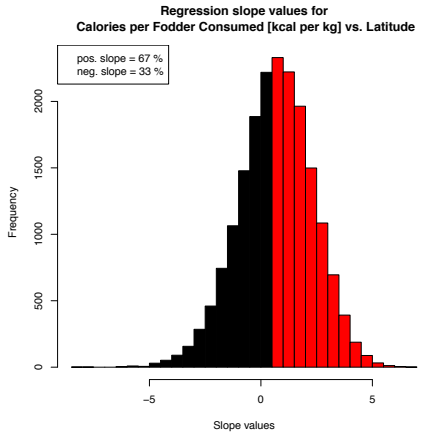
Regression slope values for
Calories per Fodder Consumed [kcal per kg] vs. Latitude
pos. slope = 67 %
neg. slope = 33 %
Frequency
0
500
1000
1500
2000
−5
0
5
Slope values

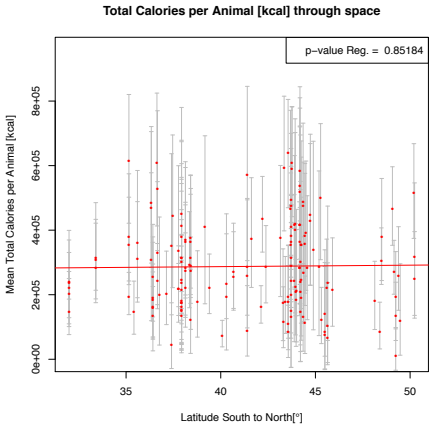
Total Calories per Animal [kcal] through space
p−value Reg. = 0.85184
Mean Total Calories per Animal [kcal]
0e+00
2e+05
4e+05
6e+05
8e+05
35
40
45
50
Latitude South to North[°]

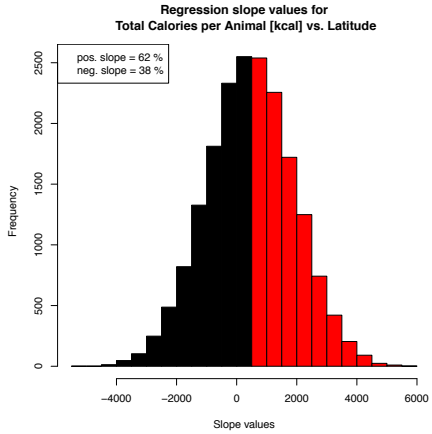
Regression slope values for
Total Calories per Animal [kcal] vs. Latitude
pos. slope = 62 %
neg. slope = 38 %
Frequency
0
500
1000
1500
2000
2500
−4000
−2000
0
2000
4000
6000
Slope values

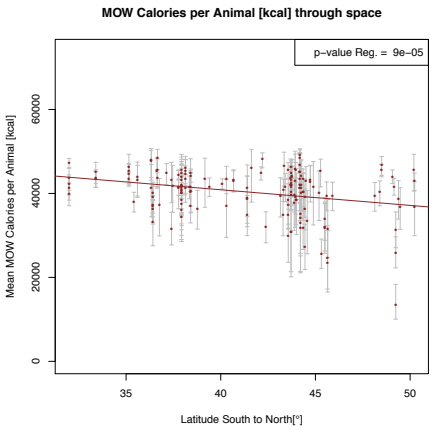
MOW Calories per Animal [kcal] through space
p−value Reg. = 9e−05
Mean MOW Calories per Animal [kcal]
0
20000
40000
60000
35
40
45
50
Latitude South to North[°]

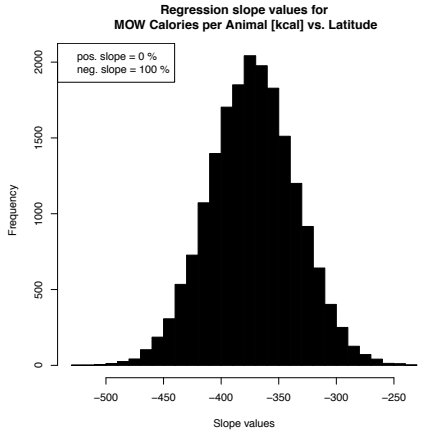
Regression slope values for
MOW Calories per Animal [kcal] vs. Latitude
pos. slope = 0 %
neg. slope = 100 %
Frequency
0
500
1000
1500
2000
−500
−450
−400
−350
−300
−250
Slope values

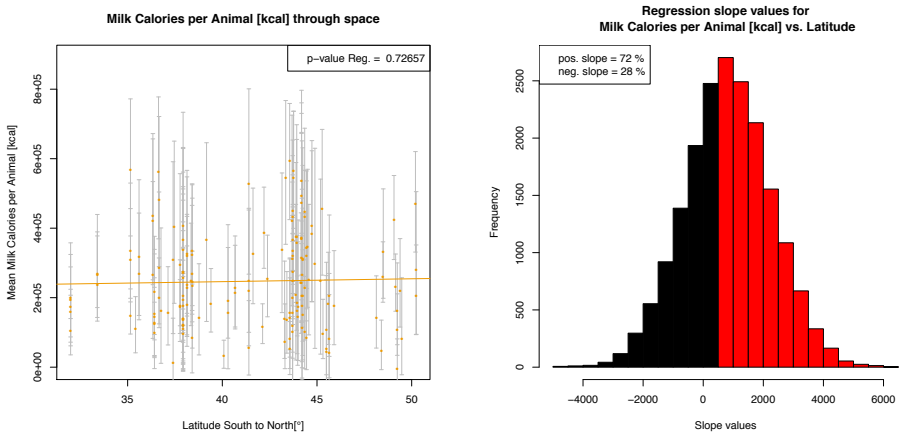

Fig. 6.6. Reproductive Output, animal product yields and macronutrient outputs inferred from 166 age-at-death profiles plotted versus latitude. Left hand plots show the means and standard deviations of the ten production estimates, plotted against latitudes, together with the correlation coefficients and p-value. The range of analysed latitudes spans from ca. 31.98 (31° 58' 48" N) to ca. 52.63 (52° 37' 48" N) degrees. Right hand plots show the distribution of regression coefficients of MCMC samples against latitudes; red = positive slopes, black = negative slopes.

Out of ten estimates, eight show a positive trend with increasing latitudes, although all but one of the mean regressions have a p-value >0.05. This one estimate is, again, MOW calories per animal. By considering the more informative distribution regression coefficients of MCMC samples against latitudes, I also obtain persuasive evidence of an increase of only MOW calories per animal with increasing latitudes.

6.6.2 Results for dataset-B (minimum number of individuals)

6.6.2.1 Product output estimate trends against time

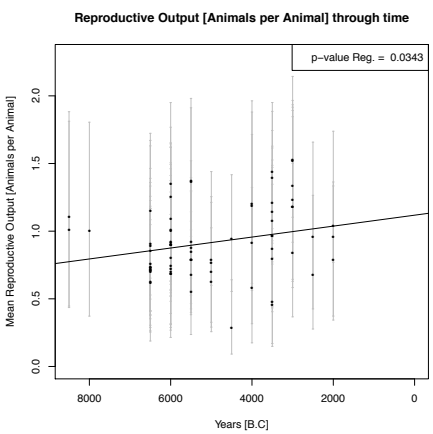

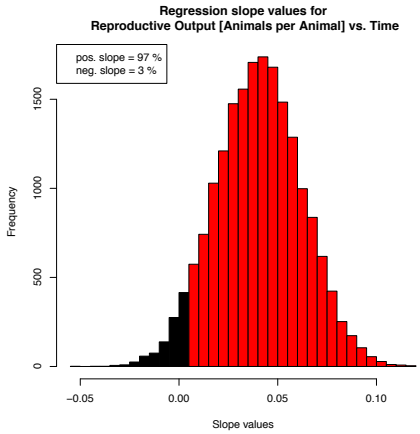

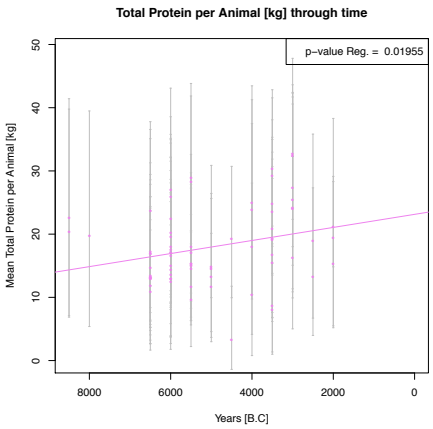

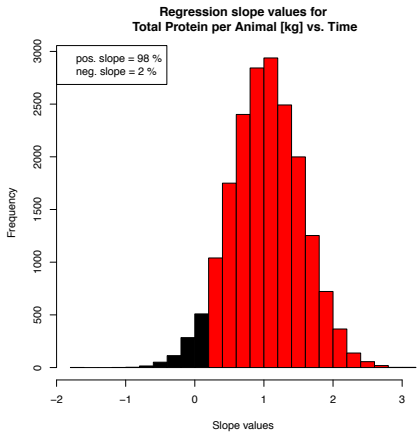

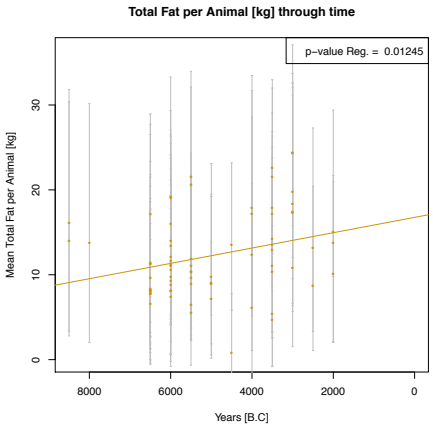

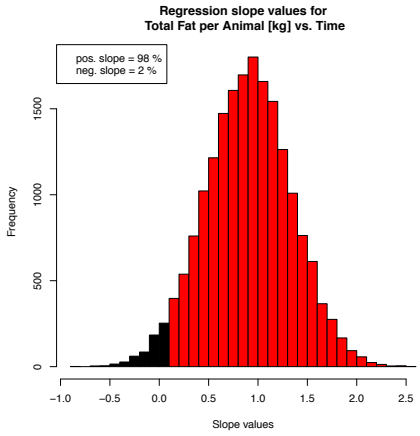

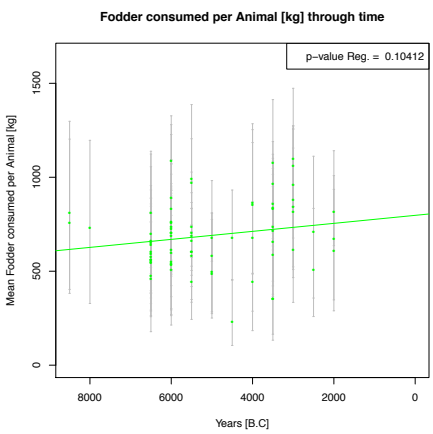
Fodder consumed per Animal [kg] through time
p−value Reg. = 0.10412
Mean Fodder consumed per Animal [kg]
0
500
1000
1500
8000
6000
4000
2000
0
Years [B.C]

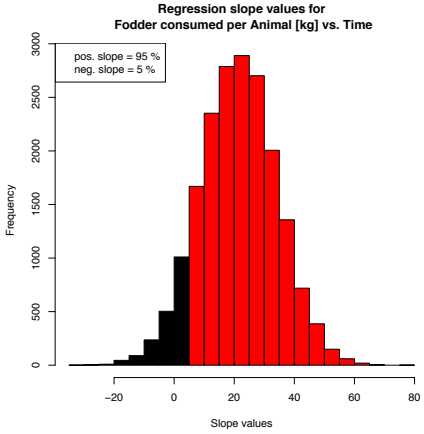
Regression slope values for
Fodder consumed per Animal [kg] vs. Time
pos. slope = 95 %
neg. slope = 5 %
Frequency
0
500
1000
1500
2000
2500
3000
−20
0
20
40
60
80
Slope values

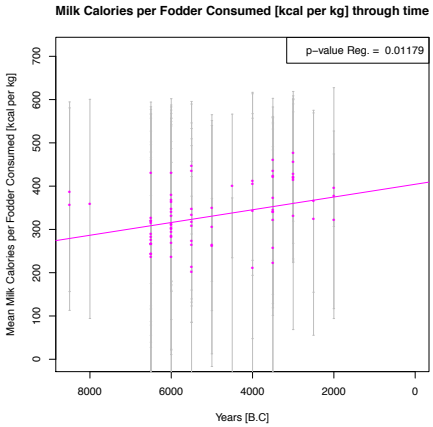
Milk Calories per Fodder Consumed [kcal per kg] through time
p−value Reg. = 0.01179
Mean Milk Calories per Fodder Consumed [kcal per kg]
0
100
200
300
400
500
600
700
8000
6000
4000
2000
0
Years [B.C]

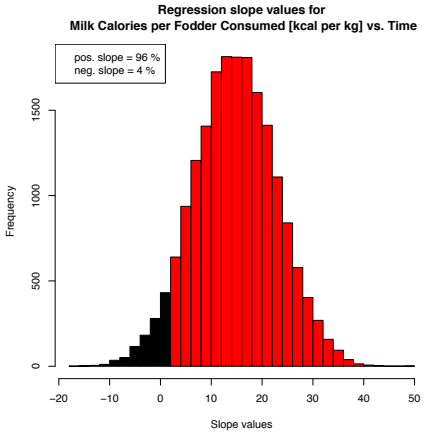
Regression slope values for
Milk Calories per Fodder Consumed [kcal per kg] vs. Time
pos. slope = 96 %
neg. slope = 4 %
Frequency
0
500
1000
1500
−20
−10
0
10
20
30
40
50
Slope values

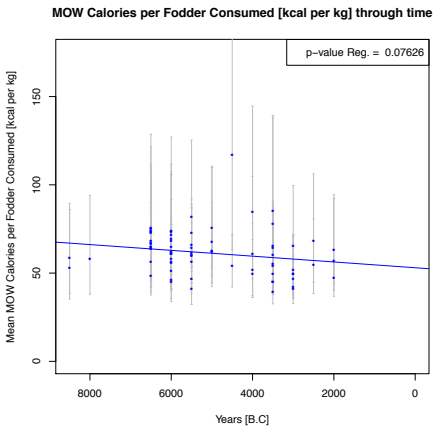
MOW Calories per Fodder Consumed [kcal per kg] through time
p−value Reg. = 0.07626
Mean MOW Calories per Fodder Consumed [kcal per kg]
0
50
100
150
8000
6000
4000
2000
0
Years [B.C]

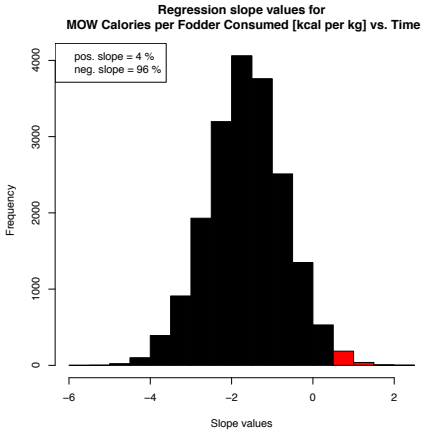
Regression slope values for
MOW Calories per Fodder Consumed [kcal per kg] vs. Time
pos. slope = 4 %
neg. slope = 96 %
Frequency
0
1000
2000
3000
4000
−6
−4
−2
0
2
Slope values

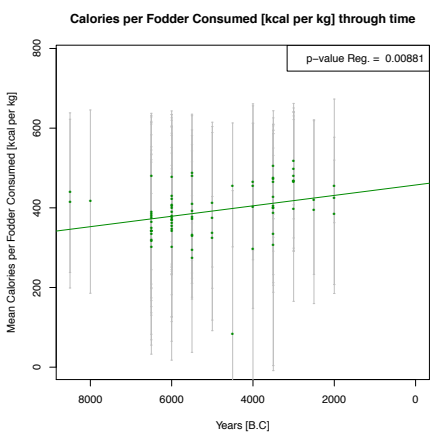
Calorie per Fodder Consumed [kcal per kg] through time
p−value Reg. = 0.00881
Mean Calories per Fodder Consumed [kcal per kg]
0
200
400
600
800
8000
6000
4000
2000
0
Years [B.C]

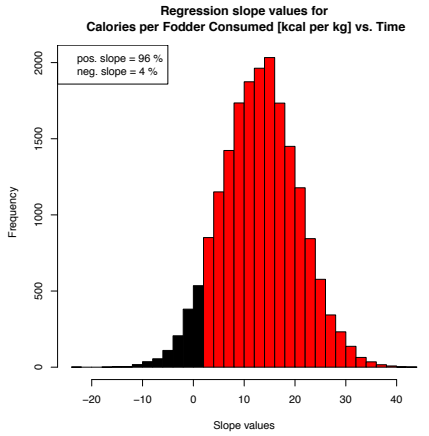
Regression slope values for
Calories per Fodder Consumed [kcal per kg] vs. Time
pos. slope = 96 %
neg. slope = 4 %
Frequency
0
500
1000
1500
2000
−20
−10
0
10
20
30
40
Slope values

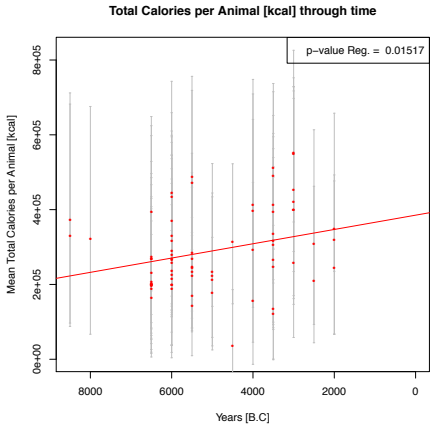
Total Calories per Animal [kcal] through time
p−value Reg. = 0.01517
Mean Total Calories per Animal [kcal]
0e+00
2e+05
4e+05
6e+05
8e+05
8000
6000
4000
2000
0
Years [B.C]

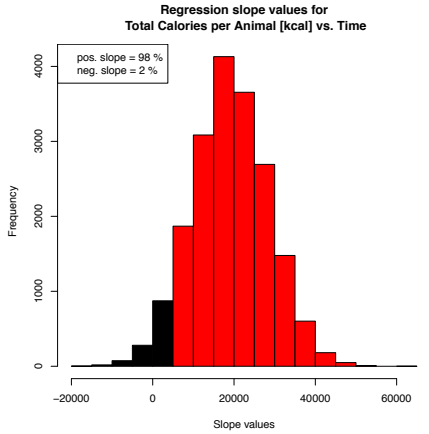
Regression slope values for
Total Calories per Animal [kcal] vs. Time
pos. slope = 98 %
neg. slope = 2 %
Frequency
0
1000
2000
3000
4000
−20000
0
20000
40000
60000
Slope values

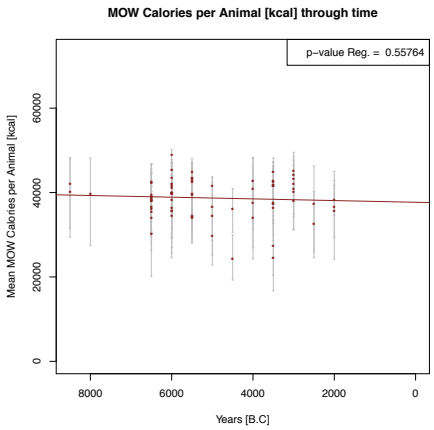
MOW Calories per Animal [kcal] through time
p−value Reg. = 0.55764
Mean MOW Calories per Animal [kcal]
0
20000
40000
60000
8000
6000
4000
2000
0
Years [B.C]

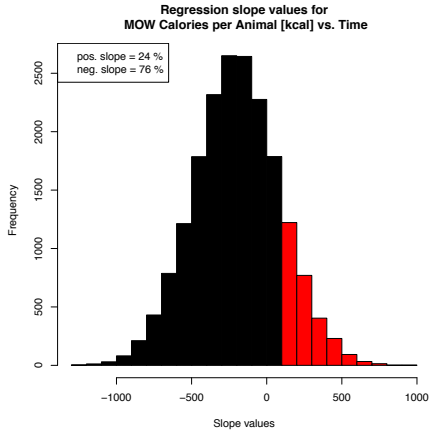
Regression slope values for
MOW Calories per Animal [kcal] vs. Time
pos. slope = 24 %
neg. slope = 76 %
Frequency
0
500
1000
1500
2000
2500
−1000
−500
0
500
1000
Slope values

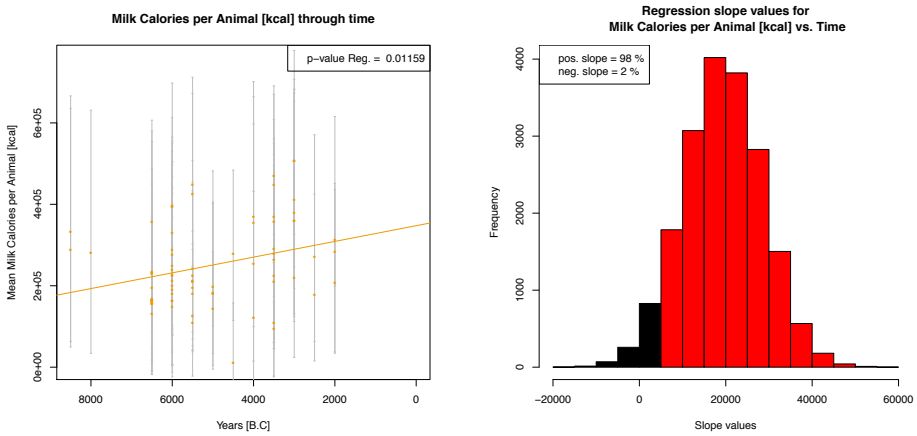

Fig. 6.7. Reproductive Outputs, animal product yields, macronutrient outputs and economic efficiencies inferred from 75 Neolithic age-at-death profiles plotted versus time (~8,000 - ~2,000 BC). Left hand plots show the means and standard deviations of the ten production estimates, plotted against time, together with the correlation coefficients and p-value (for dataset-B). Right hand plots show the distribution of regression coefficients of MCMC samples against time; red = positive slopes, black = negative slopes.

All but two estimates show a positive trend through time and seven out of ten mean regressions has a p-value <0.05. However, by considering the more informative distribution regression coefficients of MCMC samples against time, I find no persuasive evidence (as defined above) for product estimates increasing or decreasing throughout the Neolithic.

6.6.2.2 Product output estimate trends against longitude

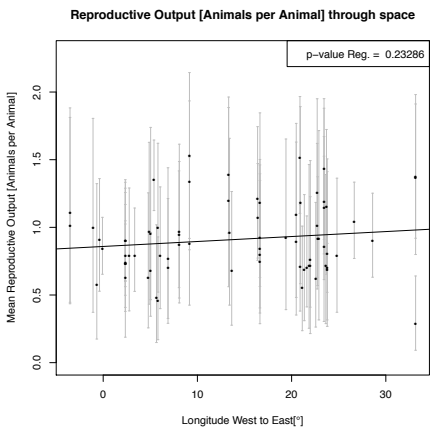

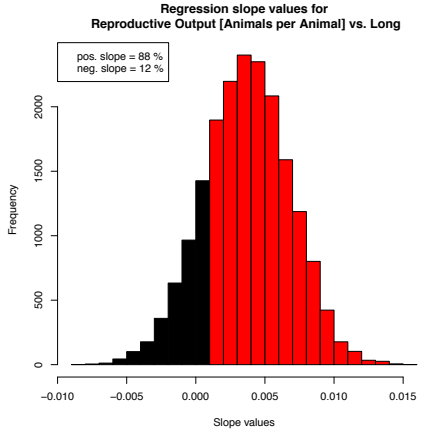

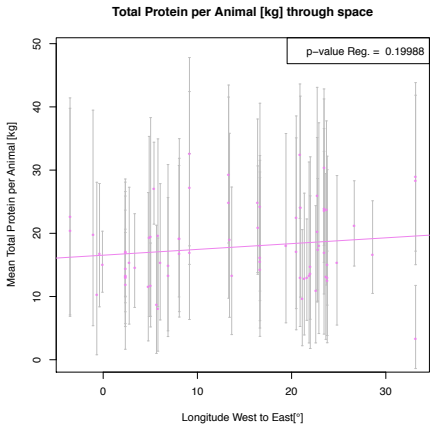

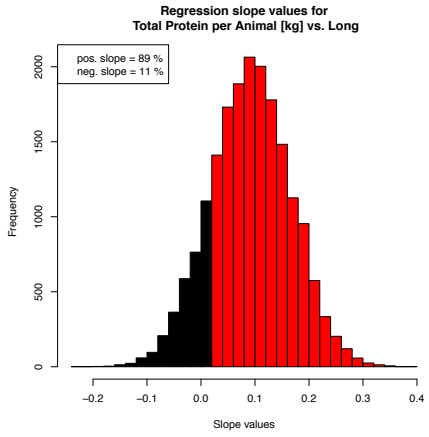

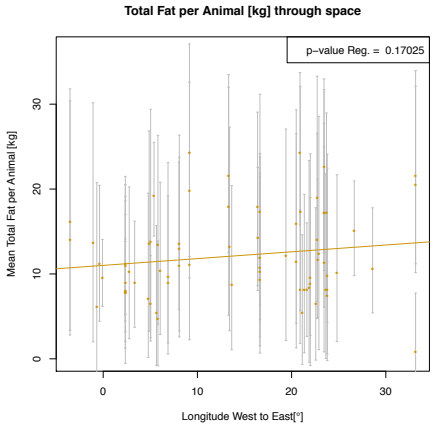

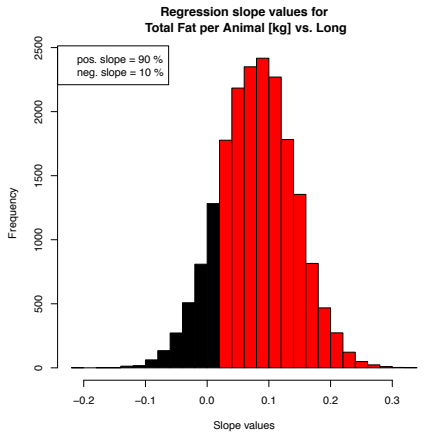

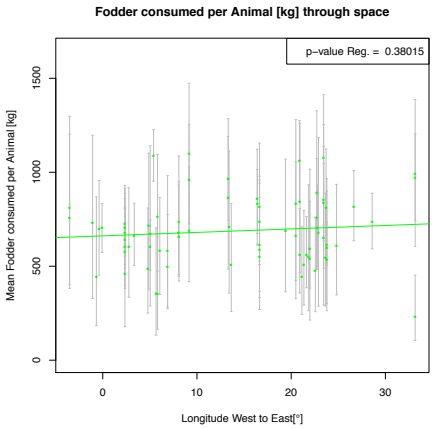
Fodder consumed per Animal [kg] through space
p−value Reg. = 0.38015
Mean Fodder consumed per Animal [kg]
Longitude West to East[°]

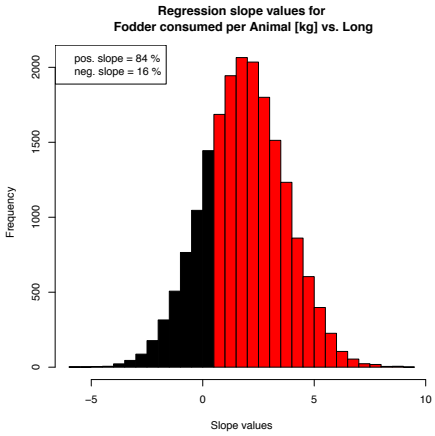
Regression slope values for
Fodder consumed per Animal [kg] vs. Long
pos. slope = 84 %
neg. slope = 16 %
Frequency
Slope values

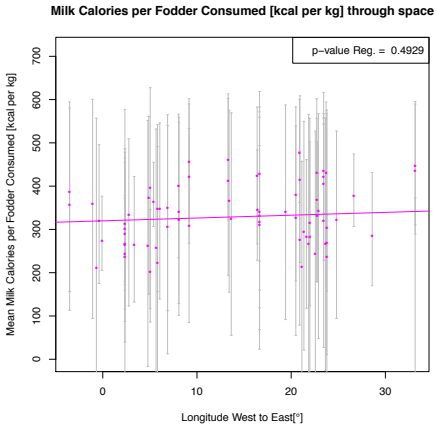
Milk Calories per Fodder Consumed [kcal per kg] through space
p−value Reg. = 0.4929
Mean Milk Calories per Fodder Consumed [kcal per kg]
Longitude West to East[°]

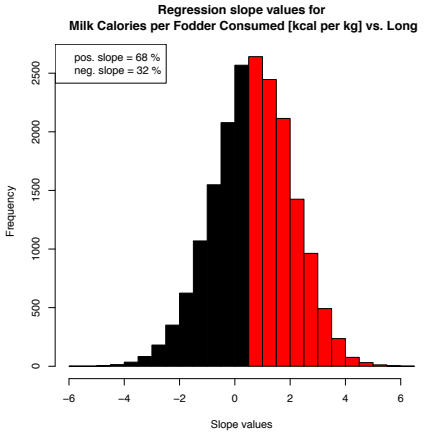
Regression slope values for
Milk Calories per Fodder Consumed [kcal per kg] vs. Long
pos. slope = 68 %
neg. slope = 32 %
Frequency
Slope values

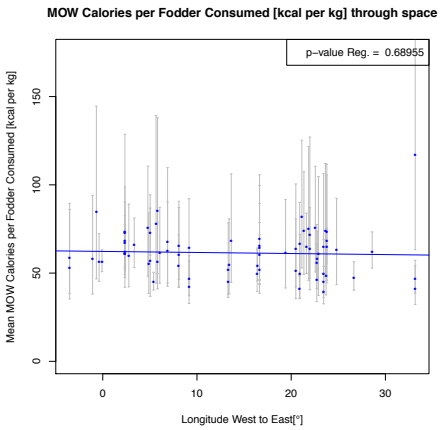
MOW Calories per Fodder Consumed [kcal per kg] through space
p−value Reg. = 0.68955
Mean MOW Calories per Fodder Consumed [kcal per kg]
Longitude West to East[°]

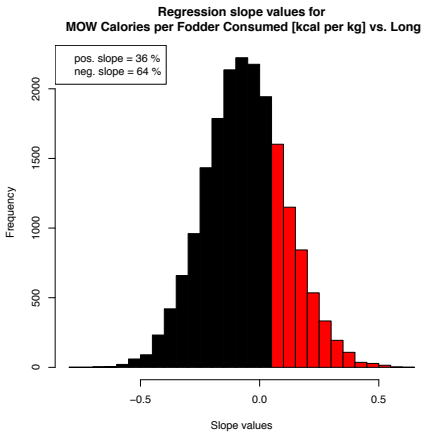
Regression slope values for
MOW Calories per Fodder Consumed [kcal per kg] vs. Long
pos. slope = 36 %
neg. slope = 64 %
Frequency
Slope values

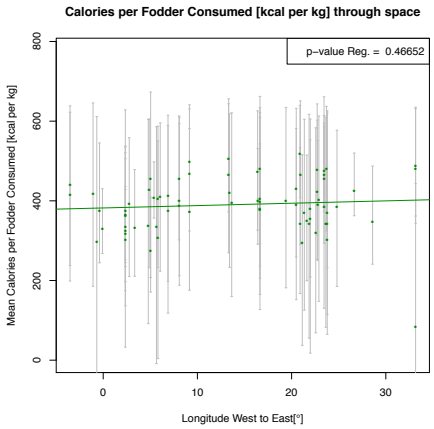
Calories per Fodder Consumed [kcal per kg] through space
p−value Reg. = 0.46652
Mean Calories per Fodder Consumed [kcal per kg]
Longitude West to East[°]

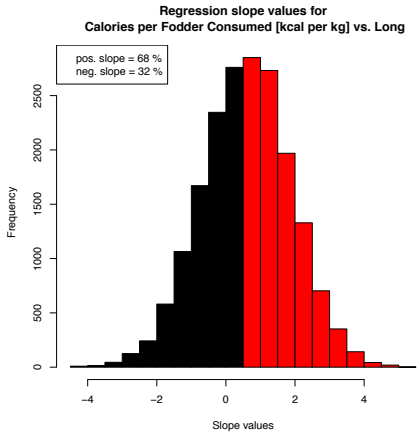
Regression slope values for
Calories per Fodder Consumed [kcal per kg] vs. Long
pos. slope = 68 %
neg. slope = 32 %
Frequency
Slope values

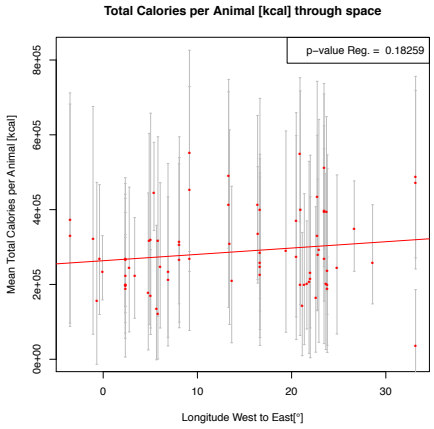
Total Calories per Animal [kcal] through space
p−value Reg. = 0.18259
Mean Total Calories per Animal [kcal]
Longitude West to East[°]

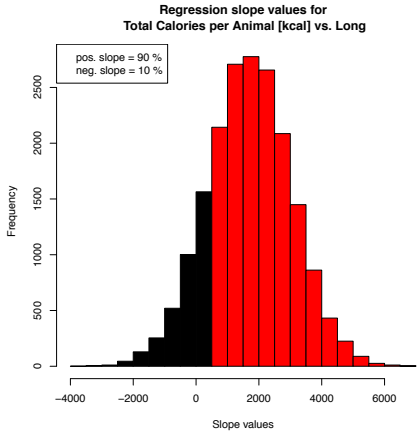
Regression slope values for
Total Calories per Animal [kcal] vs. Long
pos. slope = 90 %
neg. slope = 10 %
Frequency
Slope values

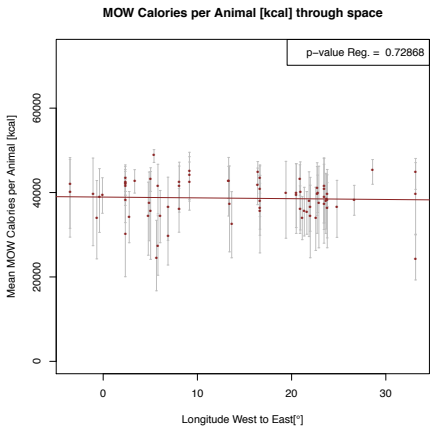
MOW Calories per Animal [kcal] through space
p−value Reg. = 0.72868
Mean MOW Calories per Animal [kcal]
Longitude West to East[°]

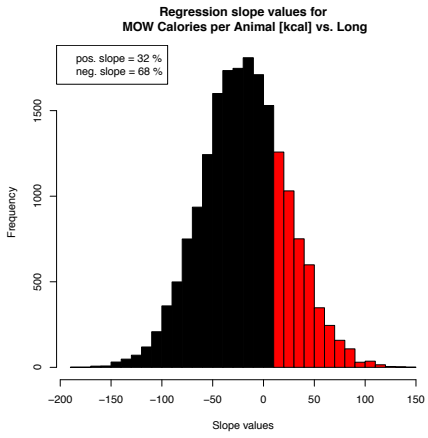
Regression slope values for
MOW Calories per Animal [kcal] vs. Long
pos. slope = 32 %
neg. slope = 68 %
Frequency
Slope values

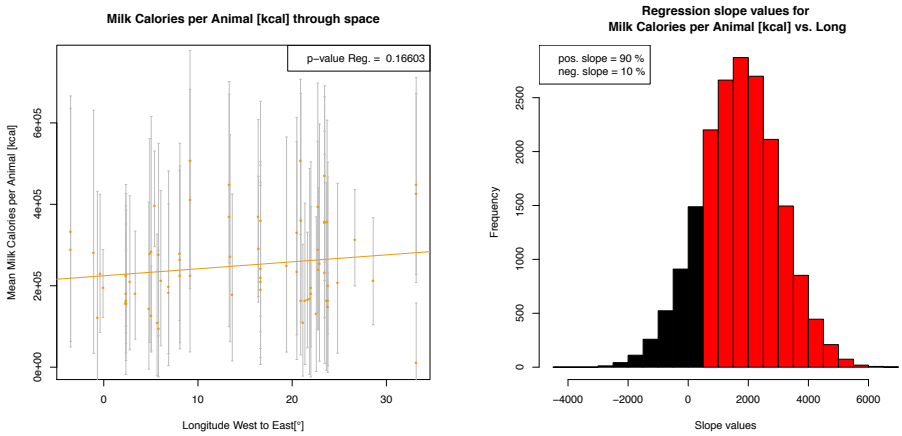

Fig. 6.8. Reproductive Output, animal product yields and macronutrient outputs inferred from 75 Neolithic age-at-death profiles plotted against longitude (West to East). Left hand plots show the means and standard deviations of the ten production estimates, plotted against longitude, together with the correlation coefficients and p-value. The range of analysed longitudes spans from -3.518915 (3°31'08.1"W) to 33.160894 (33°09'39.2"E) degrees. Right hand plots show the distribution of regression coefficients of MCMC samples against longitude; red = positive slopes, black = negative slopes.

Out of ten estimates, eight show a positive trend with increasing longitude, although none of the mean regressions have a p-value <0.05. Consistent with this, by considering the more informative distribution regression coefficients of MCMC samples against longitude I find no persuasive evidence (as defined above) for product estimates increasing or decreasing with increasing longitude.

6.6.2.3 Product output estimate trends against latitude

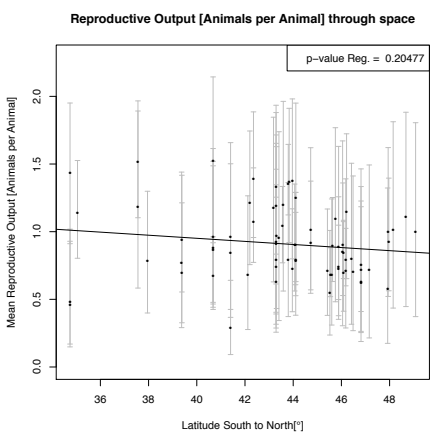

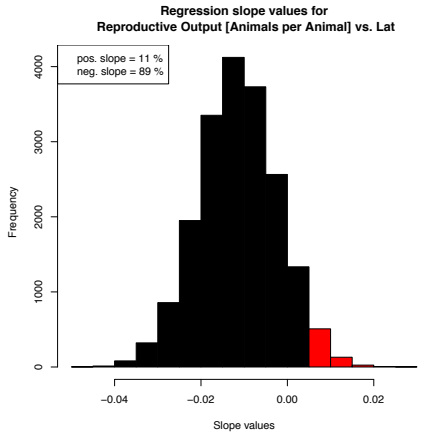

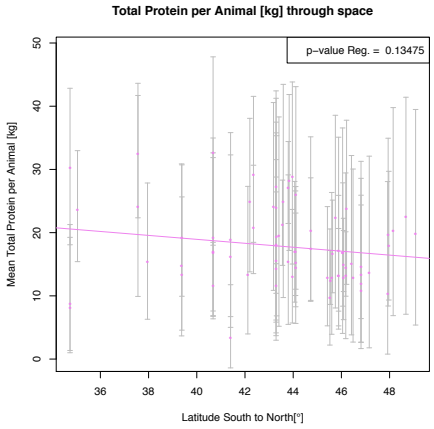

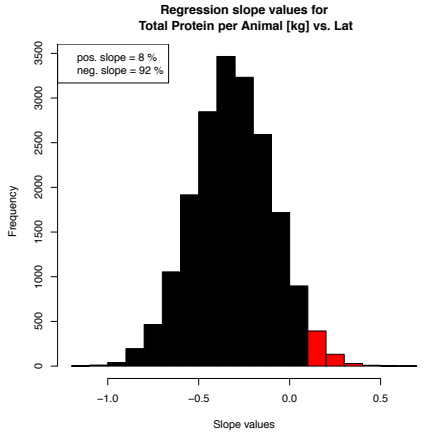

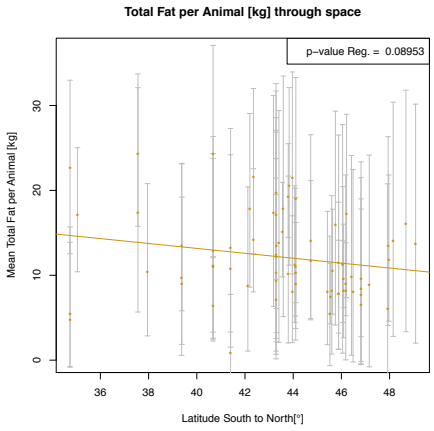

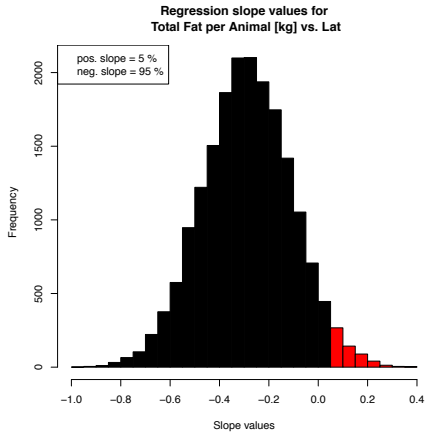

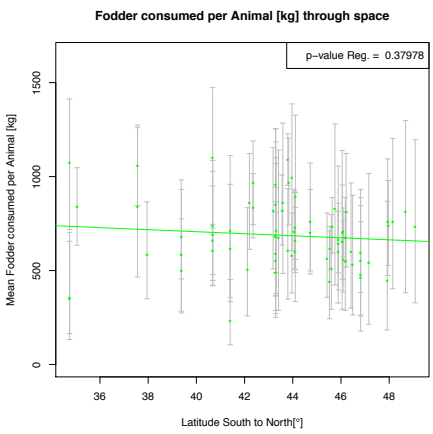
Fodder consumed per Animal [kg] through space
p−value Reg. = 0.37978
Mean Fodder consumed per Animal [kg]
0
500
1000
1500
36
38
40
42
44
46
48
Latitude South to North[°]

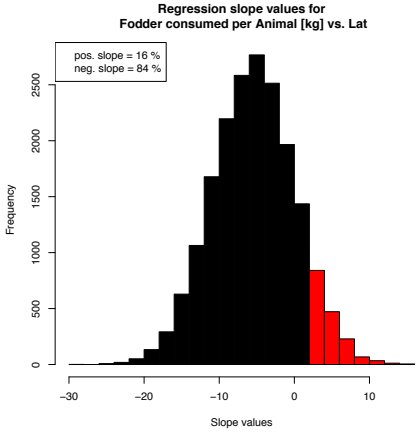
Regression slope values for
Fodder consumed per Animal [kg] vs. Lat
pos. slope = 16 %
neg. slope = 84 %
Frequency
0
500
1000
1500
2000
2500
−30
−20
−10
0
10
Slope values

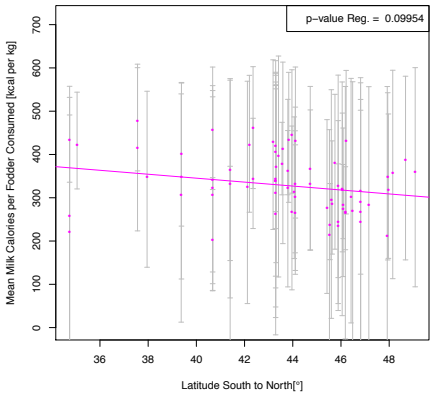
Milk Calories per Fodder Consumed [kcal per kg] through space
p−value Reg. = 0.09954
Mean Milk Calories per Fodder Consumed [kcal per kg]
0
100
200
300
400
500
600
700
36
38
40
42
44
46
48
Latitude South to North[°]

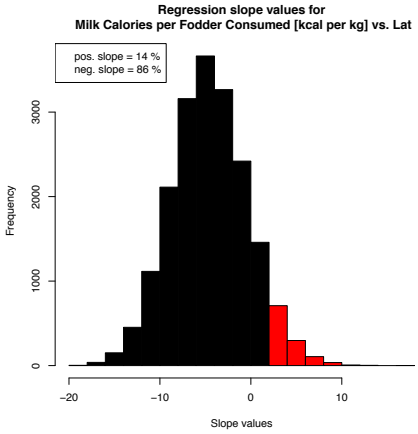
Regression slope values for
Milk Calories per Fodder Consumed [kcal per kg] vs. Lat
pos. slope = 14 %
neg. slope = 86 %
Frequency
0
1000
2000
3000
−20
−10
0
10
Slope values

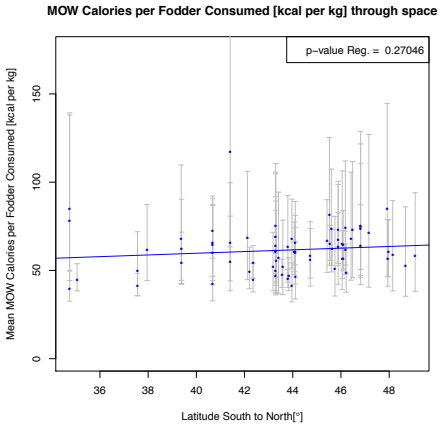
MOW Calories per Fodder Consumed [kcal per kg] through space
p−value Reg. = 0.27046
Mean MOW Calories per Fodder Consumed [kcal per kg]
0
50
100
150
36
38
40
42
44
46
48
Latitude South to North[°]

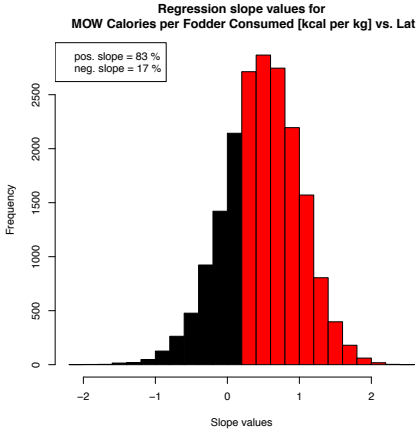
Regression slope values for
MOW Calories per Fodder Consumed [kcal per kg] vs. Lat
pos. slope = 83 %
neg. slope = 17 %
Frequency
0
500
1000
1500
2000
2500
−2
−1
0
1
2
Slope values

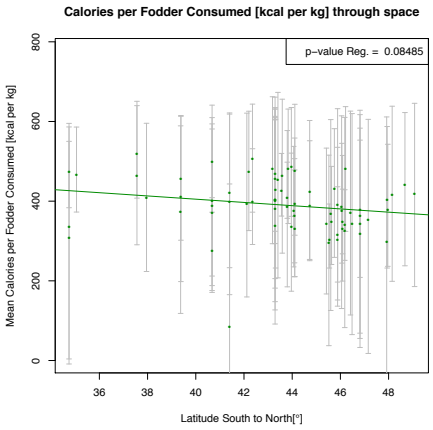
Calories per Fodder Consumed [kcal per kg] through space
p−value Reg. = 0.08485
Mean Calories per Fodder Consumed [kcal per kg]
0
200
400
600
800
36
38
40
42
44
46
48
Latitude South to North[°]

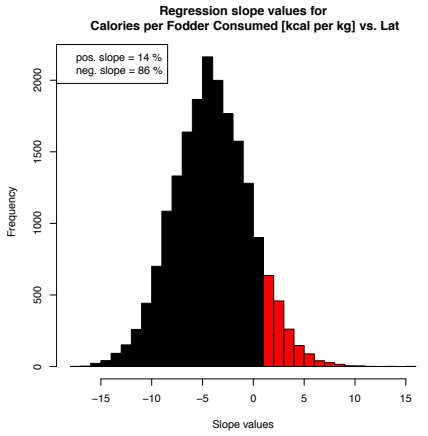
Regression slope values for
Calories per Fodder Consumed [kcal per kg] vs. Lat
pos. slope = 14 %
neg. slope = 86 %
Frequency
0
500
1000
1500
2000
−15
−10
−5
0
5
10
15
Slope values

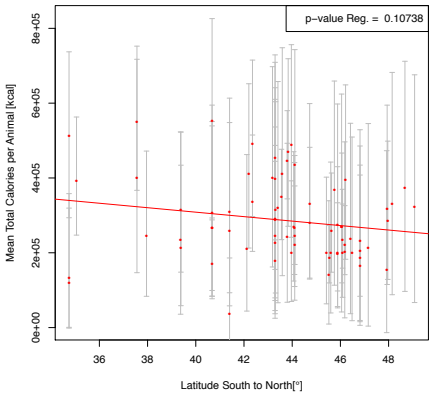
Total Calories per Animal [kcal] through space
p−value Reg. = 0.10738
Mean Total Calories per Animal [kcal]
0e+00
2e+05
4e+05
6e+05
8e+05
36
38
40
42
44
46
48
Latitude South to North[°]

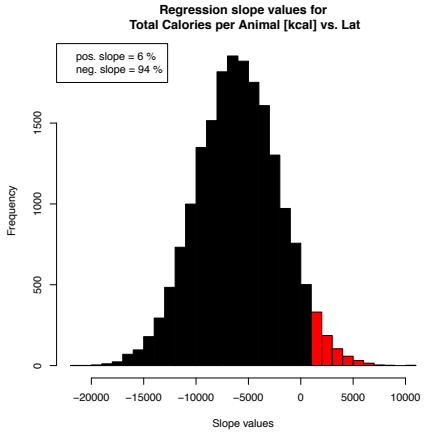
Regression slope values for
Total Calories per Animal [kcal] vs. Lat
pos. slope = 6 %
neg. slope = 94 %
Frequency
0
500
1000
1500
−20000
−15000
−10000
−5000
0
5000
10000
Slope values

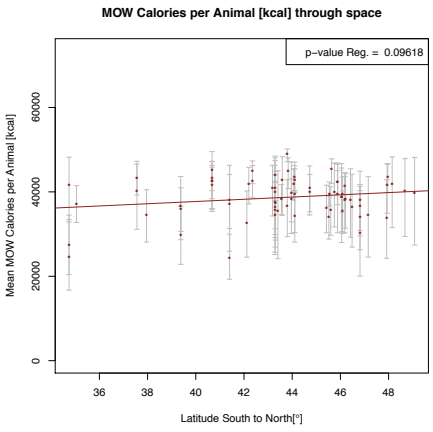
MOW Calories per Animal [kcal] through space
p−value Reg. = 0.09618
Mean MOW Calories per Animal [kcal]
0
20000
40000
60000
36
38
40
42
44
46
48
Latitude South to North[°]

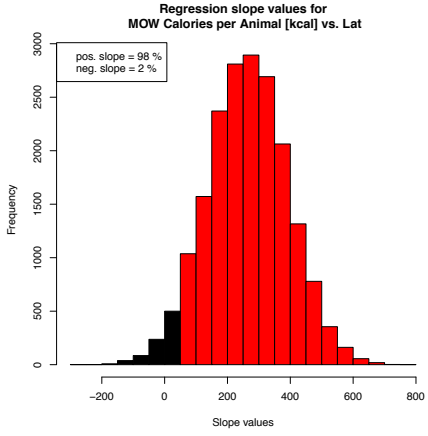
Regression slope values for
MOW Calories per Animal [kcal] vs. Lat
pos. slope = 98 %
neg. slope = 2 %
Frequency
0
500
1000
1500
2000
2500
3000
−200
0
200
400
600
800
Slope values

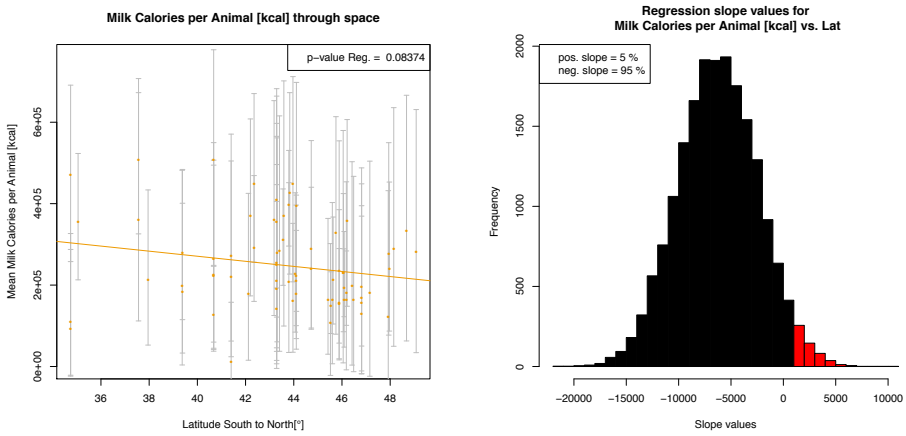

Fig. 6.9. Reproductive Output, animal product yields and macronutrient outputs inferred from 75 Neolithic age-at-death profiles plotted versus latitude (South to North Europe). Left hand plots show the means and standard deviations of the ten production estimates, plotted against latitude, together with the correlation coefficients and p-value. The range of analysed latitude spans from 34.74127 (34°44'28.6"N) to 49.07866 (49°04'43.2"N) degrees. Right hand plots show the distribution of regression coefficients of MCMC samples against latitude; red = positive slopes, black = negative slopes.

Out of ten estimates, eight show a negative trend with increasing latitude, although none of the mean regressions have a p-value <0.05. Consistent with this, by considering the more informative distribution regression coefficients of MCMC samples against latitude I find no persuasive evidence (as defined above) for product estimates increasing or decreasing with increasing latitude.

6.6.3 Results for Çukuriçi Höyük

6.6.3.1 Product output estimate trends against time

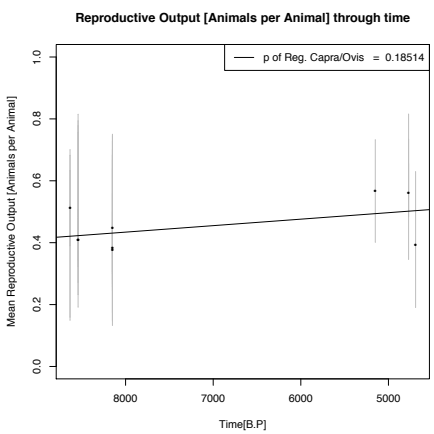

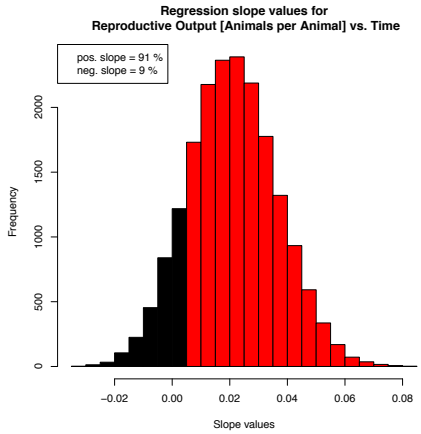

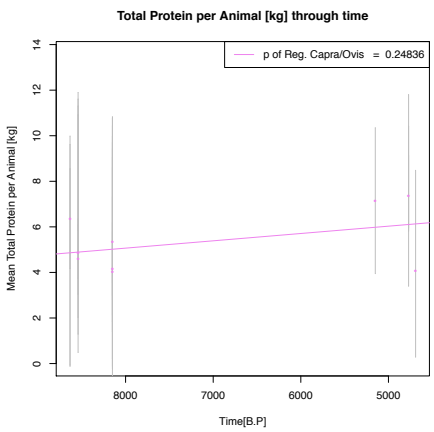

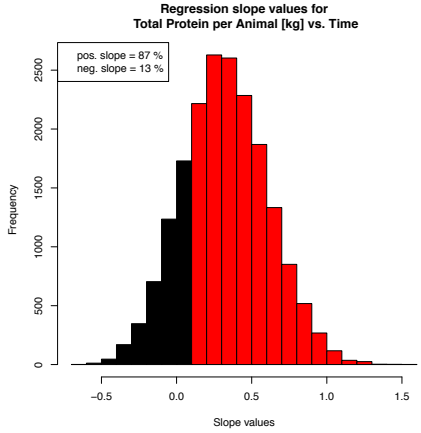

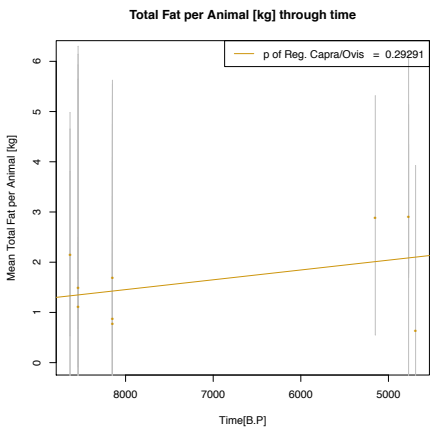

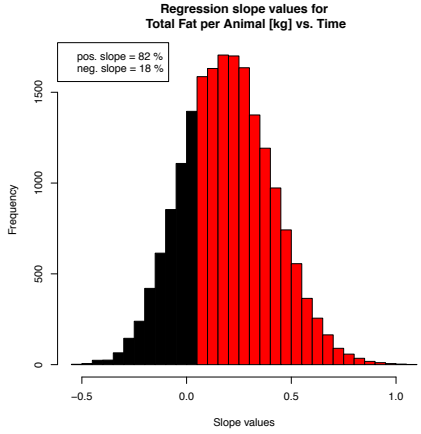

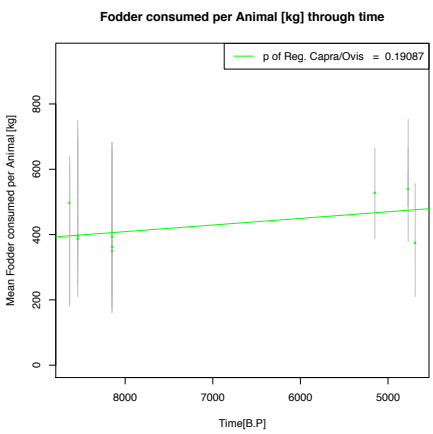
Fodder consumed per Animal [kg] through time
p of Reg. Capra/Ovis = 0.19087
Mean Fodder consumed per Animal [kg]
0
200
400
600
800
8000
7000
6000
5000
Time[B.P]

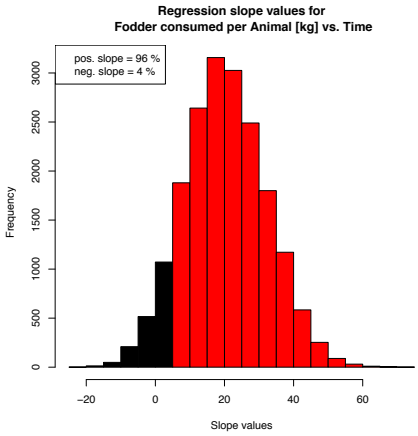
Regression slope values for
Fodder consumed per Animal [kg] vs. Time
pos. slope = 96 %
neg. slope = 4 %
Frequency
0
500
1000
1500
2000
2500
3000
−20
0
20
40
60
Slope values

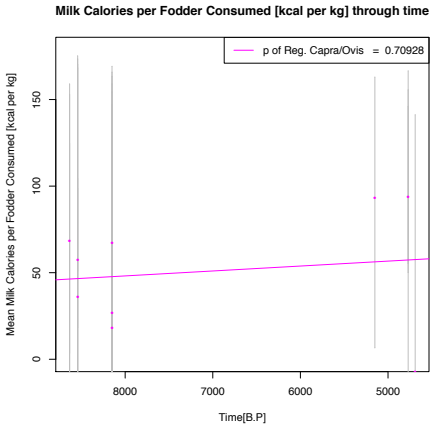
Milk Calories per Fodder Consumed [kcal per kg] through time
p of Reg. Capra/Ovis = 0.70928
Mean Milk Calories per Fodder Consumed [kcal per kg]
0
50
100
150
8000
7000
6000
5000
Time[B.P]

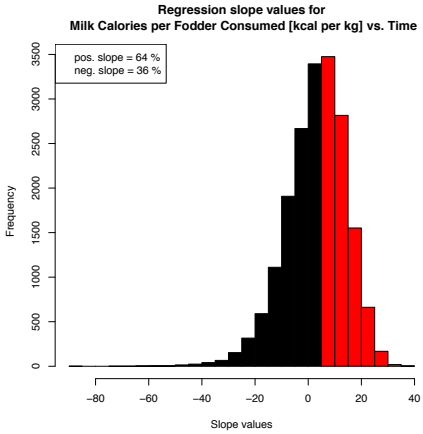
Regression slope values for
Milk Calories per Fodder Consumed [kcal per kg] vs. Time
pos. slope = 64 %
neg. slope = 36 %
Frequency
0
500
1000
1500
2000
2500
3000
3500
−80
−60
−40
−20
0
20
40
Slope values

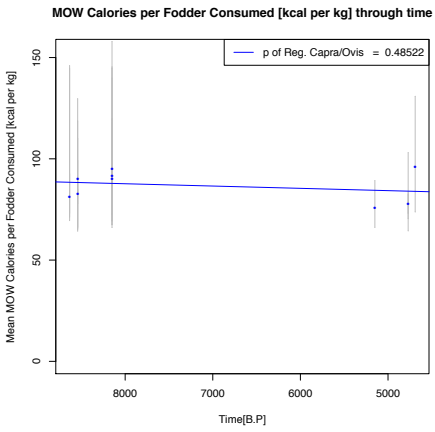
MOW Calories per Fodder Consumed [kcal per kg] through time
p of Reg. Capra/Ovis = 0.48522
Mean MOW Calories per Fodder Consumed [kcal per kg]
0
50
100
150
8000
7000
6000
5000
Time[B.P]

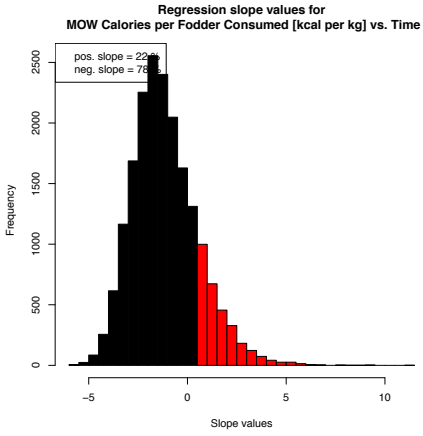
Regression slope values for
MOW Calories per Fodder Consumed [kcal per kg] vs. Time
pos. slope = 22 %
neg. slope = 78
Frequency
0
500
1000
1500
2000
2500
−5
0
5
10
Slope values

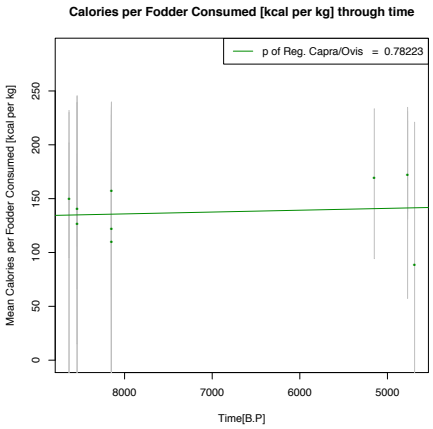
Calories per Fodder Consumed [kcal per kg] through time
p of Reg. Capra/Ovis = 0.78223
Mean Calories per Fodder Consumed [kcal per kg]
0
50
100
150
200
250
8000
7000
6000
5000
Time[B.P]

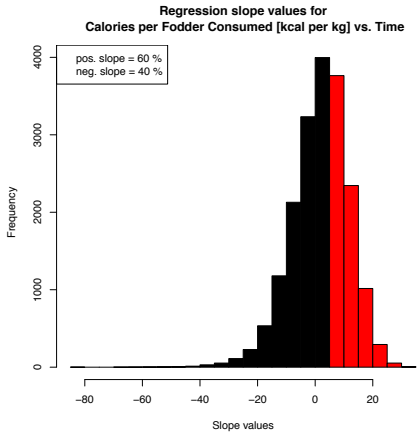
Regression slope values for
Calories per Fodder Consumed [kcal per kg] vs. Time
pos. slope = 60 %
neg. slope = 40 %
Frequency
0
1000
2000
3000
4000
−80
−60
−40
−20
0
20
Slope values

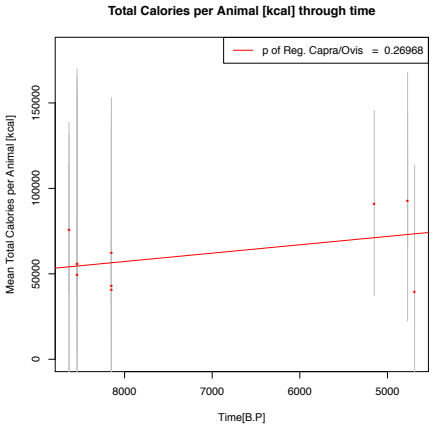
Total Calories per Animal [kcal] through time
p of Reg. Capra/Ovis = 0.26968
Mean Total Calories per Animal [kcal]
0
50000
100000
150000
8000
7000
6000
5000
Time[B.P]

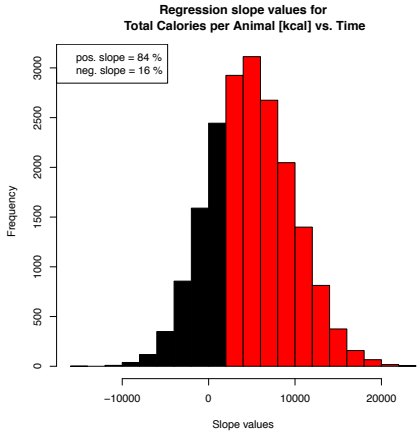
Regression slope values for
Total Calories per Animal [kcal] vs. Time
pos. slope = 84 %
neg. slope = 16 %
Frequency
0
500
1000
1500
2000
2500
3000
−10000
0
10000
20000
Slope values

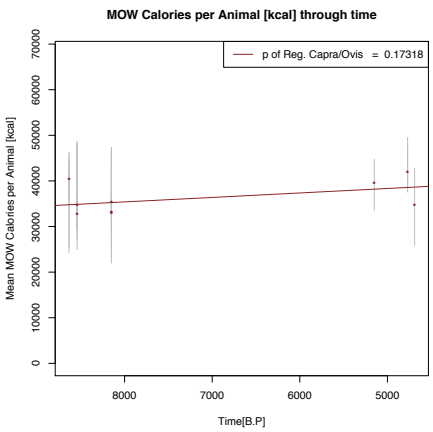
MOW Calories per Animal [kcal] through time
p of Reg. Capra/Ovis = 0.17318
Mean MOW Calories per Animal [kcal]
0
10000
20000
30000
40000
50000
60000
70000
8000
7000
6000
5000
Time[B.P]

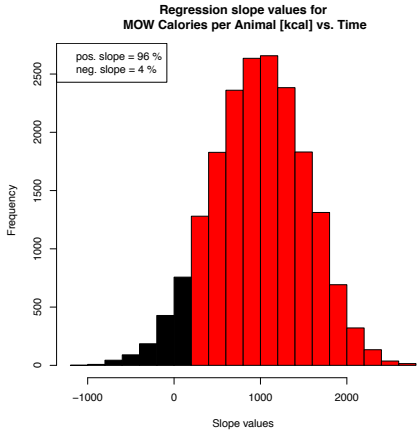
Regression slope values for
MOW Calories per Animal [kcal] vs. Time
pos. slope = 96 %
neg. slope = 4 %
Frequency
0
500
1000
1500
2000
2500
−1000
0
1000
2000
Slope values

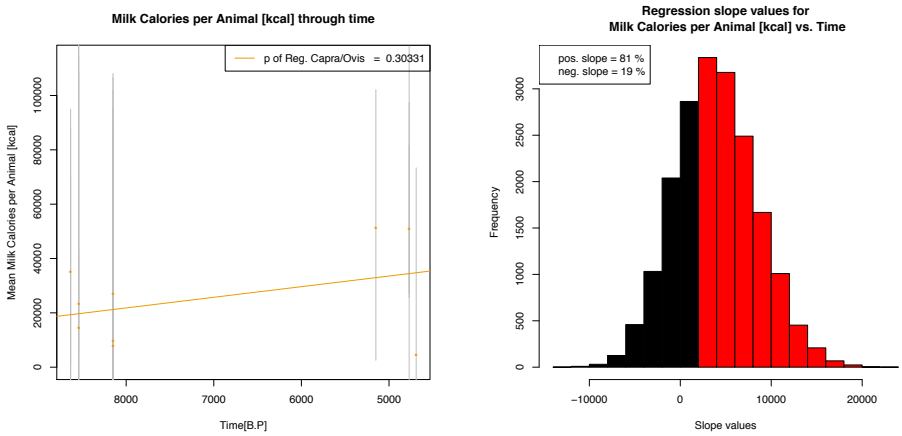

Fig. 6.10. Reproductive Output, animal product yields and macronutrient outputs inferred from 9 age-at-death sheep/goat profiles constructed from postcranial bones from different site phases ranging between the time period of the Early Neolithic to the Bronze Age from Çukuriçi Höyük plotted versus time (8,634 - 4,690 B.P). Left hand plots show the means and standard deviations of the ten production estimates, plotted against time, together with the correlation coefficients and p-value. Right hand plots show the distribution of regression coefficients of MCMC samples against time; red = positive slopes, black = negative slopes.

All but one estimate show a positive trend through time, although none of the mean regressions has a p-value <0.05. The one result with the negative trend is shown for mean MOW calories per fodder consumed. In contrast to results obtained from datasets-A and B, a positive trend is indicated for MOW calories per animal. By considering the more informative distribution of regression coefficients of MCMC samples, I find no persuasive evidence (as defined above) of an increase of decrease in product outputs with time.

6.7 Discussion

To distinguish sheep and goats from archaeozoological remains proves challenging due to their similar morphology, which is why most age-at-death profiles are constructed assuming both species are represented, but in unknown proportions. However, each species might have undergone different kill-off patterns, because sheep and goats are usually herded for different exploitation goals. One approach to

tackling this problem is thorough metric analysis of modern goat/sheep herds in order to understand detailed morphological information, which is then applied to archaeological remains (Zeder, 2001). Also, by analysing long bone epiphyseal fusion, systematic differences between sheep and goat can be detected (Zeder, 2001). Some archaeological sites with well-preserved archaeozoological material (e.g. some data from Çukuriçi Höyük or (Greenfield and Fowler, 2005)) allow for distinguishing between sheep and goats. However, this is only seen in rare cases with comparatively small total element counts (and even less counts for minimum number of individuals).

As already discussed in Chapter 5, it is important to remember that the estimates I used for fodder consumed (Food and Organization, 2003) do not represent the total food consumed by each animal. Rather, I use them as a general proxy of the economic costs of keeping animals at different ages. For this reason, the units of the estimates of product yield per fodder consumed should only be considered in relative terms, rather than as an absolute measure of product yields per food consumed. Likewise, the estimates of reproductive output, milk yields and MOW yields per animal per month at different ages (and their derivatives such as protein, fat and calorie yields) are based on estimates of mean milk produced (Dahl and Hjort, 1976; Mourad, 1992; Todaro *et al.*, 2015) milk consumed by kids / lambs (Food and Organization, 2003), meat and offal weight (MOW) produced (Tresset, 1996) and probability of giving birth (Dahl and Hjort, 1976) for each month of life in unimproved herds. I recognise that prehistoric values for such parameters may have been different; in most cases, likely lower. Nonetheless, predicted yields per animal from this model scale linearly with these parameter values, so while the absolute yield estimates should be treated with caution, their relative values in cross site and site/model comparisons should be reasonably secure.

From the analyses of dataset-B (minimum number of individuals), no 'persuasive evidence' (defined as 1% or less, or 99% or more, of the regression coefficients of

MCMC samples against time, latitude or longitude being greater than zero) of any increase of decrease of herd sustainability, product output per animal or product output per fodder consumed was found. One reason for this is that dataset-B only consisted of 75 sites. Nonetheless, there are some general trends that approached the 'persuasive evidence' threshold, including an increase in herd sustainability and increases in milk calories and total calories per animal, and per fodder consumed, and a decrease in MOW calories per animal, and per fodder consumed.

When considering dataset-A (minimum number of elements; n = 166 sites), there are similar indications of an increase of herd sustainability and the economic efficiency of calorie production over time, although again, this does not reach the significance threshold defined above as 'persuasive evidence'. With this larger dataset there is persuasive evidence of an increase in milk calories and total calories produced per animal, and of a decrease in MOW calories produced per animal. Taken together, these results suggest a shift of focus from meat to milk as the main target product of caprines. This could be seen as a soft version of the Secondary Products Revolution (Sherratt, 1981). While it is now clear that milk production was an early feature of the European Neolithic (Evershed *et al.*, 2008; Dunne *et al.*, 2012; Cramp, Evershed, *et al.*, 2014; Cramp, Jones, *et al.*, 2014), rather than something that was only 'discovered' later, its importance may have increased throughout the Neolithic, with a concomitant decrease in calories derived from meat, or the economic importance of meat calories (Ingold, 1980; A. Legge, 1981).

When considering the latitudes and longitudes of sites in dataset-A, the only trend passing the 'persuasive evidence' threshold is MOW calories produced per animal increasing with increasing longitude (East) and decreasing latitude. However, it is important to note that in both datasets-A and B, both the latitude and longitude of sites are themselves correlated with their ages, since later Neolithic sites are only found at higher latitudes and lower longitudes (East).

Çukuriçi Höyük represents a site typical of other Neolithic sites seen in Central Anatolia. However, Çukuriçi Höyük differs from other archaeological sites located around the Marmara region: sites, which are also known to represent the Fikirtepe culture. Çukuriçi Höyük resembles archaeological sites located nearby, such as Ulucak, which shows similarity in terms of architecture, material culture and diet during both, the Neolithic and Bronze age period. Those sites are usually located at the coast or mainland of Central West Anatolia and are characterized by an extensive exploitation of marine animals, together with the typical animal and crop domesticates, an elaborate knowledge of stone tool culture (with evidence for an elaborate pressure technique) with material from remote islands such as obsidian from the Greek island of Melos, as well as expertise on navigation at sea, as shown by the archaeozoological evidence provided from deep-water fishing. At Çukuriçi Höyük the main domesticates exploited are sheep and goats (likely more goats than sheep). Here, I analysed the goat / sheep husbandry strategies over time ranging from the Neolithic to the Bronze Age. The results indicate an increasing trend through time for all but one product estimate: MOW calories per fodder consumed. Whilst this change does not reach the 'persuasive evidence' threshold defined above, it is interesting to note that the same broad trend through time is seen across all the Neolithic sites in datasets A and B. However, I also note that analyses of datasets-A and B indicated a trend of decreasing MOW calories per animal with time, whereas analyses of the Çukuriçi Höyük phases indicate a general trend of increasing MOW calories per animal with time. There are indications that numbers of people increased at this site (Horejs and Schwall, 2015) (i.e. more dense architecture during the Bronze Age than during the Neolithic) and as such this may have led to increasing demand of food in general; including meat. However, others argue that milk would be more likely the food of choice to cover a high demand in food for a growing population (Ingold, 1980; A. J. Legge, 1981). Furthermore, the Bronze Age phases of the site (Horejs and Schwall, 2015) show evidence for a typical Late-Chalcolithic village life,

characterized by more sophisticated, permanent settlements with storage space and – most probably – room for domesticated animals, allowing for the expansion of animal keeping, and as such, meat production. On the other hand, the positive trend for mean MOW calories per animal through time might be seen as somewhat unusual, given that the site is located at the coast, which implies a sufficient meat supplementation from marine animals.

6.8 Conclusion

I performed this meta-analysis on three age-at-death profile datasets, together ranging between ~11,000 to ~2,000 BP. Most archaeological sites are located within the European Neolithic. I identified broad trends of change in goat/sheep herd management strategies through time and space, although given the correlations between date and latitude and / or longitude, these trends are not unrelated.

I conclude a broad positive trend toward sheep/goat herding management efficiency, reproductive outputs and product yields in Çukuriçi Höyük over time, although the small number of phases means that these trends did not reach the somewhat stringent 'persuasive evidence' threshold set above.

The clearest results obtained from datasets-A and B are strong indications of a decrease in calories obtained from meat, and a concomitant increase in calories obtained from milk of caprines. This could be viewed as a soft version of the Secondary Products Revolution (Sherratt, 1981).

Chapter 7

7 General Discussion

7.1 Summary of research

The underlying motivation for this work was to develop and apply model-based methods to address some open question in Neolithic archaeology, specifically, those concerned with the use and spread of domestic or crops and animals. The domestication of plants and animals during the Neolithic transition marks one of the most important changes in human ecology in the last 300,000 years. Whilst there is a considerable literature on the archaeology of domestic plants and animals, analyses tend to be descriptive, and formal model-based inference on the processes of spread and the economic value of those domesticates are less common. I have applied novel methods to inferring:

1. The location of origin or population expansion of seven crop and animal species, of which the origin of domestication or population expansion within a region were unknown or debated. Those species include: broomcorn millet across Eurasia, African pearl millet, taro in Africa, the Pacific rat in Polynesia and three endemic species from the island of Sulawesi.
2. Sheep and goat herd sustainability, economic efficiency and productivity from archaeological age-at-death profiles from the European Neolithic and tested those estimates over time and space.

For broomcorn millet, I inferred an east Asian origin of expansion, and formally rejected a west Eurasian origin (Jones, 2004; Hunt *et al.*, 2008, 2018). For African pearl millet, I find strong support for a northwest African origin of expansion. For taro, I find weak support for an entry into Africa via in the southwest of the continent. For the Pacific rat, I inferred the location of origin to lie around the island of Flores. The

origin of population expansion of babirusa and the Sulawesi warty pig was inferred to be in central Sulawesi, while the origin of population expansion of Anoa was inferred to lie in the west of the island.

I infer a general improvement of economic productivity of caprine herd slaughter management strategies throughout the Neolithic. Moreover, I infer decreasing calories obtained from meat and increasing calories obtained from milk from caprines over time – suggesting a trade-off between the two animal products.

7.2 Some Background to mathematical (including Bayesian), computational and spatial modelling in archaeology

There is an ongoing trend of gathering and analysing large datasets throughout various scientific disciplines with the goal to computationally infer patterns in human or animal behaviour or predict future *and* past events. Archaeology is and will be hit by the wave of a large-data driven research (Bevan, 2015). Various approaches exist to handle those types of datasets. In contrast, some computational approaches also permit management of scarcely sampled data which are also typical for archaeological datasets.

Mathematical (Bayesian) modelling has been used across various areas of archaeology, e.g. as Bayesian chronological models which aim at managing relative and absolute chronological information (Buck and Juarez, 2017). Another approach in chronological modelling via the summing of the postcalibration probability distributions (SPD) of radiocarbon dates, which can serve as a proxy for highs and lows in anthropogenic activities and human population (Rick, 1987). Here, the modelling part involves testing of significance of population fluctuations inferred from the SPDs (Shennan *et al.*, 2013). Various researchers have made use of this approach and, for example, have studied regional human population fluctuation during the Neolithic (Timpson *et al.*, 2014), or in combination with past climate data,

have suggested a link between population shifts, climate change and food production in early Neolithic Britain (Bevan *et al.*, 2017).

Spatial analysis in archaeology encompasses a wide range of approaches ranging from generating distribution maps to more elaborate spatial-statistical methods such as studying the distributions of archaeological material to understand the dynamics of trade and exchange (Bevan and Lake, 2013; Carrero-Pazos, Bevan and Lake, 2019). One such example is the study of Neolithic axehead distributions in Britain which suggests that British Neolithic people favoured particular stone sources for axehead production instead of available alternative sources (Schauer *et al.*, 2019).

A frequently used method in archaeology is Geographic Information System (GIS) which permits to display several layers of data on a map to better understand spatial patterns (Bevan and Lake, 2013). Integration of computer simulations and other statistical approaches such as Approximate Bayesian Computation (ABC) together with GIS and ancient DNA allow for the simulation of past human migration trajectories across geographic regions (e.g. Currat *et al.*, 2019).

A rather different approach to those spatial analysis approaches discussed above is the spatially-explicit modelling approach presented in chapters 2 and 3. Here, I also make use of spatial information (and a measure of diversity) in order to identify locations of origin of domesticated animals and crops. Although previous approaches also studied diversity through space (Ramachandran *et al.*, 2005; Manica *et al.*, 2007), the novelty of this method lies in the spatial kernel approach, which allows to study low genetic or morphometric heterozygosity, and statistical support to the inferences for origin locations.

In recent years the number of spatial methods has increased. However, for age-at-death data in particular, only a few statistical and computational methods have been developed to manage kill-off profile data. For instance, Gerbault (2016) and Gillis (2017) developed a method to estimate sampling uncertainties in element

counts at each age class by resampling data from the Dirichlet distribution and compressing the information into two dimensions with a correspondence analysis. One other example of statistical approaches applied in the context of age-at-death data uses a gamma distribution to model such profiles (Timpson *et al.*, 2018). The researchers suggest that the gamma distribution provides a better model to represent herd management strategies (usually inferred from age-at-death profiles by simple visualization) than other models which were proposed by others to be optimized for particular caprine herding strategies (see chapter 4 on idealised models proposed by Helmer, Redding and Payne). However, as yet, no methods have been developed to infer sexed kill-off profiles, product yields and the economic efficiency of prehistoric stock keeping from unsexed kill-off profiles. With the method presented in this thesis, I attempt to infer such information and also test whether proposed idealised age-at-death models truly reflect an optimised herding strategy.

7.3 Theoretical underpinnings of mortality profiles

Interpretations of past herding strategies from age-at-death profiles are based on a comparison of a constructed profile from archaeozoological material and a profile model which was proposed to reflect a herding strategy optimised for a particular animal product such as meat or milk or fleece (Payne, 1973). The interest for this research had grown in the archaeological community, particularly in light of Sherratt's 'secondary product revolution' model. However, some researchers contested the use of age-at-death profile models, especially the model for an optimised milk yield strategy, arguing that the construction of such idealised models underlies some strong assumptions. Halstead (1998) pointed out differences between the biology of modern and prehistoric livestock. One such difference is the variation of milk let-down suppression in prehistoric livestock after the slaughter of infants (Clutton-Brock, 1981a; McCormick, 1992). As a consequence, he assumed that high infant mortality,

which is implied by a model for a milk-oriented strategy, would have resulted in the contrary effect; i.e. low milk yields. However, Halstead compromised with research on age-at-death profiles approximating Payne's milk model under optimal herding conditions with sufficient nutritional supply as evidenced by Legge's studies on profiles from early farming sites in Switzerland (A. J. Legge, 1981). Secondly, it was suggested that prehistoric livestock was exploited to a maximum, i.e. for a combination of animal product (e.g. milk *and* meat) rather than for only one particular product. Lastly, an idealised milk profile (Payne, 1973) assumes high infant mortality resulting in insufficient animals for reproduction and as such may result in an unsustainable herding management. In fact, results shown in Fig. 5.7 c, f, i and 5.8 c, f, i, (which represent inferred productivity outcomes from ten idealised models) support some of Halstead's observations. Both, Payne's idealised milk profile and Helmer and Vigne's idealised milk profile show lower mean productivity and herd sustainability (reproductive output estimation) compared to other models proposed to be optimised for meat or fleece, a combination of product yields, herd security and energy maximisation. Those results support Halstead's argument a herd management strategy truly optimised only for milk is unlikely, because it would lead to unsustainably high mortality of offspring. He also argues that due to infant slaughter and, possibly, consequent suppression of milk let-down, an idealised strategy for optimised milk yields may have resulted in an age-at-death profile structure showing less killings in younger age classes than the milk model proposed by Payne.

Furthermore, results for the model idealised for maximizing milk yields (Helmer and Vigne's milk model) show the lowest inferred mean milk yields (yellow 'x' in Fig. 5.7 f) and as such oppose to the concept of the proposed model for milk yield optimization. Under our model assumptions, we showed an alternative profile model (Fig. 5.9) optimised for economic efficiency and herd sustainability and suggest that Neolithic herding managements may had been far from optimal.

7.4 Distinguish sheep versus goat in zooarchaeological assemblages

Due to a similar bone morphology in sheep and goats, it remains challenging to distinguish the two species from archaeozoological remains. For that reason, most age-at-death data are recorded as a combination of the two species, which is also reflected in my collection of profiles seen in datasets A and B. However, past and present sheep and goat managements differ as they may have been bred for different purposes. As a consequence, more recent research focuses on methodological developments to analyse postcranial morphometric criteria via discriminant analysis (Salvagno and Albarella, 2017). Another morphometric approach to taxonomically discriminate the two species works via the analysis of premolars (P3-P4, Halstead, Collins and Isaakidou, 2002) which is especially relevant to this study given that age-at-death profiles are usually also constructed from teeth. Furthermore and perhaps more importantly, through Zooarchaeology by Mass Spectrometry (ZooMS), a low-cost technique which asses preserved collagen or other proteins, a distinction of sheep and goats can be achieved (Buckley *et al.*, 2010) via attention to two amino acids of a peptide. A further effective but costly procedure for sheep or goat species identification would be via ancient DNA, however this is probably too costly for the purpose of age-at-death profile construction. Moreover, because collagen tends to degrade more slowly than DNA, ZooMS allows for species analysis from older archaeozoological material.

7.5 'Soft' secondary products revolution?

Revolution is usually associated with sudden change. Sherratt first referred to the exploitation of cattle, sheep and goats for dairy products as a 'secondary products revolution' (Sherratt, 1981). However, Fig. 5.10, which shows an increase of milk yield optimization, implies less of a revolution and instead more of a gradual, linear change through time.

7.6 Suggestions for future work

7.6.1 Future work concerning the model-based approach to inferring location of origin of domesticates

There are some limitations to the method for inferring the location of origin of expansion of domesticates presented here. Future work should aim to address those limitations and possibly improve the method. One such limitation is that genetic diversity is not expected to decrease with increasing distance from expansion origin location under a process of admixture with in-situ populations, since admixture is expected to increase genetic diversity. It remains to be tested what effect admixed population would have on the method or how the correlation between genetic diversity with geographic distance would behave with known admixed populations.

Another limitation is that topographical and other landscape features are not considered in the approach presented (for example, seas, mountain ranges, deserts, etc.). In theory it should be possible to take account of topographical and other landscape features if their impact on mobility were known or could be estimated. For example, such features could be factored into the estimation of geographic distance to produce a composite distance reflecting typical times taken to traverse that region. However, the impact of topograhical and other landscape features on migration is poorly studied and may be variable with time of the technologies of the populations spreading domesticates.

Additionally, this approach would benefit from introducing the possibility of extending the number of hypothesized origin locations, such that a species spreads from multiple locations at the same time, or at different times but in a way that modern genetic diversity is shaped by both expansion phases. It is very common that different archeological studies suggest multiple, different origin locations of domesticates. One such example is the hypothesized location of population expansion locales of the

three endemic species from the island of Sulawesi (personal communication with Dr. Laurent Frantz) for which more than two possible population expansion origins throughout the island were hypothesized (Frantz *et al.*, 2018).

7.6.2 Future work concerning the Bayesian Markov Chain Monte Carlo method to infer sex-specific mortality profiles and product yields from unsexed Caprini zooarchaeological remains (sheep and goats)

7.6.2.1 Sheep and goats

During the Neolithic period in Europe, sheep and goat herding may have been targeted for different products. Nowadays, goats are mainly bred for milk production while sheep are exploited for wool and meat. Moreover, they also differ in their birth rates, milk yields and even milk fat content (Haenlein and Wendorff, 2006; Haenlein, 2007). Ethological estimates for Neolithic sheep versus goat herds are not available and can therefore only be inferred from modern ethological data on unimproved herds (e.g. Dahl and Hjort, 1976), which then serve as proxy for Neolithic herds. One example is the difference in lambing/kidding of unimproved, modern sheep and goats: In general, goats give birth more often than sheep, and additionally, twins and even triplets occur more often in goats (Dahl and Hjort, 1976).

Assuming that the patterns of the idealised models as proposed by Payne (1973) and Vigne and Helmer (2004) represent differences in herding strategies targeted towards milk and meat, a simple visualization of the few available species-specific archaeological age-at-death profiles (Gillis, unpublished) indicate that, also during the Neolithic period, those mixed herds were bred for similar products. One example of an Ovis and Capra profile is from the site Füzseabony-Gubakút (Fig. 7.1), a Neolithic site in present-day Hungary, which shows that those profiles ‘look’ similar, although Capra shows more killings in the first two age classes and as such indicates a herding strategy targeted towards milk exploitation.

However, those similarities or differences remain to be tested formally with the tools I described and applied in this thesis. This, plus herd sustainability and economic efficiency, also remain to be formally tested with all available species-specific age-at-death profiles.

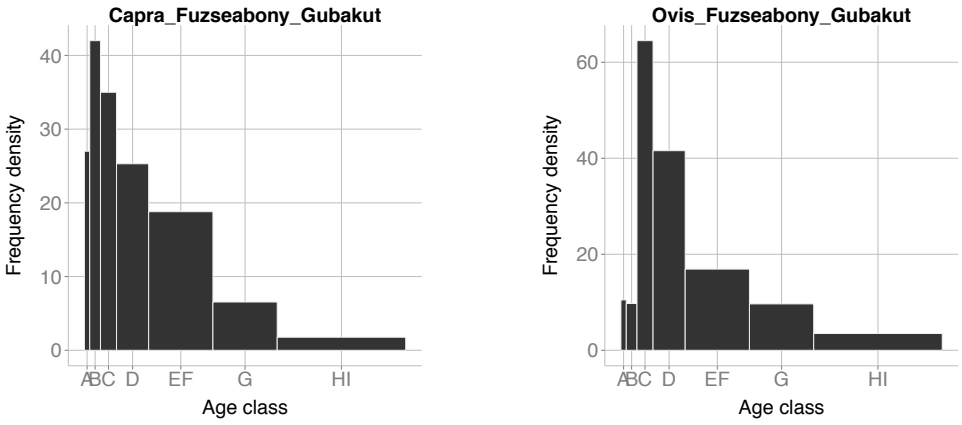

Fig. 7.1 Age-at-death profiles for Capra and Ovis from Neolithic site Füzseabony-Gubakút. Age-at-death element counts kindly provided by Gillis.

7.6.2.2 Fodder as proxy to explore efficiency

Fodder type, quality and quantity depends on location, climate and seasons. In general, modern ovicaprines mostly feed on grass, clover, and forbs. During the Neolithic, their diet consisted of an ecologically narrow range of pasture plants limited by the region of settlement of early Neolithic farmers (Vaiglova *et al.*, 2018). In my analyses, I use additional fodder supply by the farmer as an element for the proxy of economic efficiency. This is because hay collection during the summer is physically demanding and I test if the energy input by the farmer is in balance with the productivity output of the herd. However, I recognise that the farmer's energy input likely differed during the Neolithic when compared to modern times. While 'leaf hay' was a phenomenon prior to the Iron Age, and as such did not require much energy input from the Neolithic farmer, 'meadow hay' only became more common during the Middle Ages into modern times with the appearance of large hay barns and open fields and was physically more demanding (Hejcman *et al.*, 2013; Hejcmanová,

Stejskalová and Hejcman, 2014). In future, there is considerable room for improvement for a better informed estimate for fodder.

7.6.2.3 Cattle

The Bayesian method described in Chapter 5 is one that can be applied widely to other domesticated herd animals, not only to caprines Studying past cattle slaughter management and husbandry practises are of great interest to archaeologists (e.g. (Jones and Sadler, 2012; Gillis *et al.*, 2013, 2016, 2017)). Over the course of the Neolithic period, cattle became increasingly important for milk, manure and animal power rather than just for meat (Gerling *et al.*, 2017). By adjusting a number of parameters in the model to reflect cattle-specific ethological data, herd sustainability and productivity may also be inferred from cattle age-at-death profiles, for which there are no problems related to multiple species. It has been suggested that European cattle continued to reduce in size over the course of the Neolithic, Bronze Age, and pre-Roman Iron Age (Boessneck, 1962; Boessneck and Von den Driesch, 1979). This implies that cattle were large animals at the beginning of the Neolithic, which would have required high quantities of food. Therefore, testing the economic efficiency of cattle keeping would be also interesting to explore.

7.6.2.4 Model parameters

In future work it would also be useful to explore some model parameters too, for example, apply more realistic Neolithic birth rates (if data is available), since in the analyses in Chapters 5 and 6 this rate is set to 1 kid/lamb per female per year, based on empirical data from unimproved herds (Dahl and Hjort, 1976). The same applies to ethological information (if data is available) on sheep and goat milk and meat yields.

7.7 Final thoughts

This method for inferring locations of origin of domesticates allows one to research less well-known crops, plants and animals showing potentially low genetic or morphometric diversity. The origin-inference method may be used to direct archaeologists towards possible starting locations of agriculture for certain regions in the world. Secondly, with the method presented in chapter 5, we provide a statistically robust approach to quantifying (relative) sex-specific product yields, economic efficiencies and likely sustainability, all from prehistoric age-at-death profiles. Via the meta-analysis presented in chapter 6, I also analyse and contribute to a better understanding of some aspects of past agro-pastoral practise and their dynamics across time and space, especially during the European Neolithic.

Consideration of the herd sustainability inferences for individual site profiles is beyond the scope of this thesis. However, herd sustainability inferences for individual site profiles may contribute to other site-specific archaeological studies. Ideally, the application of the methods presented in this thesis would in future supplement zooarchaeological analyses of individual sites by contributing with statistically tractable inferences on herd sustainability, productivity and economic efficiency, of which the latter was inferred for the first time in any archaeozoological study from age-at-death profiles.

Model-based inference approaches in archaeology are usually concerned with population or meta-population scale questions, and can lead to the types of grand narratives (Kristiansen, 2014) that raise concerns among many archaeologists, who themselves are more interested in local-scale phenomena (Hodder, 2016) . However, while the analyses presented in this thesis are mostly performed at the population or meta-population scale, some of the methods developed – particularly those described in Chapters 4 and 5 – have potential to speak to those interested in more local-scale economic processes.

Appendix

Appendix A

Age-at-death profile datasets used in Chapters 4 – 6

A.1 Dataset-A

Table A.1 Age-at-death profiles from dataset-A. This is the dataset used for the analysis in Chapter 6. Some site names occur multiple times. This can mean that different site phases are available (as indicated by the date) but the site phase names were not provided.

Archaeological Site	BC [k]*	A	B	C	D	EF	G	HI	Latitude	Longitude
Grotta degli Zingari	5.5	4.96	4	4	0	1.01	0	1.01	45.64646	13.880954
Villa Giribaldi	5	0	0	12	10	10	12	12	43.716941	7.300215
Ulucak Höyük VI	7.5	0	2	8	3	2	10	1	38.407222	27.150278
Ulucak Höyük Vb	7	0	2	15	6	8	1	0	38.407222	27.150278
Ulucak Höyük Va	7	0	1	9	5	3	9	2	38.407222	27.150278
Ulucak Höyük IV	6	1	0	3	7	13	5	1	38.407222	27.150278
Trou Arnaud	5	6	2	2	2	5	5	0	44.568985	5.271726
Trasano III	6	0.5	2.5	16	15	22	10	5	40.67652	16.63981
Trasano II	6	0	3	18	19.5	20.5	13.5	4.5	40.67652	16.63981
Trasano I	6.5	1	3.5	15	6.75	18.08	15.08	0.58	44.182861	8.367348
Torre Sabea I	6.5	1.15	1.15	53.2	101.8	60.6	0	0	40.080873	18.007851
Testice	6.5	0.25	5.08	18.08	8.58	18	2	4	45.901603	16.161589
Suberde	7.5	0	0.54	2.16	6.84	3.42	2.16	2.52	37.4	32
Stragari	6	0	1	7	0.5	8.2	4.8	0	44.153219	20.658582
Roshiem	5.5	0	0.7	5.5	13.7	19.9	12.6	5.6	48.5	7.466667
Pupicina cave I	6	33	17	21.5	6.5	11.5	8	3.5	45.315278	14.156111
Pont de Roque-Haute	5.5	0	0	13	26	2	4	0	43.308733	3.341703
Mitreo	5	1.9	5	5	1	2	2	2	45.648388	13.872542
Ludivinono	5.5	2	2	0	1	11.7	16.7	1.7	50.2	20.9
La Draga	5.5	0	5.7	15.7	56.1	48.6	18.6	0	42.126901	2.761665
Hoyucek	8	0	2.6	1.8	5	1	4.5	4.5	37.461052	30.583134
Herxheim	5.5	0	15	42	20.25	43.9	34.4	10.4	49.151667	8.205278
Grotte Lombard	5.5	1	3	3	4	9	7	1	43.700789	6.862321
Grapceva	5	1.95	5.46	5.46	8.19	5.97	5.97	5.97	43.152267	16.655846
Grotte de l'eglise I	5	0	7	13	36	42	36	18	43.719399	6.143566
Foeni-Salas	6.5	1.5	2.1	16.5	12.6	6	11.7	0	45.595463	20.879059
Font Juvenal I	5.5	7.5	2.66	9.66	12.16	5.66	4.66	1.66	43.289993	2.350702
Etigny	5	0	8	16	9	19	8	0	48.133333	3.283333
Erbaba Höyük	6.5	0	1	35	34	19	8	11	37.768903	31.673694
Erbaba Höyük	7	0	1	7	5	5.3	3	3	37.768903	31.673694

Erbaba Höyük	7	0	0.3	59	59	81	30	18	37.768903	31.673694
Edera	5	5.7	0	5.7	1.9	0	0	0	45.640108	13.891253
Cuiry-les-Chaudardes	5.5	6.5	6.5	4	7	20	7	2	49.387103	3.770857
Cueva de la Sarsa	5.5	1	9	9	6	13	2	1	38.769122	-0.6
Cueva de Nerja I	6.5	0	4	2	4	6	0	0	36.7617	-3.8
Colle Santo Stefano	6	0	2	3	18	25	30	5	42.201395	13.641186
Combe Obscure I	5.5	2	5	10	4	4	3	7	44.447301	4.424062
Chotebudice	5.5	0	2	40	33	15	32	37	49.066667	15.566667
Cerny Vul I	5.5	0	7	0	6	1	3	4	50.237837	14.363708
Cerny Vul II	5	0	11	12	48	30	4	14	50.237837	14.363708
Caucade	5	0	0	3	2	5	1	4	43.683308	7.220049
Catignano	6.5	13.33	16.33	19.33	11	2	7	18	42.385599	13.949432
Bukovacka Cesma	6	0.5	0.5	5	1	0.33	0.33	0.33	44.21047	22.604613
Blagotin	6.5	4	1.1	13.9	26	18.2	9	16.8	43.715212	21.085681
Bischoffsheim	5.5	5	8	16.7	54.9	70.4	36.7	19.2	48.483333	7.483333
Berry au bac-Croix Maigret	5.5	1.5	1.5	9	8	6	0	0	49.476453	3.904724
Baume d'Oulen I	5.5	6	6	9.5	7.5	5.75	2.25	1	44.350528	4.405694
Barret de Lioure	5.5	0	2	9	4	8	5	1	44.366145	5.129453
Balloy Les Reaudins	5	4.165	4.165	7.33	39.32	13.99	0	0	48.400526	3.148756
Abri de Saint-Mitre I	5.5	0	1	6	2	2	3	0	43.881521	5.66421
Arene Candide II	6	0	0	0	3.25	2.95	3.25	0.5	44.182861	8.367348
Arene Candide I	6	0	0	0.5	0.5	1	2.5	1.5	44.182861	8.367348
Araguina-Sennola I	5.5	3	6.5	6.5	14	7	0	0	41.401879	9.158549
Abri II du Fraischamp	5.5	0	3	5	6	5	2	0	43.980258	5.108442
Jordan Ain Ghazal	6.5	0	0	7.3	22	0.66	13	0	31.988	35.976
Jordan Ain Ghazal	6.5	1.5	0	20.5	26.9	27.2	1.1	2.2	31.988	35.976
Jordan Ain Ghazal	6.5	0	0	19.8	42.7	107.1	12.5	0	31.988	35.976
Jordan Ain Ghazal	5.5	0	0	25.5	14.4	6	7.1	6.4	31.988	35.976
Jordan Ain Ghazal	5.5	0	4.9	14.8	26.5	8	14.1	1	31.988	35.976
Boury-en-Vexin F	5.7	16	12	11	7	18	3	5	49.240271	1.736159
Boury-en-Vexin M	5.7	16	10	0	1	0	0	0	49.240271	1.736159
Boury-en-Vexin Total	5.7	32	22	11	8	18	3	5	49.240271	1.736159
Çukuriçi Höyük I	2.74	0	3	0	1	2	1	3	37.929167	27.359444
Çukuriçi Höyük III	2.82	6	9	11	44	40	18	102	37.929167	27.359444
Çukuriçi Höyük III	2.82	0	0	1	0	0	4	11	37.929167	27.359444
Çukuriçi Höyük III	2.82	0	0	0	2	3	3	8	37.929167	27.359444
Çukuriçi Höyük VII+VI	3.2	0	3	3	3	0	3	15	37.929167	27.359444
Çukuriçi Höyük VIII - XII	6.2	9	9	9	14	5	10	21	37.929167	27.359444
Çukuriçi Höyük VIII - XII	6.2	0	0	0	1	0	0	2	37.929167	27.359444
Çukuriçi Höyük VIII - XII	6.2	0	0	0	0	1	0	1	37.929167	27.359444
Çukuriçi Höyük VIII - XII	6.2	0	0	0	0	0	0	1	37.929167	27.359444
Çukuriçi Höyük VIII - XII	6.2	32	22	14	42	35	29	73	37.929167	27.359444
Çukuriçi Höyük VIII - XII	6.2	0	0	0	3	2	6	1	37.929167	27.359444

Çukuriçi Höyük VIII - XII	6.2	1	0	0	0	3	6	3	37.929167	27.359444
Çukuriçi Höyük VIII - XII	6.2	51	21	13	52	35	43	62	37.929167	27.359444
Çukuriçi Höyük VIII - XII	6.2	0	1	3	5	3	2	7	37.929167	27.359444
Çukuriçi Höyük VIII - XII	6.2	0	0	0	1	0	2	2	37.929167	27.359444
Çukuriçi Höyük VIII - XII	6.2	0	0	0	1	0	0	1	37.929167	27.359444
Çukuriçi Höyük XI -XII	6.592	41	16	12	18	10	42	42	37.929167	27.359444
Çukuriçi Höyük XI -XII	6.592	0	0	0	3	1	1	15	37.929167	27.359444
Çukuriçi Höyük XI -XII	6.592	0	0	0	0	0	1	1	37.929167	27.359444
Çukuriçi Höyük XI -XII	6.592	20	5	18	25	13	24	37	37.929167	27.359444
Çukuriçi Höyük XI -XII	6.592	0	0	0	0	0	1	2	37.929167	27.359444
Çukuriçi Höyük XI -XII	6.592	0	0	0	0	0	1	3	37.929167	27.359444
Çukuriçi Höyük XIII	6.684	3	1	2	9	2	14	14	37.929167	27.359444
Çukuriçi Höyük XIII	6.684	0	0	0	1	1	0	1	37.929167	27.359444
Çukuriçi Höyük XIII	6.684	0	0	0	0	1	0	1	37.929167	27.359444
Iran	-2	1.6	3.26	4.9	13.1	10.4	3.4	7	32.452717	54.232391
Iran	-2	2.58	5.1	7.75	11.1	6.2	3.4	7	32.452717	54.232391
Cafer Höyük	8.3	0	0	8	4	5	2	2	38.4166	38.75
Cafer Höyük	7.675	0	3	43	28	53	38	11	38.4166	38.75
Aswad	7.675	0	1	25	21	27	14	9	33.4	36.55
Halula 5	7.675	9	12	39	30	25	14	4	36.416667	38.166667
Halula 11	6.975	3	9	24	14	12	8	3	36.416667	38.166667
Halula 12	6.975	0	4	12	4	8	3	1	36.416667	38.166667
Halula 18	6.975	3	4	9	5	4	2	1	36.416667	38.166667
Seker (base)	6.975	1	0	1	13	10	4	4	36.659742	40.366213
Aswad	6.975	0	1	33	22	25	25	10	33.4	36.55
Maghzaliyah 1/5	6.975	0	0	5	4	9	5	2	38.134927	46.484575
Maghzaliyah 6/8	6.975	0	2	13	12	10	8	1	38.134927	46.484575
Maghzaliyah 9/10	6.975	0	1	7	10	13	2	3	38.134927	46.484575
Maghzaliyah 12/14	6.975	0	0	3	7	12	4	3	38.134927	46.484575
Maghzaliyah 15/16	6.975	0	0	3	12	9	6	1	38.134927	46.484575
Seker (Late)	6.975	2	1	22	29	31	17	6	36.659742	40.366213
Ras Shamra VC1	6.975	0	2	4	7	8	9	1	35.602	35.782
Ras Shamra VC2/3	6.975	0	4	6	6	18	5	3	35.602	35.782
Qdeir	6.75	1	8	42	50.5	72	23.5	9	35.15	38.81667
Umm el Tlell	6.75	0	4	52	4	28	8	4	35.416256	39.277981
El Kowm 2 (lower levels)	6.75	3	4	10	27.5	36	19	13	35.15	38.81667
El Kowm 2 (lower levels)	6.75	3	5	6	18	38	2	14	35.15	38.81667
El Kowm 2 (PN)	5.775	0	1	4	3	6	12	8	35.15	38.81667
Sotto	5.775	0	0	2	3	2	5	0	39.166652	8.523854
Halula 25	5.775	3	6	12	14	10	11	3	36.416667	38.166667
Halula 26	5.775	8	25	48	74	56	22	18	36.416667	38.166667
Aswad	5.775	0	1	10	13	21	9	5	33.4	36.55
Seker (PN)	5.775	0	0	0	5	11	7	6	36.659742	40.366213

Khirbet Derak	5.25	1	1	6	2	10	9	12	36.630289	42.823014
Kosak Shamali (Ubaid)	5.15	0	1	3	2	7	0	1	36.3327	38.1647
Kosak Shamali (Late Ubaid)	5.15	0	0	0	2	9	6	2	36.3327	38.1647
Kosak Shamali (Post Ubaid)	5.15	0	0	1	4	11	7	3	36.3327	38.1647
Kosak Shamali (Uruk)	3.55	0	1	2	5	6	8	5	36.3327	38.1647
El Kowm 2 (Uruk)	3.55	0	7	14	49	36	11	23	35.15	38.81667
Sheikh Hassan (Mid. Uruk)	3.5	4	13	71	233	173	88	62	36.330939	39.039922
Sheikh Hassan (Late Uruk)	3.5	2	2	38	63	33	19	9	36.330939	39.039922
Mashnaqa	3.55	0	3	23	49	58	21	6	36.288425	40.79464
Rawda	2.7	22	9	21	30	36	16	7	35.181	37.633
Sidon	2.7	0	1	3	12	19	6	6	33.3338	35.2353
Mishrife	2.7	0	4	7	3	14	8	4	34.5006	36.5157
Byblos	2.7	0	1	3	3	5	3	0	34.0725	35.3904
Kutan	2.7	0	1	33	20	67	33	39	36.1425	45.3203
Tell Knedig	2.7	0	4	8	14	37	13	4	36.339328	40.752237
Tell Chuera c5	2.7	4	17	49	70	118	75	42	36.384488	39.295388
Tell Chuera c6	2.7	4	3	11	20	28	22	13	36.384488	39.295388
Tell Chuera c7	2.7	4	3	13	47	55	22	13	36.384488	39.295388
Tell Chuera c8	2.7	5	8	13	52	85	49	33	36.384488	39.295388
Kharab Sajjar	2.7	3	3	13	6	20	5	12	36.339328	40.752237
Tell Shiukh Fawqani	2.7	0	0	0	7	17	10	11	36.780259	38.038413
Mari	2.7	1	10	18	22	32	12	22	34.3258	40.5324
Baume d' Oulen c5	5.7	1	2	3	1	3	0	1	44.203	4.2728
Eglise sup_rieure c7/8	5.7	0	3	12	6	6	10	2	43.725803	6.093477
Eglise superieure c6/3	5.7	9	10	34	15	36	41	17	43.725803	6.093477
Combe Obscure c5	5.7	12	6	7	8	2	3	1	44.447301	4.424062
Baume d' Oulen c3/4	5.7	3	2	2	2	6	5	5	44.350528	4.405694
Grotte Muree c7b/10	5.7	1	6	14	8	11	18	25	43.762632	6.378675
Combe Obscure c2/3	5.7	3	7	5	8	10	6	7	44.447301	4.424062
Baume Saint-Michel	5.7	0	2	1	2	8	10	6	43.347186	5.901317
Grotte Muree c7/6	5.7	1	3	3	3	5	13	8	43.762632	6.378675
La Raverre	5.7	0	0	4	4	1	1	2	45.189529	4.865652
La Roberte	5.7	0	2	9	5	11	7	5	44.501998	4.725449
La Fare	5.7	1	2	8	36	39	8	3	43.958596	5.839358
Claparouse	5.7	1	4	13	5	8	5	9	43.893408	5.112039
La Lauziere	5.7	0	2	6	5	13	9	8	45.2733	6.2159
La Citadelle	5.7	2	6	20	16	29	30	40	43.556719	5.613496
Les Calades	5.7	1	1	10	13	6	3	2	44.248567	4.048707
Col Saint-Anne	5.7	0	2	11	12	17	1	0	43.409516	5.4833665
La Balance rue Ferruce	5.7	0	3	11	11	4	4	3	43.951152	4.805329
Les Moulins	5.7	0	11.8	52	36.5	34.5	44.9	47.3	44.349187	4.765189
Dimini	5.5	0	4.5	33	22	23	22	2.5	39.4	22.9
Franchthi Cave	6.75	2	2.2	19.6	6.2	0.66	0.66	0.66	37.4	23.1

Goebekli Tepe	8.965	0	0	7	18	20	2	1	37.1323	38.5521
Karain B1	17.4	0	16	11	18	21	25	2	37.044	30.3415
Karain B2	17.4	0	4	11	7	12	11	1	37.044	30.3415
Okuzini2	15.65	1	10	17	10	24	20	3	37.52	30.3433
Okuzini3	15.65	2	9	8	3	7	10	1	37.52	30.3433
Asikli Level 4	8.6	2	4	19	20	21	6	10	38.349	34.23
Asvan Kale	-0.4	0	2.6	18.4	14.9	10.3	7.3	9.5	38.751	39.22
Asvan Kale	0.5	0	3.8	11.6	14.8	19.5	14.2	10.4	38.751	39.22
Karain B	17.4	0	1	15	8	14	14	41	37.044	30.3415
Karain B	17.4	0	1	3	8	7	7	20	37.044	30.3415
Okuzini	15.65	0	0	3	1	1	2	11	37.52	30.3433
Okuzini	15.65	1	7	3	11	8	16	39	37.52	30.3433
Okuzini	15.65	2	6	3	6	2	6	15	37.52	30.3433
Okuzini	15.65	0	1	4	2	1	1	5	37.52	30.3433
Okuzini	15.65	0	0	1	2	0	0	8	37.52	30.3433
Blagotin (Total)	6.1	10	4.1	35.7	32.4	23	15	16.8	43.726966	21.101055
Foeni-Salas (Ovis aries)	6.1	0	1	7	1	0	0	0	45.49811	20.868992
Foeni-Salas (Ovis aries)	6.1	0	1	7.9	1.3	0	0	0	45.49811	20.868992
Foeni-Salas (Ovis aries)	6.1	1	2	12	3	2	3	0	45.49811	20.868992
Stragari (Ovis aries)	6.1	0	1	2	0	0	0	0	43.712803	21.106225
Stragari (Ovis aries)	6.1	0	1	3	0	0	0	0	43.712803	21.106225
Stragari (Ovis/Capra)	6.1	0	1	3	5	8	0	0	43.712803	21.106225
Stragari (Ovis/Capra)	6.1	0	1	3.9	8.3	8.7	0	0	43.712803	21.106225
Petnica	6.1	0	0	2	2	3	1	1	44.246767	19.92774
Petnica	6.1	0	0	3.5	4.2	6.7	3.2	1.5	44.246767	19.92774
Vinca	6.1	0	1	6	5	4	5	5	44.7313	20.5876
Vinca	6.1	0	1.1	8	5.8	7.1	6.6	5.3	44.7313	20.5876
Megalo Nisi Galanis	6.1	1	0	5	3	3	1	0	40.301504	21.786537
Megalo Nisi Galanis	6.1	1	0	8.8	11.7	14.4	8.1	0	40.301504	21.786537
Novacka Cuprija	6.1	0	0	0	1	3	0	1	43.929051	21.373649
Novacka Cuprija	6.1	0	0	0	1.5	6.5	0	2	43.929051	21.373649
Araguina-Sennola-2	5.2	3	3	4	5	8	7	0	41.401879	9.158549
Araguina-Sennola-3	5.2	1.5	0.5	3	2	3.5	0.5	8	41.401879	9.158549
Araguina-Sennola-4	5.2	2	2	4	5	6	3.5	0.5	41.401879	9.158549
Arene Candide_2	5.2	0	0	0	3.3	3	3.3	0.5	44.182861	8.367348
Arene Candide_3	5.2	0	1	3	3.3	45.6	12.7	4.3	44.182861	8.367348
Arene Candide_4	5.2	0	0	3	3	9.7	6.2	5.2	44.182861	8.367348
Arene Candide_5	5.2	0	1	1	5.2	14.5	12	9.4	44.182861	8.367348
Baume de Fontbregoua 1	5.2	13.3	13.3	13.3	33	23	0.5	0.5	43.565801	6.23097
Baume de Fontbregoua 2	5.2	5	5	5	5	5	0	0	43.565801	6.23097
Baume de Fontbregoua 3	5.2	4.3	4.3	4.3	8	15	0	0	43.565801	6.23097
Baume de Fontbregoua 4	5.2	3	3	3	10	10	1	0	43.565801	6.23097
Blagotin	6.1	1.5	2.1	16.5	12.6	6	11.7	16.8	43.715212	21.085681

Bukovacka Cesma 1	6.1	0	0.5	0.5	0	0.33	0.33	0.33	44.21047	22.604613
Bukovacka Cesma 2	6.1	0	1.5	1.5	0	0.33	0.33	0.33	44.21047	22.604613
Cala Barbarina Abri du Sanglier	6.1	0	0	0	0	9	0	0	41.620922	8.964453
Capty	6.1	1.33	1.33	1.33	5	5	0	0	44.00449	5.13206
Gomolava Block VII	6.1	0	0	1	3	1	1	1	44.890007	19.748086
Petnica	6.1	0	0	5	5	4	3	0	44.247908	19.928534

* or BP. Depends on the dating system in which the data were provided.

A.2 Dataset-B

Table A.2 Age-at-death profiles from dataset-B.

Archaeological Site	A	B	C	D	EF	G	HI	Period	Lat	Long
Silourokambos3	0	0	0.5	0.5	2	0	0	8M	34.741272	33.160894
Le Barmaz sur Collombey1	0	0	2	0	1	1	0	4M	46.181098	6.88
Pojejena Nucet IIA-IB	0	0	1	2	0	1	0	7-6M	46.4842	22.5614
Miercurea Sibiului IIB-IIA	0	1	2	1	0	1	0	6M	45.8833	23.7833
Phaistos	0	1	2	2	0	0	0	4M	35.051547	24.815941
Silourokambos1	0	0	0	2.5	1.5	0.5	0.5	9-8M	34.741272	33.160894
Silourokambos2	0	0	1.5	0.5	1	2	0	9-8M	34.741272	33.160894
Araguina-Sennola III	1	0.5	1	1	1	0.5	1	2M	41.401879	9.158549
Arma dello Stefanin	0.3	0.3	0.3	2	3	0	0	6M	44.109446	8.052864
Gornea-L I/IIB	0	0	2	1	3	0	0	7-6M	44.7281	21.8542
Kalythines Cave	1.5	1.5	1.5	1.5	0	0.5	0.5	7-6M	37.95552	23.70204
Les Calades1	1	1	0	1	3	1	0	3-2M	43.795963	5.037174
Miercurea Sibiului IB-IC	0	0	3	2	2	0	0	7-6M	45.8833	23.7833
Grotto Perusello1	1	1	1	3	1.3	0.3	0.3	6M	44.10468	8.078842
Coppetella	0	0	1	2.5	1.5	1.5	1.5	4M	43.58868	13.317947
Gura Baciului IIA-IIB	0	1	2	2	3	0	0	6M	46.813846	23.44162
Gura Baciului IVA-IVB	0	2	1	3	2	0	0	6M	46.813846	23.44162
Le Barmaz sur Collombey2	0	1	1	0	4	0	2	4M	46.181098	6.88
Moldova Veche-Rat IVA	0	0	3	1	0	4	0	6M	44.725278	21.618056
La Mercière ö Jarnac-Champagne	0	1	2	0	3	1	2	3M	45.541746	-0.390558
Nosza-Gyongypart	0	1.5	1.5	0	2	2	2	6M	46.061043	19.400039
Araguina-Sennola I	1.5	1.5	1	4	2	0	0	5M	41.401879	9.158549
Font Juvenal2	0.5	0.5	4	2	1	2	0	5M	43.289993	2.350702
Gura Baciului IA-IB	0	1	3	3	3	0	0	7-6M	46.813846	23.44162
Araguina-Sennola II	1	1	2.5	1.5	2	3	0	4-3M	41.401879	9.158549
Fontbelle	0	0	3	1	3	2	2	3M	-	-
Cueva del Mirador2	4	3	3	0	0.67	0.67	0.67	4-3M	42.352624	-3.518915
Font Juvenal7	0	0	1	2.5	1.5	4	3	3M	43.289996	2.350705
Gnadendorf	1	2	0	0	3	3	3	6-5M	48.677663	16.407165
Pont de Roque-Haute	0	0	2	5	3	2	0	6-5M	43.308733	3.341703
Font Juvenal5	0	0	2.5	4.75	2.58	2.58	0.58	4-3M	43.289996	2.350705
Le Mourre du Tendre	0	1	5	2	3	1	1	3M	44.097428	4.881125
Cueva del Mirador1	3.5	1.5	7	0	0.67	0.67	0.67	4-3M	42.352624	-3.518915
La Sauzaie ö Soubise	2	0	1	0	3	7	1	4-3M	46.213719	-1.076984
Lerna I	1	3	0	2	9	0	0	7-6M	37.558913	22.715492
Les Calades2	4	0	4	3	2	1	1	3-2M	43.795963	5.037174
Seusa-Cararea mori IB-IC	1	4	2	4	4	0	0	7-6M	46.05	23.633
Ovcarovo gorata	0	1.5	2.5	4	4	4	0	6M	43.183333	26.65
Prodromos I	0	0	3	7	6	0	0	7-6M	39.382256	21.982155

La Fare2	0	2	3	3	4	2	3	3M	43.965912	5.813354
Station See	1	3	2.5	5.5	1	3	1	2M	47.92	13.41
Clairvaux XIV	1	9	7	0.25	0.25	0.25	0.25	5-4M	48.147782	4.788136
Font Juvenal6	0.5	1	2	7.5	4.5	1	1.5	4-3M	43.289996	2.350705
Dudestii Vechi IIB	1	1	3	5	4	4	1	6M	46.091012	20.491791
Le Plan-Saint-Jean	0	2	1	3	7	4	3	3M	43.40823	6.05472
Gura Baciului IB-IIA	2	2	4	2	4	4	3	7-6M	46.813846	23.44162
Parta Tell 2/IIA	1	3	6	6	2	1	2	6M	45.6333	21.1333
Trasano V	1	4	7	2.5	0.5	4.5	1.5	6-5M	40.67652	16.63981
Foeni Salas	1	2	12	3	2	3	0	6-5M	45.6	20.9
Font Juvenal3	5	6.5	2.5	2.75	3.75	1.75	1.75	5M	43.289994	2.350703
Grotto Perusello2	3	3	3	7	4	2	2	4-3M	44.10468	8.078842
Font Juvenal1	4.5	1.16	7.16	3.16	4.34	3.34	1.34	6-5M	43.289993	2.350702
Trasano I	1	2.5	8	4.5	8.5	2.5	0	7-6M	40.67652	16.63981
Foeni-Gaz	2	5	5	6	6	4	0	7-6M	45.522065	20.887527
Miercurea Sibiului IC-IIA	4	2	6	8	4	5	1	7-6M	45.8833	23.7833
La Bremonde	0	3	7	5	7	6	5	4-3M	43.833616	5.393663
Techirghiol	0	0	7	11	7	6	2	6-5M	44.062015	28.597355
Dudestii Vechi IIA	1	4	8	6	10	6	2	6M	46.091012	20.491791
Font Juvenal4	5	3.5	7.84	6.33	4.33	5.5	4.5	5-4M	43.289995	2.350704
Trasano III	0	1.5	10	7.5	10.5	5.5	2	6M	40.67652	16.63981
Siroka U Lesa	0	3	3	7	11.7	6.7	6.7	6-5M	49.078664	16.390686
Cauce	6	7	4	11	8	6	1	7-6M	45.75	22.7666
La Citadelle	1	4	7	6	10	9	9	4-3M	43.555122	5.657915
Tiszavasvari-Deakhalm	1	1	3	16	22	2	2	6M	47.966667	21.35
Trasano II	0	1.5	10.5	13.3	14.3	7.8	2.8	6M	40.67652	16.63981
Le Camp	1	6	4	9	7	12	13	3M	45.420705	-0.076962
Prodromos II	0	0	16	13	14	9	0	7-6M	39.382256	21.982155
Trasano IV	0	1	13.3	15.8	14.2	7.3	2.3	6-5M	40.67652	16.63981
Champ-Durand	5	10	8	6	6	14	8	4-3M	46.418351	-0.67682
La Draga	0.8	2.3	7.8	23	18.5	5.5	0	6-5M	42.1182	2.7651
Lerna2	4	13	0	7	37	0	0	6-5M	37.558913	22.715492
La Fare1	0	3	8	14	21	10	6	4-3M	43.965912	5.813354
Mondees	4.33	9.33	14.33	12	2.67	17.67	10.67	2M	47.94	13.31
Colle Santo Stefano	0	1	3	15	32	29	7	6M	42.201395	13.641186
Dimini	0	4.5	33	22	23	22	2.5	5M	39.3711	22.89608
Ecsegfalva 23	15	8	8	45	23.5	23.5	0	6M	47.155793	20.927467

A.3 Dataset-C

Table A.3 Payne's idealised models

Class	**A**	**B**	**C**	**D**	**E**	**F**	**G**	**H**	**I**
Age	**0–2 months**	**2–6 months**	**6–12 months**	**1–2 years**	**2–3 years**	**3–4 years**	**4–6 years**	**6–8 years**	**8 + years**
Meat	0.15	0.10	0.05	0.20	0.20	0.05	0.05	0.10	0.10
Milk	0.52	0.05	0.03	0.04	0.07	0.05	0.04	0.10	0.10
Wool	0.15	0.10	0.05	0.05	0.07	0.06	0.06	0.26	0.20

Table A.4 Redding's idealised models

Age in years:	**0 - 0.5**	**0.5 - 1**	**1 - 2**	**2 - 3**	**3 - 4**	**4 - 5**	**5 - 6**	**6 - 7**	**7 - 8**	**8 +**
Energy offtake maximization	9.6	12.8	30	22.6	1.1	5.7	2.1	4.3	5.5	6.3
Herd security maximization	9.6	25.9	26.5	13	1.1	5.7	2.1	4.3	5.5	6.3

Table A.5 Vigne and Helmer's idealised models

Archaeological Site	**Type**	**A**	**B**	**C**	**D**	**EF**	**G**	**HI**
La Balance	Meat Type A	0	3	11	11	4	4	3
La Fare	Meat Type B	1	2	8	36	39	8	3
Combre Obscurec5	Milk Type A	12	6	7	8	2	3	1
La Lauziere	Milk Type B	0	2	6	5	13	9	8
Grotte Muree c7b/10	Fleece	1	6	14	8	11	18	25

Appendix B

B.1 Ethological data

Table B.1. Live weights, MOW, food consumed, milk consumed by kids/lambs and milk yields from unimproved, modern herds for 96 months of age.

Age in Month	Live weight (kg) per animal	Meat and offal weight MOW (kg) per animal	Food consumed (Hay in kg/month) per animal	Milk consumed by lamb-kid in kg/month	Milk yield in kg/month (egyptian goats)**
1	4.896741562	2.693207859	2.980844197	28.08	0
2	6.939236633	3.816580148	4.224193385	52.5	0
3	9.334202084	5.133811146	5.682105503	52.5	0
4	12.01126709	6.606196901	7.311742999	0	0
5	14.88420152	8.186310838	9.060614115	0	0
6	17.86223652	9.824230086	10.87346419	0	0
7	20.8594128	11.47267704	12.69796634	0	0
8	23.8010037	13.09055204	14.48863146	0	0
9	26.62696117	14.64482864	16.20890578	0	0
10	29.2928786	16.11108323	17.83175732	0	0
11	31.76918303	17.47305067	19.33918377	0	0
12	34.03926114	18.72159362	20.72107191	0	0
13	36.09709717	19.85340344	21.97375974	0	0
14	37.94483561	20.86965959	23.09855271	0	0
15	39.59052632	21.77478947	24.10035103	0	0
16	41.04618636	22.5754025	24.98647007	0	0
17	42.32622555	23.27942405	25.76568158	0	0
18	43.44622775	23.89542526	26.4474721	0	19.25
19	44.42204994	24.43212746	27.04149444	0	19.25
20	45.26918808	24.89805344	27.55718164	0	19.25
21	46.00235674	25.3012962	28.00349099	0	19.25
22	46.63523332	25.64937832	28.38874849	0	19.25
23	47.18032457	25.94917851	28.72056753	0	19.25
24	47.64892069	26.20690638	29.00582089	0	19.25
25	48.05110966	26.42811031	29.25064956	0	19.25
26	48.39583082	26.61770695	29.46049523	0	19.25
27	48.69095229	26.78002376	29.64014758	0	19.25
28	48.94336095	26.91884852	29.79379892	0	19.25
29	49.15905713	27.03748142	29.92510188	0	19.25
30	49.34324882	27.13878685	30.03722682	0	40
31	49.5004419	27.22524305	30.13291659	0	40
32	49.63452441	27.29898843	30.21453803	0	40
33	49.74884377	27.36186407	30.28412881	0	40
34	49.8462765	27.41545207	30.34344007	0	40
35	49.92929057	27.46110982	30.39397407	0	40

36	50.00000061	27.50000034	30.43701813	0	40
37	50.06021641	27.53311903	30.4736739	0	40
38	50.1114854	27.56131697	30.50488342	0	40
39	50.15512962	27.58532129	30.53145141	0	40
40	50.19227778	27.60575278	30.55406499	0	40
41	50.22389295	27.62314112	30.57331042	0	40
42	50.25079648	27.63793806	30.5896877	0	45.83333333
43	50.27368855	27.6505287	30.60362303	0	45.83333333
44	50.29316585	27.66124122	30.61547964	0	45.83333333
45	50.30973671	27.67035519	30.62556699	0	45.83333333
46	50.32383409	27.67810875	30.63414863	0	45.83333333
47	50.33582664	27.68470465	30.64144897	0	45.83333333
48	50.34602823	27.69031553	30.64765909	0	45.83333333
49	50.35470604	27.69508832	30.65294162	0	45.83333333
50	50.36208746	27.6991481	30.65743501	0	45.83333333
51	50.36836602	27.70260131	30.66125703	0	45.83333333
52	50.37370637	27.70553851	30.6645079	0	45.83333333
53	50.37824865	27.70803676	30.66727296	0	45.83333333
54	50.38211206	27.71016163	30.66962479	0	48.16666667
55	50.38539802	27.71196891	30.67162507	0	48.16666667
56	50.38819281	27.71350605	30.6733264	0	48.16666667
57	50.39056983	27.7148134	30.67477337	0	48.16666667
58	50.3925915	27.71592533	30.67600405	0	48.16666667
59	50.39431095	27.71687102	30.67705074	0	48.16666667
60	50.39577334	27.71767534	30.67794096	0	48.16666667
61	50.3970171	27.7183594	30.67869808	0	48.16666667
62	50.3980749	27.7189412	30.679342	0	48.16666667
63	50.39897455	27.719436	30.67988968	0	48.16666667
64	50.3997397	27.71985683	30.68035545	0	48.16666667
65	50.40039044	27.72021474	30.68075159	0	48.16666667
66	50.40094389	27.72051914	30.68108849	0	49.58333333
67	50.40141458	27.72077802	30.68137503	0	49.58333333
68	50.4018149	27.7209982	30.6816187	0	49.58333333
69	50.40215536	27.72118545	30.68182595	0	49.58333333
70	50.40244492	27.72134471	30.68200221	0	49.58333333
71	50.40269118	27.72148015	30.68215214	0	49.58333333
72	50.40290062	27.72159534	30.68227961	0	49.58333333
73	50.40307874	27.72169331	30.68238806	0	49.58333333
74	50.40323023	27.72177663	30.68248028	0	49.58333333
75	50.40335907	27.72184749	30.68255869	0	49.58333333
76	50.40346865	27.72190775	30.6826254	0	49.58333333
77	50.40356183	27.72195901	30.68268214	0	49.58333333
78	50.40364109	27.7220026	30.68273038	0	48.16666667
79	50.4037085	27.72203967	30.68277141	0	48.16666667
80	50.40376582	27.7220712	30.68280632	0	48.16666667

81	50.40381458	27.72209802	30.682836	0	48.16666667
82	50.40385604	27.72212082	30.68286123	0	48.16666667
83	50.4038913	27.72214022	30.68288269	0	48.16666667
84	50.4039213	27.72215671	30.68290095	0	48.16666667
85	50.4039468	27.72217074	30.68291647	0	48.16666667
86	50.4039685	27.72218267	30.68292968	0	48.16666667
87	50.40398694	27.72219282	30.68294091	0	48.16666667
88	50.40400264	27.72220145	30.68295047	0	48.16666667
89	50.40401598	27.72220879	30.68295859	0	48.16666667
90	50.40402733	27.72221503	30.6829655	0	45.83333333
91	50.40403698	27.72222034	30.68297138	0	45.83333333
92	50.40404519	27.72222485	30.68297637	0	45.83333333
93	50.40405217	27.72222869	30.68298063	0	45.83333333
94	50.40405811	27.72223196	30.68298422	0	45.83333333
95	50.40406316	27.72223474	30.6829873	0	45.83333333
96	50.40406745	27.7222371	30.68298991	0	45.83333333

B.2 Selected age-at-death profiles for analysis described in Chapter5

Table B.2. Archaeological age-at-death profile data represented in bone-element counts in 7 age classes (A - HI) from a dataset of 76 (see Chapter 4) with 10 smallest and 10 largest sample sizes (N).

Site	A	B	C	D	EF	G	HI	N	Period	Region	Reference:
Silourokambos3	0	0	0.5	0.5	2	0	0	3	8M	Eastmed	Vigne *et al.*, 2011
Le Barmaz sur Collombey1	0	0	2	0	1	1	0	4	4M	Central	Chaix, 1976
Pojejena Nucet IIA-IB	0	0	1	2	0	1	0	4	7-6M	Balkans	El Susi, 2008
Miercurea Sibiului IIB-IIA	0	1	2	1	0	1	0	5	6M	Balkans	El Susi, 2008
Phaistos	0	1	2	2	0	0	0	5	4M	Aegean	Wilkens, 1996
Silourokambos1	0	0	0	2.5	1.5	0.5	0.5	5	9-8M	Eastmed	Vigne et al., 2011
Silourokambos2	0	0	1.5	0.5	1	2	0	5	9-8M	Eastmed	Vigne et al., 2011
Araguina-Sennola III	1	0.5	1	1	1	0.5	1	6	2M	Franco-Iberian	Vigne, 1988
Arma dello Stefanin	0.333	0.333	0.333	2	3	0	0	6	6M	Adriatic	Barker *et al.*, 1990
Gornea-L I/IIB	0	0	2	1	3	0	0	6	7-6M	Balkans	El Susi, 2008
Prodromos II	0	0	16	13	14	9	0	52	7-6M	Aegean	Halstead and Jones, 1980
Trasano IV	0	1	13.3	15.8	14.2	7.3	2.3	54	6-5M	Adriatic	Braguier, 2000
Champ-Durand	5	10	8	6	6	14	8	57	4-3M	North-west	Gillis, 2012
La Draga	0.8	2.3	7.8	23	18.5	5.5	0	58	6-5M	Franco-Iberian	Gillis, 2012
Lerna2	4	13	0	7	37	0	0	61	6-5M	Mainland Greece	Gejvall *et al.*, 1969
La Fare1	0	3	8	14	21	10	6	62	4-3M	Franco-Iberian	Blaise, 2009
Mondees	4.33	9.33	14.33	12	2.67	17.67	10.67	71	2M	Central	Wolff, 1977
Colle Santo Stefano	0	1	3	15	32	29	7	87	6M	Adriatic	Salque, 2012
Dimini	0	4.5	33	22	23	22	2.5	107	5M	Mainland Greece	Halstead, 1992
Ecsegfalva 23	15	8	8	45	23.5	23.5	0	123	6M	Balkans	Bartosiewicz and Gál, 2007

B.3 Sex ratio datasets

Table B.3. Sex ratio datasets of modern and archaeological goat/sheep herds.

Ali Kosh Goats Zeder SCORES (archaeological site)			Male		Female		sex ratios
Age (months)	Age_start	Age_ends	n	%	n	%	
0-6	0	6	100	NA	98	NA	1.020408163
06-12	6	12	96	NA	95	NA	1.010526316
12-18	12	18	93	NA	98	NA	0.948979592
18-30	18	30	54	NA	82	NA	0.658536585
30-48	30	48	25	NA	47	NA	0.531914894
Total							

Ali kosh GAZELLES Zeder SCORES (archaeological site)			Male		Female		sex ratios
Age (months)	Age_start	Age_ends	n	%	n	%	
0-6	0	6	99	NA	100	NA	0.99
06-12	6	12	100	NA	96	NA	1.041666667
12-18	12	18	98	NA	97	NA	1.010309278
18-30	18	30	75	NA	89	NA	0.842696629
30-48	30	48	66	NA	53	NA	1.245283019
Total							

Jarmo Goats Zeder SCORES (archaeological site)			Male		Female		sex ratios
Age (months)	Age_start	Age_ends	n	%	n	%	
0-6	0	6	99	NA	99	NA	1
06-12	6	12	100	NA	98	NA	1.020408163
12-18	12	18	88	NA	99	NA	0.888888889
18-30	18	30	88	NA	96	NA	0.916666667
30-48	30	48	46	NA	59	NA	0.779661017
Total							

Ganj Dareh Goats Zeder SCORES (archaeological site)			Male		Female		sex ratios
Age (months)	Age_start	Age_ends	n	%	n	%	
0-6	0	6	97	NA	0	NA	NA
06-12	6	12	100	NA	100	NA	1
12-18	12	18	100	NA	100	NA	1
18-30	18	30	100	NA	100	NA	1
30-48	30	48	100	NA	50	NA	0
Total							

Boury-en-Vexin Sheep/Goat (archaeological site)			Male		Female		sex ratios
Age (months)	Age_start	Age_ends	n	%	n	%	
0-12	0	12	16	NA	16	NA	1
12-24	12	24	10	NA	12	NA	0.833333333
24-36	24	36	0	NA	11	NA	0
36-48	36	48	1	NA	7	NA	0.142857143
48-60	48	60	0	NA	10	NA	0
60-72	60	72	0	NA	8	NA	0
72-84	72	84	0	NA	3	NA	0
84-96	84	96	0	NA	5	NA	0
Total							

Gani Dareh Zeder SCORES (archaeological site)			Male		Female		sex ratios
Age (months)	Age_start	Age_ends	n	%	n	%	
0-6	0	6	98	NA	96	NA	1.020833333
06-12	6	12	94	NA	91	NA	1.032967033
12-18	12	18	74	NA	93	NA	0.795698925
18-30	18	30	21	NA	74	NA	0.283783784
30-48	30	48	4	NA	27	NA	0.148148148
Total							

Ganj Dareh LEVEL E Goats Zeder SCORES (archaeological site)			Male		Female		sex ratios
Age (months)	Age_start	Age_ends	n	%	n	%	
0-6	0	6	100	NA	88	NA	1.136363636
06-12	6	12	83	NA	91	NA	0.912087912
12-18	12	18	57	NA	91	NA	0.626373626
18-30	18	30	23	NA	72	NA	0.319444444
30-48	30	48	6	NA	25	NA	0.24
Total							

Ganj Dareh Goats LEVEL A-D Zeder SCORES (archaeological site)			Male		Female		sex ratios
Age (months)	Age_start	Age_ends	n	%	n	%	
0-6	0	6	97	NA	94	NA	1.031914894
06-12	6	12	97	NA	83	NA	1.168674699
12-18	12	18	86	NA	94	NA	0.914893617
18-30	18	30	20	NA	74	NA	0.27027027
30-48	30	48	7	NA	28	NA	0.25
Total							

Ganj Dareh Goats Zeder REAL COUNTS (archaeological site)			Male		Female		sex ratios	
Age (months)	Age_start	Age_ends	n	%	n	%		
0-10	0	10	100	NA	164	NA	0.609756098	
10-13	10	13	61	NA	61	NA		1
13-16	13	16	30	NA	43	NA	0.697674419	
16-24	16	24	92	NA	13	NA	7.076923077	
24-30	24	30	101	NA	194	NA	0.520618557	
30-36	30	36	90	NA	91	NA	0.989010989	
Total								

Shanidar Goats Zeder SCORES (archaeological site)			Male		Female		sex ratios	
Age (months)	Age_start	Age_ends	n	%	n	%		
0-6	0	6	100	NA	100	NA		1
06-12	6	12	0	NA	100	NA		0
12-18	12	18	99	NA	79	NA	1.253164557	
18-30	18	30	83	NA	50	NA	1.66	
30-48	30	48	80	NA	0	NA	NA	
Total								

Sahel Goats			Male		Female		sex ratios	
Age (months)	Age_start	Age_ends	n	%	n	%		
0-<12	0	12	35	18.5	34	18	1.029411765	
12-<24	12	24	11	5.8	32	16.9	0.34375	
24- <36	24	36	8	4.2	19	10.1	0.421052632	
36-<48	36	48	0	0	18	9.6		0
48+	48	96	0	0	32	16.9		0
Total			54	28.5	135	71.5		

Sokoto red Goats			Male		Female		sex ratios	
Age (months)	Age_start	Age_ends	n	%	n	%		
0-<12	0	12	148	22.9	190	29.3	0.778947368	
12 -<24	12	24	41	6.3	99	15.3	0.414141414	
24-<36	24	36	3	0.5	56	8.7	0.053571429	
36-<48	36	48	0	0	56	8.7		0
48+	48	96	0	0	54	8.3		0
Total			192	29.7	455	70.3		

Confined Goats Nigeria (Group 3)			Male		Female		sex ratios	
Age (months)	Age_start	Age_ends	n	%	n	%		
0 -<6	0	6	15	NA	21	NA	0.714285714	
6 -<12	6	12	1	NA	5	NA	0.2	
12 -<24	12	24	2	NA	15	NA	0.133333333	
24 -<36	24	36	0	NA	7	NA		0
36 -<48	36	48	0	NA	8	NA		0
48 - <60	48	60	0	NA	6	NA		0
>60	60	96	0	NA	3	NA		0
Total			18		65			

Confined Goats Nigeria (Group 4)			Male		Female		sex ratios
Age (months)	Age_start	Age_ends	n	%	n	%	
0 -<6	0	6	20	18.9	20	18.8	1
6 - <12	6	12	6	5.7	9	8.5	0.666666667
12 -<24	12	24	1	0.9	8	7.6	0.125
24 -<36	24	36	0	0	9	8.5	0
36 - <48	36	48	0	0	12	11.3	0
48 - <60	48	60	0	0	10	9.4	0
>60	60	96	0	0	11	10.4	0
Total			27	25.5	79	74.5	

Confined Goats Nigeria (Group 2)			Male		Female		sex ratios
Age (months)	Age_start	Age_ends	n	%	n	%	
0 -<6	0	6	6	NA	5	NA	1.2
6-<12	6	12	2	NA	3	NA	0.666666667
12-<24	12	24	1	NA	5	NA	0.2
24 - <36	24	36	0	NA	3	NA	0
36 - <48	36	48	0	NA	1	NA	0
48 -<60	48	60	0	NA	1	NA	0
>60	60	96	0	NA	1	NA	0
Total			9		19		

Ethiopian Goats All			Male		Female		sex ratios
Age (months)	Age_start	Age_ends	n	%	n	%	
0-<6	0	6	2533036	11.12	2865173	12.57	0.884077855
6-<12	6	12	1276786	5.6	1662469	7.3	0.7680059
12-<24	12	24	1033521	4.54	1791990	7.86	0.576744848
24+	24	96	1984080	8.71	9639892	42.3	0.205819733
Total			6827423	29.97	15959524	70.03	

Ethiopian Sheep All			Male		Female		sex ratios
Age (months)	Age_start	Age_ends	n	%	n	%	
0-<6	0	6	3270863	12.82	3506824	13.75	0.93271376
6-<12	6	12	1099170	4.31	1459251	5.72	0.753242588
12-<24	12	24	934179	3.66	1657483	6.5	0.56361302
24+	24	96	1662047	6.52	11919187	46.73	0.139442984
Total			6966259	27.31	18542745	72.69	

Sheep/Goats modern Zeder REAL COUNTS			Male		Female		sex ratios	
Age (months)	Age_start	Age_ends	n	%	n	%		
0-10	0	10	12	NA	11	NA	1.090909091	
Oct-13	10	13	36	NA	31	NA	1.161290323	
13-16	13	16	44	NA	39	NA	1.128205128	
16-24	16	24	24	NA	24	NA		1
24-30	24	30	11	NA	12	NA	0.916666667	
30-36	30	36	12	NA	11	NA	1.090909091	
Total								

Sheep Free Range (Group WAD in Nigeria)			Male		Female		sex ratios	
Age (months)	Age_start	Age_ends	n	%	n	%		
0 - <6	0	6	17	NA	22	NA	0.772727273	
6 - <12	6	12	10	NA	16	NA	0.625	
12 -<24	12	24	4	NA	24	NA	0.166666667	
24 -<36	24	36	0	NA	18	NA		0
36 -<48	36	48	0	NA	11	NA		0
48- <60	48	60	0	NA	2	NA		0
>60	60	96	0	NA	10	NA		0
Total			31		103			

Goats Free Range (Group WAD in Nigeria)			Male		Female		sex ratios	
Age (months)	Age_start	Age_ends	n	%	n	%		
0-<6	0	6	29	NA	40	NA	0.725	
6-<12	6	12	0	NA	15	NA		0
12 - <24	12	24	1	NA	25	NA	0.04	
24 - <36	24	36	0	NA	19	NA		0
36 - <48	36	48	0	NA	12	NA		0
48 -<60	48	60	0	NA	9	NA		0
>60	60	96	0	NA	7	NA		0
Total			30		127			

Sheep North Nigeria			Male		Female		sex ratios	
Age (months)	Age_start	Age_ends	n	%	n	%		
0 -<12	0	12	221	21.8	247	24.5	0.894736842	
12 -<24	12	24	98	9.7	146	14.6	0.671232877	
24 - <36	24	36	3	0.3	66	6.5	0.045454545	
36 -<48	36	48	0	0	83	8.2		0
48+	48	96	0	0	146	14.5		0
Total			322	31.8	688	68.3		

Sheep (Group 2) Seasonally Confined in Nigeria			Male		Female		sex ratios
Age (months)	Age_start	Age_ends	n	%	n	%	
0 - <6	0	6	12	NA	6	NA	2
6 -<12	6	12	3	NA	2	NA	1.5
12 -<24	12	24	1	NA	6	NA	0.166666667
24 -<36	24	36	0	NA	9	NA	0
36 - <48	36	48	0	NA	9	NA	0
48 - <60 -	48	60	0	NA	3	NA	0
>60	60	96	0	NA	7	NA	0
Total			16		42		

Sheep, Seasonally Confined in Nigeria			Male		Female		sex ratios
Age (months)	Age_start	Age_ends	n	%	n	%	
0 - <6	0	6	7	NA	6	NA	1.166666667
6 -<12	6	12	1	NA	6	NA	0.166666667
12 - <24	12	24	2	NA	6	NA	0.333333333
24 -<36	24	36	0	NA	4	NA	0
36 - <48	36	48	1	NA	10	NA	0.1
48 -<60	48	60	0	NA	1	NA	0
>60	60	96	0	NA	1	NA	0
Total			11		34		

Goats (group WAD Nigeria) 'cut and carry'			Male		Female		sex ratios
Age (months)	Age_start	Age_ends	n	%	n	%	
0 -<6	0	6	31	NA	29	NA	1.068965517
6-<12	6	12	12	NA	11	NA	1.090909091
12 - <24	12	24	4	NA	22	NA	0.181818182
24 - <36	24	36	1	NA	24	NA	0.041666667
36 - <48	36	48	0	NA	28	NA	0
48 - <60	48	60	2	NA	21	NA	0.095238095
>60	60	96	0	NA	27	NA	0
Total			51		162		

Goats (group WAD Nigeria)			Male		Female		sex ratios
Age (months)	Age_start	Age_ends	n	%	n	%	
0 -<12	0	12	141	21	179	26.6	0.787709497
12-<24	12	24	13	1.9	81	12.1	0.160493827
24 - <36	24	36	1	0.1	73	10.8	0.01369863
36 -<48	36	48	4	0.6	72	10.7	0.055555556
48+	48	96	2	0.3	107	15.9	0.018691589
Total			161	23.9	512	76.1	

Sheep (Group WAD Nigeria)			Male		Female		sex ratios	
Age (9months)	Age_start	Age_ends	n	%	n	%		
0 -<12	0	12	75	20.7	92	25.3	0.815217391	
12 -<24	12	24	15	4.1	49	13.5	0.306122449	
24 -<36	24	36	0	0	39	10.7		0
36 -<48	36	48	1	0.3	45	12.4	0.022222222	
48+	48	96	1	0.3	46	12.7	0.02173913	
Total			92	25.4	271	74.6		

Iran/Iraq Sheep/Goats MODERN WILD (Zeder et al.,)			Male		Female		sex ratios	
Age (months)	Age_start	Age_ends	n	%	n	%		
0-6 (A)	0	6	3	NA	0	NA	NA	
6-12 (B)	6	12	0	NA	5	NA		0
12-18 (C)	12	18	9	NA	2	NA	4.5	
18-30 (D)	18	30	15	NA	8	NA	1.666666667	
30-48 (E)	30	48	6	NA	12	NA	0.428571429	
48+ (F)	48	96	20	NA	20	NA	0.952380952	
Total			53		47			

B.4 Protein and calories in sheep/goat milk and meat

Table B.4. Macronutrient quantity in 100g of meat and milk in sheep or goats.

Sheep/Goats meat and milk	Protein in g/100g in meat or milk	Calories in cal /100g in meat or milk	Reference
Goat raw meat	21	109	U.S. Department of Agriculture, 2015
Goat roasted meat	27	144	U.S. Department of Agriculture, 2015
Lamb, 1/4" fat, meat	25	267	U.S. Department of Agriculture, 2015
Lamb raw meat	16.56	282	U.S. Department of Agriculture, 2015
Goat raw meat	20.6	109	U.S. Department of Agriculture, 2015
Goat meat	16	253	Redding, 1981, Book, p. 103
Sheep meat	18.4	157	Redding, 1981, Book, p. 103
Goat milk	3.69	63	Giles Abie, Nall Kacia, 2015
Sheep milk	6	108	U.S. Department of Agriculture, 2015
Goat milk	3.56	69	U.S. Department of Agriculture, 2015
Sheep milk	5.98	108	U.S. Department of Agriculture, 2015
Goat milk	3.3	66.8	Redding, 1981, Book, p. 114
Sheep milk	6.18	109.6	Redding, 1981, Book, p. 114
goat/sheep mean meat	20.65	188.71	
goat/sheep mean milk	4.78	87.4	

B.5 Meat and Milk datasets for sheep and goats

Tables B.5 - 21 contain information on live weights, meat weights and carcass weights for goat or sheep herds from rural Asia and Africa. The tables below show total of female and male animal weights (presented either as live weights or a combination of live weights, carcass weights and meat weights). Data are presented per individual or as single, twin and triplets at various types of ages in either months or days with different intervals of ages per dataset (Redding, 1981, FAO, 2003). Those datasets, which share same age structure are combined into one table. The datasets contain weights in kg for various breeds on sheep and goats from Turkey, Sudan, Nigeria, Uganda, Tanzania, Iran, Yemen and Rajasthan in India as well as

unknown locations (Redding, 1981). Live weights and meat weights from all datasets were considered to provide information for Table B.1.

Goat datasets:

Table B.5 Meat weights in kg measured at birth, 3 months, 6 months, 9 months and 12 months for 12 Indian goat breeds (FAO, 2003).

Rajasthan (India) goats - Meat body weight in kg												
Goat Breed	Sihori	Matwari	Beetal	Barbari	Jam-napari	Chokla	Nali	Marwari	Magra	Malpura	Sonadi	Muzza-farnagari
At birth	2.82 ± 0.02	2.29 ± 0.05	2.80 ± 0.01	1.739 ± 0.018	4.27 ± 0.04	2.37 ± 0.02Ê	2.88 ± 0.03Ê	2.98 ± 0.02Ê	2.98	2.52 ± 0.01Ê	2.40 ± 0.02Ê	3.01 ± 0.63Ê
3 months	9.92 ± 0.12	6.00 ± 0.85	9.26 ± 0.09	6.661 ± 0.095	12.11 ± 0.45	11.13 ± 0.13Ê	10.19 ± 0.14Ê	8.16 ± 0.84Ê	11.7	9.14 ± 0.09Ê	9.29 ± 0.13Ê	10.76 ± 0.39Ê
6 months	13.48 ± 0.19	8.70 ± 1.35	12.18 ± 0.21	7.800 ± 0.476	15.56 ± 1.67	13.46 ± 0.18Ê	13.30 ± 0.20Ê	9.40 ± 0.20Ê	37.97	12.55 ± 0.13Ê	13.22 ± 0.21Ê	14.56 ± 0.59Ê
9 months	16.95 ± 0.21	13.70 ± 1.58	15.42 ± 0.65	12.566 ± 1.215	24.00 ± 1.16	15.40 ± 0.17Ê	14.54 ± 0.21Ê	14.65 ± 0.25Ê	21.82	17.26 ± 0.18Ê	16.19 ± 0.24Ê	18.39 ± 0.93Ê
12 months	21.27 ± 0.23	16.25 ± 2.79	21.83 ± 0.83	14.517 ± 0.765	29.65	17.89 ± 0.215Ê	17.74 ± 0.31Ê	21.06 ± 0.04Ê	27.99	20.63 ± 0.29Ê	18.95 ± 0.26Ê	25.01 ± 2.16Ê

Table B.6. Meat weights, Live weights and Carcass weights in kg measured at birth, 0 – 12 months, 12+ months for Goats (Redding, 1981).

Goats, Redding				
Age Class / Sex	Age in months	Live weight in kg	Expected carcass weight in kg	Expected meat weight in kg
Females at birth	0	1.9	0.9	0.6
Males at birth	0	2.1	1	0.6
F yearlings	0 - 12	26	13	8.9
M yearlings	0 - 12	41	20.5	14.1
Female adults	12 - 96	35	175	12.6
Male adults	12 - 96	65	32.5	23.4

Table B.7. Live weights in kg measured at birth, 42 days, 150 days, 180 days 275 days and 365 days of age for 2 Ugandan goat and sheep breeds (FAO, 2003).

Goats and Sheep from Uganda – Live weights in kg		
Age in days	Small Boer Goat/Sheep	Small East African
0	2.06±0.4	2.3±0.5
42	8.3±1.5	6.9±1.3
150	19.7±2.5	14.9±2.7
180	21.8±2.8	16.2±2.9
275	28.2±2.8	20.2±2.3
365	34.3±2.4	20.0±3.1

Table B.8. Live weights in kg measured at birth, 0 - 1 months, 1 – 2 months, 2 – 3 months, 2 – 3 months of age and 3 – 6 months of age for single, twin, triplet male and female Nigerian goats (FAO, 2003).

Sokoto Nigeria goats - live weights in kg						
Age in months	Male			Female		
	Single	Twin	Triplet	Single	Twin	Triplet
0	2.1	1.8	1.5	2.1	2.1	1.4
0 - 1	3	3.9	3	3.7	4.4	3
1 - 2	6.1	5.8	5.4	5	5	4.2
2 - 3	7.7	7	6.8	7.5	7.5	4.4
3 - 6	10.3	10.1	10.9	10.4	11.1	6.5

Table B.9. Live weights, carcass weights and meat weights in kg measured at birth, 0 - 12 months and 12+ months of age for Sudanese female and male goats (FAO, 2003).

Goats from Sudanese desert - Live weight/ carcass/meat in kg						
Age in months	Male live weight	Female live weight	M carcass	F carcass	M meat	F meat
0	2.1	1.9	1	0.9	0.6	0.6
0-12	41	26	20.5	13	14.1	8.9
12+	65	35	32.5	17.5	23.4	12.6

Table B.10. Live weights in kg measured at birth, 0 - 4 months, 4 - 6 months, 6 – 12 months and 12+ months of age for Tanzanian female and male goats (FAO, 2003).

Goats in Tanzania – Live weight in kg		
Age in months	Male	Female
0	2.7	2.5
0 - 4	13.5	11.5
4 - 6	15.5	13.3
6 - 12	20.9	19.1
12 - 18	30.2	20.4

Table B.11. Live weights in kg measured at birth, 4 months, and 12+ months of age for Turkish female and male goats (FAO, 2003).

Turkey, Angora goats (breed) - Live weight in kg		
Age in months	Male	Female
0	2.6	2.3
4	16.8	14.7
12+	24.3	18.8

Table B.12. Live weights in kg measured at birth, 0 - 6 months, 6 - 9 months, 9 – 12 months, 12 – 18 months, 18 – 24 months and 24 – 36 months for Yemeni goats (FAO, 2003).

Yemen Goats	
Age in months	Live weight in kg
0	2
0 - 6	11
6 - 9	13
9 - 12	16
12 - 18	21
18 - 24	23
24 -36	27

Sheep datasets:

Table B.13. Live weights in kg measured at birth, 45 days, 105 days and 180 days of age for Central Anatolian female and male Merino sheep (FAO, 2003).

Turkish sheep – breed: Central Anatolian Merino - Live weight in kg		
Age in days	Male	Female
Birth	4.7	4.5
45	15.5	14.7
105	28.9	26.8
180	34.2	31.3

Table B.14. Live weights, Carcass weights and meat weights in kg measured at birth, 0 – 12 months and 12+ months of age for Iranian female and male sheep (FAO, 2003).

Sheep in Iran Live weight/ carcass/meat in kg						
Age in months	Male Live weight	Female Live weight	M carcass	F carcass	M meat	F meat
0	4.3	4	2.2	2	1.5	1.4
0 - 12	41	30	21.3	15.6	16.2	11.8
12+	68	40	35.4	20.8	26.9	15.8

Table B.15. Live weights, Carcass weights and meat weights in kg measured at birth, 0 – 12 months and 12+ months of age for female and male sheep (Redding, 1981).

Meat from Sheep, Redding 1981				
Age and Sex Class	Age in months	Live weight (kg)	Expected carcass weight (kg)	Expected meat weight (kg)
Females at birth	0	4	2	1.4
Males at birth	0	4.3	2.2	1.5
F yearlings	0-12	30	15.6	11.8
M yearlings	0-12	41	21.4	16.2
Female adults	12-96	40	20.8	15.8
Male adults	12-96	68	35.4	26.9

Table B.16. Live weights in kg measured at birth, 45 days, 75 days and 105 days and older than 105 days of age for Turkish sheep (FAO, 2003).

Sheep in Turkey	
Age in days	live weight in kg
0 - 45	3.92
45 -75	14.01
75 -105	18.93
105+	23.61

Table B.17. Live weights in kg measured at birth, 0 – 3 months, 3 – 6 months, 6 – 9 months, 9 – 12 months of age for Turkish sheep (FAO, 2003).

Turkey sheep – Sakiz Greek island	
Age in months	Live weight in kg
0	4.6
0 - 3	27.4
3 - 6	35.9
6 - 9	42.4
9 - 12	46.2

Table B.18. Live weights in kg measured at birth, 93 days and 6+ months of age for 2 Turkish breed sheep (FAO, 2003).

Turkey sheep – different breeds - Live weight in kg			
Age in days and months	Red Karaman	Daglic Male	Daglic Female
Birth weight	3.4	3.5	3.4
Weaning weight (93 days)	20.03	14.4	13.4
6 months +	28.7	25	22.8

Table B.19. Live weights in kg measured at birth, 45 days, 75 days, 110 days and 180 days of age for Turkish Merino sheep (FAO, 2003).

Turkey sheep - Turkish Merinos	
Age in days	Live weights in kg
Birth	4.4
45	15.2
75	22.4
110	28.8
180	39.9

Table B.20. Live weights in kg measured at birth, 45 days, 75 days, 105 days and 180 days of Turkish Karavaka sheep (FAO, 2003).

Turkey sheep – Karayaka	
Age in days	Live weights in kg
Birth	3.8
45	12.1
75	17.6
105	22.3
180	28.7

Table B.21. Live weights in kg measured at birth, 60 days, 120 days, 180 days of age for 3 male and female Turkish sheep breeds (FAO, 2003).

Turkey sheep - other breeds - Live weights in kg						
Age in days	Awassi M	Awassi F	Kivircjk M	Kivircjk F	Gokceada M	Gokceada F
Birth	4.4	4.1	4.3	4	4	3.9
60	17.7	16.4	16.4	15.7	18.1	16.3
120	28.7	25.3	19.4	18.8	27.3	23.5
180	37.3	34.8	25.9	24.1	32.3	28

B.6 Means and medians for ten production estimates for 20 age-at-death profiles from dataset-B and idealised models

Table B.22. Mean, Median and HPD of posterior distributions for outputs 'total calories per animal', 'reproductive output', 'milk calories per animal', 'MOW calories per animal', 'total calories per animal', total protein per animal', 'fodder consumed per animal, 'calories per fodder consumed', 'milk calories per fodder consumed' and 'mow calories per fodder consumed' for archaeological sites (10 smallest and 10 largest sample sizes from dataset-B) and idealized models.

	Total Calories per Animal (kcal)			
Age-at-Death profile	**Mean.1**	**Median.1**	**Confl.1**	**ConflI.1**
Eitzum	356.54	337.35	50.36	764.1
Cochstedt I	328.8	304.9	55.22	721.85
Cueva da la Dehesilla	220.16	191.73	-1.76	596.06
Cueva del Forcon	296.79	274.5	19.91	687.72
Cochstedt II	402.71	389.57	102.8	771.64
Gatersleben II	373.46	360.5	75.69	742.89
Silourokambos I	321.73	304.14	66.98	675.79
Le Barmaz sur Collombey1	292.05	274.76	45.56	641.24
Pojejena Nucet IIA-IB	269.77	245.95	41.83	624.32
Miercurea Sibiului IIB-IIA	214.57	192.21	3.98	545.44
Prodromos II	197.48	190.86	97.92	333.67
Trasano4	222.23	215.15	109.82	378.7
Champ-Durand	393.19	388.38	247.22	562.95
La Draga	169.24	162.75	83.56	293.05
Lerna2	233.69	229.9	158.87	330.38
La Fare1	335.96	327.39	203.73	514.81
Lanycsok-Egettmalom	271.41	263.84	158.04	425.55
Colle Santo Stefano	446.02	440.69	344.14	579.91
Dimini	222.43	218.65	141.47	326.03
Ecsegfalva 23	187.5	184.28	119.45	273.36
Helmer Meat Type A	221.81	213.14	99.49	391.61
Helmer Meat Type B	256.19	250.39	206.76	325.96
Helmer Milk Type A	112.69	103.95	17.83	257.74
Helmer Milk Type B, Meat Type A	310.58	301.35	177.17	488.37
Helmer Fleece, Milk Type B, Meat Type A	614.07	611.1	421.53	820.39
Payne Meat	324.16	327.32	313.2	330.43
Payne Milk	325.97	327.52	316.95	330.98
Payne Fleece	687.95	687.58	681.14	696.65
Redding Energy Max.	264.6	264.58	257.46	268.84
Redding Herd Security	244.44	248.17	233.23	250.53

	Reproductive Output (Animals per Animal)			
Age-at-Death profile	**Mean.2**	**Median.2**	**Confl.2**	**Confll.2**
Eitzum	1.05	1.02	0.3	2
Cochstedt I	0.99	0.94	0.33	1.9
Cueva da la Dehesilla	0.73	0.67	0.19	1.6
Cueva del Forcon	0.91	0.87	0.24	1.82
Cochstedt II	1.17	1.15	0.45	2.01
Gatersleben II	1.1	1.08	0.38	1.95
Silourokambos I	1	0.97	0.37	1.81
Le Barmaz sur Collombey1	0.91	0.88	0.32	1.72
Pojejena Nucet IIA-IB	0.85	0.8	0.3	1.67
Miercurea Sibiului IIB-IIA	0.72	0.67	0.21	1.49
Prodromos II	0.74	0.72	0.5	1.05
Trasano4	0.79	0.78	0.53	1.14
Champ-Durand	1.14	1.13	0.8	1.53
La Draga	0.68	0.66	0.47	0.96
Lerna2	0.84	0.84	0.65	1.07
La Fare1	1.07	1.06	0.77	1.47
Lanycsok-Egettmalom	0.89	0.87	0.63	1.23
Colle Santo Stefano	1.35	1.34	1.12	1.65
Dimini	0.79	0.78	0.6	1.02
Ecsegfalva 23	0.68	0.68	0.52	0.88
Helmer Meat Type A	0.78	0.76	0.49	1.16
Helmer Meat Type B	0.88	0.87	0.77	1.04
Helmer Milk Type A	0.43	0.41	0.2	0.77
Helmer Milk Type B, Meat Type A	1.02	1.01	0.71	1.42
Helmer Fleece, Milk Type B, Meat Type A	1.69	1.68	1.25	2.14
Payne Meat	0.98	0.99	0.95	0.99
Payne Milk	0.88	0.88	0.85	0.89
Payne Fleece	1.77	1.77	1.75	1.79
Redding Energy Max.	0.88	0.88	0.86	0.89
Redding Herd Security	0.81	0.82	0.79	0.82

	Milk Calories per Animal (kcal)			
Age-at-Death profile	**Mean.3**	**Median.3**	**Confl.3**	**Confll.3**
Eitzum	319.16	299.25	24.12	717.68
Cochstedt I	289.94	266.14	22.81	675.52
Cueva da la Dehesilla	185.64	156.75	-27.06	551.78
Cueva del Forcon	261.71	239.14	-6.13	644.2
Cochstedt II	361.76	348.29	68.4	725.15
Gatersleben II	335.57	322.13	47.04	697.22
Silourokambos I	282.02	263.71	33.99	631.12
Le Barmaz sur Collombey1	254.49	237.33	14.94	597.16
Pojejena Nucet IIA-IB	230.83	206.96	8.95	579.69
Miercurea Sibiului IIB-IIA	180.1	158	-23.93	504.4
Prodromos II	155.11	148.43	57.47	289.75
Trasano4	179.38	172.24	68.55	334.32
Champ-Durand	355.93	351	212.85	523.23
La Draga	125.9	119.33	42.01	248.42
Lerna2	194.19	190.09	122.34	289.04
La Fare1	291.05	282.4	159.94	468.97
Lanycsok-Egettmalom	228.2	220.57	116.29	381.18
Colle Santo Stefano	397.11	391.81	295.82	530.74
Dimini	180.91	177.02	101.12	283.83
Ecsegfalva 23	147.86	144.66	81.06	232.67
Helmer Meat Type A	180.41	171.8	60.06	348.9
Helmer Meat Type B	210.5	204.63	161.39	280.07
Helmer Milk Type A	85.5	76.97	-7.14	226.58
Helmer Milk Type B, Meat Type A	267.33	258.07	136.4	443.49
Helmer Fleece, Milk Type B, Meat Type A	567.7	564.6	377.6	772.1
Payne Meat	285.37	288.45	274.56	291.56
Payne Milk	300.56	302	291.81	305.54
Payne Fleece	647.92	647.46	641.29	656.52
Redding Energy Max.	226.68	226.66	219.49	230.9
Redding Herd Security	209	212.77	197.57	215.32

	MOW Calories per Animal (kcal)			
Age-at-Death profile	**Mean.4**	**Median.4**	**Confl.4**	**Confll.4**
Eitzum	37.38	38.34	21.4	48.5
Cochstedt I	38.86	39.77	24.78	48.12
Cueva da la Dehesilla	34.52	35.02	21.15	45.38
Cueva del Forcon	35.08	35.52	21.18	46.47
Cochstedt II	40.95	41.92	28.14	48.87
Gatersleben II	37.89	38.46	25.06	47.75
Silourokambos I	39.72	40.41	27.4	48.17
Le Barmaz sur Collombey1	37.55	37.81	26.9	46.24
Pojejena Nucet IIA-IB	38.94	39.48	28	46.71
Miercurea Sibiului IIB-IIA	34.46	34.56	24.55	43.6
Prodromos II	42.36	42.42	39.43	45.03
Trasano4	42.85	42.93	39.87	45.41
Champ-Durand	37.26	37.29	32.74	41.48
La Draga	43.34	43.44	40.27	45.86
Lerna2	39.5	39.56	35.09	43.5
La Fare1	44.92	45	41.95	47.33
Lanycsok-Egettmalom	43.21	43.28	40.35	45.62
Colle Santo Stefano	48.91	49	47.13	50.16
Dimini	41.52	41.53	39.28	43.66
Ecsegfalva 23	39.65	39.68	36.68	42.33
Helmer Meat Type A	41.4	41.46	37.92	44.49
Helmer Meat Type B	45.69	45.7	44.95	46.37
Helmer Milk Type A	27.19	27.17	21.86	32.68
Helmer Milk Type B, Meat Type A	43.25	43.38	39.07	46.67
Helmer Fleece, Milk Type B, Meat Type A	46.37	46.57	42.34	49.34
Payne Meat	38.79	38.87	38.64	38.87
Payne Milk	25.41	25.48	25.1	25.53
Payne Fleece	40.03	40.05	39.81	40.3
Redding Energy Max.	37.92	37.92	37.86	37.99
Redding Herd Security	35.44	35.42	35.21	35.65

	Total Fat Calories per Animal (kcal / kg)			
Age-at-Death profile	**Mean.5**	**Median.5**	**Confl.5**	**Confll.5**
Eitzum	15.43	14.5	1.46	34.25
Cochstedt I	14.08	12.96	1.48	32.24
Cueva da la Dehesilla	9.13	7.78	-0.95	26.44
Cueva del Forcon	12.7	11.65	0.03	30.74
Cochstedt II	17.47	16.83	3.62	34.58
Gatersleben II	16.2	15.57	2.55	33.26
Silourokambos I	13.71	12.87	2.01	30.16
Le Barmaz sur Collombey1	12.4	11.6	1.07	28.57
Pojejena Nucet IIA-IB	11.3	10.18	0.82	27.74
Miercurea Sibiului IIB-IIA	8.87	7.84	-0.79	24.16
Prodromos II	7.79	7.48	3.19	14.13
Trasano4	8.94	8.6	3.72	16.22
Champ-Durand	17.15	16.92	10.41	25.03
La Draga	6.43	6.13	2.48	12.19
Lerna2	9.59	9.41	6.18	14.06
La Fare1	14.2	13.79	8.04	22.56
Lanycsok-Egettmalom	11.23	10.88	5.97	18.42
Colle Santo Stefano	19.22	18.97	14.46	25.5
Dimini	8.99	8.81	5.23	13.83
Ecsegfalva 23	7.42	7.27	4.27	11.41
Helmer Meat Type A	8.97	8.56	3.29	16.88
Helmer Meat Type B	10.43	10.16	8.13	13.7
Helmer Milk Type A	4.34	3.94	-0.04	11
Helmer Milk Type B, Meat Type A	13.07	12.63	6.9	21.36
Helmer Fleece, Milk Type B, Meat Type A	27.2	27.05	18.26	36.81
Payne Meat	13.86	14.01	13.35	14.15
Payne Milk	14.41	14.48	13.99	14.64
Payne Fleece	30.88	30.86	30.57	31.29
Redding Energy Max.	11.1	11.1	10.76	11.29
Redding Herd Security	10.24	10.41	9.7	10.53

	Total Protein Calories per Animal (kcal / kg)			
Age-at-Death profile	**Mean.6**	**Median.6**	**Confl.6**	**Confll.6**
Eitzum	21.55	20.53	4.24	44.34
Cochstedt I	20.11	18.79	4.6	42
Cueva da la Dehesilla	13.93	12.42	1.28	34.92
Cueva del Forcon	18.15	16.95	2.45	40.06
Cochstedt II	24.27	23.57	7.47	44.73
Gatersleben II	22.5	21.82	5.68	43.13
Silourokambos I	19.77	18.84	5.38	39.48
Le Barmaz sur Collombey1	18.03	17.1	4.14	37.48
Pojejena Nucet IIA-IB	16.89	15.58	4.06	36.56
Miercurea Sibiului IIB-IIA	13.62	12.37	1.78	32.1
Prodromos II	13.12	12.77	7.58	20.66
Trasano4	14.5	14.11	8.27	23.1
Champ-Durand	23.54	23.28	15.41	32.97
La Draga	11.63	11.29	6.87	18.47
Lerna2	14.94	14.75	10.68	20.34
La Fare1	20.83	20.36	13.52	30.66
Lanycsok-Egettmalom	17.21	16.79	10.94	25.7
Colle Santo Stefano	27.07	26.79	21.45	34.41
Dimini	14.44	14.23	9.95	20.13
Ecsegfalva 23	12.43	12.25	8.64	17.19
Helmer Meat Type A	14.4	13.93	7.61	23.78
Helmer Meat Type B	16.51	16.2	13.79	20.34
Helmer Milk Type A	7.65	7.17	2.3	15.73
Helmer Milk Type B, Meat Type A	19.35	18.86	11.93	29.17
Helmer Fleece, Milk Type B, Meat Type A	36.12	35.97	25.48	47.49
Payne Meat	19.85	20.03	19.24	20.2
Payne Milk	19.22	19.31	18.71	19.49
Payne Fleece	39.82	39.8	39.43	40.3
Redding Energy Max.	16.55	16.55	16.16	16.78
Redding Herd Security	15.31	15.51	14.71	15.63

	Fodder consumed per Animal (kg)			
Age-at-Death profile	**Mean.7**	**Median.7**	**Confl.7**	**Confll.7**
Eitzum	763.21	743.33	254.62	1394.97
Cochstedt I	729.13	702.51	288.61	1299.48
Cueva da la Dehesilla	541.73	511.42	179.85	1067.03
Cueva del Forcon	658.99	631.67	211.04	1254.82
Cochstedt II	847.59	834.9	387.33	1380.4
Gatersleben II	788.5	775.55	316.62	1348.79
Silourokambos I	731.51	724.39	328.42	1196.63
Le Barmaz sur Collombey1	678.51	658.88	287.39	1184.73
Pojejena Nucet IIA-IB	651.38	624.11	293.65	1138.51
Miercurea Sibiului IIB-IIA	540.67	511.27	213.72	1016.48
Prodromos II	640.05	635.81	488.26	815.08
Trasano4	659.26	655.81	503.92	835.15
Champ-Durand	838.46	836.38	634.22	1047.23
La Draga	603.55	600.84	478.48	746.15
Lerna2	704.18	704.45	573.25	832.96
La Fare1	833.97	831.39	674.06	1015.53
Lanycsok-Egettmalom	725.43	721.71	581.6	890.02
Colle Santo Stefano	1089.75	1089.09	953.01	1227.56
Dimini	676.53	674.64	553.15	809.41
Ecsegfalva 23	614.35	612.52	505	735.3
Helmer Meat Type A	645.98	640.89	472.47	847.29
Helmer Meat Type B	758.19	757.84	706.52	810.64
Helmer Milk Type A	346.67	336.29	202.03	543.32
Helmer Milk Type B, Meat Type A	787.75	784.43	612.89	975.84
Helmer Fleece, Milk Type B, Meat Type A	1215.71	1218.92	967.93	1448.59
Payne Meat	803.87	810.62	790.84	810.62
Payne Milk	665.93	668.7	655.24	671.9
Payne Fleece	1348.66	1350	1328.11	1363.33
Redding Energy Max.	764.48	764.29	751.34	769.27
Redding Herd Security	703.9	705.17	693.16	711.16

	Calories per Fodder Consumed (kcal / kg)			
Age-at-Death profile	**Mean.8**	**Median.8**	**Confl.8**	**Confll.8**
Eitzum	0.44	0.45	0.18	0.65
Cochstedt I	0.42	0.43	0.17	0.65
Cueva da la Dehesilla	0.36	0.37	-0.01	0.64
Cueva del Forcon	0.41	0.43	0.09	0.64
Cochstedt II	0.46	0.46	0.24	0.65
Gatersleben II	0.45	0.46	0.22	0.65
Silourokambos I	0.42	0.42	0.19	0.65
Le Barmaz sur Collombey1	0.4	0.41	0.15	0.61
Pojejena Nucet IIA-IB	0.39	0.39	0.13	0.61
Miercurea Sibiului IIB-IIA	0.35	0.37	0.02	0.61
Prodromos II	0.3	0.3	0.2	0.44
Trasano4	0.33	0.32	0.21	0.48
Champ-Durand	0.47	0.46	0.37	0.59
La Draga	0.28	0.27	0.17	0.41
Lerna2	0.33	0.32	0.27	0.43
La Fare1	0.4	0.39	0.29	0.53
Lanycsok-Egettmalom	0.37	0.36	0.26	0.5
Colle Santo Stefano	0.41	0.4	0.36	0.5
Dimini	0.33	0.32	0.25	0.43
Ecsegfalva 23	0.3	0.3	0.23	0.39
Helmer Meat Type A	0.34	0.33	0.21	0.49
Helmer Meat Type B	0.34	0.33	0.29	0.41
Helmer Milk Type A	0.3	0.31	0.08	0.51
Helmer Milk Type B, Meat Type A	0.39	0.38	0.27	0.53
Helmer Fleece, Milk Type B, Meat Type A	0.5	0.49	0.41	0.62
Payne Meat	0.4	0.4	0.4	0.41
Payne Milk	0.49	0.49	0.48	0.5
Payne Fleece	0.51	0.51	0.51	0.52
Redding Energy Max.	0.35	0.35	0.34	0.35
Redding Herd Security	0.35	0.35	0.34	0.35

	Milk Calories per Fodder Consumed (kcal / kg)			
Age-at-Death profile	**Mean.9**	**Median.9**	**Confl.9**	**Confll.9**
Eitzum	0.39	0.4	0.08	0.61
Cochstedt I	0.37	0.38	0.07	0.6
Cueva da la Dehesilla	0.29	0.31	-0.14	0.59
Cueva del Forcon	0.35	0.38	-0.03	0.6
Cochstedt II	0.41	0.41	0.16	0.61
Gatersleben II	0.4	0.41	0.14	0.61
Silourokambos I	0.36	0.36	0.09	0.6
Le Barmaz sur Collombey1	0.34	0.36	0.05	0.57
Pojejena Nucet IIA-IB	0.32	0.33	0.03	0.57
Miercurea Sibiului IIB-IIA	0.28	0.3	-0.11	0.56
Prodromos II	0.24	0.23	0.12	0.38
Trasano4	0.27	0.26	0.13	0.42
Champ-Durand	0.42	0.41	0.32	0.54
La Draga	0.2	0.2	0.09	0.35
Lerna2	0.27	0.27	0.21	0.38
La Fare1	0.34	0.34	0.23	0.48
Lanycsok-Egettmalom	0.31	0.3	0.19	0.45
Colle Santo Stefano	0.36	0.36	0.31	0.46
Dimini	0.26	0.26	0.18	0.37
Ecsegfalva 23	0.24	0.24	0.16	0.33
Helmer Meat Type A	0.27	0.27	0.12	0.44
Helmer Meat Type B	0.28	0.27	0.23	0.35
Helmer Milk Type A	0.22	0.23	-0.03	0.45
Helmer Milk Type B, Meat Type A	0.33	0.33	0.21	0.48
Helmer Fleece, Milk Type B, Meat Type A	0.47	0.45	0.37	0.58
Payne Meat	0.35	0.36	0.35	0.36
Payne Milk	0.45	0.45	0.44	0.46
Payne Fleece	0.48	0.48	0.48	0.49
Redding Energy Max.	0.3	0.3	0.29	0.3
Redding Herd Security	0.3	0.3	0.29	0.3

	MOW Calories per Fodder Consumed (kcal / kg)			
Age-at-Death profile	**Mean.10**	**Median.10**	**Confl.10**	**Confll.10**
Eitzum	0.05	0.05	0.03	0.1
Cochstedt I	0.06	0.06	0.04	0.1
Cueva da la Dehesilla	0.07	0.07	0.04	0.13
Cueva del Forcon	0.06	0.06	0.03	0.11
Cochstedt II	0.05	0.05	0.03	0.08
Gatersleben II	0.05	0.05	0.03	0.09
Silourokambos I	0.06	0.06	0.04	0.09
Le Barmaz sur Collombey1	0.06	0.06	0.04	0.1
Pojejena Nucet IIA-IB	0.07	0.06	0.04	0.11
Miercurea Sibiului IIB-IIA	0.07	0.07	0.04	0.13
Prodromos II	0.07	0.07	0.05	0.08
Trasano4	0.07	0.07	0.05	0.08
Champ-Durand	0.04	0.04	0.04	0.05
La Draga	0.07	0.07	0.06	0.09
Lerna2	0.06	0.06	0.05	0.06
La Fare1	0.05	0.05	0.05	0.06
Lanycsok-Egettmalom	0.06	0.06	0.05	0.07
Colle Santo Stefano	0.05	0.04	0.04	0.05
Dimini	0.06	0.06	0.05	0.07
Ecsegfalva 23	0.06	0.06	0.06	0.08
Helmer Meat Type A	0.07	0.06	0.05	0.08
Helmer Meat Type B	0.06	0.06	0.06	0.06
Helmer Milk Type A	0.08	0.08	0.06	0.12
Helmer Milk Type B, Meat Type A	0.06	0.06	0.05	0.07
Helmer Fleece, Milk Type B, Meat Type A	0.04	0.04	0.03	0.05
Payne Meat	0.05	0.05	0.05	0.05
Payne Milk	0.04	0.04	0.04	0.04
Payne Fleece	0.03	0.03	0.03	0.03
Redding Energy Max.	0.05	0.05	0.05	0.05
Redding Herd Security	0.05	0.05	0.05	0.05

Bibliography

Aiello, L. C. and Wheeler, P. (1995) 'The expensive-tissue hypothesis: the brain and the digestive system in human and primate evolution', *Current anthropology*. University of Chicago Press, 36(2), pp. 199–221.

Al-Aifari, R., Daubechies, I. and Lipman, Y. (2013) 'Continuous Procrustes distance between two surfaces', *Communications on Pure and Applied Mathematics*. Wiley Online Library, 66(6), pp. 934–964.

Albarella, U. (1999) 'The animal economy after the eruption of Avellino pumice: the case of La Starza (Avellino, Southern Italy)'.

Albarella, U. *et al.* (2009) *Norwich Castle: Excavations and historical surveys 1987-98. Part III: a Zooarchaeological Study*. Norfolk.

Albarella, U. and Davis, S. J. M. (1996) 'Mammals and birds from Launceston Castle, Cornwall: decline in status and the rise of agriculture', *Circaea*, 12(1).

Allaby, R. G., Fuller, D. Q. and Brown, T. A. (2008) 'The genetic expectations of a protracted model for the origins of domesticated crops', *Proceedings of the National Academy of Sciences*. National Acad Sciences, 105(37), pp. 13982–13986.

Van Andel, T. H. and Runnels, C. N. (1988) 'An essay on the 'emergence of civilization'in the Aegean world', *Antiquity*. Cambridge University Press, 62(235), pp. 234–247.

Van Andel, T. H. and Runnels, C. N. (1995) 'The earliest farmers in Europe', *Antiquity*. Cambridge University Press, 69(264), pp. 481–500.

Van Andel, T. H. and Shackleton, J. C. (1982) 'Late Paleolithic and Mesolithic coastlines of Greece and the Aegean', *Journal of Field Archaeology*, 9(4), pp. 445–454.

Atici, A. L. (2007) *Before the revolution: A comprehensive zooarchaeological*

approach to terminal pleistocene forager adaptations in the Western Taurus Mountains, Turkey. Harvard University.

Audoin-Rouzeau, F. (1991) *La taille du boeuf domestique en Europe de l'Antiquité aux temps modernes*. APDCA.

Austerlitz, F. *et al.* (1997) 'Evolution of coalescence times, genetic diversity and structure during colonization', *Theoretical Population Biology*. Elsevier, 51(2), pp. 148–164.

Balaresque, P. *et al.* (2010) 'A predominantly neolithic origin for European paternal lineages', *PLoS Biol*, 8(1), p. e1000285.

Baltensperger, D. D. (2002) 'Progress with proso, pearl and other millets', *Trends in new crops and new uses*. ASHS Press Alexandria, VA, pp. 100–103.

Bar-Yosef, O. and Meadow, R. H. (1995) 'The origins of agriculture in the Near East', *Last hunters, first farmers: New perspectives on the prehistoric transition to agriculture*. School of American Research Press Santa Fe, pp. 39–94.

Barker, G. *et al.* (1990) 'FROM HUNTING T0 HERDING IN THE VAL PENNAVAIRA (Liguria-northern Italy)'.

Barton, L. *et al.* (2009) 'Agricultural origins and the isotopic identity of domestication in northern China', *Proceedings of the National Academy of Sciences*. National Acad Sciences, 106(14), pp. 5523–5528.

Bartosiewicz, L. (1999) 'The role of sheep versus goat in meat consumption at archaeological sites', *Transhumant Pastoralism in Southern Europe. Archaeolingua, Budapest*, pp. 47–60.

Bartosiewicz, L. and Gál, E. (2007) 'Sample size and taxonomic richness in mammalian and avian bone assemblages from archaeological sites', *Archeometriai Műhely*, 1, pp. 37–44.

Bayes, T., Price, R. and Canton, J. (1763) 'An essay towards solving a problem

in the doctrine of chances'.

Beaujard, P. (2011) 'The first migrants to Madagascar and their introduction of plants: linguistic and ethnological evidence', *Azania: Archaeological Research in Africa*. Taylor & Francis, 46(2), pp. 169–189.

Beaumont, M. A., Zhang, W. and Balding, D. J. (2002) 'Approximate Bayesian computation in population genetics', *Genetics*. Genetics Soc America, 162(4), pp. 2025–2035.

Bellwood, P. (2004) 'The origins and dispersals of agricultural communities in Southeast Asia'.

Bellwood, P. S. (2005) 'First farmers: the origins of agricultural societies'. Blackwell Oxford.

Van den Bergh, G. D., de Vos, J. and Sondaar, P. Y. (2001) 'The Late Quaternary palaeogeography of mammal evolution in the Indonesian Archipelago', *Palaeogeography, Palaeoclimatology, Palaeoecology*. Elsevier, 171(3–4), pp. 385–408.

Bergner, M., Horejs, B. and Pernicka, E. (2009) 'Zur Herkunft der Obsidianartefakte vom Çukuriçi Höyük', *Studia Troica*, 18, pp. 249–272.

Bertorelle, G., Benazzo, A. and Mona, S. (2010) 'ABC as a flexible framework to estimate demography over space and time: some cons, many pros', *Molecular ecology*. Wiley Online Library, 19(13), pp. 2609–2625.

Bevan, A. *et al.* (2017) 'Holocene fluctuations in human population demonstrate repeated links to food production and climate', *Proceedings of the National Academy of Sciences*. National Acad Sciences, 114(49), pp. E10524–E10531.

Bevan, A. H. (2015) 'The data deluge', *Antiquity: a quarterly review of archaeology*, 89(345), pp. 1473–1484.

Bevan, A. and Lake, M. (2013) *Computational approaches to archaeological*

spaces. Left Coast Press.

Bickle, P. and Whittle, A. (2013) *The first farmers of central Europe: diversity in LBK lifeways*. Oxbow Books.

Binford, L. R. (1968) *New perspectives in archeology*. Aldine Pub. Co.

Blaise, E. (2006) 'Référentiel actuel de brebis «Préalpes du Sud»(Digne, Alpes-de-Haute-Provence, France): pratiques d'élevage et âges dentaires', *Anthropozoologica*, 41(2), pp. 191–214.

Blaise, E. (2009) *Economie animale et gestion des troupeaux au Néolithique final en Provence: approche archéozoologique et contribution des analyses isotopiques de l'émail dentaire (version non corrigée)*. Université de Provence-Aix-Marseille I.

Blench, R. (1996) 'The ethnographic evidence for long-distance contacts between Oceania and East Africa', *The Indian Ocean in Antiquity*. Kegan Paul International London and New York, pp. 417–438.

Blench, R. (2009) 'Bananas and plantains in Africa: re-interpreting the linguistic evidence'.

Bocquet-Appel, J.-P. (2011) 'When the world's population took off: the springboard of the Neolithic Demographic Transition', *Science*. American Association for the Advancement of Science, 333(6042), pp. 560–561.

Boessneck, J. (1962) 'Die neuen Tierknochenfunde aus dem keltischen Oppidum bei Manching im Vergleich mit den früheren', *Zeitschrift für Tierzüchtung und Züchtungsbiologie*. Wiley Online Library, 77(1-4), pp. 47–61.

Boessneck, J. and Von den Driesch, A. (1979) *Die Tierknochenfunde aus der neolithischen Siedlung auf dem Fikirtepe bei Kadiköy am Marmarameer*. Universität München, Institut für Palaeoanatomie, Domestikationsforschung ….

Bokonyi, S. (1974) 'History of domestic mammals in Central and Eastern Europe'. Akadémiai Kiadó.

Bollongino, R. *et al.* (2012) 'Modern taurine cattle descended from small number of Near-Eastern founders', *Molecular biology and evolution*, p. mss092.

Bosse, M. *et al.* (2014) 'Untangling the hybrid nature of modern pig genomes: a mosaic derived from biogeographically distinct and highly divergent Sus scrofa populations', *Molecular ecology*. Wiley Online Library, 23(16), pp. 4089–4102.

Bourke, R. M. (2009) 'History of agriculture in Papua New Guinea', *Food and Agriculture in Papua New Guinea*. JSTOR, pp. 10–26.

Bowles, S. and Choi, J.-K. (2013) 'Coevolution of farming and private property during the early Holocene', *Proceedings of the National Academy of Sciences*. National Acad Sciences, 110(22), pp. 8830–8835.

Box, G. E. P. (1976) 'Science and statistics', *Journal of the American Statistical Association*, 71(356), pp. 791–799.

Boyazoglu, J. and Morand-Fehr, P. (2001) 'Mediterranean dairy sheep and goat products and their quality: A critical review', *Small Ruminant Research*, 40(1), pp. 1–11.

Boyd, R., Richerson, P. J. and Henrich, J. (2011) 'Rapid cultural adaptation can facilitate the evolution of large-scale cooperation', *Behavioral ecology and sociobiology*. Springer, 65(3), pp. 431–444.

Braguier, S. (2000) *Economie alimentaire et gestion des troupeaux au Néolithique récent/final dans le centre-ouest de la France*. ANRT, Université de Lille III.

Braidwood, L. S. (1983) *Prehistoric archeology along the Zagros Flanks*. Oriental Inst Pubns Sales.

Bramanti, B. *et al.* (2009) 'Genetic discontinuity between local hunter-gatherers and central Europe's first farmers', *science*. American Association for the Advancement of Science, 326(5949), pp. 137–140.

Britsch, C. and Horejs, B. (2014) ‘The Role of Textile Production and Fishing in the EBA Metallurgical Centre of Çukuriçi Höyük (Turkey)’, *Ägypten und Levante*. Verlag Der Österreichischen Akademie Der Wissenschaften, 24, pp. 229–242.

Bronson, B. (1977) ‘The earliest farming: Demography as cause and consequence’, *Origins of agriculture*. Mouton The Hague, pp. 23–48.

Broushaki, F. *et al.* (2016) ‘Early Neolithic genomes from the eastern Fertile Crescent’, *Science*. American Association for the Advancement of Science, 353(6298), pp. 499–503.

Buck, C. E. and Juarez, M. (2017) ‘Bayesian radiocarbon modelling for beginners’, *arXiv preprint arXiv:1704.07141*.

Buckley, M. *et al.* (2010) ‘Distinguishing between archaeological sheep and goat bones using a single collagen peptide’, *Journal of Archaeological Science*. Elsevier, 37(1), pp. 13–20.

Burgarella, C. *et al.* (2018) ‘A western Sahara centre of domestication inferred from pearl millet genomes’, *Nature ecology & evolution*. Nature Publishing Group, 2(9), p. 1377.

Burger, J. and Thomas, M. G. (2011) ‘The palaeopopulationgenetics of humans, cattle and dairying in Neolithic Europe’, *Human bioarchaeology of the transition to agriculture*. Wiley Online Library, pp. 369–384.

Burkill, I. H. (1966) ‘A dictionary of the economic products of the Malay Peninsula’, *A Dictionary of the Economic Products of the Malay Peninsula.*, 2(2nd edition).

Çakırlar, C. (2012) ‘The evolution of animal husbandry in Neolithic central-west Anatolia: the zooarchaeological record from Ulucak Höyük (c. 7040–5660 cal. BC, Izmir, Turkey)’, *Anatolian Studies*. Cambridge University Press, 62, pp. 1–33.

De Candolle, A. (1883) *Origine des plantes cultivées*. Germer-Baillière.

Carrero-Pazos, M., Bevan, A. and Lake, M. W. (2019) 'The spatial structure of Galician megalithic landscapes (NW iberia): A case study from the Monte Penide region', *Journal of Archaeological Science*. Elsevier, 108, p. 104968.

Carter, R. J. (1997) 'Age estimation of the roe deer (Capreolus capreolus) mandibles from the Mesolithic site of Star Carr, Yorkshire, based on radiographs of mandibular tooth development', *Journal of Zoology*. Wiley Online Library, 241(3), pp. 495–502.

Caussinus, H., Courgeau, D. and Mandelbaum, J. (2010) 'Estimating age without measuring it: A new method in paleodemography', *Population*. INED, 65(1), pp. 117–144.

Cavalli-Sforza, L. L., Barrai, I. and Edwards, A. W. F. (1964) 'Analysis of human evolution under random genetic drift', in *Cold Spring Harbor symposia on quantitative biology*. Cold Spring Harbor Laboratory Press, pp. 9–20.

Chaix, L. (1976) 'La faune néolithique du Valais (Suisse): ses caractères et ses relations avec les faunes néolithiques des régions proches'.

Charlesworth, B. and Charlesworth, D. (2017) 'Population genetics from 1966 to 2016', *Heredity*. Nature Publishing Group, 118(1), p. 2.

Childe, V. G. (1936) 'Man makes himself London', *Watts and Company*.

Childe, V. G. (1950) 'The urban revolution', *Town Planning Review*. Liverpool University Press, 21(1), p. 3.

Çilingiroğlu, Ç. (2005) 'The concept of "Neolithic package": considering its meaning and applicability', *Documenta Praehistorica*, 32, pp. 1–13.

Clark, P. U. *et al.* (2009) 'The last glacial maximum', *science*. American Association for the Advancement of Science, 325(5941), pp. 710–714.

Clutton-Brock, J. (1981a) 'Contributions to discussion', *Farming practice in British prehistory*. Edinburgh University Press: Edinburgh, pp. 218–220.

Clutton-Brock, J. (1981b) ‘Domesticated animals from early times.’, *Domesticated animals from early times.* British Museum (Natural History) and William Heinemann Ltd.

Colledge, S. and Conolly, J. (2007) *The origins and spread of domestic plants in Southwest Asia and Europe*. Left Coast Press Walnut Creek.

Cordain, L. *et al.* (2005) ‘Origins and evolution of the Western diet: health implications for the 21st century’, *The American journal of clinical nutrition*. Oxford University Press, 81(2), pp. 341–354.

Cramp, L. J. E., Jones, J., *et al.* (2014) ‘Immediate replacement of fishing with dairying by the earliest farmers of the northeast Atlantic archipelagos’, *Proceedings of the Royal Society B: Biological Sciences*. The Royal Society, 281(1780), p. 20132372.

Cramp, L. J. E., Evershed, R. P., *et al.* (2014) ‘Neolithic dairy farming at the extreme of agriculture in northern Europe’, *Proceedings of the Royal Society B: Biological Sciences*. The Royal Society, 281(1791), p. 20140819.

Crawford, G. W. (2006) ‘East Asian plant domestication’, *archaeology of asia*. Wiley Online Library, pp. 77–95.

Currat, M. *et al.* (2019) ‘SPLATCHE3: simulation of serial genetic data under spatially explicit evolutionary scenarios including long-distance dispersal’, *Bioinformatics*. Oxford University Press, 35(21), pp. 4480–4483.

Curry, A. (2013) ‘Archaeology: the milk revolution’, *Nature News*, 500(7460), p. 20.

Dahl, G. and Hjort, A. (1976) *Having herds: pastoral herd growth and household economy*. Department of Social Anthropology, University of Stockholm.

Darwin, C. (1859) *The Origin of Species; And, the Descent of Man*. Modern library.

Denham, T., Haberle, S. and Lentfer, C. (2004) 'New evidence and revised interpretations of early agriculture in Highland New Guinea', *Antiquity*. Cambridge University Press, 78(302), pp. 839–857.

Ducos, P. (1968) 'L'Origine des animaux domestiques en Palestine, Publications de l'Institute de Prehistoire de l'Université de Bordeaux', *Mémoire 6Delmas, Bordeaux*.

Dunne, J. *et al.* (2012) 'First dairying in green Saharan Africa in the fifth millennium BC', *Nature*. Nature Publishing Group, 486(7403), p. 390.

Düring, B. S. (2010) *The prehistory of Asia Minor: from complex hunter-gatherers to early urban societies*. Cambridge University Press.

Dussert, Y. *et al.* (2013) 'Polymorphism pattern at a miniature inverted-repeat transposable element locus downstream of the domestication gene Teosinte-branched1 in wild and domesticated pearl millet', *Molecular ecology*, 22(2), pp. 327–340.

Dussert, Y., Snirc, A. and Robert, T. (2015) 'Inference of domestication history and differentiation between early-and late-flowering varieties in pearl millet', *Molecular ecology*, 24(7), pp. 1387–1402.

Edmonds, C. A., Lillie, A. S. and Cavalli-Sforza, L. L. (2004) 'Mutations arising in the wave front of an expanding population', *Proceedings of the National Academy of Sciences*. National Acad Sciences, 101(4), pp. 975–979.

Edwards, C. J. *et al.* (2007) 'Mitochondrial DNA analysis shows a Near Eastern Neolithic origin for domestic cattle and no indication of domestication of European aurochs', *Proceedings of the Royal Society B: Biological Sciences*. The Royal Society London, 274(1616), pp. 1377–1385.

Enattah, N. S. *et al.* (2002) 'Identification of a variant associated with adult-type hypolactasia', *Nature genetics*. Nature Publishing Group, 30(2), p. 233.

ETHIOPIA, F. D. R. O. F. and AGENCY, C. S. (2011) *AGRICULTURAL SAMPLE SURVEY 2010/11 [2003 E.C.], VOLUME IIREPORT ON LIVESTOCK AND LIVESTOCK CHARACTERISTICS (PRIVATE PEASANT HOLDINGS)*. ADDIS ABABA: FEDERAL DEMOCRATIC REPUBLIC OF ETHIOPIACENTRAL STATISTICAL AGENCY.

Evershed, R. P. *et al.* (2008) 'Earliest date for milk use in the Near East and southeastern Europe linked to cattle herding', *Nature*. Nature Publishing Group, 455(7212), p. 528.

Excoffier, L., Foll, M. and Petit, R. J. (2009) 'Genetic consequences of range expansions', *Annual Review of Ecology, Evolution, and Systematics*. Annual Reviews, 40, pp. 481–501.

Fairnell, E. H. and E. (2014) 'Animal Bones and Archaeology Guidlines for Best Practice'.

Flannery, K. V (1969) 'Origins and ecological effects of early domestication in Iran and the Near East.', *Origins and ecological effects of early domestication in Iran and the Near East.* Gerald Duckworth & Co., London.

Food and Organization, A. (2003) *World agriculture: towards 2015/2030: an FAO perspective*. FAO.

François, O. *et al.* (2010) 'Principal component analysis under population genetic models of range expansion and admixture', *Molecular biology and evolution*. Oxford University Press, 27(6), pp. 1257–1268.

Frantz, L. A. F. *et al.* (2018) 'Synchronous diversification of Sulawesi's iconic artiodactyls driven by recent geological events', *Proceedings of the Royal Society B: Biological Sciences*. The Royal Society, 285(1876), p. 20172566.

Fuller, D. Q. (2003) 'African crops in prehistoric South Asia: a critical review'.

Fuller, D. and Rowlands, M. (2011) 'Ingestion and food technologies: maintaining

differences over the long-term in West, South and East Asia', in. Oxbow Books Ltd.

Furuse, Y., Suzuki, A. and Oshitani, H. (2010) 'Origin of measles virus: divergence from rinderpest virus between the 11 th and 12 th centuries', *Virology journal*. BioMed Central, 7(1), p. 52.

Gallagher, E. M., Shennan, S. J. and Thomas, M. G. (2015) 'Transition to farming more likely for small, conservative groups with property rights, but increased productivity is not essential', *Proceedings of the National Academy of Sciences*. National Acad Sciences, 112(46), pp. 14218–14223.

Gallagher, E., Shennan, S. and Thomas, M. G. (2019) 'Food Income and the evolution of Forager Mobility', *Scientific reports*. Nature Publishing Group, 9(1), p. 5438.

Gautier, A. (1987) 'Prehistoric men and cattle in North Africa: A dearth of data and a surfeit of models', *Prehistory of Arid North Africa, Southern Methodist University Press, Dallas*, pp. 163–187.

Gejvall, Nils-Gustaf *et al.* (1969) *Lerna: A Preclassical Site in the Argolid: Results of Excavations Conducted by the American School of Classical Studies at Athens. The Fauna*. American School of Classical Studies at Athens.

Gelman, A. and Rubin, D. B. (1992) 'Inference from iterative simulation using multiple sequences', *Statistical science*, 7(4), pp. 457–472.

Gerbault, P. *et al.* (2012) 'Domestication and migrations: Using mitochondrial DNA to infer domestication processes of goats and horses', *Population Dynamics in Pre-and Early History New Approaches by Stable Isotopes and Genetics*. De Gruyter, pp. 17–30.

Gerbault, P. *et al.* (2014) 'Storytelling and story testing in domestication', *Proceedings of the National Academy of Sciences*. National Acad Sciences, 111(17), pp. 6159–6164.

Gerbault, P. *et al.* (2016) 'Statistically robust representation and comparison of mortality profiles in archaeozoology', *Journal of Archaeological Science*, 71, pp. 24–32.

Gerling, C. *et al.* (2017) 'High-resolution isotopic evidence of specialised cattle herding in the European Neolithic', *PloS one*. Public Library of Science, 12(7), p. e0180164.

Gillis, R. (2012) *Osteological and isotopic contributions to the study of dairy husbandry during the European Neolithic*. Paris, Muséum national d'histoire naturelle.

Gillis, R. *et al.* (2013) 'Sophisticated cattle dairy husbandry at Borduşani-Popină (Romania, fifth millennium BC): the evidence from complementary analysis of mortality profiles and stable isotopes', *World Archaeology*. Taylor & Francis, 45(3), pp. 447–472.

Gillis, R. *et al.* (2016) 'Neonatal mortality, young calf slaughter and milk production during the Early Neolithic of north western Mediterranean', *International Journal of Osteoarchaeology*. Wiley Online Library, 26(2), pp. 303–313.

Gillis, R., Chaix, L. and Vigne, J.-D. (2011) 'An assessment of morphological criteria for discriminating sheep and goat mandibles on a large prehistoric archaeological assemblage (Kerma, Sudan)', *Journal of Archaeological Science*, 38(9), pp. 2324–2339.

Gillis, R. E. *et al.* (2017) 'The evolution of dual meat and milk cattle husbandry in Linearbandkeramik societies', *Proc. R. Soc. B*. The Royal Society, 284(1860), p. 20170905.

Goldstein, D. B. *et al.* (1995) 'An evaluation of genetic distances for use with microsatellite loci', *Genetics*, 139(1), pp. 463–471.

Greenfield, H. J. and Fowler, K. D. (2005) *The secondary products revolution in Macedonia: the zooarchaeological remains from Megalo Nisi Galanis, a late neolithic-*

early bronze age site in Greek Macedonia. British Archaeological Reports.

Groves, C. P. (1984) 'Of mice and men and pigs in the Indo-Australian Archipelago', *Canberra Anthropology*. Taylor & Francis, 7(1–2), pp. 1–19.

Haak, W. *et al.* (2010) 'Ancient DNA from European early neolithic farmers reveals their near eastern affinities', *PLoS Biol*, 8(11), p. e1000536.

Haenlein, G. F. W. (2007) 'About the evolution of goat and sheep milk production', *Small ruminant research*. Elsevier, 68(1–2), pp. 3–6.

Haenlein, G. F. W. and Wendorff, W. L. (2006) 'Sheep milk', *Handbook of milk of non-bovine mammals*. Wiley Online Library, pp. 137–194.

Halstead, P. (1998) 'Mortality models and milking: problems of uniformitarianism, optimality and equifinality reconsidered', *Anthropozoologica*, 27(1998), pp. 3–20.

Halstead, P., Collins, P. and Isaakidou, V. (2002) 'Sorting the sheep from the goats: morphological distinctions between the mandibles and mandibular teeth of AdultOvis and Capra', *Journal of Archaeological Science*. Elsevier, 29(5), pp. 545–553.

Halstead, P. and Jones, G. (1980) 'Early Neolithic economy in Thessaly: some evidence from excavations at Prodromos', *Anthropologika*, 1, pp. 93–117.

Hanotte, O. *et al.* (2002) 'African pastoralism: genetic imprints of origins and migrations', *Science*. American Association for the Advancement of Science, 296(5566), pp. 336–339.

Hardy, K. *et al.* (2015) 'The importance of dietary carbohydrate in human evolution', *The Quarterly review of biology*. The University of Chicago Press, 90(3), pp. 251–268.

Harlan, J. R. (1971) 'Agricultural origins: centers and noncenters', *Science*. American Association for the Advancement of Science, 174(4008), pp. 468–474.

Harlan, J. R. (2011) *Origins of African plant domestication*. Walter de Gruyter.

Hassan, F. A. (1986) 'Desert environment and origins of agriculture in Egypt', *Norwegian Archaeological Review*. Taylor & Francis, 19(2), pp. 63–76.

Hassan, F. A. (1988) 'The predynastic of Egypt', *Journal of World Prehistory*. Springer, 2(2), pp. 135–185.

Hejcman, M. *et al.* (2013) 'Origin and history of grasslands in C entral E urope–a review', *Grass and Forage Science*. Wiley Online Library, 68(3), pp. 345–363.

Hejcmanová, P., Stejskalová, M. and Hejcman, M. (2014) 'Forage quality of leaf-fodder from the main broad-leaved woody species and its possible consequences for the Holocene development of forest vegetation in Central Europe', *Vegetation History and Archaeobotany*. Springer, 23(5), pp. 607–613.

Helmer, D. (1992) 'La domestication des animaux par les hommes préhistoriques, coll. Préhistoire, Ed'. Masson, Paris, Milan, Barcelone, Bonn.

Helmer, D. *et al.* (2005) 'L'élevage des caprinés néolithiques dans le sud-est de la France: saisonnalité des abattages, relations entre grottes-bergeries et sites de plein air', *Anthropozoologica*, 40(1), pp. 167–189.

Helmer, D., Gourichon, L. and Vila, E. (2007) 'The development of the exploitation of products from Capra and Ovis (meat, milk and fleece) from the PPNB to the Early Bronze in the northern Near East (8700 to 2000 BC cal.)', *Anthropozoologica*, 42(2), pp. 41–69.

Helmer, D. and Vigne, J. D. (2004) 'La gestion des cheptels de caprinés au Néolithique dans le midi de la France', in *Approches fonctionnelles en Préhistoire (Actes XXVe Congres Préhistorique de France Nanterre, 24–26 novembre 2000), Paris: Société Préhistorique Française Édition*, pp. 397–407.

Henry, D. O., Leroi-Gourhan, A. and Davis, S. (1981) 'The excavation of Hayonim Terrace: An examination of terminal Pleistocene climatic and adaptive changes',

Journal of Archaeological Science. Elsevier, 8(1), pp. 33–58.

Hesse, B. (1982) 'Slaughter patterns and domestication: the beginnings of pastoralism in western Iran', *Man*, pp. 403–417.

Heun, M. *et al.* (1997) 'Site of einkorn wheat domestication identified by DNA fingerprinting', *Science*. American Association for the Advancement of Science, 278(5341), pp. 1312–1314.

Higham, C. F. W. (1968) 'Stock rearing as a cultural factor in prehistoric Europe', in *Proceedings of the Prehistoric Society*. Cambridge University Press, pp. 84–106.

Hillman, G. *et al.* (2001) 'New evidence of Lateglacial cereal cultivation at Abu Hureyra on the Euphrates', *The Holocene*. Sage Publications Sage CA: Thousand Oaks, CA, 11(4), pp. 383–393.

Hodder, I. (2016) *Studies in Human-thing Entanglement*. Ian Hodder.

Hodos, T. (2016) '1: Globalization: some basics. An introduction to The Routledge Handbook of Archaeology and Globalization', in *The Routledge Handbook of Archaeology and Globalization*. Routledge, pp. 27–35.

Holden, C. and Mace, R. (2009) 'Phylogenetic analysis of the evolution of lactose digestion in adults', *Human biology*. BioOne, 81(5/6), pp. 597–620.

Horejs, B. *et al.* (2011) 'Aktivitäten und Subsistenz in den Siedlungen des Çukuriçi Höyük. Der Forschungsstand nach den Ausgrabungen 2006–2009', *Praehistorische Zeitschrift*. Walter de Gruyter GmbH & Co. KG, 86(1), pp. 31–66.

Horejs, B. (2014) 'Proto-Urbanisation without Urban Centres? A Model of Transformation for the Izmir Region in the 4th Millennium BC'.

Horejs, B. *et al.* (2015) 'The Aegean in the Early 7th Millennium BC: Maritime Networks and Colonization', *Journal of World Prehistory*, 28(4), pp. 289–330.

Horejs, B. (2016) 'Aspects of Connectivity on the centre of the Anatolian Aegean

coast in the 7th millennium BC', *Of Odysseys and oddities: Scales and modes of interaction between prehistoric Aegean societies and their neighbours. Sheffield Studies in Aegean Archaeology*, 10.

Horejs, B. and Schwall, C. (2015) *New Light on a Nebulous Period – Western Anatolia in the 4th Millennium BC: Architecture and Settlement Structures as Cultural Patterns?*, *Neolithic and Copper Age between the Carpathians and the Aegean Sea. Chronologies and Technologies from the 6th to the 4thMillennium BCE*. Edited by S. Hansen, P. Raczky, and A. Anders. Bonn.

Horejs, B. and Weninger, B. (2016) 'Early Troy and its significance for the Early Bronze Age in Western Anatolia', p. 133.

Huang, Z. (1994) 'On the origin of rice agriculture in southern China and its propagation in East Asia', *Chinese Geographical Science*. Springer, 4(4), pp. 289–294.

Hudson, R. R. (1983) 'Properties of a neutral allele model with intragenic recombination', *Theoretical population biology*. Elsevier, 23(2), pp. 183–201.

Hunt, H. V *et al.* (2008) 'Millets across Eurasia: chronology and context of early records of the genera Panicum and Setaria from archaeological sites in the Old World', *Vegetation history and archaeobotany*, 17(1), pp. 5–18.

Hunt, H. V *et al.* (2011) 'Genetic diversity and phylogeography of broomcorn millet (Panicum miliaceum L.) across Eurasia', *Molecular ecology*. Wiley Online Library, 20(22), pp. 4756–4771.

Hunt, H. V *et al.* (2018) 'Genetic evidence for a western Chinese origin of broomcorn millet (Panicum miliaceum)', *The Holocene*. SAGE Publications Sage UK: London, England, 28(12), pp. 1968–1978.

Ingold, T. (1980) *Hunters, pastoralists and ranchers: reindeer economies and their transformations*. Cambridge University Press Cambridge.

Itan, Y. *et al.* (2009) 'The origins of lactase persistence in Europe', *PLoS computational biology*. Public Library of Science, 5(8), p. e1000491.

Ito, M. *et al.* (2017) 'Food preparation behaviour of babirusa (Babyrousa celebensis)'. European Association of Zoos and Aquaria.

Jobling, M., Hurles, M. and Tyler-Smith, C. (2013) *Human evolutionary genetics: origins, peoples & disease*. Garland Science.

Jones, A. M. (1971) *Africa and Indonesia: the evidence of the xylophone and other musical and cultural factors*. Brill Archive.

Jones, G. G. and Sadler, P. (2012) 'Age at death in cattle: methods, older cattle and known-age reference material', *Environmental Archaeology*. Taylor & Francis, 17(1), pp. 11–28.

Jones, M. (2004) *Between fertile crescents: minor grain crops and agricultural origins*. na.

Jones, M. *et al.* (2011) 'Food globalization in prehistory', *World Archaeology*. Taylor & Francis, 43(4), pp. 665–675.

Khoury, C. K. *et al.* (2016) 'Origins of food crops connect countries worldwide', *Proceedings of the Royal Society B: Biological Sciences*. The Royal Society, 283(1832), p. 20160792.

Kingman, J. F. C. (1982) 'On the genealogy of large populations. Stoch', in *Proc. Appl*, pp. 235–248.

Kitchen, J. L. and Allaby, R. G. (2012) 'The limits of mean-field heterozygosity estimates under spatial extension in simulated plant populations', *PloS one*. Public Library of Science, 7(8), p. e43254.

Klein, R. G. *et al.* (1981) 'The use of dental crown heights for constructing age profiles of red deer and similar species in archaeological samples', *Journal of Archaeological Science*. Elsevier, 8(1), pp. 1–31.

Klopfstein, S., Currat, M. and Excoffier, L. (2005) 'The fate of mutations surfing on the wave of a range expansion', *Molecular biology and evolution*. Oxford University Press, 23(3), pp. 482–490.

Kristiansen, K. (2014) 'Towards a new paradigm', *The third science revolution and its possible consequences in archaeology. Current Swedish Archaeology*, 22, pp. 11–34.

Lazaridis, I. *et al.* (2016) 'Genomic insights into the origin of farming in the ancient Near East', *Nature*. Nature Publishing Group, 536(7617), p. 419.

Lebot, V. (2009) *Tropical root and tuber crops: cassava, sweet potato, yams and aroids*. Cabi.

Lebot, V. and Aradhya, K. M. (1991) 'Isozyme variation in taro (Colocasia esculenta (L.) Schott) from Asia and Oceania', *Euphytica*. Springer, 56(1), pp. 55–66.

Lee-Thorp, J. A., van der Merwe, N. J. and Brain, C. K. (1994) 'Diet of Australopithecus robustus at Swartkrans from stable carbon isotopic analysis', *Journal of Human Evolution*. Elsevier, 27(4), pp. 361–372.

Lee-Thorp, J. A., Sealy, J. C. and Van Der Merwe, N. J. (1989) 'Stable carbon isotope ratio differences between bone collagen and bone apatite, and their relationship to diet', *Journal of archaeological science*. Elsevier, 16(6), pp. 585–599.

Lee, G.-A. *et al.* (2007) 'Plants and people from the Early Neolithic to Shang periods in North China', *Proceedings of the National Academy of Sciences*. National Acad Sciences, 104(3), pp. 1087–1092.

Legge, A. (1981) 'Grimes Graves; the agricultural economy'', *Mercer, RJ, The Excavation of a Flint Mine Shaft at Grimes Graves, Norfolk, England. Society of Antiquaries, London*.

Legge, A. J. (1981) 'Aspects of cattle husbandry', *Farming practice in British prehistory*, pp. 169–181.

Lichardus, J. and Lichardus-Itten, M. (1985) 'Diffusion de la civilization néolithique en Europe et évolution historico-culturelle jusqu'à la fin du Néolithique', *J. Lichardus, M. Lichardus-Itten, G. Bailloud and J. Cauvin, La protohistoire de l'Europe. Le Néolithique et le Chalcolithique entre la Méditerranée et la Mer Baltique. Presses Universitaires de France, Paris*, pp. 207–515.

Lightfoot, E., Liu, X. and Jones, M. K. (2013) 'Why move starchy cereals? A review of the isotopic evidence for prehistoric millet consumption across Eurasia', *World Archaeology*. Taylor & Francis, 45(4), pp. 574–623.

Lipson, M. *et al.* (2014) 'Reconstructing Austronesian population history in island Southeast Asia', *Nature communications*. Nature Publishing Group, 5, p. 4689.

Lipson, M. *et al.* (2018) 'Population turnover in remote Oceania shortly after initial settlement', *Current Biology*. Elsevier, 28(7), pp. 1157–1165.

Loog, L. *et al.* (2017) 'Estimating mobility using sparse data: Application to human genetic variation', *Proceedings of the National Academy of Sciences*. National Acad Sciences, 114(46), pp. 12213–12218.

Loy, T. H., Spriggs, M. and Wickler, S. (1992) 'Direct evidence for human use of plants 28,000 years ago: starch residues on stone artefacts from the northern Solomon Islands', *Antiquity*. Cambridge University Press, 66(253), pp. 898–912.

Lu, H. *et al.* (2009) 'Earliest domestication of common millet (Panicum miliaceum) in East Asia extended to 10,000 years ago', *Proceedings of the National Academy of Sciences*. National Acad Sciences, 106(18), pp. 7367–7372.

MacDonald, K. C. (2000) 'The origins of African livestock: indigenous or imported', *The origins and development of African livestock: Archaeology, genetics, linguistics and ethnography*. London: UCL Press, 2, p. 17.

Madsen, D. B. and Elston, R. G. (2007) 'Variation in Late Quaternary central Asian climates and the nature of human response', *Developments in Quaternary*

Sciences. Elsevier, 9, pp. 69–82.

Malher, X., Seegers, H. and Beaudeau, F. (2001) 'Culling and mortality in large dairy goat herds managed under intensive conditions in western France', *Livestock Production Science*, 71(1), pp. 75–86.

Manica, A. *et al.* (2007) 'The effect of ancient population bottlenecks on human phenotypic variation', *Nature*, 448(7151), pp. 346–348.

Manning, K. *et al.* (2015) 'Size reduction in early European domestic cattle relates to intensification of Neolithic herding strategies', *PloS one*. Public Library of Science, 10(12), p. e0141873.

Manning, K. and Fuller, D. (2013) 'Early Millet Farmers in the Lower Tilemsi Valley, Northeastern Mali', *Archaeology of African Plant Use*, 61, p. 73.

Manning, K. and Shennan, S. (2013) 'The Origins and Spread of Domestic Animals in Southwest Asia and Europe'. Left Coast Press, Walnut Creek. California.

Marshall, F. and Hildebrand, E. (2002) 'Cattle before crops: the beginnings of food production in Africa', *Journal of World Prehistory*. Springer, 16(2), pp. 99–143.

Maschner, H. D. G. (2003) 'Historical Traditions and Darwinian Theory: Genes, Memes and Human History: Darwinian Archaeology and Cultural Evolution, by Stephen Shennan, 2002. London: Thames & Hudson; ISBN 0-500-051186 hardback,£ 19.95 & US $34.95, 304 pp., 47 ills.-', *Cambridge Archaeological Journal*. Cambridge University Press, 13(2), pp. 283–285.

Matolcsi, J. (1970) 'Historische Erforschung der Körpergröße des Rindes auf Grund von ungarischem Knochenmaterial', *Zeitschrift für Tierzüchtung und Züchtungsbiologie*. Wiley Online Library, 87(1-4), pp. 89–137.

Matthews, P. J. (2002) 'Taro storage systems', *Vegeculture in Eastern Asia and Oceania (S. Yoshida and PJ Matthews, eds.). The Japan Center for Area Studies, Osaka*, pp. 135–163.

McCormick, F. (1992) ‘Early faunal evidence for dairying’, *Oxford journal of archaeology*. Wiley Online Library, 11(2), pp. 201–210.

Meadow, R. H. (1989) ‘Osteological evidence for the process of animal domestication’, *The walking larder: patterns of domestication, pastoralism, and predation*. Unwin-Hyman: London, pp. 80–90.

Meniel, P. (1987) ‘Le dépôt d’animaux du fossé chasséen de Boury-en-Vexin (Oise)’, *Revue archéologique de Picardie*, 1(1), pp. 3–26.

Méniel, P. (1984) ‘Contribution à l’histoire de l’élevage en Picardie. Du Néolithique à la fin de l’Age du Fer’, *Revue archéologique de Picardie*. Société Archéologique de Picardie, 3(1), pp. 1–56.

Millard, A. R. (2006) ‘A Bayesian approach to ageing sheep/goats from toothwear’, *Recent advances in ageing and sexing animal bones*, pp. 145–154.

Mithen, S. J. (1996) ‘The Prehistory of the Mind a Search for the Origins of Art, Religion and Science’.

Molloy, B. (2016) *Of Odysseys and Oddities: Scales and Modes of Interaction Between Prehistoric Aegean Societies and their Neighbours*. Casemate Publishers.

Motuzaite-Matuzeviciute, G. *et al.* (2013) ‘The early chronology of broomcorn millet (Panicum miliaceum) in Europe’, *Antiquity*. Cambridge University Press, 87(338), pp. 1073–1085.

Mourad, M. (1992) ‘Effects of month of kidding, parity and litter size on milk yield of Alpine goats in Egypt’, *Small Ruminant Research*, 8(1–2), pp. 41–46.

Munson, P. J. (2000) ‘Age-correlated differential destruction of bones and its effect on archaeological mortality profiles of domestic sheep and goats’, *Journal of Archaeological Science*, 27(5), pp. 391–407.

Murdock, G. P. (1959) ‘Africa: its peoples and their culture history’.

Nei, M. (1978) ‘Estimation of average heterozygosity and genetic distance from a small number of individuals’, *Genetics*, 89(3), pp. 583–590.

Nei, M., Maruyama, T. and Chakraborty, R. (1975) ‘The bottleneck effect and genetic variability in populations’, *Evolution*. Wiley Online Library, 29(1), pp. 1–10.

Nei, M. and Tajima, F. (1981) ‘DNA polymorphism detectable by restriction endonucleases’, *Genetics*. Genetics Soc America, 97(1), pp. 145–163.

Nugraha, A. M. S. and Hall, R. (2018) ‘Late cenozoic palaeogeography of Sulawesi, Indonesia’, *Palaeogeography, palaeoclimatology, palaeoecology*. Elsevier, 490, pp. 191–209.

Orton, D. C. (2008) *Beyond Hunting and Herding: Humans, animals, and the political economy of the Vinča period*. University of Cambridge.

Oumar, I. *et al.* (2008) ‘Phylogeny and origin of pearl millet (Pennisetum glaucum [L.] R. Br) as revealed by microsatellite loci’, *Theoretical and Applied Genetics*, 117(4), pp. 489–497.

Ozainne, S. *et al.* (2014) ‘A question of timing: spatio-temporal structure and mechanisms of early agriculture expansion in West Africa’, *Journal of Archaeological Science*, 50, pp. 359–368.

Özdoğan, M. (2011) ‘Archaeological evidence on the westward expansion of farming communities from eastern Anatolia to the Aegean and the Balkans’, *Current Anthropology*. University of Chicago Press Chicago, IL, 52(S4), pp. S415–S430.

Payne, S. (1973) ‘Kill-off patterns in sheep and goats: the mandibles from Aşvan Kale’, *Anatolian studies*, 23, pp. 281–303.

Payne, S. (1988) ‘Animal bones from Tell Rubeidheh’, *Tell Rubeidheh, an Uruk Village in the Jebel Hamrin (Iraq Archaeological Reports 2)*, pp. 98–135.

Peters, J. *et al.* (2013) ‘The long and winding road. Ungulate exploitation and domestication in early Neolithic Anatolia (10,000-7,000 cal BC)’, *The origins and*

spread of domestic animals in southwest Asia and Europe.

Powell, A., Shennan, S. and Thomas, M. G. (2009) 'Late Pleistocene demography and the appearance of modern human behavior', *Science*. American Association for the Advancement of Science, 324(5932), pp. 1298–1301.

Prendergast, M. E. *et al.* (2019) 'Ancient DNA reveals a multistep spread of the first herders into sub-Saharan Africa', *Science*. American Association for the Advancement of Science, p. eaaw6275.

Price, M., Wolfhagen, J. and Otarola-Castillo, E. (2016) 'Confidence intervals in the analysis of mortality and survivorship curves in zooarchaeology', *American Antiquity*, 81(1), pp. 157–173.

Purugganan, M. D. and Fuller, D. Q. (2009) 'The nature of selection during plant domestication', *Nature*. Nature Publishing Group, 457(7231), p. 843.

Ramachandran, S. *et al.* (2005) 'Support from the relationship of genetic and geographic distance in human populations for a serial founder effect originating in Africa', *Proceedings of the National Academy of Sciences of the United States of America*, 102(44), pp. 15942–15947.

Redding, R. W. (1981) *Decision making in subsistence herding of sheep and goats in the Middle East*. University of Michigan.

Reed, C. A. (1977) 'model for the origin of agriculture in the Near East', *Origins of agriculture*.

Ren, X. *et al.* (2016) 'Foothills and intermountain basins: Does China's Fertile Arc have "Hilly Flanks"?', *Quaternary international*. Elsevier, 426, pp. 86–96.

Richerson, P. J., Boyd, R. and Bettinger, R. L. (2001) 'Was agriculture impossible during the Pleistocene but mandatory during the Holocene? A climate change hypothesis', *American Antiquity*. Cambridge University Press, 66(3), pp. 387–411.

Rick, J. W. (1987) 'Dates as data: an examination of the Peruvian preceramic

radiocarbon record', *American Antiquity*. JSTOR, pp. 55–73.

RIM. (1992) *Nigerian livestock resources. Four volume report to the Federal Government of Nigeria by Resource Inventory and Management Limited: I. Executive summary and atlas; II. National synthesis; III. State reports; IV. Urban reports and commercially managed live*.

Roberts, M. (1991) 'Origin, dispersal routes, and geographic distribution of Rattus exulans, with special reference to New Zealand'.

Robusto, C. C. (1957) 'The cosine-haversine formula', *The American Mathematical Monthly*. JSTOR, 64(1), pp. 38–40.

Rodríguez, R. *et al.* (2011) '50,000 years of genetic uniformity in the critically endangered Iberian lynx', *Molecular Ecology*. Wiley Online Library, 20(18), pp. 3785–3795.

Rozzi, R. (2017) 'A new extinct dwarfed buffalo from Sulawesi and the evolution of the subgenus Anoa: An interdisciplinary perspective', *Quaternary Science Reviews*. Elsevier, 157, pp. 188–205.

Salque, M. *et al.* (2012) 'New insights into the Early Neolithic economy and management of animals in Southern and Central Europe revealed using lipid residue analyses of pottery vessels', *Anthropozoologica*, 47(2), pp. 45–62.

Salvagno, L. and Albarella, U. (2017) 'A morphometric system to distinguish sheep and goat postcranial bones', *PloS one*. Public Library of Science San Francisco, CA USA, 12(6), p. e0178543.

Scanes, C. G. (2018) 'The Neolithic Revolution, Animal Domestication, and Early Forms of Animal Agriculture', in *Animals and Human Society*. Elsevier, pp. 103–131.

Schauer, P. *et al.* (2019) 'British Neolithic Axehead Distributions and Their Implications', *Journal of Archaeological Method and Theory*. Springer, pp. 1–24.

Scheu, A. *et al.* (2015) 'The genetic prehistory of domesticated cattle from their

origin to the spread across Europe', *BMC genetics*. BioMed Central, 16(1), p. 54.

Schrider, D. R. and Kern, A. D. (2018) 'Supervised machine learning for population genetics: a new paradigm', *Trends in Genetics*. Elsevier, 34(4), pp. 301–312.

Séfériadès, M. (2007) 'Complexity of the processes of Neolithization: tradition and modernity of the Aegean world at the dawn of the Holocene period (11–9 kyr)', *Quaternary International*. Elsevier, 167, pp. 177–185.

Shennan, S. (2009) 'Evolutionary demography and the population history of the European early Neolithic', *Human Biology*. BioOne, 81(3), pp. 339–355.

Shennan, S. *et al.* (2013) 'Regional population collapse followed initial agriculture booms in mid-Holocene Europe', *Nature communications*. Nature Publishing Group, 4(1), pp. 1–8.

Sherratt, A. (1981) 'Plough and pastoralism: aspects of the secondary products revolution'.

Silva, F. *et al.* (2015) 'Modelling the geographical origin of rice cultivation in Asia using the rice archaeological database', *PLoS One*. Public Library of Science, 10(9), p. e0137024.

Simoons, F. J. (1979) 'Dairying, milk use, and lactose malabsorption in Eurasia: A problem in culture history', *Anthropos*. JSTOR, (H. 1./2), pp. 61–80.

Skoglund, P. *et al.* (2016) 'Genomic insights into the peopling of the Southwest Pacific', *Nature*. Nature Publishing Group, 538(7626), p. 510.

Slatkin, M. (1995) 'A measure of population subdivision based on microsatellite allele frequencies', *Genetics*, 139(1), pp. 457–462.

Slatkin, M. and Racimo, F. (2016) 'Ancient DNA and human history', *Proceedings of the National Academy of Sciences*. National Acad Sciences, 113(23), pp. 6380–6387.

Spengler, R. *et al.* (2014) 'Early agriculture and crop transmission among Bronze Age mobile pastoralists of Central Eurasia', *Proceedings of the Royal Society B: Biological Sciences*. The Royal Society, 281(1783), p. 20133382.

Sponheimer, M. and Lee-Thorp, J. A. (1999) 'Isotopic evidence for the diet of an early hominid, Australopithecus africanus', *Science*. American Association for the Advancement of Science, 283(5400), pp. 368–370.

Stein, G. (1986) 'Herding strategies at neolithic Gritille', *Expedition*, 28(2), p. 35.

Stiner, M. C. *et al.* (2014) 'A forager–herder trade-off, from broad-spectrum hunting to sheep management at Aşıklı Höyük, Turkey', *Proceedings of the National Academy of Sciences*, 111(23), pp. 8404–8409.

Stiner, M. C. and Munro, N. D. (2011) 'On the evolution of diet and landscape during the Upper Paleolithic through Mesolithic at Franchthi Cave (Peloponnese, Greece)', *Journal of Human Evolution*, 60(5), pp. 618–636.

Stock, F. *et al.* (2013) 'In search of the harbours: New evidence of Late Roman and Byzantine harbours of Ephesus', *Quaternary International*. Elsevier, 312, pp. 57–69.

El Susi, G. (2008) 'The comparative analyze of faunal samples from Sites dated in Starčevo-Körös-Criş Culture–phases IB-IIA from Transylvania and Banat', in *Acta Terrae Septemcastrensis Journal, Proceedings of the 7th International Colloquium of Funerary Archaeology, Special number (Bibliotheca Septemcastrensis, XVII)*, pp. 91–106.

Svizzero, S. (2015) 'Farmers' spatial behaviour, demographic density dependence and the spread of Neolithic agriculture in Central Europe', *Documenta Praehistorica*, 42, pp. 133–146.

Sweeney, M. and McCouch, S. (2007) 'The complex history of the domestication of rice', *Annals of Botany*. Oxford University Press, 100(5), pp. 951–957.

Thomson, V. *et al.* (2014) 'Molecular Genetic Evidence for the Place of Origin of the Pacific Rat, Rattus exulans', *PloS one*, 9(3), p. e91356.

Timpson, A. *et al.* (2014) 'Reconstructing regional population fluctuations in the European Neolithic using radiocarbon dates: a new case-study using an improved method', *Journal of Archaeological Science*. Elsevier, 52, pp. 549–557.

Timpson, A. *et al.* (2018) 'Modelling caprine age-at-death profiles using the Gamma distribution', *Journal of Archaeological Science*. Elsevier, 99, pp. 19–26.

Todaro, M. *et al.* (2015) 'Aseasonal sheep and goat milk production in the Mediterranean area: Physiological and technical insights', *Small Ruminant Research*, 126, pp. 59–66.

Tostain, S. (1992) 'Enzyme diversity in pearl millet (Pennisetum glaucum L.)', *Theoretical and Applied Genetics*, 83(6–7), pp. 733–742.

Trentacoste, A., Nieto-Espinet, A. and Valenzuela-Lamas, S. (2018) 'Pre-Roman improvements to agricultural production: Evidence from livestock husbandry in late prehistoric Italy', *PloS one*. Public Library of Science, 13(12), p. e0208109.

Tresset, A. (1996) *Le rôle des relations homme/animal dans l'évolution économique et culturelle des sociétés des Ve-IVe millénaires en Bassin Parisien: approche ethno-zootechnique fondée sur les ossements animaux*. Paris 1.

Trifonov, V. A. *et al.* (2017) 'Directly dated broomcorn millet from the northwestern Caucasus: Tracing the Late Bronze Age route into the Russian steppe', *Journal of Archaeological Science: Reports*. Elsevier, 12, pp. 288–294.

Tringham, R. (2000) 'Southeastern Europe in the transition to agriculture in Europe: bridge, buffer or mosaic', *Europe's first farmers*. Cambridge University Press Cambridge, pp. 19–56.

Tsegaye, A. (2002) *On indigenous production, genetic diversity and crop ecology of enset (Ensete ventricosum (Welw.) Cheesman)*.

U.S. Department of Agriculture, A. R. S. (2015) *USDA National Nutrient Database for Standard Reference.* Available at: http://www.ars.usda.gov/nutrientdata.

Ungar, P. S. and Teaford, M. F. (2002) *Human diet: its origin and evolution*. Greenwood Publishing Group.

Vaiglova, P. *et al.* (2018) 'Of cattle and feasts: Multi-isotope investigation of animal husbandry and communal feasting at Neolithic Makriyalos, northern Greece', *PloS one*. Public Library of Science San Francisco, CA USA, 13(6), p. e0194474.

Valenzuela-Lamas, S. and Albarella, U. (2017) 'Animal husbandry across the Western Roman Empire: changes and continuities', *European Journal of Archaeology*. Cambridge University Press, 20(3), pp. 402–415.

Vavilov, N. I. (1951) 'The origin, variation, immunity and breeding of cultivated plants', *Soil Science*, 72(6), p. 482.

Vigne, J.-D. (1988) 'Les mammifères post-glaciaires de Corse. Étude archéozoologique', *Supplément à Gallia Préhistoire*, 26, pp. 1–337.

Vigne, J.-D. (1991) 'The meat and offal weight (MOW) method and the relative proportion of ovicaprines in some ancient meat diets of the north-western Mediterranean', *Rivista di Studi Liguri*, 57(1–4), pp. 21–47.

Vigne, J.-D. and Helmer, D. (2007) 'Was milk a "secondary product" in the Old World Neolithisation process? Its role in the domestication of cattle, sheep and goats', *Anthropozoologica*, 42(2), pp. 9–40.

Vigne, J.-D., Peters, J. and Helmer, D. (2005) *The first steps of animal domestication*. Oxford: Oxbow Books.

Voight, B. F. *et al.* (2005) 'Interrogating multiple aspects of variation in a full resequencing data set to infer human population size changes', *Proceedings of the National Academy of Sciences*. National Acad Sciences, 102(51), pp. 18508–18513.

Warinner, C. *et al.* (2014) 'Direct evidence of milk consumption from ancient human dental calculus', *Scientific reports*. Nature Publishing Group, 4, p. 7104.

Wenke, R. J. (1989) 'Egypt: Origins of complex societies', *Annual Review of Anthropology*. Annual Reviews 4139 El Camino Way, PO Box 10139, Palo Alto, CA 94303-0139, USA, 18(1), pp. 129–155.

White, J. P., Clark, G. and Bedford, S. (2000) 'Distribution, present and past, of Rattus praetor in the Pacific and its implications.', *Pacific Science*, 54(2), pp. 105–117.

White, T. E. (1953) 'A method of calculating the dietary percentage of various food animals utilized by aboriginal peoples', *American Antiquity*. Cambridge University Press, 18(4), pp. 396–398.

Wilkens, B. (1996) 'Faunal remains from Italian excavations on Crete', *Pleistocene and Holocene Fauna of Crete and Its First Settlers (Monographs in World Archaeology 28)*, pp. 241–261.

Willcox, G. (2004) 'Measuring grain size and identifying Near Eastern cereal domestication: evidence from the Euphrates valley', *Journal of archaeological science*. Elsevier, 31(2), pp. 145–150.

Wilson, I. J. and Balding, D. J. (1998) 'Genealogical inference from microsatellite data', *Genetics*. Genetics Soc America, 150(1), pp. 499–510.

Wolff, P. (1975) *Die Jagd-und Haustierfauna der spätneolithischen Pfahlbauten des Mondsees*. na.

Yen, D. E. and Wheeler, J. M. (1968) 'Introduction of taro into the Pacific: the indications of the chromosome numbers', *Ethnology*. JSTOR, 7(3), pp. 259–267.

Zeder, M. (2008) 'Animal domestication in the Zagros: an update and directions for future research', *Travaux de la Maison de l'Orient et de la Méditerranée*, 49(1), pp. 243–277.

Zeder, M. A. (2001) ‘A Metrical Analysis of a Collection of Modern Goats (Capra hircus aegargus and C. h. hircus) from Iran and Iraq: Implications for the Study of Caprine Domestication’, *Journal of Archaeological Science*, 28(1), pp. 61–79.

Zeder, M. A. (2006a) ‘Archaeological approaches to documenting animal domestication’, *Documenting domestication: new genetic and archaeological paradigms*. University of California Press Berkeley, pp. 171–180.

Zeder, M. A. *et al.* (2006) ‘Documenting domestication: the intersection of genetics and archaeology’, *TRENDS in Genetics*. Elsevier, 22(3), pp. 139–155.

Zeder, M. A. (2006b) ‘Reconciling rates of long bone fusion and tooth eruption and wear in sheep (Ovis) and goat (Capra)’, *Recent advances in ageing and sexing animal bones*, pp. 87–118.

Zeder, M. A. (2008) ‘Domestication and early agriculture in the Mediterranean Basin: Origins, diffusion, and impact’, *Proceedings of the national Academy of Sciences*. National Acad Sciences, 105(33), pp. 11597–11604.

Zeder, M. A. (2011) ‘The origins of agriculture in the Near East’, *Current Anthropology*. University of Chicago Press Chicago, IL, 52(S4), pp. S221–S235.

Zhao, Z. (2011) ‘New archaeobotanic data for the study of the origins of agriculture in China’, *Current Anthropology*. University of Chicago Press Chicago, IL, 52(S4), pp. S295–S306.

Zhimin, A. (1988) ‘PREHISTORIC AGRICULTURE IN CHINA [J]’, *Acta Archaeologia Sinica*, 4, pp. 369–381.

Zimmo, S., Blanco, J. and Nebel, S. (2012) ‘The use of stable isotopes in the study of animal migration’, *Nature Education Knowledge*, 3(12), p. 3.

Zohary, D., Hopf, M. and Weiss, E. (2012) *Domestication of Plants in the Old World: The origin and spread of domesticated plants in Southwest Asia, Europe, and the Mediterranean Basin*. Oxford University Press on Demand.